



If you have discovered material in AURA which is unlawful e.g. breaches copyright, (either yours or that of a third party) or any other law, including but not limited to those relating to patent, trademark, confidentiality, data protection, obscenity, defamation, libel, then please read our [Takedown Policy](#) and [contact the service](#) immediately

AZIDOPROFEN AS A SOFT ANTI-INFLAMMATORY AGENT FOR THE
TOPICAL TREATMENT OF PSORIASIS

by

AARTI NAIK

A thesis submitted for the degree of
Doctor of Philosophy
at
Aston University, Birmingham

December 1990

This copy of the thesis has been supplied on condition that anyone who consults it is understood to recognise that its copyright rests with its author and that no quotation from the thesis and no information derived from it may be published without the author's prior, written consent.

Aston University, Birmingham.

**AZIDOPROFEN AS A SOFT ANTI-INFLAMMATORY AGENT FOR THE TOPICAL
TREATMENT OF PSORIASIS**

by
Aarti Naik

Submitted for the degree of Doctor of Philosophy, 1990

SUMMARY

Azidoprofen {2-(4-azidophenyl)propionic acid; AZP}, an azido-substituted arylalkanoic acid, was investigated as a model soft drug candidate for a potential topical non-steroidal anti-inflammatory agent (NSAIA).

Reversed-phase high performance liquid chromatography (HPLC) methods were developed for the assay of AZP, a series of ester analogues and their degradation products. ¹H-NMR spectroscopy was also employed as an analytical method in selected cases.

Reduction of the azido-group to the corresponding amine has been proposed as a potential detoxification mechanism for compounds bearing this substituent. An *in vitro* assay to measure the susceptibility of azides towards reduction was developed using dithiothreitol as a model reducing agent. The rate of reduction of AZP was found to be base-dependent, hence supporting the postulated mechanism of thiol-mediated reduction *via* nucleophilic attack by the thiolate anion.

Prodrugs may enhance topical bioavailability through the manipulation of physico-chemical properties of the parent drug. A series of ester derivatives of AZP were investigated for their susceptibility to chemical and enzymatic hydrolysis, which regenerates the parent acid. Use of alcoholic cosolvents with differing alkyl functions to that of the ester resulted in transesterification reactions, which were found to be enzyme-mediated.

The skin penetration of AZP was assessed using an *in vitro* hairless mouse skin model, and silastic membrane in some cases. The rate of permeation of AZP was found to be a similar magnitude to that of the well established NSAIA ibuprofen. Penetration rates were dependent on the vehicle pH and drug concentration when solutions were employed. In contrast, flux was independent of pH when suspension formulations were used. Pretreatment of the skin with various enhancer regimes, including oleic acid and azone in propylene glycol, promoted the penetration of AZP.

An intense IR absorption due to the azide group serves as a highly diagnostic marker, enabling azido compounds to be detected in the outer layers of the stratum corneum following their application to skin, using attenuated total reflectance Fourier transform infrared spectroscopy (ATR-FTIR). This novel application enabled a non-invasive examination of the percutaneous penetration enhancement of a model azido compound *in vivo* in man, in the presence of the enhancer oleic acid.

Keywords: Azidoprofen; percutaneous absorption; attenuated total reflectance Fourier transform infrared spectroscopy; non-steroidal anti-inflammatory; psoriasis.

... call to Dr. Guy...

... for the quality...

... laboratory to keep...

... Guy and his colleagues...

... of California, San...

To my family

... and

... general to

... discussions

... and staff at

... stay

... Research Council (SERC) for...

... SERC for additional...

... encouragement

... of the manuscript

ACKNOWLEDGEMENTS

I would like to express my appreciation to Dr Bill Irwin for his continual supervision, advice and optimism and to Dr Roger Griffin not only for his guidance and encouragement but also for the equally constant supply of compounds which emerged from his laboratory to keep me occupied throughout this project.

My sincere thanks must also be extended to Dr Richard Guy and his colleagues at the Department of Pharmaceutical Chemistry, University of California, San Francisco (UCSF), USA, for their generous hospitality, collaboration and friendship during my visit in the summer of 1990. I am especially grateful to Drs D Bommaman and Richard Guy for their expertise, helpful discussions and advice, and useful comments on the relevant chapter.

Thanks to my fellow postgraduate friends and colleagues, lecturers and staff at Aston for their companionship and cooperation throughout my stay.

I am grateful to the Science and Engineering Research Council (SERC) for the award of a research grant and to both the UCSF and SERC for additional financial support.

Finally, I must thank my parents and family for their support, encouragement and profound patience, particularly during the preparation of this manuscript, and my mother for her love and confidence, always.

CONTENTS

	<u>Page</u>
Title page	1
Thesis summary	2
Dedication	3
Acknowledgements	4
Contents	5
List of figures	10
List of tables	17
Abbreviations	20
CHAPTER ONE	
INTRODUCTION: THE POTENTIAL ROLE OF NON-STEROIDAL ANTI-INFLAMMATORY AGENTS IN THE TREATMENT OF PSORIASIS	23
1.1 Structure and protective function of skin	24
1.1.1 Cutaneous inflammatory response	26
1.1.1.1 Arachidonic acid metabolites as inflammatory mediators in the skin	27
1.2 Psoriasis	33
1.2.1 Historical perspective	33
1.2.2 Epidemiology and aetiology of psoriasis	33
1.2.3 Clinical features of psoriasis	37
1.2.4 Pathogenesis of psoriasis	39
1.2.4.1 Proliferative aspects	40
1.2.4.2 Inflammatory aspects	40
1.2.5 Treatments for psoriasis	42
1.2.5.1 Anti-proliferative approaches	43
1.2.5.2 Anti-inflammatory approaches	46
1.2.5.2.1 Dietary manipulation	47
1.2.5.2.2 Non-steroidal anti-inflammatory agents	47

1.3 Strategies for the development of novel antipsoriatic agents	52
1.3.1 The soft-drug approach	53
1.3.2 Non-steroidal anti-inflammatory drugs and the soft-drug approach	55
1.3.3 Azidoprofen	59
1.4 Aims and objectives of present study	60

CHAPTER TWO

ASSAY PROCEDURES FOR AZIDOPROFEN AND RELATED COMPOUNDS 61

2.1 Materials	62
2.2 Instrumentation	62
2.2.1 Analytical	62
2.2.2 Subsidiary	64
2.3 Methods	65
2.3.1 High-performance liquid chromatography method development	65
2.3.2 Analysis of azidoprofen and related compounds	73
2.4 Summary	89

CHAPTER THREE

MODEL FOR BIOREDUCTION OF AROMATIC AZIDES 90

3.1 Introduction	91
3.2 Experimental	93
3.2.1 Reduction kinetics of azidoprofen	93
3.2.1.1 Effect of pH on the rate of reduction	93
3.2.1.2 NMR analysis	94
3.2.1.3 Comparative study between NMR and HPLC analysis	95
3.2.2 Murine liver metabolism of azidoprofen	96

3.2.3	Reduction kinetics for the alkyl esters of azidoprofen	96
3.2.3.1	Preliminary studies with azidoprofen-propyl ester	96
3.2.3.2	Anaerobic reduction of azidoprofen and its alkyl esters	98
3.3	Results and discussion	99
3.4	Summary	119
CHAPTER FOUR		120
METABOLIC TRANSFORMATION OF AZIDOPROFEN ESTERS		120
4.1	Introduction	121
4.2	Experimental	125
4.2.1	Enzymatic hydrolysis	125
4.2.1.1	Porcine liver esterase studies	126
4.2.1.2	Hairless mouse skin homogenate studies	128
4.2.2	Chemical hydrolysis	129
4.3	Results and discussion	129
4.4	Summary	146
CHAPTER FIVE		147
PERCUTANEOUS ABSORPTION STUDIES		147
5.1	Introduction	148
5.1.1	NSAIDs and topical delivery	148
5.1.2	Properties influencing percutaneous absorption	151
5.1.2.1	Formulation factors	151
5.1.3	Permeation studies	157
5.1.3.1	Mathematical analysis of skin permeation	161
5.2	Experimental	167
5.2.1	Preparation of membranes	167
5.2.2	Diffusion cell design	167
5.2.3	Preparation of test vehicles	168
5.2.4	Permeation procedure	170

5.2.5 Solubility determinations	171
5.2.6 Partition coefficient measurements	172
5.2.7 pK _a determinations	175
5.3 Results and discussion	177
5.3.1 Measurement of physico-chemical parameters	177
5.3.2 Percutaneous absorption studies	191
5.3.2.1 Permeation studies with azidoprofen and ibuprofen	192
5.3.2.2 Effect of pH on the percutaneous absorption of AZP	196
5.3.2.3 Effect of drug concentration on the percutaneous absorption of AZP	209
5.3.2.4 Effect of cosolvent concentration on the percutaneous absorption of AZP	212
5.3.2.5 Effect of penetration enhancers on the percutaneous absorption of AZP	212
5.4 Summary	223
CHAPTER SIX	
MEASUREMENT OF PERCUTANEOUS PENETRATION <i>IN VIVO</i> BY ATTENUATED TOTAL REFLECTANCE FOURIER TRANSFORM INFRARED SPECTROSCOPY	
	225
6.1 Introduction	226
6.1.1 <i>In vivo</i> percutaneous absorption studies	227
6.2 Attenuated total reflectance Fourier transform infrared spectroscopy	230
6.2.1 Principles of ATR-FTIR	230
6.2.1.1 Infrared spectroscopy	230
6.2.1.2 Attenuated total reflectance	231
6.3 Experimental	235
6.3.1 Attenuated total reflectance Fourier transform infrared spectroscopy	235

6.3.2 <i>In vivo</i> measurements	235
6.3.3 Calibration	236
6.4 Results and discussion	237
6.4.1 Spectral analysis	237
6.4.2 Removal of stratum corneum	243
6.4.3 Distribution of MZPES	248
6.4.4 Stratum corneum lipids	253
6.5 Summary	259
CHAPTER SEVEN	
GENERAL SUMMARY	260
REFERENCES	265
APPENDICES	302
Appendix 1: List of suppliers	303
Appendix 2: Composition of buffers	305

LIST OF FIGURES

<u>Figure</u>		<u>Page</u>
1.1	Schematic cross-sections of the skin.	25
1.2 A	Schematic representation of the metabolic transformation of arachidonic acid <i>via</i> the cyclooxygenase pathway.	29
1.2 B	Schematic representation of the metabolic transformation of arachidonic acid <i>via</i> the lipoxygenase pathway.	31
1.3	Biotransformation of Fluocortin-butylester in man.	54
1.4	Example of a 2-aryloxazolopyridine type NSAID.	54
1.5	Chemical classification of non-steroidal anti-inflammatory agents.	56
1.6	Basic structural features of an arylpropionic acid type NSAID.	57
1.7	The bioreduction of MZP to MAP as its postulated inactivation mechanism.	58
1.8	Schematic representation of azidoprofen, a model azido-substituted arylalkanoic acid.	59
2.1	Structural formulae of compounds used during the study.	63
2.2	UV absorption spectra for AZP and AMP.	68
2.3	Example HPLC chromatogram of a 2 component mixture.	72
2.4	Effect of acetonitrile concentration on the separation of AZP (a), corresponding Methyl (b), Ethyl (c), and Propyl (d) esters and internal standard (e).	75
2.5	Effect of acetonitrile concentration on the separation of AZP (a), corresponding THF (b) and THP (c) esters and internal standard (d).	76
2.6	Typical calibration graph for AZP using HPLC system A.	80

2.7	Typical calibration graphs for AZP and its corresponding methyl, ethyl and propyl esters using HPLC system A.	81
2.8	Typical calibration graphs for the methyl, ethyl and propyl esters of AZP using HPLC system B.	82
2.9	Typical calibration graph for AZP and its corresponding THF and THP esters using HPLC system B.	83
2.10 A	Example chromatogram of AZP and glycolamide ester with methyl paraben as IS.	84
2.10 B	Typical calibration graphs for AZP and the corresponding glycolamide ester using HPLC system F.	84
2.11 A	Example chromatogram of AZP and IBP with butyl paraben as IS; using HPLC system G.	87
2.11 B	Typical calibration graph for AZP and IBP using HPLC system G.	87
2.12 A	Example chromatogram of caffeine and theophylline (IS) using HPLC system H.	88
2.12 B	Typical calibration graph for caffeine using HPLC system H.	88
3.1	Example HPLC chromatogram for the reduction of AZP in phosphate buffer, pH 7.21 at 37°C.	100
3.2	Effect of pH on the first-order reduction kinetics of azidoprofen at 37°C.	101
3.3	pH-rate profile for the base-catalyzed reduction of AZP in phosphate buffer at 37°C.	103
3.4	Proposed mechanism of reduction for aryl azides.	106
3.5	NMR spectrum illustrating the upfield chemical shift of the <i>ortho</i> and <i>meta</i> protons as AZP is reduced to AMP.	108
3.6	Time courses for AZP and AMP during reduction at pD 6.95, as determined by NMR spectroscopy.	109

3.7	Effect of DTT concentration on the reduction of AZP at pD 6.95, as determined by NMR spectroscopy.	110
3.8	First-order plots for the reduction of AZP, determined by NMR and HPLC analysis.	111
3.9	Schematic illustration of decomposition pathways for the alkyl esters of AZP.	113
3.10	Reduction of the propyl ester of AZP in 50% acetonitrile-buffer, pH 7.4 at 37°C.	115
3.11	Example HPLC chromatograms for the methyl (A), ethyl (B) and propyl (C) esters of AZP.	117
3.12	First-order reduction profiles for AZP and its alkyl esters in 30% acetonitrile-buffer, pH 7.4 at 37°C.	118
4.1	Postulated decomposition pathways for esters of AZP.	122
4.2	Example chromatogram for the enzymatic degradation of AZP-methyl ester in 20% propylene glycol at 37°C.	130
4.3	Reaction profiles for the enzymatic hydrolysis of AZP-methyl ester in (A) 10% acetonitrile and (B) 20% propylene glycol at 37°C.	131
4.4	Example chromatogram for the enzymatic degradation of AZP-methyl ester in 10% ethanol at 37°C.	133
4.5	Reaction profile for the enzymatic decomposition of AZP-methyl ester in 10% ethanol-Tris buffer, pH 7.44, by 55 units % esterase at 37°C.	134
4.6	Scheme illustrating the possible transesterification intermediates from reaction between AZP esters and propylene glycol.	135
4.7	Reaction profile for enzymatic hydrolysis of the AZP-THF ester in 10% acetonitrile-Tris buffer, pH 7.44, by 55 units % esterase at 37°C.	140

4.8	First-order plots for the enzymatic hydrolysis of various esters of AZP.	141
4.9	First-order plots for the chemical hydrolysis of various esters of AZP.	143
4.10	Reaction profile for the cutaneous metabolism of AZP-methyl ester at 37°C.	145
5.1	Schematic representation of percutaneous absorption.	150
5.2	Structures of some penetration enhancers.	156
5.3	Schematic representation of a typical penetration profile through a membrane, using a two-compartment diffusion cell.	162
5.4	Schematic representation of a Franz-type diffusion cell.	169
5.5	Schematic representation of a titration assembly to determine ionization constants.	176
5.6	Plot of log octanol/20% propylene glycol-water partition coefficients against alkyl chain length for alkyl esters of AZP.	181
5.7	Effect of pH on the apparent partition coefficient of AZP between octanol and McIlvaine buffer at 20°C.	182
5.8	Effect of pH on the apparent partition coefficient of AZP between IPM and McIlvaine buffer at 20°C.	183
5.9	Effect of pH on the partitioning data of AZP between hairless mouse skin and 10% propylene glycol-buffer at 37°C.	186
5.10	Effect of propylene glycol concentration on the partitioning of AZP between hairless mouse skin and propylene-glycol water mixtures.	187
5.11	Partitioning data for AZP between hairless mouse skin, pretreated with various regimens, and 10% PG-buffer.	189

5.12	Effect of pH on the partitioning of AZP between hairless mouse skin pretreated with 3% v/v azone in PG for 12 hours and 10% PG-buffer.	190
5.13	Steady-state phases of the permeation profiles for AZP and IBP across silastic membrane from saturated solutions in 10% PG-buffer, pH 5.50.	194
5.14	Steady-state phases of the permeation profiles for AZP and IBP across silastic membrane from 1mM solutions in 10% PG-buffer, pH 5.50.	195
5.15	Effect of pH on the permeation of AZP across hairless mouse skin from 15 mM solutions in 10% PG-buffer vehicles.	197
5.16	Plot of the steady-state flux of AZP across hairless mouse skin from solutions of differing pH, as a function of the degree of ionization.	199
5.17	Plot of the observed flux of AZP (k_{obs})/ α as a function of $(1-\alpha)/\alpha$, in order to determine k_u and k_i .	199
5.18	Plot of the steady-state flux of AZP across hairless mouse skin from solutions of differing pH, as a function of saturation.	201
5.19	Effect of pH on the penetration of AZP across silastic membrane from 5 mM solutions in 10% PG-buffer.	202
5.20	Effect of pH on the penetration of AZP across silastic membrane from 5 mM solutions in 10% PG-buffer. Plots of steady-state flux as a function of (A) fraction of unionized drug and (B) fraction of saturation of donor vehicle.	204
5.21	Effect of pH on the penetration of AZP across hairless mouse skin from suspensions in 10% PG-buffer. Plot of steady state flux as a function of fraction of drug unionized.	206
5.22	Plot of log permeability coefficient (K_p) for AZP across hairless mouse skin against pH of donor formulation.	208

5.23	Plot of $\log K_p$ of AZP against the apparent \log skin/ aqueous propylene glycol partition coefficient.	208
5.24	Effect of solute concentration on the penetration of AZP across hairless mouse skin from solutions in 10% PG-buffer (pH 4.50).	210
5.25	Effect of the degree of donor phase saturation on the penetration rate of AZP across hairless mouse skin from solutions in 10% PG (pH 4.50).	211
5.26	Effect of propylene glycol concentration on the penetration of AZP across hairless mouse skin from buffered suspensions (pH 4.50).	213
5.27	Example permeation profiles of AZP across hairless mouse skin from suspensions in 10% PG-buffer (pH 4.50) following various 12 hour pretreatments.	216
5.28	Permeation profile for caffeine across hairless mouse skin with and without a 1 hr pretreatment with 0.5% DCA in PG.	220
5.29	Example permeation profiles of AZP across hairless mouse skin from suspensions in buffered 10% PG vehicles (pH 4.50-6.50) following pretreatment with 3% azone in PG.	221
6.1	A schematic diagram of an ATR-FTIR sampling device.	231
6.2	Example IR spectra of (A) untreated human SC, (B) MZPES and (C) human SC following application of a 5% w/v solution of MZPES in propylene glycol.	238
6.3	Normalization of an IR absorbance to correct for variations in skin/IRE contact.	241
6.4	Calibration plot for MZPES, illustrating the linear relationship between MZPES concentration and IR absorbance.	242

6.5	Distribution of radioactivity in the SC after topical application of 4-chlortestosterone acetate.	244
6.6	Cumulative weight per unit area of SC removed by sequential tape-stripping.	246
6.7	Semi-logarithmic plots of the normalized MZPES level as a function of (A) tape-strip number and (B) cumulative weight of SC removed.	247
6.8	Normalized MZPES level as a function of SC 'depth' following treatment for 1 hr with either a 5% w/v solution of MZPES in propylene glycol or the identical solution containing 5% w/v oleic acid.	249
6.9	Normalized MZPES level as a function of SC 'depth' following treatment for 2 hr with either a 5% w/v solution of MZPES in propylene glycol or the identical solution containing 5% w/v oleic acid.	250
6.10	Normalized MZPES level as a function of SC 'depth' following treatment for 3 hrs with either a 5% w/v solution of MZPES in propylene glycol or the identical solution containing 5% w/v oleic acid.	251
6.11	IR spectra of human SC in the C-H stretching region.	255
6.12	Frequency shift of the C-H asymmetric stretching absorbance as a function of tape-strip number following (A) 1 hour, (B) 2 hour and (C) 3 hour treatment with either a 5% w/v solution of MZPES in propylene glycol (control) or an identical solution containing 5% w/v oleic acid (OA treatment).	257

LIST OF TABLES

<u>Table</u>		<u>Page</u>
1.1	Summary of pro-inflammatory actions of eicosanoids in human skin.	32
2.1	Molar absorption coefficients for AZP and AMP at various wavelengths under neutral and acidic conditions.	68
2.2	The effect of varying acetonitrile concentration on the HPLC parameters of AZP and corresponding esters.	77
2.3	Summary of HPLC conditions for compounds analyzed during the study.	78
2.4	Typical calibration statistics for AZP using HPLC system A.	80
2.5	Calibration statistics for Figure 2.7.	81
2.6	Calibration statistics for Figure 2.8.	82
2.7	Calibration statistics for Figure 2.9	83
2.8	Calibration statistics for Figure 2.10 B	84
2.9	Summary of HPLC conditions for the analysis of azido and amino alkyl ester derivatives of AZP.	85
2.10	Calibration statistics for Figure 2.11 B	87
2.11	Calibration statistics for Figure 2.12 B	88
3.1	Conditions used to collect NMR spectra.	94
3.2	Analytical conditions for the assay of AZP and corresponding esters.	98
3.3	Effect of pH on the rate of reduction of azidoprofen at 37°C.	102

3.4	Reduction data for AZP and its alkyl esters in 30% acetonitrile-buffer, pH 7.4 at 37°C.	118
4.1	Example biotransformation reactions in the skin.	123
4.2	Examples of prodrugs developed for topical use.	124
4.3	Transesterification and hydrolysis rates for AZP esters at 37°C.	138
4.4	Kinetic data for the enzymatic hydrolysis of various esters of AZP.	141
4.5	Kinetic data for the chemical hydrolysis of various esters of AZP.	143
5.1	Example ionization constants.	177
5.2	Effect of pH on the saturated solubility of AZP in 10% propylene glycol-buffer at 32°C.	179
5.3	Effect of propylene glycol concentration on the saturated solubility of AZP in buffered vehicles (pH 4.50), at 32°C.	179
5.4	Partitioning data for AZP and corresponding alkyl esters between octanol and 20% propylene glycol in water at 20°C.	181
5.5	Partitioning data for AZP between various systems.	185
5.6	Permeation data for AZP and IBP across silastic membrane from dilute and saturated solutions in 10% PG-buffer, pH 5.50.	195
5.7	Permeation data for AZP across hairless mouse skin from a series of equimolar (15 mM) solutions in 10% PG-buffer.	196
5.8	Permeation data for AZP across silastic membrane from a series of equimolar (5 mM) solutions in 10% PG-buffer.	202

5.9	Permeation data for AZP across hairless mouse skin from a series of suspensions in 10% PG-buffer.	205
5.10	Permeation data for AZP across hairless mouse skin from solutions of varying concentration in 10% PG-buffer.	210
5.11	Permeation data for AZP across hairless mouse skin from buffered propylene glycol suspensions (pH 4.50).	213
5.12	Permeation data for AZP across hairless mouse skin from suspensions in 10% PG-buffer (pH 4.50) following a 1 or 12 hour pretreatment with various penetration enhancers.	215
5.13	Effect of dodecylamine on the permeation of AZP across hairless mouse skin from a suspension in buffered 10% PG.	218
5.14	Permeation data for AZP across hairless mouse skin from suspensions in buffered 10% PG (pH 4.50-6.50) following a 12 hour pretreatment with 3% azone in PG.	221
6.1	Infrared band assignments for stratum corneum constituents.	239
6.2	Relative amounts of MZPES in the SC following various treatment protocols.	252

ABBREVIATIONS

AA	arachidonic acid
ATR-FTIR	attenuated total reflectance-fourier transform infra-red
AUFS	absorbance units full scale
AMP	aminoprofen
AZP	azidoprofen
AZP-Na	azidoprofen sodium salt
cm	centimetres
¹⁴ C	carbon-14 radiolabelled
CO	cyclooxygenase
DCHA	docosahexaenoic acid
DCMS	decylmethyl sulphoxide
DHFR	dihydrofolate reductase
DMSO	dimethyl sulphoxide
DNA	deoxyribonucleic acid
DTT	dithiothreitol
DW	distilled water
EPA	eicosapentaenoic acid
EtOH	ethanol
g	grammes
g	gravity
GA	glycolamide
GSH	glutathione
h	hours
³ H	tritium radiolabelled
¹ H-NMR	proton nuclear magnetic resonance
HCl	hydrochloric acid
HETE	hydroxy-5,8,10,14-eicosatetraenoic acid
HLA	human lymphocyte antigen
HPETE	hydroperoxy-5,8,10,14-eicosatetraenoic acid
HPLC	high performance liquid chromatography
i.d.	internal diameter

IBP	ibuprofen
IPM	isopropyl myristate
IR	infra-red
IS	internal standard
IU	international units
kV	kilovolts
KBr	potassium bromide
K _p	permeability coefficient
ln	natural logarithm (to base 2)
log	logarithm (to base 10)
LO	lipoxygenase
LTB ₄	leukotriene B ₄
LTC ₄	leukotriene C ₄
LTD ₄	leukotriene D ₄
LTE ₄	leukotriene E ₄
mg	milligrammes
min	minutes
ml	millilitres
mM	millimolar
mmol	millimoles
MAP	<i>m</i> -aminopyrimethamine
MeCN	methyl cyanide (acetonitrile)
MeOH	methanol
MHC	major histocompatibility complex
MHz	megahertz
MZP	<i>m</i> -azidopyrimethamine
MZPES	<i>m</i> -azidopyrimethamine ethanesulphonate
nm	nanometres
NADP	nicotinamide adenine dinucleotide phosphate
NADPH	nicotinamide adenine dinucleotide phosphate (reduced form)
NMR	nuclear magnetic resonance
NSAID(s)	non-steroidal anti-inflammatory drug(s)
OA	oleic acid

ODS	octadecylsilane
phrs	peak height ratios
pK _a	log ₁₀ dissociation constant
P	partition coefficient
PBS	phosphate buffered saline
PG	propylene glycol
PGD ₂	prostaglandin D ₂
PGE ₂	prostaglandin E ₂
PGF _{2α}	prostaglandin F _{2α}
PGG ₂	prostaglandin G ₂
PGH ₂	prostaglandin H ₂
PGI ₂	prostacyclin I ₂
PLA ₂	phospholipase A ₂
PMNL	polymorphonuclear leukocyte
PUVA	psoralen plus UV-A
r	correlation coefficient
rpm	revolutions per minute
sem	standard error of the mean
SC	stratum corneum
SRS-A	slow reacting substance of anaphylaxis
THF	tetrahydrofuranylmethyl
THP	tetrahydropyranylmethyl
TXA ₂	thromboxane A ₂
UV	ultra-violet
v/v	volume in volume
w/v	weight in volume (g/100 ml)
μA	microamps
μg	micrograms
μl	microlitres
μM	micromolar
μmol	micromoles
%	percentage
°C	degrees celcius

CHAPTER ONE
INTRODUCTION:
THE POTENTIAL ROLE OF NON-STEROIDAL ANTI-INFLAMMATORY AGENTS IN THE
TREATMENT OF PSORIASIS

INTRODUCTION:

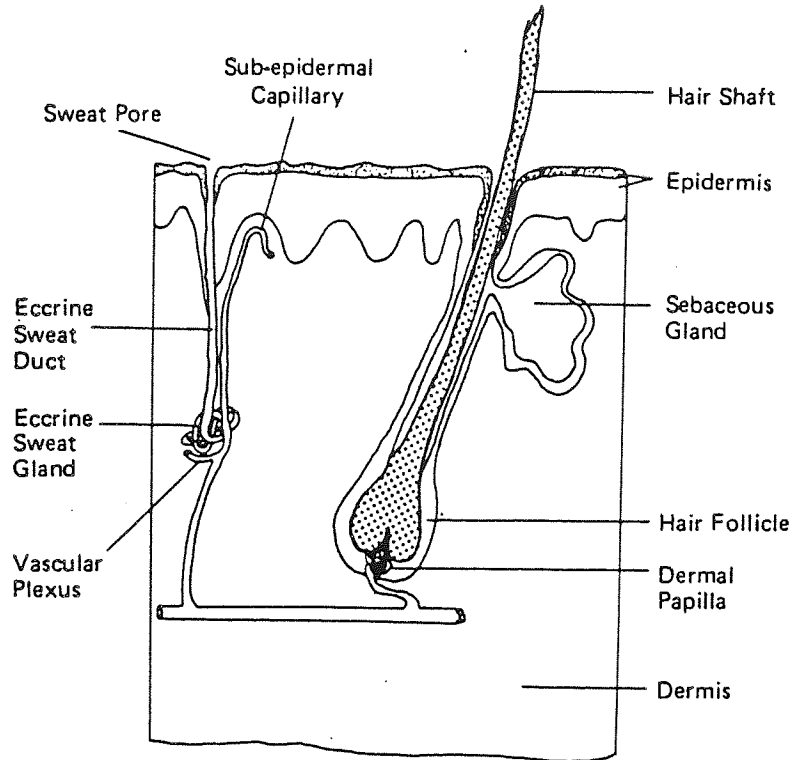
THE POTENTIAL ROLE OF NON-STEROIDAL ANTI-INFLAMMATORY AGENTS IN THE TREATMENT OF PSORIASIS

1.1 STRUCTURE AND PROTECTIVE FUNCTION OF SKIN

Skin, the interface between man and his environment, is the single heaviest organ of the body. During the course of evolution, it has undergone many structural modifications in order to perform the functions currently attributed to it. Ideally situated for its primary role of protection, this flexible envelope maintains homeostasis of the *milieu intérieur* by preventing the loss of essential body fluids, the entrance of toxic agents and microorganisms as well as providing resistance to physical injury from mechanical forces and radiation. In addition, it plays a sensory, thermoregulatory, endocrine and communicatory role. Indeed, the immense heterogeneity of the skin is testimony to the multitude of requirements it must fulfill. The detailed anatomy and physiology of the skin has been reviewed by several excellent texts (Barry, 1983; Greaves and Shuster, 1989; Montagna and Parakkal, 1974) and will be discussed only briefly here.

Human skin is essentially composed of two layers, the outer epidermis and the underlying dermis, beneath which resides a layer of subcutaneous fat also termed the hypodermis (Figure 1.1 A). The dermis is essentially an acellular collagen-based connective tissue which harbours a dense capillary and nerve network. Sweat glands, hair follicles and associated sebaceous glands are supported by this matrix before they reach the skin surface. In contrast, the avascular and cellular epidermis is structurally unique, consisting of stacked layers of both viable and non-viable cells, in a state of constant transition. A transverse epidermal section is effectively a "freeze frame" displaying one cell type in different phases of maturation which constitute the epidermis (Figure 1.1 B).

A



B

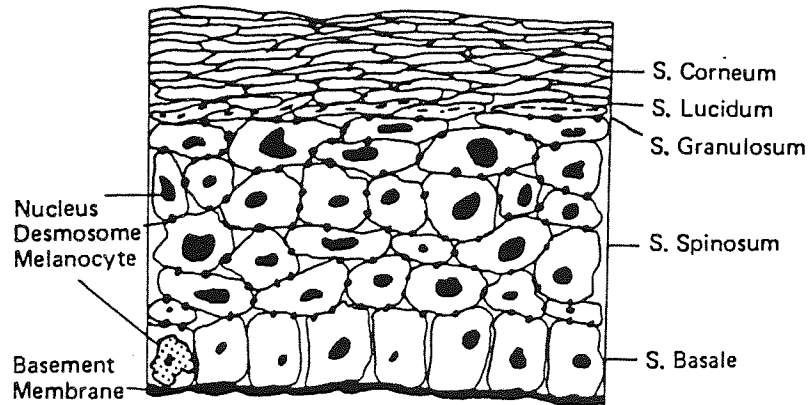


Figure 1.1 Schematic cross-sections of the skin. (A) Full-thickness skin and (B) an expansion of the epidermis. (From Barry, 1983).

This is the result of a complex chain of events, during which cells migrate from the proliferative basal layer towards the skin surface before desquamation. As they ascend, the metabolically active and rapidly dividing columnar keratinocytes undergo a process of ordered differentiation which culminates in the formation of dead, anucleated, flattened and elongated corneocytes rich in keratin. These protein-enriched cells at the final stages of differentiation together with their intercellular lipid matrix, give rise to the outermost layer of the epidermis, the stratum corneum (Elias, 1983). Predominantly lipophilic and considered to be the principal epidermal permeability barrier, its formation has been described as the ultimate goal of the epidermal differentiation process (Elias, 1988) and the *raison d'être* of the epidermis (Kligman, 1964).

Besides the ability of the skin to present a physical armour against the hostilities of the external surroundings, it is also equipped with a secondary defence mechanism should the primary barrier be impaired. Hence, the skin is able to respond to a wide variety of noxious stimuli in the form of an immune or nonimmune-mediated cutaneous inflammatory response. The epidermis also serves as an immunologically competent organ, harbouring a macrophage-like population of cells known as Langerhans cells. First described in 1868 by Paul Langerhans, they are thought to play an essential role in immunologically mediated inflammatory conditions (Stingl and Wolff, 1982).

1.1.1 Cutaneous inflammatory response

Inflammation can be defined as the response of living tissues to an injurious stimulus. Recognition of a foreign body or mechanically inflicted trauma triggers a series of events designed to minimize local damage and inhibit its progression. It is characterized by a local vascular response consisting of transient vasoconstriction followed by vasodilatation and increased vascular permeability. This is accompanied by the accumulation of fluids and phagocytic cells at the site of injury which attempt to remove the intruder and rectify the situation. Failure to do so results in the continuous influx of leucocytes and the onset of a chronic inflammatory reaction, often with an immunological involvement.

Although Cornelius Celsus in the first century AD, is noteworthy for his classical description of the four cardinal signs of inflammation: *Tumor* (swelling), *Rubor* (redness), *Calor* (heat) and *Dolor* (pain), it was not until the 18th Century that John Hunter (1728-1793) introduced an essentially modern concept of inflammation. He described it as a "salutary" reaction in response to disease or injury and not a disease itself, although he also appreciated that it could be harmful and wrote: "when it cannot accomplish that salutary purpose.... it does mischief". To Julius Cohnheim (1839-1884) we owe the descriptions of the vascular and cellular events and to Elie Metchnikoff (1845-1916) the concept of phagocytosis and its central role in the inflammatory process. These vital observations and subsequent research have led to an appreciation of the complexity of the inflammatory process involving interactions from numerous chemical mediators and regulators. We now recognize that many common dermatoses such as psoriasis present as varying degrees of inflammation and possibly reflect an imbalance of the intracellular mediators and associated biochemical pathways. Prior to examining the evidence for this, a brief discussion of the putative inflammatory mediators in skin is warranted.

1.1.1.1 Arachidonic acid metabolites as inflammatory mediators in the skin

The study of the role of chemical mediators in cutaneous inflammation has received much attention and has the distinct advantage of a unique accessibility to the organ of interest (Camp and Greaves, 1987; Greaves, 1988; Ruzicka and Printz, 1984). Realization in the 1960's that vasoactive amines and short chain peptides could not alone account for the pathophysiological events of clinical inflammation, prompted a search for alternative mediators. Furthermore, the endogenous substance responsible for leukocyte migration, a key event in inflammation, had yet to be identified. Isolation and structural elucidation of a family of pharmacologically active lipids in the 1960's and 70's and the discovery that aspirin-like nonsteroidal anti-inflammatory drugs inhibited the biosynthesis of some of these lipids (Vane, 1971; Smith and Willis, 1971)) have helped to explain many of the molecular events underlying the inflammatory response.

Arachidonic acid (AA), an unsaturated fatty acid, is the precursor of a group of pharmacologically active metabolites collectively referred to as eicosanoids, several of which have been implicated in the dermal inflammatory response. The preliminary event in their synthesis is the liberation of free AA by hydrolytic cleavage from cell membrane phospholipids, where it is esterified to the 2-acyl position in phosphatidylcholine. This is catalyzed by the calcium-dependent enzyme phospholipase A₂ (PLA₂), the activity of which is the rate-limiting step in eicosanoid synthesis, since esterified or unreleased AA is incapable of being metabolized. Epidermal PLA₂ may be activated by a variety of stimuli including cellular damage and agents capable of inducing transmembrane flux of calcium ions. In the absence of PLA₂ stimulation, the *in vivo* epidermal free AA content appears to be barely detectable. However, once released, free AA may undergo biotransformation by one of several routes (Figure 1.2).

Conversion by the the microsomal enzyme cyclooxygenase yields a family of metabolites which possess a cyclic structure within the 20-carbon monocarboxylic acid chain (Figure 1.2 A). The first step involves addition of oxygen, isomerization and cyclization of AA to form the unstable cyclic endoperoxide prostaglandin G₂ (PGG₂), which undergoes further peroxidation to generate PGH₂. Both PGG₂ and PGH₂ are highly unstable and although possessing pharmacological activity, probably serve as transitory intermediates in the formation of more stable metabolites. Thus, PGH₂ assumes a central position as an intermediate in prostanoid synthesis and serves as a substrate for enzymatic conversion to the prostaglandins of which the most important are PGE₂, PGF_{2α} and PGD₂. In addition, it may also be converted to the chemically unstable thromboxane A₂ (TXA₂) and prostacyclin I₂ (PGI₂), which undergo spontaneous hydrolytic rearrangement to the stable, relatively inactive substances TXB₂ and 6-keto-PGF_{1α}.

...synthesizing several products of
 ...and PGI_2 (Barry *et al.*, 1984);
 ...

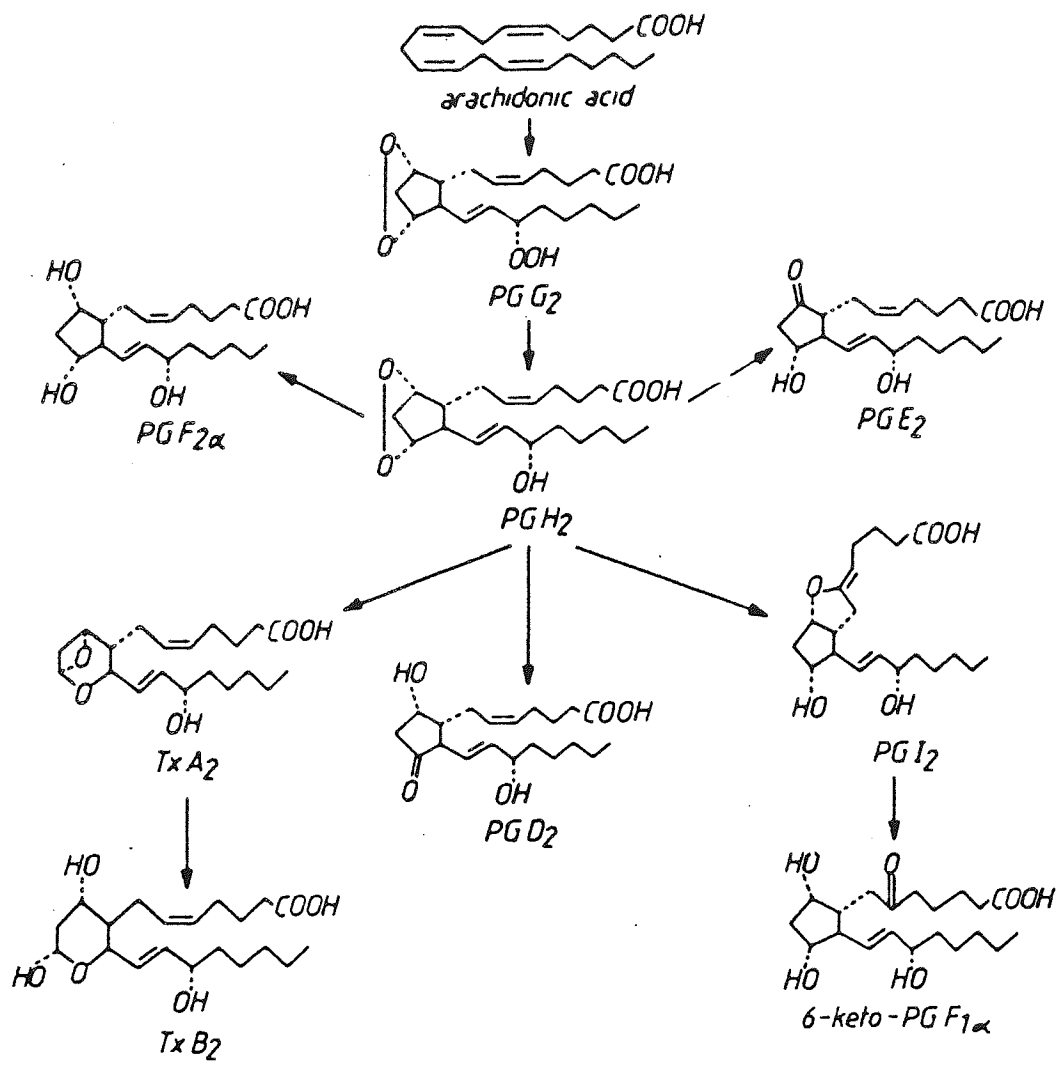


Figure 1.2 A Schematic representation of the metabolic transformation of arachidonic acid *via* the cyclooxygenase pathway. (From Church *et al.*, 1989).

Human skin has been shown to be capable of synthesizing several products of the cyclooxygenase pathway, namely; PGE₂, PGF_{2α} and PGD₂ (Barr *et al*, 1986; Greaves and McDonald-Gibson, 1972; Jonsson and Anggard, 1972), the most predominant of which is PGE₂. Although, TXB₂ and 6-keto-PGF_{1α} have also been identified in suction blister fluid from human skin (Oikarinen *et al*, 1981), the presence of blood products in this fluid makes it difficult to identify the exact source of these metabolites.

Arachidonic acid may also be converted by a series of lipoxygenase enzymes, classified according to the carbon atom they act upon as 5-, 12- and 15-lipoxygenase (LO) (Figure 1.2 B). In contrast to the products of the CO pathway, these metabolites lack a cyclic structure in the molecule. Hamberg and Samuelson (1974) and Nugteren (1975) first described the 12-LO pathway in platelets which catalyzes the conversion of AA to the hydroxy acid, 12-hydroxy-5,8,10,14-eicosatetraenoic acid (12-HETE) *via* the hydroperoxy intermediate 12-HPETE. The enzyme which has generated most interest in the skin is however 5-lipoxygenase which initially catalyzes the conversion of AA to the unstable epoxide, leukotriene A₄ (LTA₄) *via* 5-hydroperoxyeicosatetraenoic acid (5-HPETE). LTA₄ may then be further metabolized *via* two routes. It can be hydrolysed enzymatically to leukotriene B₄ (LTB₄). Alternatively, it may be conjugated with glutathione yielding LTC₄ which can undergo further transformation to LTD₄ and LTE₄; these latter three metabolites form the major components of slow-reacting substance of anaphylaxis (SRS-A). Finally, the activity of both 5-LO and 12-LO is inhibited by 15-hydroxyeicosatetraenoic acid (15-HETE), a product of the 15- LO pathway (Kragballe *et al*, 1986a; Vanderhook *et al*, 1980;). Evidence for the presence of lipoxygenase activity in human epidermis has been derived from studies of isolated keratinocytes (Brain *et al*, 1982a; Grabbe *et al*, 1984), epidermal enzyme preparations (Ziboh *et al*, 1984) and keratome biopsies (Duell *et al*, 1988) which demonstrate either the presence or synthesis of 12-HETE and LTB₄.

The preceding discussion have
 been available (1) and have been
 ...

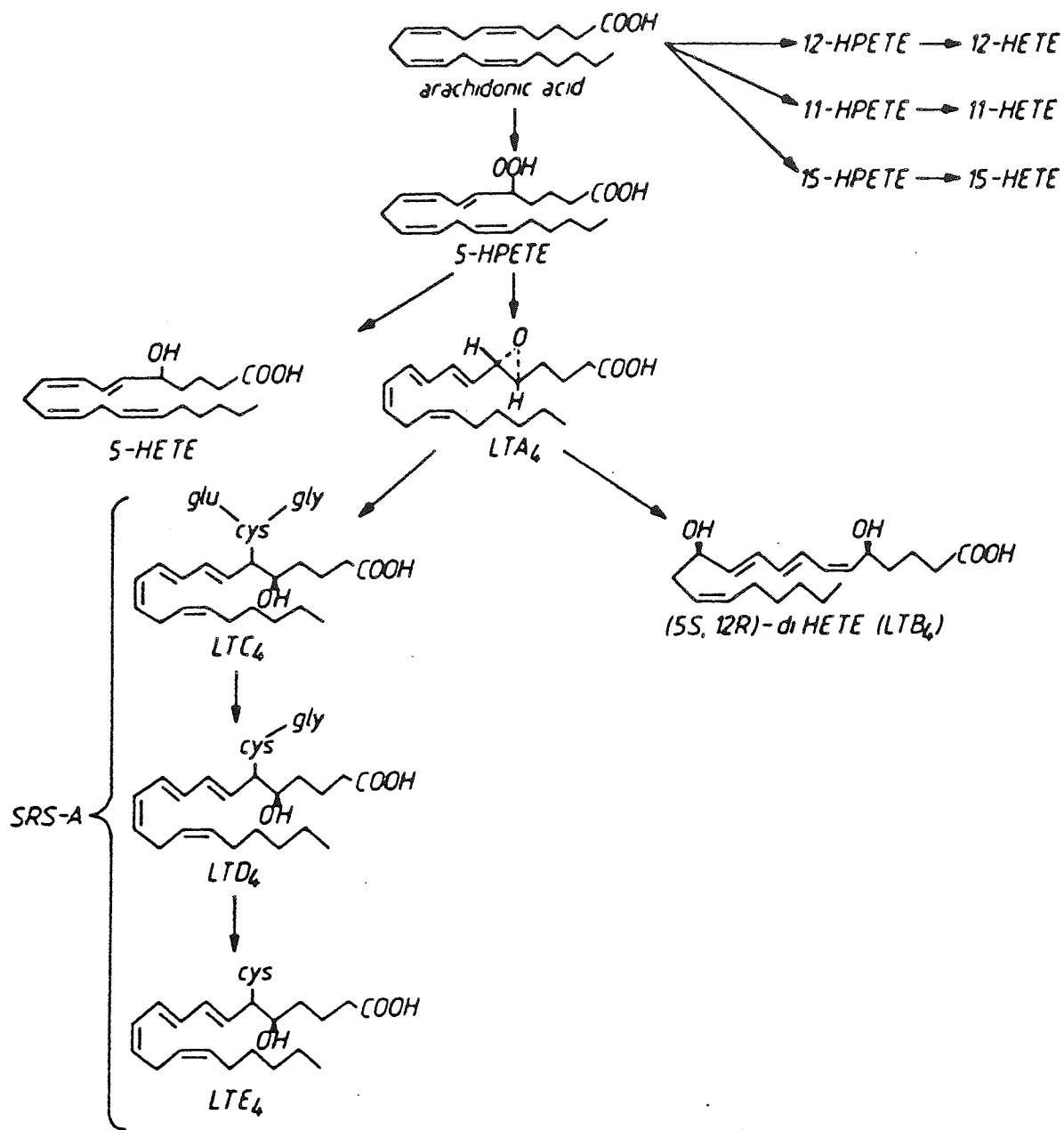


Figure 1.2 B Schematic representation of the metabolic transformation of arachidonic acid *via* the lipoxygenase pathways. (From Church *et al*, 1989).

Several of the AA metabolites mentioned in the preceding discussion have been shown to possess pro-inflammatory properties (Table 1.1) and have been investigated for their pathogenic significance in inflammatory disorders of the skin based on the criteria of Dale (1934), which should be satisfied if a substance is to be held responsible for an inflammatory process (Camp, 1988). A skin disease which has been the subject of relatively detailed investigations in order to provide clues to the aetiology of the condition is psoriasis.

Table 1.1 Summary of pro-inflammatory actions of eicosanoids in human skin

Eicosanoid	Vasodilatation	Vascular permeability	Chemotactic
PGE ₂	+	+*	-
PGD ₂	+	+*	-
PGI ₂	+	?	-
LTB ₄	-	‡	+
12-HETE	?	?	+

? information not available for human skin

* acts synergistically with other mediators

‡ related to its chemotactic ability

1.2 PSORIASIS

1.2.1 Historical perspective

Psoriasis is a chronic hyperproliferative and inflammatory skin disorder whose history has been described as being "... as interesting and puzzling as the disease itself" (van de Kerkhof, 1986) and forms the subject of detailed monographs by Bechet (1936) and Pusey (1933). Celsus (25 BC - 45 AD) is credited with the first recognizable description of psoriasis almost 2000 years ago, however it was Galen (133 - 200 AD) who first used the word 'psoriasis', derived from the Greek *psora* for itch, albeit probably for a condition which we recognize as eczema today. The first accurate description of psoriasis and its various manifestations was provided by Robert Willan in 1809 (Willan, 1809). From the onset however, psoriasis was grouped with leprosy, the social stigma of which also made psoriatic patients the victims of ostracism. This confusion remained for many centuries and it was not until 1841 that Hebra definitively separated the two disease entities.

1.2.2 Epidemiology and aetiology of psoriasis

Psoriasis remains one of the commonest skin disorders, affecting an estimated 2% of the Western European population (Zachariae, 1986) though subject to racial and geographical variation with prevalence in the general population ranging from 0.1% (Convit, 1963) to 2.8% (Lomholt, 1963). It occurs in males and females with equal frequency and may become apparent at any time between birth and the final years of life, although in an extensive census study by Farber and Nall (1974), 58% of patients had an age of onset before 30 years. Hence, it is a global disease affecting persons of all ages, both sexes and almost all ethnic groups. It is recognized as a lifelong disorder characterized by chronic recurrent exacerbations and remissions of erythematous scaly lesions, which although rarely life-threatening are physically and emotionally debilitating. Described as a disease of the total skin, any site on otherwise symptomless skin has the potential to elicit a psoriatic response. This condition, for which there is no known cure and whose aetiology remains a mystery, has attracted

universal research efforts which have helped to unravel some of the etiopathogenetic events in the course of the disease.

The view that psoriasis has a genetic predisposition has long been accepted, although the precise mode of inheritance is still unclear. Early reports proposed the inheritance of a single dominant gene with incomplete penetrance in a classical Mendelian fashion (Abele *et al*, 1963). Subsequent family studies (Watson *et al*, 1972) and analysis of earlier census investigations (Ananthakrishnan *et al*, 1973 and 1974) have excluded simple monogenic types of inheritance and support the concept of polygenic and multifactorial inheritance, implicating the effect of several genes as the causative factor. In recent years, many inherited diseases have been linked with histocompatibility antigens (human lymphocyte antigen; HLA). These antigens are inheritable membrane surface components of human cells of importance in the immune response, which are coded for by genes in the major histocompatibility complex (MHC) on the short arm of chromosome number six. A greater than expected frequency (a disequilibrium) of a given HLA antigen in a certain disease has led to the assumption that the genes responsible for that disease reside near the HLA complex. Psoriasis has been associated with several HLA antigens with different clinical patterns correlated to different markers (Beckman *et al*, 1977; Krulig *et al*, 1975); determination of the HLA status therefore has the potential to give a good indication of the risk and clinical nature of the disease. Epidemiological studies suggest that although psoriasis has an undisputed genetic component, a number of exogenous factors are also important in precipitating and influencing the course of the disease (Farber and Nall, 1983).

The Koebner or isomorphic phenomenon describes the appearance of a lesion in clinically uninvolved skin of psoriatic patients at the site of local trauma resulting from such events as surgical wounds, irritation, sunburn or mechanical injury and was first reported by Heinrich Koebner in 1876 (Koebner, 1876). Both dermal and epidermal damage is necessary to elicit the response (Farber *et al*, 1965; Pedace *et al*, 1969) and patients may shift between the Koebner positive and negative states at different times during the course of

the disease. An estimated 25% of psoriatic patients are Koebner positive according to Eyre and Krueger (1982) who also introduced the term 'the reverse Koebner phenomenon', describing the appearance of clinically uninvolved skin following removal of an area of plaque psoriasis, the two reactions being mutually exclusive. The identity of the factor governing the transient nature of the phenomenon remains unknown, although relative levels of T suppressor and helper cells may be of importance (Baker, 1984).

The role of infections in the aetiology of psoriasis is well established (Holzmann *et al*, 1974; Norholm-Pederson, 1952; Norrlind, 1947). From these reports, a significant association emerges between upper respiratory tract infection, particularly streptococcal tonsillitis, and childhood guttate psoriasis. Although streptococcal infection is now regarded as the major precipitating factor in guttate psoriasis, the causal relationship is still not understood. Various explanations have been forwarded including cross-reactivity between streptococcal antigens and keratinocyte components (Swerlick, 1986) and certain HLA antigens (Hirata and Terasaki, 1970), as well as the inability to produce normal amounts of antibody to streptolysin O in patients genetically predisposed to guttate psoriasis (Bertrams *et al*, 1974).

Certain drugs have been reported to precipitate or exacerbate psoriasis; these include, lithium, beta blockers, antimalarials and nonsteroidal anti-inflammatory drugs. Considering the range of pharmacological activities which these drugs possess, they may be influencing the psoriatic process through intervention at various biochemical and molecular levels. Similarly, the underlying condition being treated may also modulate the course of the disease. Additionally, since drugs may cause a variety of cutaneous reactions, a secondary Koebner phenomenon following a primary drug eruption should also be considered (Abel *et al*, 1986). These authors have reviewed the associated literature and stress the need for controlled studies in order to fully comprehend the role of these drugs in the disease process. Evaluation of the pharmacological effects of drugs which exacerbate psoriasis may provide clues to the etiopathogenesis of the disorder. Thus, reports that indomethacin (Ellis

et al, 1983; Katayama and Kawada, 1981) and meclofenamate (Meyerhoff, 1983) aggravated the condition denoted the significance of inflammatory eicosanoids in the pathogenesis of psoriasis. Other literature (Ellis *et al*, 1986a; Green and Shuster, 1987) however is not in agreement with these observations, and even includes reports of improvement with meclofenamate (Winthrop, 1982); therefore experience with respect to the effect of NSAIDs on psoriasis is quite variable.

Hormonal changes such as those encountered during puberty, menopause and pregnancy have been known to influence the course of psoriasis. Hence, it may first become manifest around puberty or the menopause and improve or worsen during pregnancy (Farber and Nall, 1974).

Perhaps one of the single most important triggering and aggravating factors in psoriasis is psychological stress (Farber and Nall, 1983). Not only may an episode of stress precipitate an attack, but the presence of the lesions may then cause secondary stress, exacerbating the condition with the establishment of a vicious circle. Hormonal and immunological processes which may be affected by stress could in turn influence the clinical course of psoriasis. The inability to quantify stress objectively poses further difficulty in the precise evaluation of its role. The psychosocial aspects of psoriasis together with its management have been discussed extensively by several authors (Duller and van Veen-Vietor, 1986; Seville, 1986).

Climatic changes may also modulate the disease. Increased humidity may have a beneficial effect as does exposure to sunlight. In a few patients, sun exposure may have an adverse effect but this is probably a result of sunburn which may elicit a Koebner response. Geographical variation in the prevalence of psoriasis has also been linked to environmental factors (Yasuda *et al*, 1971).

Hypocalcaemia has been associated with an exacerbation of psoriasis (Baker and Ryan, 1968; Risum, 1973). This observation may throw light on the pathogenesis of this disorder, since vitamin D has been reported to benefit

psoriasis (Smith *et al*, 1988) as have sunlight and ultraviolet-B therapy which enhance the production of vitamin D in the skin.

Identification of such a vast range of aetiological factors not only contributes to an understanding of the etiopathogenesis of the disease but provides avenues through which preventative and control measures may be taken to improve the prognosis of the condition (Farber and Nall, 1984).

1.2.3 Clinical features of psoriasis

Psoriasis is characterized by the appearance of cutaneous lesions whose distinctive macromorphology is a valuable diagnostic tool for dermatologists. The lesions vary in size depending on the clinical form of the disease but usually present as sharply-defined, erythematous, elevated plaques covered with a silvery-white scale. The epidermal thickening or acanthosis due to hyper and parakeratosis cause the lesions to be slightly raised from the adjoining skin, while air spaces separating the layers reflect light to produce the distinctive silver appearance of the scale. Removal of the scale reveals small bleeding points referred to as *signe d'Auspitz*, indicative of dermal vascular changes. In the fully-developed psoriatic lesion this is accompanied by cellular invasion of the epidermis by polymorphonuclear leukocytes, which aggregate within the parakeratotic mounds of the stratum corneum to form Munro's micro-abscesses (Pinkus and Mehregan, 1981). The underlying epidermal cells of the stratum spinosum may be intermingled with neutrophils forming small spongiform pustules of Kogoj (Lever and Schaumburg-Lever, 1983) which together with Munro's abscesses are highly diagnostic of psoriasis. Development of this epidermal histopathology is preceded by changes in the dermal microvasculature, most notably enhanced dilatation and tortuosity of the increased number of dermal capillaries, which coil upwards in the papillae towards the epidermis. The repeated abrupt and sudden exocytosis from the convoluted capillaries of the elongated papillae ('squirting papillae') gives rise to an oedematous infiltrate composed of lymphocytes, neutrophils, monocytes and macrophages. These cells migrate into the epidermis where neutrophils

become incorporated into abscesses and pustules, leaving an infiltrate of the remaining cells in the superficial dermis and lower half of the epidermis.

Psoriasis exists in several different morphological forms. Although each of these will display a varying histological profile, the above description presents an overview of the microscopic dermal and epidermal changes accompanying the development of a lesion. The morphological variants are;

Chronic plaque psoriasis

This is the most common form, also known as psoriasis vulgaris, affecting some 90% of psoriatic patients. It is characterized by sharply defined erythematous squamous plaques usually distributed fairly symmetrically and most commonly affecting the knees, elbows and lumbar region. The size of the lesion varies from coin-sized (nummular) to large assemblies of coalescent lesions (psoriasis geographica).

Guttate psoriasis

This form describes the shower of small 'drop-like' lesions distributed over most of the body surface, particularly the trunk and limbs. It is most commonly seen in children, often following an episode of stress or a streptococcal throat infection, and usually resolves with minimal therapy in the course of six to twelve weeks.

Pustular psoriasis

This clinical manifestation involves the eruption of sterile, superficial pustules resulting from neutrophil accumulation, often in association with psoriatic lesions and causing severe disability. Two forms may be distinguished; the localized variant is usually limited to the palms and soles (palmoplantar pustulosis) whereas a widespread form of the less common generalized type affects the entire body surface. The latter entity (von Zumbusch psoriasis) is one of the most severe and disabling forms of psoriasis.

Erythrodermic psoriasis

This exfoliative form involves the entire skin surface, with generalized erythema and scaling replacing the characteristic psoriatic lesion. It may lead to systemic complications, notably thermal irregularity, dehydration, protein loss with renal and cardiac failure in extreme cases.

The appearance of various clinical manifestations may be modified at certain anatomical locations and consequently be classified accordingly. Examples include flexural, palmoplantar and seborrhoeic psoriasis. Extracutaneous manifestations may also affect the nails, mucosal membranes and joints. The latter variant, psoriatic arthritis, is a frequent complication of psoriasis and may occur in the absence of cutaneous lesions. Typically affecting the distal interphalangeal joints and less frequently the spine and sacroiliac joints, it is regarded as a specific disease entity as opposed to a variant of rheumatoid arthritis.

As previously mentioned, the entire skin is potentially abnormal in psoriatic patients and as such even symptomless skin may be histologically and biochemically involved (Farber *et al*, 1985). Increased DNA synthesis, capillary dilatation, dermal lymphocytic infiltration with activated T helper and suppressor cells, and abnormal arachidonic acid metabolism are all features of clinically uninvolved (nonlesional) as well as involved (lesional) psoriatic epidermis.

1.2.4 Pathogenesis of psoriasis

That psoriasis is an inflammatory and epidermoproliferative disorder is undisputed. The subject of debate is whether the condition is primarily vascular and inflammatory with secondary epidermal alterations or whether the dermal inflammatory changes are secondary to an initial epidermal hyperplasia. As early as 1896, Unna in his textbook *Histopathology of Skin Diseases* described the inflammation and hyperproliferation associated with psoriasis but was undecided as to which was the primary event. Almost 100

years later, there are still two schools of thought regarding the primary pathogenic event.

1.2.4.1 Proliferative aspects

Most of the clinical features of psoriasis can be attributed to the epidermal hyperplasia and perhaps for this reason the principal force of research was initially directed at this event. The investigations of van Scott and Ekel (1963) reported a 27-fold increase in the mitotic rate of psoriatic keratinocytes together with a decreased epidermal turnover time as compared to normal skin. An uncontrolled cellular proliferation of epidermal cells was therefore regarded as the primary disorder in psoriasis and concomitantly, anti-mitotic drugs a beneficial treatment modality. Several investigators (Weinstein and Frost, 1968; Weinstein and McCullough, 1973) associated the increased mitosis and shortened transit times to decreased cell cycle times. More recent work, however, suggests that the increased epidermal turnover in psoriasis is not due to any major alteration in the cell cycle time, but is the result of a larger proliferative cell population (germinative compartment) and an increase in the proportion of these cells recruited to the active cycling phase (Bauer, 1986). Moreover, increased mitosis *per se* cannot account for the histological features of psoriasis since similar mitotic counts are also observed in certain other skin disorders which do not develop psoriatic lesions.

1.2.4.2 Inflammatory aspects

A feature of psoriasis not explained by the rapid epidermal turnover is inflammation. The earliest histological changes consist of transepidermal migration of inflammatory cells originating from dermal, perivascular infiltrates when epidermal proliferation is only present to a minor degree (Braun-Falco and Schmoeckel, 1977; Chowaniec *et al*, 1981). Accordingly, the last decade has seen a resurgence of interest in the inflammatory aspects of the disease in order to assess its pathogenic significance. One of the most prominent features of the psoriatic lesion is the accumulation of polymorphonuclear leucocytes (PMNL's) in the upper regions of the epidermis where they form characteristic Munro's microabscesses and spongioform

pustules (Ragaz and Ackerman, 1979). Attempts to elucidate the mechanisms underlying this process, in particular the local production of neutrophil chemoattractants, have produced some interesting observations. The pioneering work of Hammarstrom *et al* (1975) first introduced the possibility that altered arachidonic acid (AA) metabolism may play a possible role in the pathogenesis of psoriasis. These investigators demonstrated an abnormally high level of free AA and 12-HETE in keratome slices of psoriatic lesions, with only modest elevations in PGE₂ and PGF_{2α} levels, compared to uninvolved epidermis. An increased phospholipase A₂ activity has been associated with the elevated AA levels (Foster *et al*, 1983) whilst the apparent deficiency in the cyclooxygenase (CO) system has been attributed to the presence of an endogenous CO inhibitor in psoriatic plaques (Penneys *et al*, 1975). Reduction of AA metabolism *via* the CO pathway would be expected to divert the substrate to the alternative lipoxygenase pathways. The greatly increased 12-HETE levels in psoriatic lesions complies with this scenario. Additionally, elevated and biologically active levels of leukotriene B₄ (LTB₄) have been detected in scale and chamber fluid extracts from abraded psoriatic lesions by Brain *et al* (1982b, 1984a and 1984b). Ziboh *et al* (1984), subsequently demonstrated increased 5-LO activity in enzyme preparations from involved, compared to uninvolved, psoriatic epidermis. The pathophysiological significance of these observations lies in the fact that both 12-HETE and LTB₄ are potent neutrophil chemoattractants and could therefore play a role in eliciting the neutrophil infiltrates seen in psoriasis. Although the chemoattractant potency of LTB₄ is far greater than that of 12-HETE, the presence of the latter in correspondingly larger amounts suggests that both these mediators may be of equal importance. Recent studies have also shown that psoriatic 12-HETE is not stereochemically identical to platelet 12-(S)-HETE (Woollard, 1986) as previously assumed, and that psoriatic 12-(R)-HETE is a more potent stimulant of leukocyte chemokinesis than its stereoisomer (Cunningham *et al*, 1986). Topical application of nanomolar doses of LTB₄ to normal skin causes erythema and swelling characterized histologically by intraepidermal neutrophil microabscesses (Camp *et al*, 1984). This reaction is less pronounced following application of 12-HETE (Dowd *et al*, 1985).

However, since neither LTB₄ nor racemic 12-HETE elicit the lesions of psoriasis they are unlikely to be the primary modulators of the pathogenesis of psoriasis. Equally, if the major source of LTB₄ is the infiltrating neutrophil as opposed to resident keratinocytes, it cannot be invoked as the chemotactic factor responsible for the initial invasion. This has yet to be unequivocally determined and therefore the current understanding that 12-HETE is synthesized by epidermis but not by neutrophils makes it a more likely candidate mediator for the preliminary cellular invasion. The generation of 15-HETE, a metabolite of the 15-LO pathway which has been shown to inhibit the activities of epidermal 5- and 12-LO, is also significantly reduced in uninvolved psoriatic epidermis (Kragballe *et al*, 1986b) suggesting that one of the endogenous systems controlling the formation of inflammatory eicosanoids may be defective. The chemotactic responses of mononuclear and polymorphonuclear cells are also reported to be enhanced in moderate and severe psoriasis (Ternowitz *et al*, 1986; Wahba *et al*, 1978). Thus, both the abnormalities of cellular chemotactic response and presence of chemoattractant factors in the epidermis may be of importance in the pathogenesis of psoriasis.

Other noneicosanoid chemoattractants such as platelet-activating factor (Mallet and Cunningham, 1985), complement (Schroder and Christophers, 1986) and an interleukin-1-like cytokine (Fincham *et al*, 1988) have also been implicated in psoriasis. The presence of the latter mediator together with the effectiveness of cyclosporin A in psoriasis (Ellis *et al*, 1986b) has implications for the involvement of T lymphocyte-mediated immune mechanisms in the disease process (Valdimarsson *et al*, 1986). The preceding discussion has however pertained to the role of eicosanoid chemotactic factors in the pathogenesis of psoriasis, with a view to pharmacological intervention by drugs which affect arachidonic acid metabolism.

1.2.5 Treatments for psoriasis

One hundred years ago the most effective remedy for psoriasis was arsenic taken orally (Fry, 1988). Other oral treatments during this period included mercury, phosphorus and potassium iodide, whilst topical preparations

comprised of turpentine, ammoniated mercury, pyrogallic acid, thymol, β -naphthol, coal tar and chrysarobin. Although this vast range of antipsoriatic therapy has been somewhat modified for today's psoriatic patient, it has hardly diminished in number and is perhaps indicative of our ignorance concerning the aetiology of psoriasis. Most of the currently available therapeutic regimens have been based on empirical observations and are aimed at controlling only one aspect - that of epidermal hyperproliferation. Despite such a wide array of therapy, no current drug treatment is able to induce a permanent remission or provide a truly safe and effective amelioration without the attendant side effects.

1.2.5.1 Antiproliferative approaches

The proliferative nature of psoriasis has prompted the therapeutic use of a number of topical and systemic antiproliferative agents. Topical therapy offers the advantage of direct drug access to the diseased skin thus minimizing unwanted systemic effects and represents a fundamental approach to the treatment of psoriasis. It includes traditional treatments such as dithranol and coal tar as well as the more cosmetically acceptable PUVA and corticosteroid regimens, of which the latter may also be helpful in suppressing the inflammatory aspects of the disease. Systemic treatments such as methotrexate and the retinoids are usually reserved for severe forms and certain clinical variants of psoriasis which are not amenable to topical treatment since they are associated with greater hazards.

Dithranol

Dithranol or Anthralin is a descendant of chrysarobin, an active ingredient of the antifungal 'Goa powder' imported by the Portuguese into India *via* Goa, and found to be effective for psoriasis following misdiagnosis (Squire, 1876). One of the most long standing and effective topical antipsoriatic remedies currently available for chronic plaque psoriasis, its popularity is restricted owing to the staining of skin and clothing and contact irritation of the surrounding uninvolved skin. Patient compliance has however been aided by the advent of short contact therapy comprising shorter exposure periods of

higher dithranol concentrations (Schaefer, 1980). The oxidative formation of highly reactive free radical intermediates is thought to be responsible for both its clinical activity and skin irritancy. Dithranol is known to interfere with various cellular processes including mitochondrial function (Ashton *et al*, 1983) and consequently its clinical antiproliferative effect may be associated with modulation of these processes.

Corticosteroids

Although the proven therapeutic benefit and cosmetic acceptability of topical corticosteroids renders them particularly attractive for the management of psoriasis, their long-term clinical use is severely limited by well documented side-effects. These include skin atrophy, spontaneous bruising and striae formation. Rebound or destabilization of psoriasis following withdrawal of treatment and tachyphylaxis are also well recognized, as is adrenal suppression following systemic absorption. The correlation between steroid potency and antipsoriatic effect is also reciprocated with side-effects. Their mode of action may involve several independent mechanisms such as reduction of DNA synthesis and epidermal proliferation (Fisher and Maibach, 1971), suppression of the synthesis of inflammatory mediators *via* the reduction of phospholipase A₂ activity (Hong and Levine, 1976), and modulation of the immunocompetent cell population (Fauci, 1979).

Coal Tar

Although coal tar alone does have an antipsoriatic effect, it is most commonly used synergistically in combination with ultraviolet-B light in the Goeckerman regimen. The unpleasant physical properties of tar and the prolonged nature of the treatment restrict it to inpatient use. The theoretical increased risk of skin malignancies with topical use of tars does not appear to be reflected in clinical practice but imposes a need for caution.

Photochemotherapy (PUVA)

The beneficial effect of sunlight on psoriasis has already been mentioned. Similarly, utilization of artificial ultraviolet radiation particularly as an adjunct to other treatments, for example in the Goeckerman regimen, has been well established. PUVA describes either the topical or oral administration of psoralens (P) followed by exposure to long-wave ultraviolet radiation (UV-A). Psoralens such as 8-methoxypsoralen are photoactivated to form DNA adducts which produce a dose-dependent temporary inhibition of DNA synthesis and cell proliferation. An immunomodulatory effect of PUVA may also partly be responsible for its antipsoriatic activity. Although undoubtedly an effective and established treatment for psoriasis which is also acceptable to patients, serious reservations concerning its long-term safety with respect to premature ageing, carcinogenicity and cataract formation still exist.

Methotrexate

This cytostatic agent is an inhibitor of the enzyme dihydrofolate reductase which is essential for the synthesis of certain pyrimidine and purine precursors of nucleic acid biosynthesis, suppression of which results in impaired protein synthesis and consequently cytostasis. Despite its long standing and valuable role in the management of severe and disabling psoriasis, its potential to cause hepatotoxicity resulting in fibrosis and cirrhosis remains a long-term concern and necessitates serial liver biopsies in patients receiving prolonged treatment.

Retinoids

The retinoids are a group of vitamin A derivatives of which etretinate has found a use in the treatment of psoriasis, particularly pustular variants. The initial enthusiasm for this drug has diminished in light of its potential hazards, most notably teratogenicity but also hepatotoxicity, skeletal damage and abnormal lipid metabolism. The risk of these adverse effects is potentiated by its protracted 120 day half-life.

Vitamin D₃

Several recent reports have indicated that the biologically active metabolite of vitamin D, 1,25-dihydroxyvitamin D₃ and its analogues may be useful for the treatment of psoriasis following oral or topical administration (Kato *et al*, 1986; Morimoto *et al*, 1986; Smith *et al*, 1988). The existence of vitamin D₃ receptors on epidermal cell membranes, and the observation of dose-dependent reduction of proliferation and induction of terminal differentiation of cultured keratinocytes in the presence of vitamin D₃ (Smith *et al*, 1986) has provided further impetus to this research. The long-term therapeutic benefit of this therapy has however been questioned in light of the potential risks of vitamin D₃ toxicity.

Cyclosporin

Cyclosporin is an immunosuppressive agent which has been reported to have a beneficial effect in psoriasis (Griffiths *et al*, 1986; Meuller and Hermann, 1979). Although its precise mechanism of antipsoriatic action is not understood, several theories have been postulated (Bos, 1988) including suppression of T helper lymphocytes which are thought to be activated in psoriatic epidermis. Adverse effects such as nephrotoxicity and hypertension which are also seen in organ transplant patients in whom cyclosporin is normally used are expected to limit its use.

1.2.5.2 Anti-inflammatory approaches

One of the characteristic biochemical abnormalities of psoriatic skin is altered arachidonic acid metabolism. Recognition of this has provided an alternative target for therapeutic intervention and in recent years has prompted attempts to inhibit the generation of pro-inflammatory lipoygenase products which are markedly elevated in the psoriatic lesion and considered to play a role in the pathogenesis of the disease.

1.2.5.2.1 Dietary manipulation

Consistent with this approach is dietary modulation of arachidonic acid metabolism. Epidemiological studies have shown a lower prevalence of inflammatory disorders in populations who consume large amounts of fish oils (Kromann and Green, 1980). This may be of significance since fish oils are an important source of eicosapentaenoic acid (EPA), an unsaturated fatty acid which competes with arachidonic acid as a substrate for the CO and LO pathways. Transformation of EPA *via* these pathways results in the generation of less potent eicosanoids (Prescott, 1984; Terano *et al*, 1984). In contrast, docosahexaenoic acid (DCHA) only appears to be a competitive inhibitor of AA for the CO pathway (Corey *et al*, 1983), possibly diverting AA metabolism towards the LO pathway. High EPA/DCHA ratios in epidermal tissue have been correlated with a clinical improvement in psoriasis whereas low EPA/DCHA ratios have been associated with nonclearance of lesions (Ziboh *et al*, 1986). Similarly, a diet rich in linoleic acid and dihomo γ -linoleic acid derived from vegetable seed oils may also improve psoriasis by manipulation of AA metabolism.

1.2.5.2.2 Non-steroidal anti-inflammatory agents

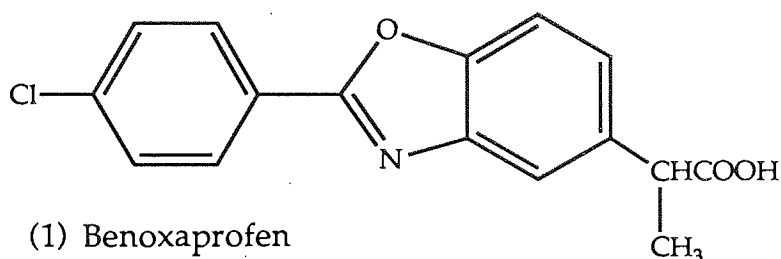
NSAIDs are amongst the most widely used drugs in man. Vane's hypothesis that NSAIDs owed their anti-inflammatory activity, at least in part, to the inhibition of enzymatic transformation of arachidonic acid to its pro-inflammatory prostaglandin metabolites has become well established (Vane, 1971). Specifically, suppression of prostaglandin synthesis by NSAIDs is the result of cyclooxygenase inhibition. Such compounds do not arrest leukocyte accumulation associated with inflammation probably due to their inability to prevent formation of chemotactic lipoxygenase products. It has therefore become increasingly evident that suppression of the second main pathway of arachidonic acid metabolism, the lipoxygenase pathway, is equally important in contributing to anti-inflammatory activity. Dual inhibitors may be of even greater therapeutic value, since the complexity of the AA cascade means that depression of one pathway is often compensated by substrate diversion to another.

Cyclooxygenase inhibitors

Despite their potent anti-inflammatory activity and widespread use in rheumatological disorders, cyclooxygenase inhibitors have not found a useful place in the treatment of inflammatory dermatoses, suggesting that prostaglandins *per se* contribute little to such disorders. An exception is sunburn or ultraviolet B-induced erythema, where the elevation of PGE₂ levels during the early phase of the reaction may be inhibited by the cyclooxygenase inhibitor indomethacin with a concurrent reduction in the inflammatory reaction (Kobza Black *et al*, 1978). The experience with cyclooxygenase inhibitors in this model inflammatory reaction, which is also used as an assay for their evaluation, is however not translated to clinical inflammatory skin disease. By contrast, cyclooxygenase inhibitors have been reported to aggravate a number of dermatoses including idiopathic urticaria and dermatitis herpetiformis (Griffiths *et al*, 1985) although studies suggesting indomethacin induced exacerbation of psoriasis (Ellis *et al*, 1983; Katayama and Kawada, 1981) remain controversial (Green and Shuster, 1987).

Lipoxygenase inhibitors

Substantial evidence exists for the role of lipoxygenase products as mediators of inflammation, not only in psoriasis but other skin diseases such as allergic contact dermatitis (Barr *et al*, 1984) and atopic dermatitis (Ruzicka *et al*, 1986). Further support for the pathogenic significance of these mediators in inflammatory dermatoses, particularly psoriasis, appeared to be provided by the NSAID, benoxaprofen (1).



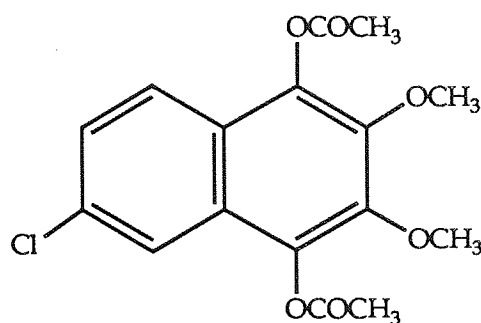
In 1977, Cashin and co-workers (Cashin *et al*, 1977) reported the unusual pharmacological profile of this novel NSAID, as demonstrated by its potent anti-inflammatory effect yet weak cyclooxygenase inhibitory activity. It was subsequently reported to be an inhibitor of arachidonate lipoxygenase in isolated leukocytes (Harvey *et al*, 1979; Walker and Dawson, 1979) suggesting that it differed significantly in its mode of action from other NSAIDs.

The chance finding of improvement in psoriatic skin lesions during use as an anti-inflammatory agent in rheumatoid patients led to an open study (Allen and Littlewood, 1982), which reported the beneficial effect of benoxaprofen in severe psoriasis. The effectiveness of benoxaprofen was substantiated in further controlled studies (Allen and Littlewood, 1983; Kragballe and Herlin, 1983), the latter report indicating substantial improvement in 75% of patients receiving oral treatment. These investigations demonstrated the effectiveness of benoxaprofen in various grades of psoriasis as well as palmoplantar pustulosis (Fenton and Wilkinson, 1982). In view of the earlier reports on the mode of action of benoxaprofen, its therapeutic efficacy in psoriasis was

attributed to 5-lipoxygenase inhibition which further encouraged support for the pathogenetic role of lipoxygenase products in the disorder. Later studies have, however, questioned the drug's 5-lipoxygenase inhibitory activity since it does not appear to effectively inhibit the enzyme in *in vitro* (Masters and McMillan, 1984) or *in vivo* (Salmon *et al*, 1984) systems. In addition to psoriasis, cystic acne and nodular prurigo which are typified by neutrophil infiltration and epidermal hyperplasia have also been shown to respond to benoxaprofen therapy in case reports (Hindson *et al*, 1982a and 1982b) although it is not known whether these conditions are also characterized by elevated leukotriene levels. The ability of benoxaprofen to impede the migration of monocytes into sites of inflammation possibly by suppressing their chemotactic response (Meacock *et al*, 1979) may also contribute to its antipsoriatic action, since these features are enhanced in patients with psoriasis (Czarnetzki, 1985). Interestingly, a normalization of *in vitro* monocyte chemotaxis in patients receiving benoxaprofen has been demonstrated prior to clinical resolution of the lesions (Kragballe *et al*, 1985). During the course of its use as an antiarthritic agent, a high incidence of side-effects especially photosensitivity, onycholysis and hepatotoxicity as well as a number of fatalities, particularly in elderly patients suffering from renal or hepatic failure resulted in its withdrawal from clinical use in 1982. Disappointingly, the therapeutic mechanism of one of the most effective drugs in psoriasis therefore remains unresolved.

Efforts to develop lipoxygenase inhibitors, primarily targeted towards asthma and arthritis, initially proved to be disappointing with many contenders failing because of low efficacy or toxicity, however several interesting compounds are still under evaluation.

The chloronaphthalene derivative lonapalene (2) (Jones *et al*, 1986) is a selective and potent inhibitor of human PMN 5-lipoxygenase with negligible inhibitory activity against cyclooxygenase or 12-lipoxygenase. In a trial in Finland, topical lonapalene (0.5%) and fluocinolone acetonide (0.025%) were found to be equally effective in the treatment of chronic plaque psoriasis, although some patients experienced local irritation (Lassus and Forstrom, 1985). Clinical improvement has also been associated with a selective decrease of LTB₄ in lesional skin (Camp *et al* 1988).



(2) Lonapalene

Certain established antipsoriatic therapies have also been shown to possess lipoxygenase inhibitory activity. Examples include dithranol which selectively inhibits the 12-lipoxygenase of mouse epidermal cells (Bedford *et al*, 1982) and several retinoids which suppress the generation of LTB₄ by rat leukocytes (Bray, 1984). However, the *in vivo* 5-lipoxygenase inhibiting properties of these drugs in psoriasis have yet to be confirmed.

Recently the potent *in vitro* 5-LO inhibitor, R 68 151, was found to significantly reduce the scaling and erythema associated with psoriatic lesions following topical application in a controlled study (Degreef *et al*, 1990). The orally inactive 5-LO inhibitors L-651 392 and L-651 896, aimed at topical application for psoriasis, have also been investigated in animal models of epidermal hyperproliferation (Chan *et al*, 1987). It should also be noted that *in vitro* lipoxygenase inhibitory activity does not always confer antipsoriatic activity as demonstrated by the example of nordihydroguaiaretic acid (NDGA). NDGA is an antioxidant of plant origin which has also been shown to inhibit the 5-LO

enzyme (Bokoch and Reed, 1981), however during an evaluation of its topical antipsoriatic activity it did not display any such effect (Newton *et al*, 1988). Whether the absence of a clinical response was also associated with a lack of *in vivo* pharmacological activity was not established.

Leukotriene antagonists

An alternative approach to the regulation of chemotactic inflammatory mediators would be to design specific antagonists for these eicosanoids. Several such compounds have been synthesized by the systematic modification of the natural agonist¹. These are still under evaluation and as yet no reports of their clinical activity in psoriasis have emerged.

1.3 STRATEGIES FOR THE DEVELOPMENT OF NOVEL ANTIPSORIATIC AGENTS

The treatment of psoriasis remains palliative, providing only temporary remission from an often interminable disease which has been recognized since biblical times. The chronic nature of the condition means that treatment may correspondingly continue for several decades thus potentiating the drawbacks of currently available therapies and reiterating the need for safe and effective therapeutic agents.

Benoxaprofen was undoubtedly one of the most interesting NSAIDs to have emerged in the last decade, setting an important precedent in the treatment of psoriasis and attempting to fill the void that exists in the therapeutics of inflammatory dermatoses by this group of drugs. The nature of the pharmacological action responsible for its remarkable antipsoriatic activity unfortunately remains unresolved, hampering the development of safer analogues. However, one fact is clear whatever the mechanism of action; the systemic toxicity of such drugs needs to be minimized without compromising their efficacy.

¹ Update on Leukotriene Research. (Proceedings of the Society for Drug Research Symposium on Leukotrienes), *Pharm J*, 244 (1990) 203

1.3.1 The soft drug approach

Various strategies are available to the drug designer to achieve this goal. Amongst these is the design of "soft-drugs", defined as biologically active, therapeutic chemical compounds (drugs) characterized by a predictable and controllable *in vivo* destruction (metabolism) to inactive non-toxic moieties, once their therapeutic role is achieved. This concept was introduced by Bodor (1982) as a means of designing safe and effective drugs; the essence of which is to direct the metabolism-elimination of a drug towards a more predictable route. Incorporation of a metabolically sensitive handle into the molecule which is the preferential route for a one-step controllable deactivation not involving highly reactive intermediates, is one way of achieving such a goal.

One of the best examples of a topical soft drug is that of the corticosteroid fluocortin butyl ester (FCB), which utilizes the skin's natural metabolizing capacity to minimize systemic availability and therefore toxicity of the active parent drug (Kapp, 1977). Figure 1.3 shows the main biotransformation pathways of fluocortin butyl ester in humans. Ester hydrolysis which is initiated in the skin leads to the formation of locally and systemically inactive metabolites. Inactivation as a result of the very first biotransformation step distinguishes FCB from other corticosteroid esters of similar structure and is therefore especially advantageous in those particularly susceptible to their adverse effects such as infants, the elderly and pregnant women.

With respect to the design of *soft* NSAIDs, a group of 2-aryloxazopyridines (Figure 1.4) have shown promise toward this approach. Several members in this series are comparable to indomethacin as cyclooxygenase inhibitors *in vitro*, and as topical anti-inflammatory agents in certain *in vivo* assays. However, when given orally or parentally, these compounds are devoid of activity and toxicity as a result of their facile *in vivo* metabolic inactivation (Coombs *et al*, 1973; Shen, 1977).

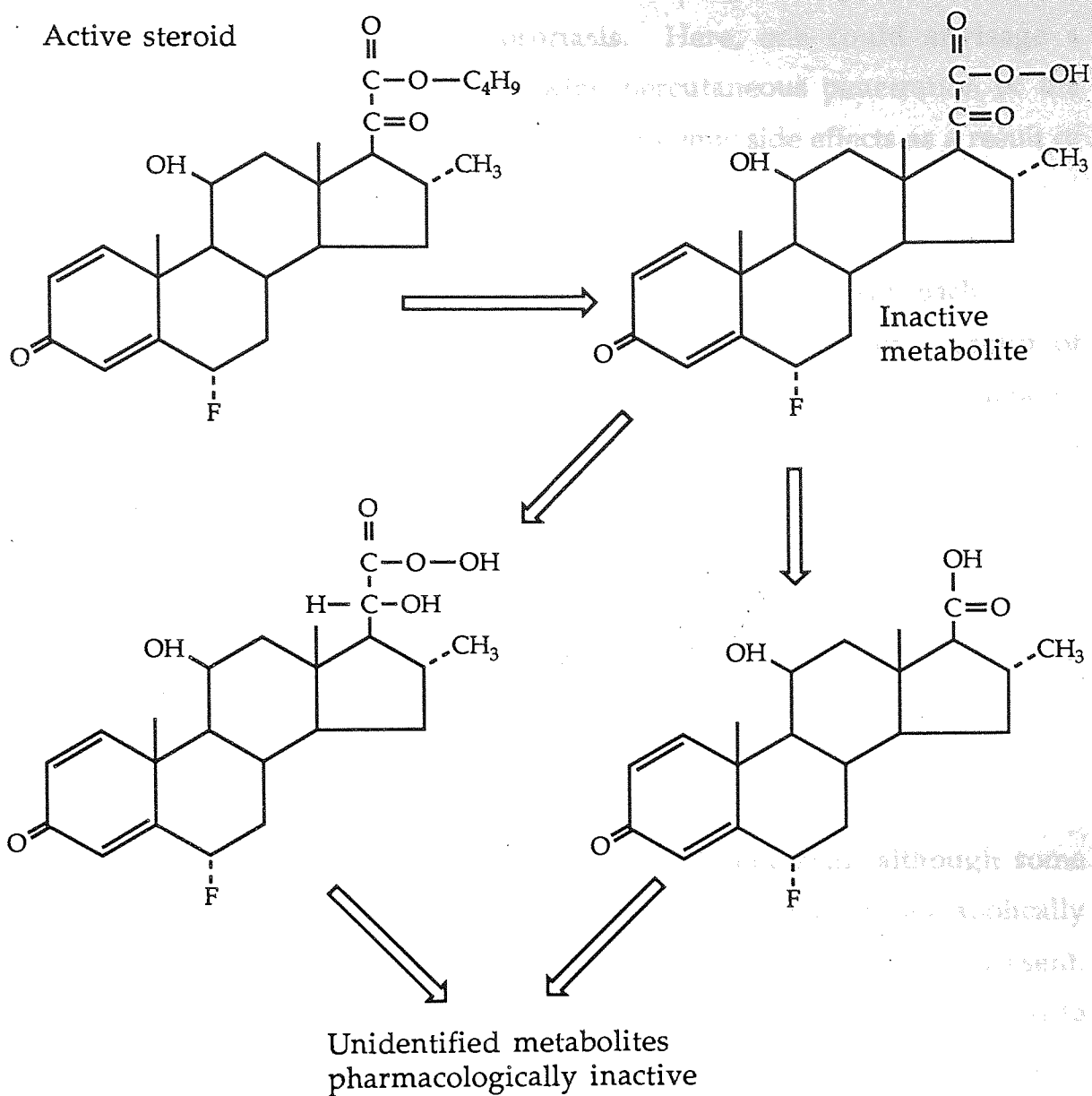


Figure 1.3 Biotransformation of Fluocortin-butylester in man (Herz-Hübner, 1977; Mützel, 1976)

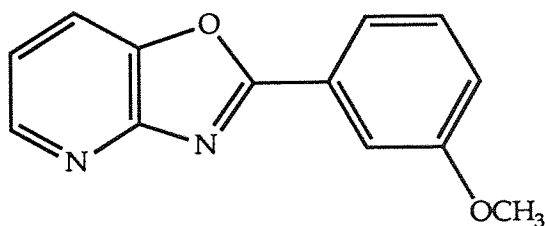


Figure 1.4 Example of a 2-aryloxazolo[5,4-b]pyridine type NSAID.

The soft drug approach could be utilized in the design of topical NSAIDs for inflammatory dermatoses such as psoriasis. Here, one could envisage a localized anti-inflammatory effect following percutaneous penetration of the soft drug to the diseased site in the absence of systemic side effects as a result of subsequent cutaneous or systemic detoxification.

1.3.2 Non-steroidal anti-inflammatory drugs and the soft drug approach

Non-steroidal anti-inflammatory drugs (NSAIDs) are a diverse group of chemically heterogeneous compounds which share similar therapeutic actions, namely, anti-inflammatory, analgesic and antipyretic activity through a common pharmacological mode of action. They may be classified chemically according to Figure 1.5. The arylalkanoic acids represent the largest and most successful group of NSAIDs and include amongst their ranks the widely prescribed ibuprofen (3) and naproxen (4). The basic structural features are an aromatic ring which has both a hydrophobic and a polar substituent (Figure 1.6).

The polar substituent is usually an acetic or α -propionic acid, although some carboxyl derivatives such as esters and amides which may be metabolically converted to the active carboxylic acid side chain may also be present. Depending on the nature of the polar substituent, they may also be referred to as arylacetic or arylpropionic acids. Quantitative structure-activity relationships including conformational studies of NSAIDs have been extensively reviewed by Gund and Jensen (1983). The propionic acid side chain possesses an asymmetric centre, the α -carbon atom, and anti-inflammatory activity has been associated with the S (+) isomer (Shen, 1981). Studies have also revealed that this group of NSAIDs may undergo a stereoselective inversion of the R (-) to the pharmacologically more active S (+) isomer *in vivo*. The presence of a hydrogen atom on the α -carbon atom also appears to be necessary for activity (Juby, 1972; Smeyers *et al*, 1985).

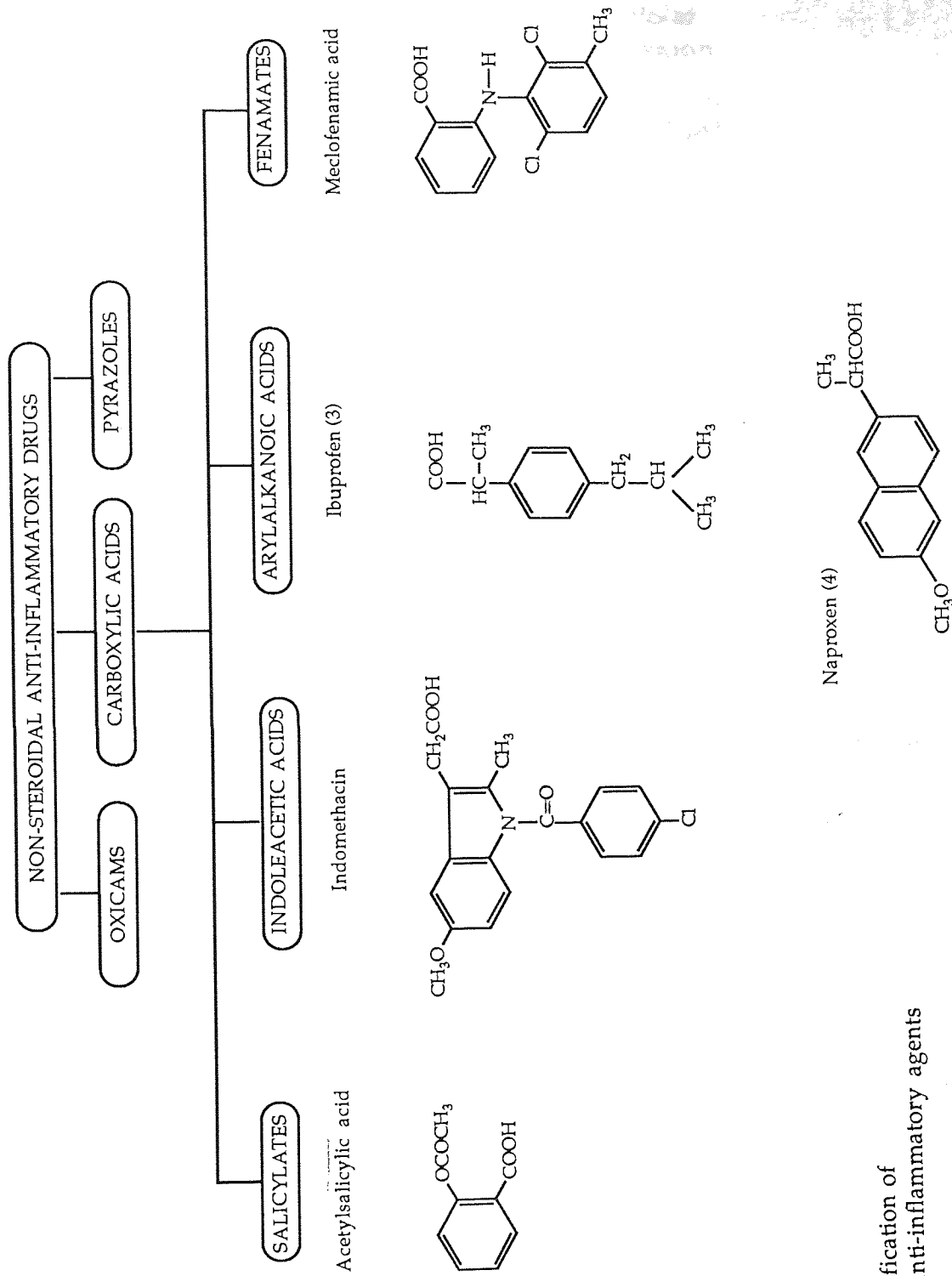
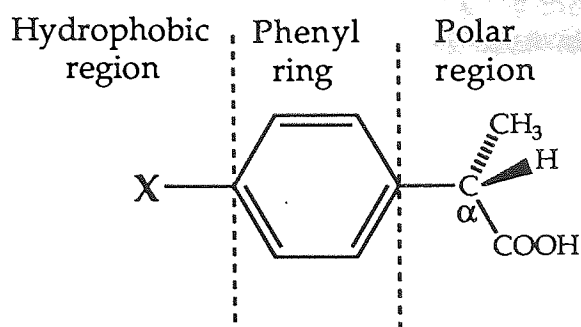


Figure 1.5
 Chemical classification of
 non-steroidal anti-inflammatory agents

Figure 1.6 Basic structural features of an arylpropionic acid type NSAID.

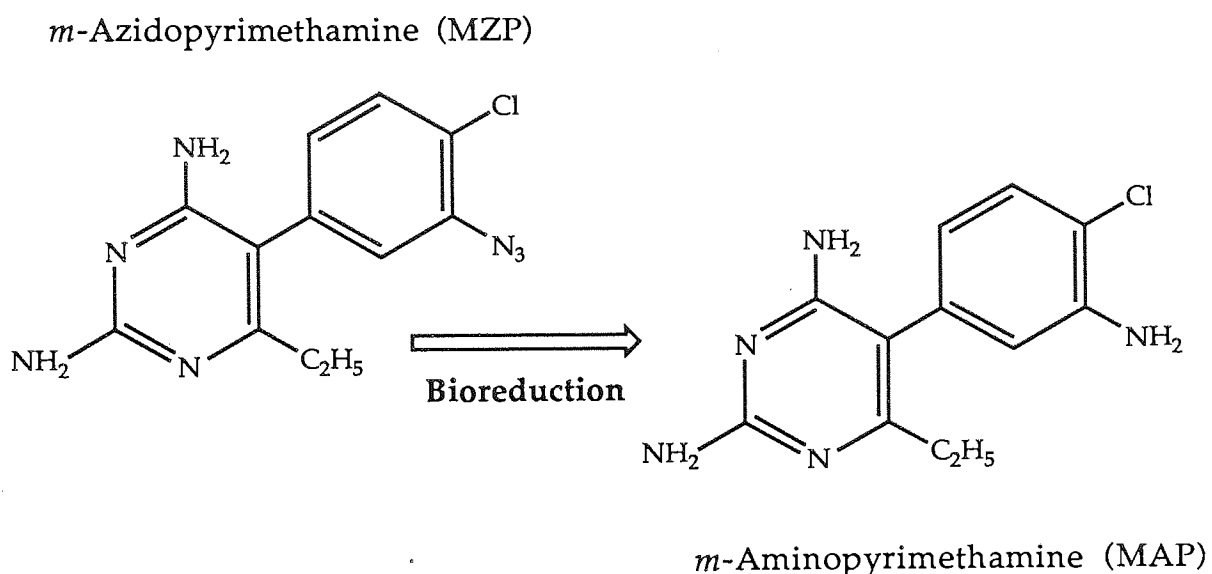


In contrast, the nature of the hydrophobic substituent shows substantial variation. It is usually a less rigid aliphatic or alicyclic residue which is able to adopt a non-planar configuration. Strategies involving modification of this hydrophobic residue could form the basis for the design of a soft drug, where biotransformation would yield an inactive, polar species ensuring rapid inactivation and elimination.

Several arylalkanoic acids, including benoxaprofen, the most promising anti-psoriatic member of the group contain a *p*-chlorophenyl residue in the hydrophobic region. The azido-substituent (N₃) has certain properties such as lipophilicity and electronic characteristics in common with halogen atoms *e.g.*, the chloro group, and for this reason is frequently referred to as a *pseudohalide*. Studies with dihydrofolate reductase inhibitors have demonstrated that the azido residue can be substituted for a chloro group without a dramatic reduction in activity or change in isosteric configuration (Griffin, personal communication). Interest in the azido functionality is further accentuated by the suggestion that incorporation of this group into a drug molecule may also provide a means of bioinactivation (Stevens *et al*, 1987), a prerequisite of the soft drug approach. Aryl azides are susceptible to thiol-mediated chemical reduction to the corresponding amine under physiological conditions (Staros *et al*, 1978), a process which has also been shown to occur *in vivo* (Bliss *et al*, 1979) either enzymatically or chemically *via* endogenous thiols. In addition, the novel lipophilic antifolate, *m*-azidopyrimethamine (MZP), an experimental antitumour and potential antipsoriatic agent, has been shown to

undergo bioreductive transformation to the more polar and inactive arylamine, *m*-aminopyrimethamine (MAP) *in vitro* in murine tissues (Kamali *et al*, 1988) and *in vivo* in mice (Slack *et al*, 1986) as illustrated in Fig.1.7.

Figure 1.7 The bioreduction of MZP to MAP as its postulated inactivation mechanism



This bioreduction has been postulated as an inactivation mechanism responsible for the relatively short biological half-life of MZP compared to its analogue metoprin. In support of this view are the observations that MAP has a diminished dihydrofolate reductase inhibitory activity compared to MZP and is also devoid of antitumour activity *in vivo* (Griffin, personal communication); its increased polarity compared to the parent azide would also be expected to aid rapid elimination from the body. The short half-life of MZP and thus the possibility of reduced toxicity, by design, demonstrates the utility of aromatic azides as soft drugs.

1.3.3 Azidoprofen

Extension of this concept to NSAIDs has led to the development of azidoprofen [2-(4-azidophenyl)propionic acid; AZP; 5], a model azido-substituted NSAID, where the hydrophobic residue common to arylalkanoic acids is replaced with an azido moiety; rendering it susceptible to bioinactivation (Figure.1.8). AZP was synthesized by reduction of the corresponding nitro compound, followed by diazotization and azidation of the resultant amine analogue (Griffin, unpublished results). The sodium salt (AZP-Na) and a series of ester derivatives have also been prepared to overcome low aqueous solubility problems and to provide a range of lipophilicities respectively.

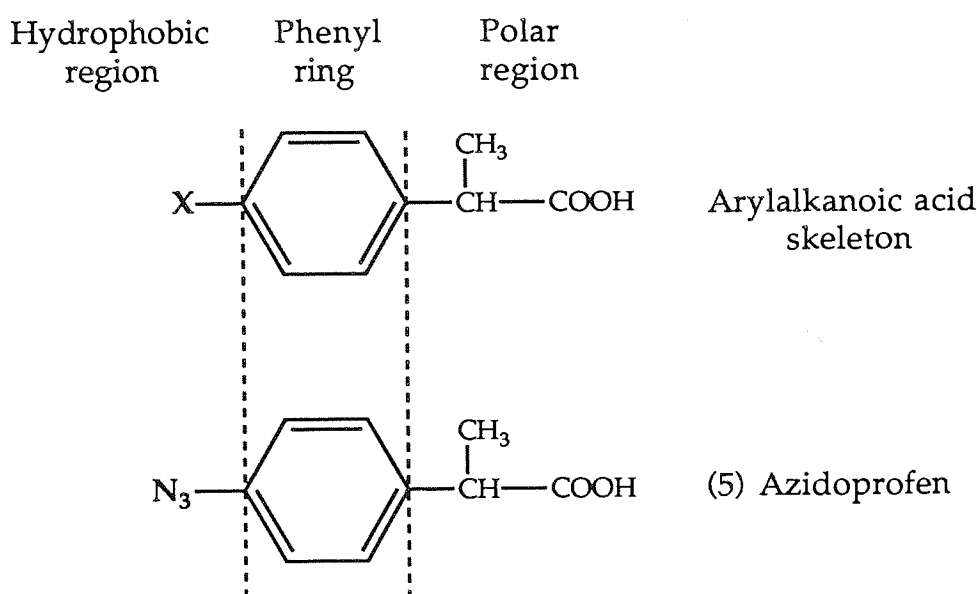


Figure 1.8 Schematic representation of azidoprofen, a model azido-substituted arylalkanoic acid.

Azidoprofen and its analogues may therefore be considered to represent model compounds incorporating both potential anti-inflammatory activity and a metabolically labile azido 'hot-spot', enabling assessment of the soft drug approach in controlling their pharmacokinetic profile. In this context, the previously described scenario of topical NSAID soft drugs may be further extrapolated to include an azido-substituted NSAID which after eliciting a topical anti-inflammatory response may be expected to undergo cutaneous or

systemic bioreduction to the inactive and polar amine metabolite, ensuring rapid elimination and minimal side-effects.

1.4 AIMS AND OBJECTIVES OF PRESENT STUDY

Implicit in the design of topical NSAID soft drugs is the requirement for such compounds to *penetrate the skin* to produce a localized therapeutic response, followed by *biotransformation* to yield inactive, non-toxic metabolites. The overall aim of this project was therefore to investigate the potential role of azides as topical soft drugs with respect to both these requirements; using AZP and related ester analogues as model compounds, which were synthesized for the purpose of this study. The first objective was to examine the degradation kinetics of these compounds under a range of conditions using an *in vitro* model developed for the preliminary assessment of this proposed reductive detoxification mechanism for aromatic azides. Secondly, to monitor the susceptibilities of the ester analogues towards chemical and enzymatic activation, which regenerate the active parent acid. Finally, to assess the role of the azido group in the control of topical delivery by a study of *in vitro* and *in vivo* percutaneous penetration and the factors influencing this process.

CHAPTER TWO
ASSAY PROCEDURES FOR AZIDOPROFEN AND RELATED COMPOUNDS

2.1 MATERIALS

2-(4-azidophenyl)propionic acid [azidoprofen; AZP], 2-(4-aminophenyl)propionic acid [aminoprofen; AMP] and a series of corresponding esterified analogues were synthesized by Dr R J Griffin, Pharmaceutical Sciences Institute, Aston University. The structural formulae of these compounds which formed the basis of this study are illustrated in Figure 2.1. Azidoprofen was prepared by the stepwise reduction, diazotisation and azidation of the corresponding nitro-analogue, 2-(4-nitrophenyl) propionic acid. The latter two stages were omitted in the synthesis of aminoprofen. Ester derivatives were prepared from the parent acid by established methods of esterification.

Ibuprofen was supplied by the Boots Company, Nottingham, England. All other chemicals and solvents were purchased from appropriate chemical suppliers as listed in Appendix 1 and were used as received. HPLC grade solvents were used for the preparation of HPLC mobile phases whilst other chemicals were either analar or reagent grade as appropriate. Double distilled water was used throughout for the preparation of analyte solutions and mobile phases.

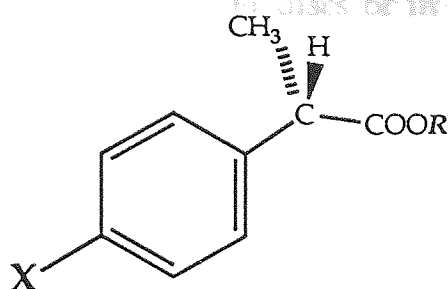
2.2 INSTRUMENTATION

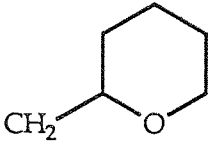
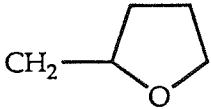
2.2.1 Analytical

Ultra-violet absorption

UV absorption readings were measured using a Cecil C292 Digital Ultraviolet spectrophotometer while UV spectra were recorded using a Pye Unicam SP8000 Ultraviolet scanning spectrophotometer. In both instances, 10 mm quartz cells were employed.

Figure 2.1 Structural formulae of compounds used during the study.



X	R	Compound
N ₃	H	Azidoprofen (AZP)
<u>Esters of AZP</u>		
N ₃	CH ₃	Methyl
N ₃	C ₂ H ₅	Ethyl
N ₃	C ₃ H ₇	Propyl
N ₃	CH ₂ CONH ₂	Glycolamide
N ₃	CH ₂ CON(Et) ₂	N-diethyl glycolamide
N ₃		Tetrahydropyranyl-methyl ester (THP)
N ₃		Tetrahydrofuranlyl-methyl ester (THF)
NH ₂	H	Aminoprofen (AMP)
<u>Esters of AMP</u>		
NH ₂	CH ₃	Methyl
NH ₂	C ₂ H ₅	Ethyl
NH ₂	C ₃ H ₇	Propyl

Infra-red absorption

Infra-red spectra were recorded either in KBr discs or in Nujol mulls on a Pye Unicam SP 200 Infra-red spectrophotometer.

Mass spectrometry

Mass spectra were recorded on a VG Micromass 12 spectrometer, operating at an accelerating voltage of 4 kV, a trap current of 100 μ A and a source temperature of 250 °C.

Nuclear magnetic resonance spectroscopy

¹H-NMR spectroscopy was conducted either at 60 MHz on a Varian EM 360A spectrometer or at 300 MHz on a Bruker AC 300 spectrometer.

High-performance liquid chromatography

HPLC analyses were performed using a system constructed from a number of basic components. An Altex 100A dual reciprocating, solvent-metering pump delivered mobile phases typically at a flow rate of 1 ml min⁻¹ to a stainless-steel column (10 cm x 4.6 mm; column length x internal diameter) packed with 5 μ m Hypersil-ODS (Shandon, UK) reversed-phase material. Samples were introduced through a Rheodyne 7120 injection valve fitted with a 10 μ l, 20 μ l, 50 μ l or 100 μ l loop as appropriate and UV detection was accomplished with a Pye Unicam LC3 variable wavelength UV detector equipped with a 8 μ l flow cell. Chromatograms were recorded using either a JJ instruments CR452 or an Omniscrite D5000 chart recorder operated at chart speeds of 12.0 cm hr⁻¹ and 12.5 cm hr⁻¹ respectively.

2.2.2 Subsidiary

All pH measurements were undertaken using a Radiometer PHM 62 Standard pH meter (2 decimal place display) or a WPA CD 660 Digital pH meter (3 decimal place display) in conjunction with a Gallenkamp combination glass electrode, appropriately calibrated with Colourkey® buffer solutions (BDH Ltd).

A range of electronic balances; Sartorius 1601 MP8 and analytic A200S four decimal place or research R200D five decimal place instruments were used for accurate weighing purposes.

A Kerry laboratory sonicator was employed where sonication was required as an aid to dissolution or solvent de-gassing.

2.3 EXPERIMENTAL

The techniques of infra-red spectroscopy and mass spectrometry were predominantly used for qualitative identification and purity assessment of the novel azido and amino compounds following their synthesis. $^1\text{H-NMR}$ spectroscopy was used for similar purposes and also for the kinetic profiling of certain AZP reduction studies (see Chapter 3). These spectroscopic methods will not be further discussed here and the following account will pertain to the development of high-performance liquid chromatography (HPLC) methods used for the quantitative analysis of AZP and related analogues during the course of this study.

2.3.1 High-performance liquid chromatography method development

HPLC is undoubtedly one of the most valuable and versatile analytical techniques currently available to the pharmaceutical scientist. Its attributes include the ability to efficiently separate and detect a wide range of molecules with varying molecular weights, polarities and thermal labilities. The technique is especially valuable in the analytical separation of groups of closely related compounds such as enantiomers, degradation products, metabolites and structural analogues. This latter quality is of particular relevance to the nature of the current study. In addition, the provision of a rapid, specific, sensitive and readily quantifiable assay system makes HPLC an ideal analytical method for this purpose.

Comprehensive accounts of the theoretical principles and practical aspects of HPLC may be found in several texts (Knox *et al*, 1978; Simpson, 1978). Very simply, the system involves the delivery of a mobile phase through an injection valve onto a solid-phase chromatographic column, thereby introducing the sample onto the latter component. A combination of partitioning and adsorption processes of the analyte between the solid stationary phase and liquid mobile phase, by nature of their physicochemical characteristics, result in separation and elution of the analytes onto a detection device where they may be quantified.

Also available are reviews of the pharmaceutical application of HPLC (Irwin and Scott, 1982; Li Wan Po and Irwin, 1980) as well as texts and monographs devoted to the analysis of therapeutic compounds (Moffat, 1986; Tsuji and Morozowich, 1978-79). Clearly evident in this literature is the extensive use of the technique in the analysis of NSAIDs in formulation and stability studies as well as pharmacokinetic investigations.

The development of a suitable assay procedure may be achieved by the modification of several variables which determine the efficient chromatographic separation of compounds. Once the basic components of the system are assembled, selection of an appropriate column-stationary phase is the initial criterion. A number of these are available and a single stationary phase may be used for the analysis of a multitude of compounds. System selectivity and separation of individual components is however achieved by the careful choice of mobile phase. Changes in solvent composition together with selection of an appropriate UV detection wavelength are used to achieve optimal detection and resolution which may be quantified in terms of various mathematical parameters. Internal standards may be incorporated into samples to aid standardization by minimising errors caused by fluctuations in column performance, while analyte concentrations are determined by interpolation from calibration plots which are validated in terms of their linearity. The development of HPLC methods for AZP and analogues will be discussed with respect to these variables.

Choice of UV wavelength

The use of an UV detector to monitor the presence and concentration of analytes separated on the chromatographic column requires a preliminary knowledge of the UV absorption characteristics of the compounds of interest. Hence, UV spectra of AZP and analogues as well as those of internal standard candidates were initially studied in the range of 200-350 nm. UV spectra of AZP and AMP, typifying the UV absorption profiles of azido and amino analogues respectively are illustrated in Fig. 2.2 together with their molar absorptivity coefficients at various wavelengths (Table 2.1). The data clearly show the pH dependence of the UV absorption for the amino species. At acidic pH (0.1 M HCl), protonation of the NH_2 residue to the NH_3^+ species, results in an alteration of the UV absorbing chromophore and consequent change in UV absorption profile. All compounds were found to absorb over the range of study and a wavelength of 250 nm, allowing high sensitivity with minimal interference from mobile phase constituents which might compromise specificity, was chosen for most HPLC analyses.

Choice of stationary phase

The majority of HPLC separations are performed on porous silica-based stationary phases with a controlled particle size of 3-10 μm , which may be either untreated or chemically-modified. In the case of untreated silica, the surface silanol groups (Si-OH) which are polar in character may be exploited in normal-phase chromatography where the separation process is dependent on adsorption of solute from a relatively non-polar mobile phase by interaction with these silanol functions. Alternatively, these surface silanol groups may be modified by chemical reaction with hydrocarbon derivatives to yield a non-polar surface coat. Of these, the octadecylsilane (ODS, C_{18}) bonded phase is probably the most widely used and was selected as the packing material for the duration of the current work. The hydrophobic alkyl bonded phase permits the use of highly polar mobile phases. This process is termed *reversed-phase* chromatography, and enables the separation of polar compounds which would not be eluted from normal phase systems.

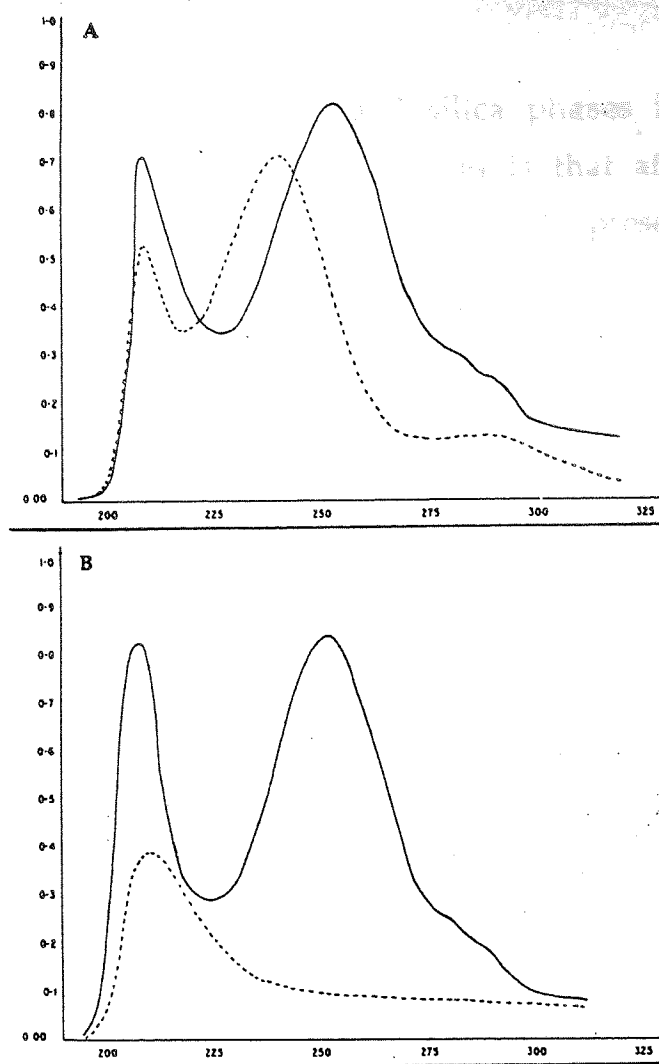


Figure 2.2 UV absorption spectra for AZP (—) and AMP (----) in 95% Ethanol (A) and 0.1 M Hydrochloric acid (B)

Table 2.1 Molar absorption coefficients for AZP and AMP at various wavelengths under neutral and acidic conditions.

Wavelength (nm)	Molar absorption coefficient (1 molar, 1cm)			
	AZP		AMP	
	95% EtOH	0.1 M HCl	95% EtOH	0.1 M HCl
210	15297	13958	7781	7434
220	4627	3423	4064	3750
230	3557	3557	8079	1702
240	6941	8968	11400	760
250	13480	14245	7731	512

Although chromatography using bonded silica phases is a very popular technique, a major problem with such phases is that after derivatization, residual (unreacted) surface silanol groups may still be present. This gives rise to a bifunctional surface consisting of both non-polar (C₁₈) and the usually acidic, polar (Si-OH) regions. Certain compounds, particularly basic substances such as amines exhibiting both hydrophobic and hydrophilic molecular regions, will interact with both types of functional groups, resulting in broad asymmetrical tailing peaks. Most efforts to suppress peak tailing are aimed at minimizing these silanol interactions and include "end capping" or secondary bonding reactions with a short chain silane after the primary reaction. Additionally, chromatography may be improved by the inclusion of organic additives in the mobile phase which is discussed more fully below.

Silica-based bonded phases are also prone to degradation at pH extremes. Consequently, they were operated between the suggested guidelines of pH 2.5 and pH 7.0. At low pH values (pH<2.5) there may be loss of bonded phase whereas at higher pH values (pH>7) the silica particles are prone to dissolution. Column performance may also be impaired by prolonged use and deposition of lipid and proteinaceous sample impurities on the stationary phase towards the top of the column. In the case of the octadecylsilane columns, a deterioration in peak shape was indicative of this damage and could be easily remedied by the manual replacement of the top 1 to 2 mm of the column packing with a slurried suspension of the stationary phase in propan-2-ol.

Choice of mobile phase

It is generally accepted that modifying mobile phase characteristics such as polarity and pH imparts the main selectivity to the system. Thus, development of isocratic elution systems suitable for different compounds was achieved by systematic quantitative changes in solvent composition. Mobile phases composed of varying proportions of acetonitrile and water were employed to optimize peak resolution whilst maintaining a relatively short analysis time.

The complications of poor chromatography due to surface silanol group interactions have already been mentioned. The problem may also be partly resolved by the addition of an organic modifier to the mobile phase, which as a result of strong polar interactions with the residual silanol groups, minimizes similar associations with the sample compound. Several of the amino compounds in this study exhibited broad tailing peaks which were dramatically improved by the addition of diethylamine (0.1% v/v) at acidic pH (~2.5) to the mobile phase. Use of this additive also appeared to improve the overall chromatography of the azido analogues and was therefore included in most analytical methods. Adjusting the pH of the mobile phase to ensure that the sample molecules are in a neutral form also reduces acidic and basic silanol interactions. Consequently, most mobile phases were acidified to a pH of 2.5 with orthophosphoric acid to maintain AZP in an unionized form thus improving chromatography.

Selectivity may be further increased by modifying the mobile phase to achieve ion-pair chromatography. The technique for weak bases involves adjusting the mobile phase pH to effect ionization together with the addition of a strong electrolyte such as an alkyl sulphonate (*e.g.*, octanesulphonic acid) or alkyl sulphate (*e.g.*, sodium lauryl sulphate). Formation of a reversible complex between the ionized analyte and added counter-ion ($R_3NH^+ \dots R'SO_4^-$) favours partitioning into the hydrophobic stationary phase due to increased lipophilicity of the complex and results in increased retention. This technique was useful in the concurrent analysis of azido and amino compounds where the large variation in polarities of the two moieties made their simultaneous analysis difficult (early peak of polar amine incompletely resolved whereas the late peak of lipophilic azide broad and indistinct). Ion-pairing with octanesulphonic acid increased retention of the amine, helping to minimize the problem.

Dissolved gases can cause deterioration in chromatography by out-gassing in the detector flow-cell or formation of UV-absorbing complexes with solvents

(Bakalyer *et al*, 1978). To minimize these problems, mobile phases were degassed by vacuum filtration or sonication prior to HPLC analyses.

Mathematical parameters

The HPLC systems used may be quantified by a number of mathematical parameters which define their chromatographic performance in terms of retention and resolution. Figure 2.3 illustrates a typical HPLC chromatogram for a two-component mixture where:

t_0 , t_A and t_B are the retention times of an unretained solute, component A and component B respectively; t_0 is commonly recognized as the first disturbance in the baseline, usually observed as the solvent front, with which the unretained solute is considered to co-elute. The corresponding retention volumes (V_0 , V_A , V_B) may be calculated from the mobile phase flow rate (F ml/min):

$$V_0 = t_0 F \quad (2.1)$$

V_0 is the column void volume (or dead volume) and is a measure of the inter- and intraparticle pores. For a 4.6 mm i.d column, it may also be estimated by the following equation (Dolan, 1988):

$$V_0 \cong (0.1 \text{ ml/cm}) (L) \quad (2.2)$$

where L is the column length in centimeters.

The column capacity factor, k' , a measure of the sample retention is probably the most useful separation parameter and may be calculated using the formula:

$$k' = \frac{(t_A - t_0)}{t_0} \quad (2.3)$$

where t_A is the retention time of the band of interest (component A). This is effectively also a measure of the volume of mobile phase, in column void

volumes (V_0), required to elute the given sample component. For good isocratic separation, k' should be in the range of 1 to 10. Values outside this range should be avoided since small capacity factors, less than 1, indicate inadequate separation from the solvent front whilst large values of k' , greater than 10, are associated with long retention times and broadened peaks.

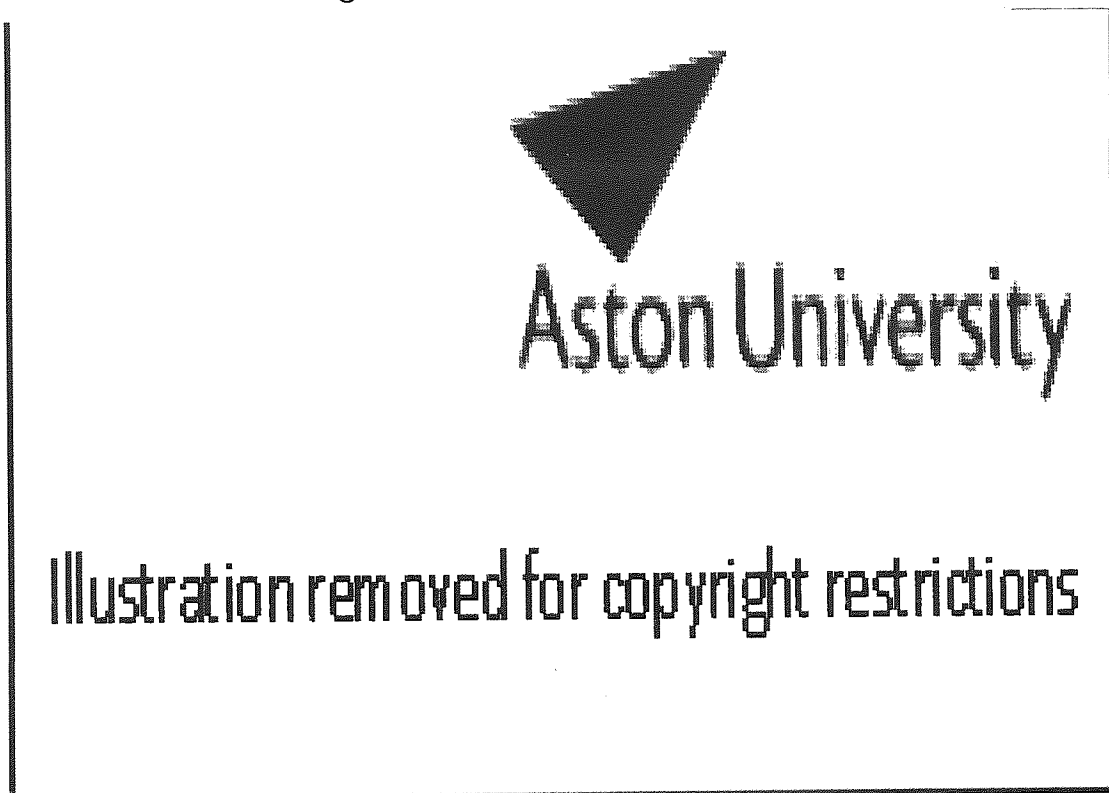


Figure 2.3 Example HPLC chromatogram of a two-component mixture (From Li Wan Po and Irwin, 1980).

The number of theoretical plates, N , gives a measure of the column efficiency which is dependent on the degree of band broadening relative to the time taken to elute. For the test chromatogram in Figure 2.3., this may be defined by the equation:

$$N = 16 (t_A / W_A)^2 \quad (2.4)$$

where W_A is the base width of peak A. N is usually expressed per metre of column length (derived by dividing the above formulae by column length in metres) and for typical systems, should be in the range of 2500 to 10000.

Columns with large N values will produce narrow peaks and better resolution than those with lower N values. The efficiency may also be expressed as the height equivalent of a theoretical plate, H :

$$H = \frac{L}{N} \quad (2.5)$$

where L is the column length in μm . Values of H should lie between 25 and 100 μm .

The resolution, R_S , of a system is a measure of the efficiency of the separation of different components and may be represented by the equation:

$$R_S = \frac{2(t_B - t_A)}{(W_A + W_B)} \quad (2.6)$$

An R_S value of 1.0 indicates a satisfactory separation with $\sim 2\%$ overlap, whilst a value of 1.5 represents almost total separation.

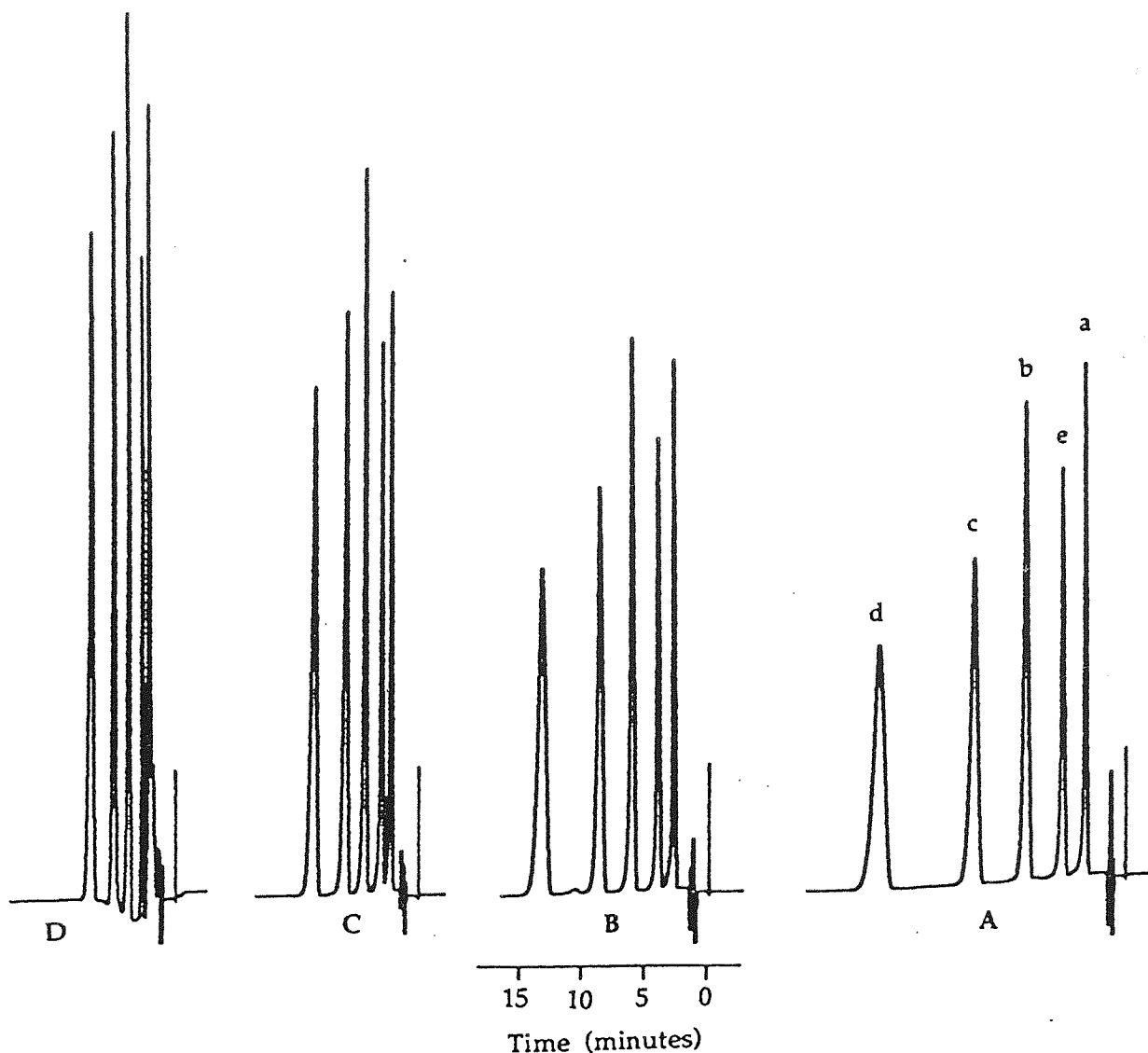
2.3.2 Analysis of azidoprofen and related compounds

AZP and related ester analogues were generally analyzed using mobile phases consisting of varying concentrations of acetonitrile in distilled water and 0.1% v/v diethylamine, adjusted to a final pH of 2.5 with orthophosphoric acid. A flow rate of 1 ml min^{-1} was employed and the column eluant was usually measured spectrophotometrically at 250 nm. Sample injection volumes were typically 10 μl but were increased up to 100 μl according to the specific experimental conditions. Similarly, sensitivity settings ranged from 0.08 to 1.28 AUFS.

During the development of suitable systems for these compounds, the effect of varying acetonitrile content (40-65%) on their retention and resolution was investigated and examples of the resulting chromatograms for AZP and its alkyl, tetrahydrofuranyl-methyl (THF) and tetrahydropyranyl-methyl (THP) esters are shown in Figures 2.4 and 2.5 together with calculations of resolution (R_s) between adjacent peaks. Values of t_R , k' , N , and H , quantifying the chromatographic efficiency of these systems, are summarized in Table 2.2. The values of these parameters were useful indicators in the final choice of a mobile phase for each compound or group of compounds.

The final selection of a solvent system was also dependent on the specific experimental conditions which determined whether a particular substance was to be analyzed separately or in conjunction with other analogues, metabolites, degradation or reaction products. Subtle variations in column performance amongst different columns were also occasionally noticeable; these occurred rarely and were usually negligible. However, analysis of compounds with capacity factors close to 1 or those resolving close to other peaks sometimes necessitated minor changes in solvent composition with different columns for efficient chromatography. As a result of these factors, different mobile phases were sometimes employed for analysis of the same compound under varying test procedures. The solvent systems and conditions used for these compounds are summarized in Table 2.3. Following the testing of a number of candidates, butyl paraben (*n*-butyl-*p*-aminobenzoate) was selected as an internal standard for the majority of systems. Methyl paraben, ethyl and *n*-propyl salicylate were also used as internal standards in selected assays.

AZP, alone, was analyzed using a mobile phase comprising 50% v/v acetonitrile in distilled water, 0.1% v/v diethylamine, acidified to pH 2.5 with orthophosphoric acid. The corresponding alkyl, THF and THP esters generally required elution with solvents comprising higher acetonitrile concentrations due to their greater lipophilicity and consequent increased retention by the stationary phase. Many ester metabolism studies, however, required the concurrent analysis of both the ester and hydrolytic product, AZP.



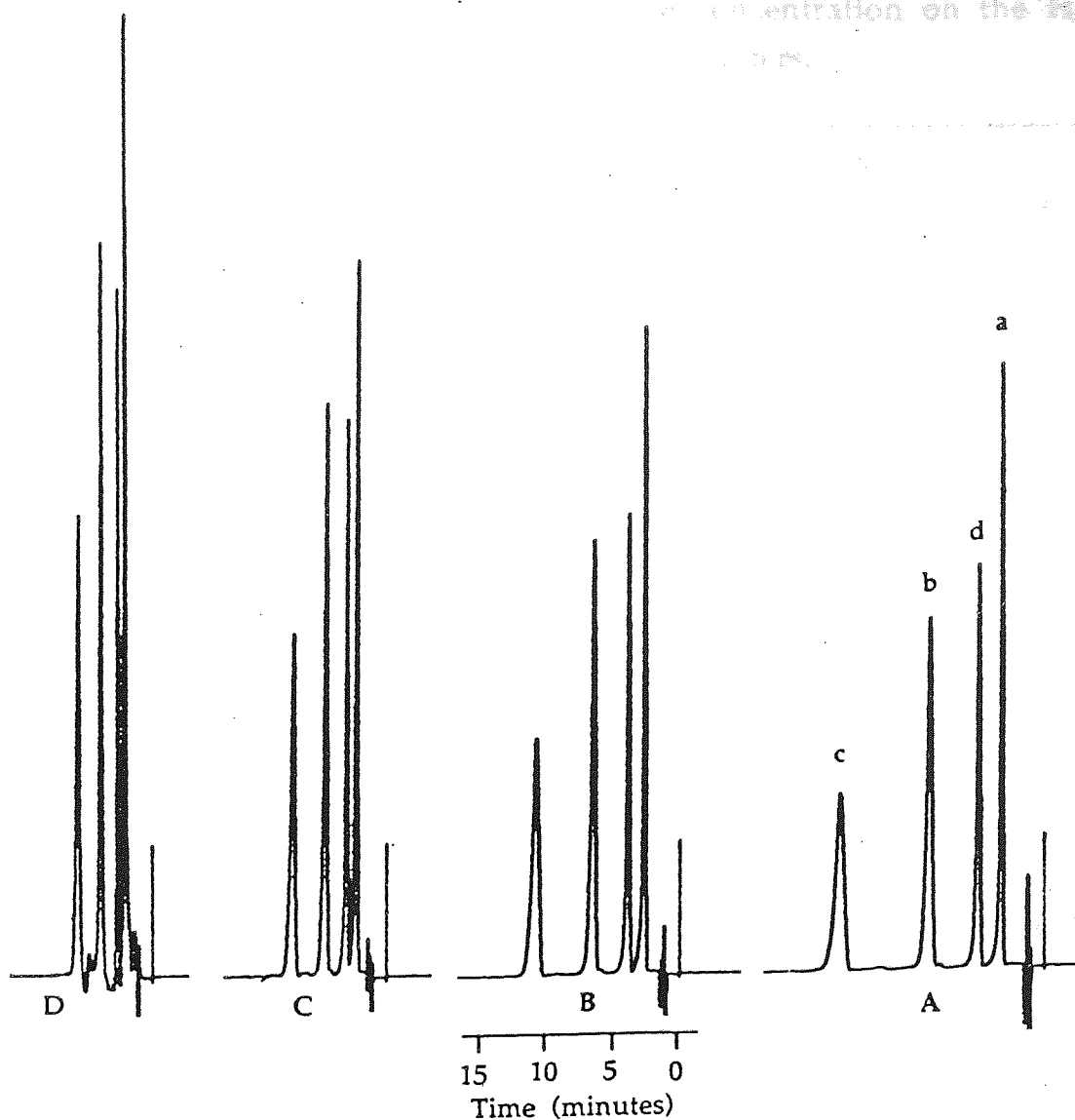
Peaks	Resolution			
	D	C	B	A
a + e	1.2	1.6	2.2	2.6
b + e	1.6	2.2	2.7	3.5
b + c	1.7	2.3	3.2	3.5
c + d	2.3	3.0	3.8	4.2

Figure 2.4 Effect of acetonitrile concentration on the separation of AZP (a), corresponding Methyl (b), Ethyl (c) and Propyl (d) esters and internal standard (e) using:

(A) 50% MeCN; (B) 55% MeCN; (C) 60% MeCN and (D) 65% MeCN in distilled water with 0.1% diethylamine and adjusted to pH 2.5.

HPLC conditions:

Column: 5 μ m ODS-Hypersil (10cm x 4.6 mm i.d); Flow rate: 1ml min⁻¹ ; Loop size: 10 μ l
 Chart speed: 2mm min⁻¹; Sensitivity: 0.08 AUFS; Wavelength: 250 nm; I.S = Butyl paraben



Peaks	Resolution			
	D	C	B	A
a + d	1.2	1.6	2.2	2.6
b + d	2.4	2.7	3.5	4.5
c + d	5.1	6.0	7.5	9.6

Figure 2.5 Effect of acetonitrile concentration on the separation of AZP (a), corresponding THF (b) and THP (c) esters and internal standard (d) using: (A) 50% MeCN; (B) 55% MeCN; (C) 60% MeCN and (D) 65% MeCN in distilled water with 0.1% diethylamine and adjusted to pH 2.5.

HPLC conditions:

Column: 5 μ m ODS-Hypersil (10cm x 4.6 mm i.d); Flow rate: 1ml min⁻¹; Loop size: 10 μ l
 Chart speed: 2mm min⁻¹; Sensitivity: 0.08 AUFS; Wavelength: 250 nm; I.S = Butyl paraben

Table 2.2 The effect of varying acetonitrile concentration on the HPLC parameters of AZP and corresponding esters.

<i>Compound</i>	acetonitrile (%)	t_R (min)	k'	N (m^{-1})	H (μm)
<i>AZP</i>	50	3.1	2.1	4271	23.4
	55	2.6	1.6	4326	23.1
	60	2.2	1.2	4840	20.7
	65	1.9	0.9	2310	43.3
<i>Methyl ester</i>	50	7.8	6.8	9734	10.3
	55	5.7	4.7	8123	12.3
	60	4.1	3.1	7471	13.4
	65	3.4	2.4	5138	19.5
<i>Ethyl ester</i>	50	12.0	11.0	11755	8.5
	55	8.4	7.4	13938	7.2
	60	5.6	4.6	10240	9.8
	65	4.5	3.5	6612	15.1
<i>Propyl ester</i>	50	19.2	18.2	14746	6.8
	55	12.8	11.8	13375	7.5
	60	8.0	7.0	12642	7.9
	65	6.2	5.2	9610	10.4
<i>Tetrahydrofuranyl-methyl ester</i>	50	8.6	7.6	11834	8.5
	55	6.1	5.1	12150	8.2
	60	4.4	3.4	8605	11.6
	65	3.7	2.7	8762	11.4
<i>Tetrahydropyranyl-methyl ester</i>	50	15.4	14.4	16865	5.9
	55	10.2	9.2	13757	7.3
	60	6.8	5.8	11560	8.7
	65	5.3	4.3	12484	8.0

Table 2.3 Summary of HPLC conditions for compounds analysed during the study.

Compound	System	Mobile phase (% MeCN)*	Internal Standard	Detection wavelength (nm)
<i>AZP</i>	A	50	Butyl paraben	250
	B	55	Butyl paraben	250
<u>Esters</u>				
<i>Methyl</i>	A	50	Butyl paraben	250
	B	55	Butyl paraben	250
	C	60	Propyl salicylate	250
<i>Ethyl</i>	A	50	Butyl paraben	250
	B	55	Butyl paraben	250
	D	60	Ethyl salicylate	250
<i>Propyl</i>	A	50	Butyl paraben	250
	B	55	Butyl paraben	250
	E	65	Ethyl salicylate	250
<i>Glycolamide</i>	F	40	Methyl paraben	250
<i>THF</i>	B	55	Butyl paraben	250
<i>THP</i>	B	55	Butyl paraben	250
<u>Miscellaneous</u>				
<i>Ibuprofen</i>	G	50	Butyl paraben	230
<i>Caffeine</i>	H	10	Theophylline	273

* MeCN content (%) in a basic mobile phase composed of acetonitrile, distilled water and 0.1% diethylamine, acidified to pH 2.5 with phosphoric acid.

HPLC conditions:

Column: 5 μ m ODS-Hypersil (10cm x 4.6 mm i.d); Flow rate: 1ml min⁻¹; Loop size: 10 to 100 μ l
Chart speed: 2mm min⁻¹; Sensitivities: 0.08 to 1.28 AUFS

In these instances, the highest acetonitrile concentration which could be employed was 55%, allowing sufficient resolution of the early AZP peak from the solvent front to enable quantification without greatly compromising chromatography of the slower eluting esters (Figures 2.4 and 2.5). In contrast, the glycolamide ester was analysed using a mobile phase with a lower acetonitrile content of 40% v/v (Figure 2.10).

Quantification of sample peak responses was achieved by way of calibration measurements. These were performed for the test compounds during each assay procedure, under the conditions of that particular experiment and in an appropriate concentration range. The validity of this technique was assessed by examining the linearity of the calibration plots of peak height ratios (azide: internal standard) against azide concentration. Example calibration plots are illustrated in Figures 2.6-2.10 with corresponding statistical parameters in Tables 2.4-2.8.

AZP and AMP could not be monitored simultaneously due to large differences in polarity. Despite manipulation of the mobile phase with ion-pairing agents, retention of the highly polar AMP could not be increased sufficiently to allow separation from the solvent front whilst maintaining acceptable chromatography of the better retained and late eluting AZP. Consequently, a mobile phase comprising of 10% v/v acetonitrile in distilled water with 0.1% v/v diethylamine, adjusted to pH 2.5 was used for the separate analysis of AMP when required.

Preliminary degradation studies of azido-substituted alkyl-esters also necessitated the simultaneous detection of the reduction product; amino-ester and hydrolysis product; AZP, in order to determine the major degradative pathway. Thus, HPLC methods enabling concurrent analysis of AZP, the amino-ester and azido-ester species for each of the alkyl esters were developed.

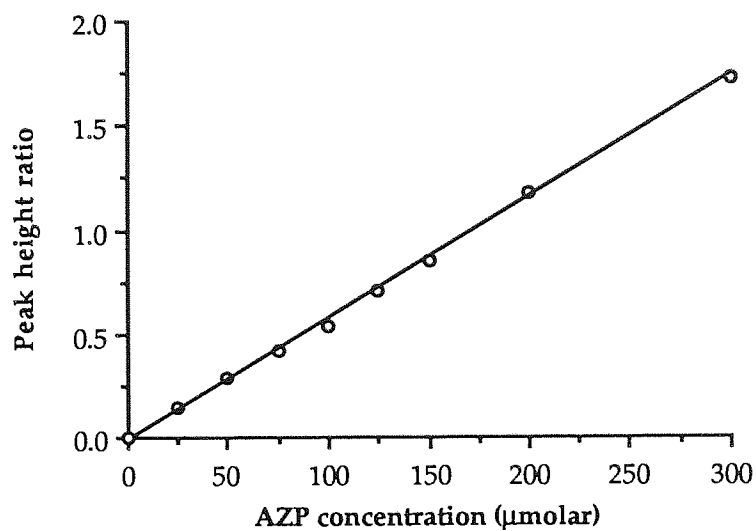


Figure 2.6 Typical calibration graph for AZP using HPLC system A.

Other HPLC conditions:

Loop size: 10 µl; Sensitivity: 0.64 AUFS; Butyl paraben (I.S): 40 µg ml⁻¹

Table 2.4 Typical calibration statistics for AZP using HPLC system A.

Compound	Slope ($\times 10^3$)	Intercept ($\times 10^2$)	Correlation coefficient
AZP	5.7977	-1.0704	0.9995

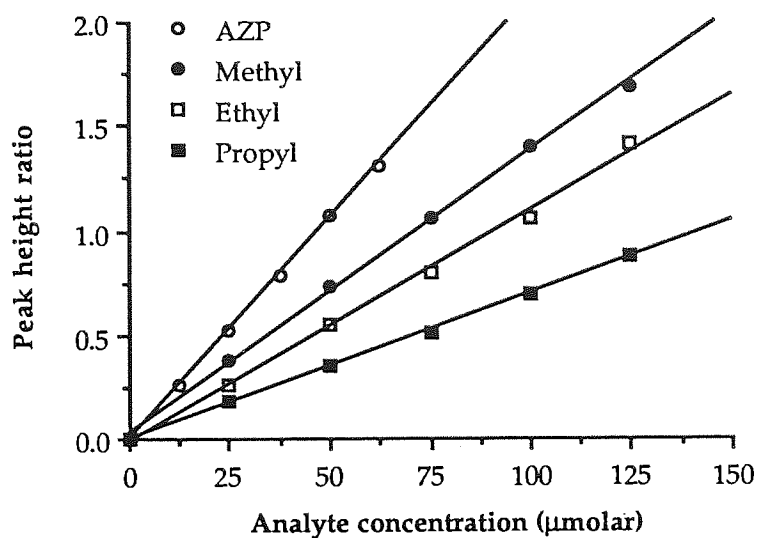


Figure 2.7 Typical calibration graphs for AZP and its corresponding methyl, ethyl and propyl esters using HPLC system A.

Other HPLC conditions:

Loop size: 10 µl; Sensitivity: 0.16 AUFS; Butyl paraben (I.S): 10 µg ml⁻¹

Table 2.5 Calibration statistics for Figure 2.7.

Compound	Slope ($\times 10^2$)	Intercept ($\times 10^2$)	Correlation coefficient
AZP	2.1042	0.2095	0.9997
Methyl ester	1.3518	3.0810	0.9992
Ethyl ester	1.1063	-1.0476	0.9986
Propyl ester	0.6941	0.1381	0.9997

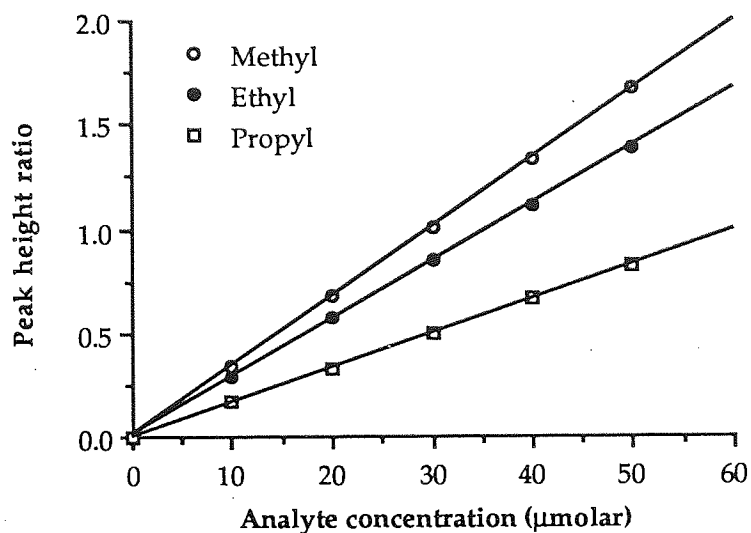


Figure 2.8 Typical calibration graphs for the methyl, ethyl and propyl esters of AZP using HPLC system B.

Other HPLC conditions:

Loop size: 50 µl; Sensitivity: 0.32 AUFS; Butyl paraben (I.S): 2 µg ml⁻¹.

Table 2.6 Calibration statistics for Figure 2.8.

Compound	Slope (x 10 ²)	Intercept (x 10 ³)	Correlation coefficient
Methyl ester	3.3196	8.2333	1.0000
Ethyl ester	2.7768	8.2333	0.9999
Propyl ester	1.6416	4.6238	0.9999

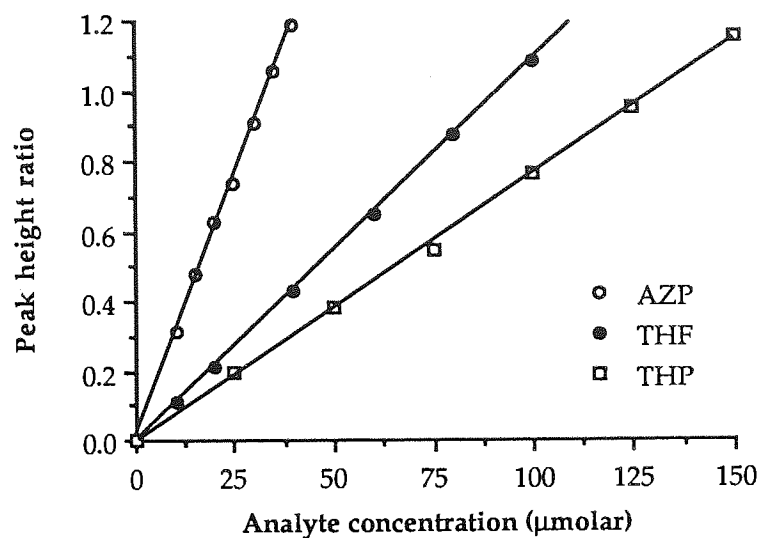


Figure 2.9 Typical calibration graph for AZP and its corresponding THF and THP esters using HPLC system B.

Other HPLC conditions:

Loop size: 10 µl; Sensitivity: 0.08 AUFS; Butyl paraben (I.S): 7.5 µg ml⁻¹.

Table 2.7 Calibration statistics for Figure 2.9.

Compound	Slope ($\times 10^2$)	Intercept ($\times 10^3$)	Correlation coefficient
AZP	2.9735	14.144	0.9994
THF ester	1.0941	-2.2761	1.0000
THP ester	0.7722	-4.5250	0.9996

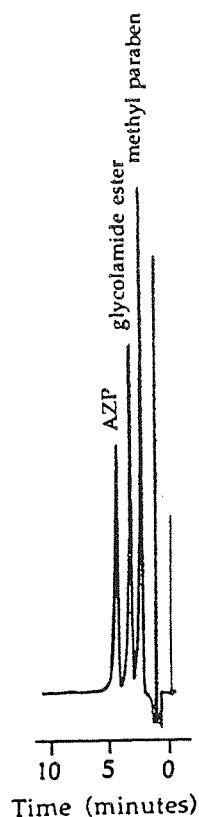


Figure 2.10 A
Example chromatogram of AZP and glycolamide ester with methyl paraben as I.S.

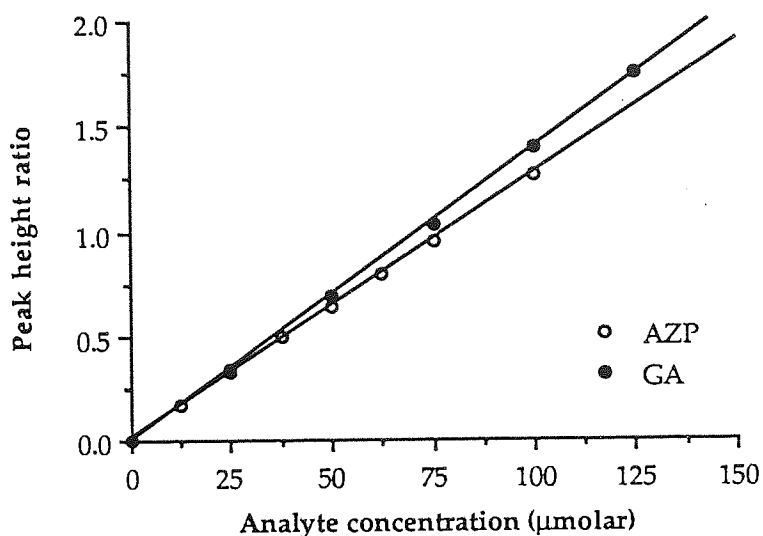


Figure 2.10 B
Typical calibration graphs for AZP and the corresponding glycolamide ester using HPLC system F.

Other HPLC conditions:

Loop size: 10 µl; Sensitivity: 0.08 AUFS; Methyl paraben (I.S): 2.5 µg ml⁻¹.

Table 2.8 Calibration statistics for Figure 2.10 B.

Compound	Slope (x 10 ²)	Intercept (x 10 ³)	Correlation coefficient
AZP	1.2653	9.5163	0.9999
Glycolamide ester	1.4003	-6.0476	0.9999

Since the amino-acid derivative (AMP) could not be analyzed with the systems utilized, its formation was assessed by mass balance as three of the four potential components of the system could be quantified. The systems and conditions employed are summarized in Table 2.9. Difficulties in analyzing both the azido and amino moieties together, due to the large difference in their molar extinction coefficients under the acidic environment of the mobile phase used (Table 2.1), was overcome by the use of two UV detectors and recorders connected in series. Each detector was operated at a different sensitivity allowing detection of both derivatives in the same molar concentration range.

Table 2.9 Summary of HPLC conditions for the analysis of azido and amino alkyl ester derivatives of AZP

Ester (HPLC system)	Mobile phase MeCN: H ₂ O: 1-octanesulphonic acid sodium salt	Internal Standard	Wavelength, Flow rate, Sample size	Sensitivity (AUFS) detector	
				1 [†]	2 [‡]
Methyl (I)	45: 55: 0.02 M	Butyl paraben [†] Methyl <i>p</i> -nitro- benzoate [‡]	245 nm 1ml min ⁻¹ 10 µl	0.04	0.32
Ethyl (J)	40: 60: 0.03 M	Butyl paraben [†] Methyl <i>p</i> -nitro- benzoate [‡]	245 nm 1ml min ⁻¹ 20µl	0.04	0.32
Propyl (K)	50: 50: 0.01 M	Ethyl salicylate [†] Propyl salicylate [‡]	245 nm 1ml min ⁻¹ 100 µl	0.04	0.32

[†] for amino-derivative (detector 1) [‡] for azido-derivative (detector 2)

Several comparative permeation studies of ibuprofen (IBP) and azidoprofen were performed. Here, 50 μl samples of both substances were analyzed using a mobile phase consisting of 50% v/v acetonitrile in distilled water with 0.1% v/v diethylamine, acidified to a pH of 2.5 with orthophosphoric acid, at sensitivity settings ranging from 0.08 to 1.28 AUFS. The column eluant was monitored at 230 nm; this choice of wavelength enabled both IBP and AZP to exhibit comparable molar absorptivities. Butyl paraben was employed as an internal standard. An example chromatogram is shown in Figure 2.11 A. Calibration plots of peak height ratio against analyte concentration were linear and examples are shown in Figure 2.11 B, with corresponding statistical parameters in Table 2.10.

Analysis of caffeine was required for a certain permeation study, investigating the effect of ionization on penetration enhancement. In this case, 20 μl samples were analysed using a solvent system comprising 10% v/v acetonitrile in distilled water, 0.1% v/v diethylamine, adjusted to pH 2.5. The detector was operated at a wavelength of 273 nm and a sensitivity of 0.16 AUFS. The related xanthine, theophylline was selected as an internal standard. Example chromatograms and calibration plots are shown in Figure 2.12 with corresponding statistical parameters in Table 2.11.

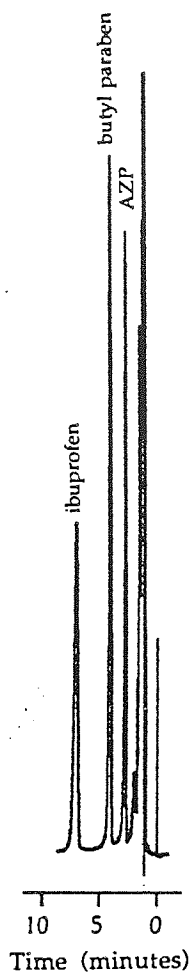


Figure 2.11 A
Example chromatogram of AZP and IBP with butyl paraben as I.S; using HPLC system G.

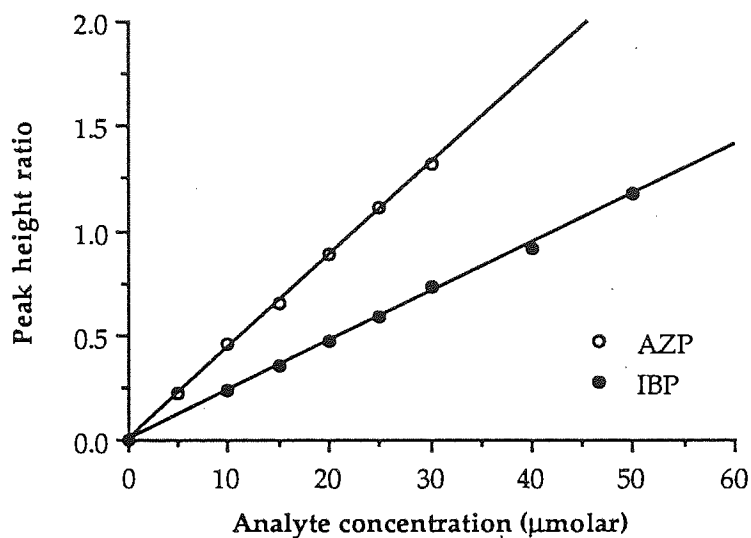


Figure 2.11 B
Typical calibration graph for AZP and IBP using HPLC system G.

Other HPLC conditions:

Loop size: 50 µl; Sensitivity: 0.08 AUFS; Butyl paraben (I.S): 4 µg ml⁻¹.

Table 2.10 Calibration statistics for Figure 2.11 B.

Compound	Slope (x 10 ²)	Intercept (x 10 ³)	Correlation coefficient
AZP	4.4072	3.4067	0.9998
IBP	2.3539	-0.1871	0.9995

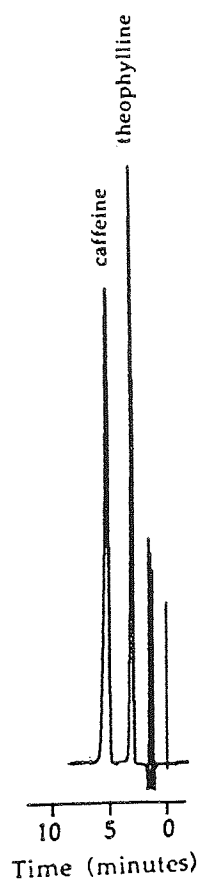


Figure 2.12 A
 Example chromatogram of caffeine and theophylline (I.S) using HPLC system H.

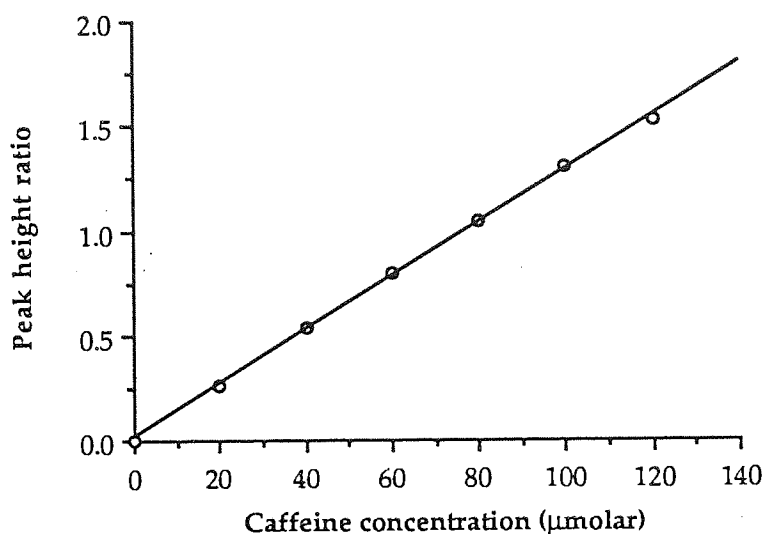


Figure 2.12 B
 Typical calibration graph for caffeine using HPLC system H.

Other HPLC conditions:

Loop size: 20 µl; Sensitivity: 0.16 AUFS; Theophylline (I.S): 7.5 µg ml⁻¹.

Table 2.11 Calibration statistics for Figure 2.12 B.

Compound	Slope ($\times 10^2$)	Intercept ($\times 10^2$)	Correlation coefficient
Caffeine	1.2842	1.2536	0.9997

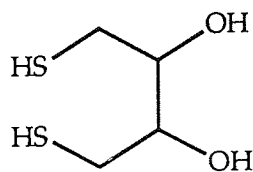
2.4 SUMMARY

Reversed phase HPLC methods suitable for the assay of compounds under study were developed. These enabled sensitive and specific analysis under a range of experimental conditions, allowing separation of individual components from mixtures of analogous reaction and degradation products, and subsequent quantification. These methods, as techniques for quantitative analysis, were validated in terms of linearity of calibration plots with respect to analyte concentration. The linear regression correlation coefficients of these plots were determined to be ≥ 0.999 , thus validating the assay procedure for each compound.

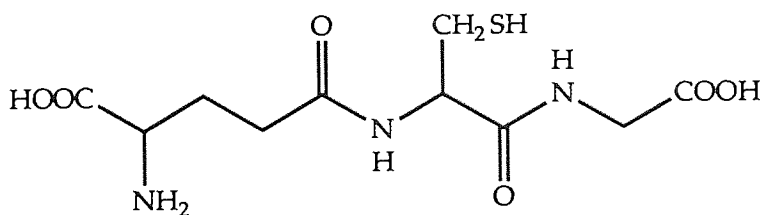
CHAPTER THREE
MODEL FOR BIOREDUCTION OF AROMATIC AZIDES

3.1 INTRODUCTION

The ability of soft drugs to undergo controlled *in vivo* bioinactivation is a fundamental requirement for their therapeutic success. The potential of azido-substituted drugs to offer the advantages of soft drugs is therefore largely dependent on this criterion. Bioreduction to the corresponding amine has been postulated as a detoxification mechanism for azides and evidence for this process occurring both *in vitro* and *in vivo* for various aryl azides was presented earlier (section 1.3.2). Additionally, aryl azides have been reported to undergo a facile thiol-mediated chemical reduction to the corresponding amine under physiological (Cartwright *et al*, 1976; Staros *et al*, 1978) and non-physiological (Baker *et al*, 1989) conditions. Similarly, alkyl azides have also been shown to be readily reduced by thiols at room temperature (Bayley *et al*, 1978). More recently, the antiretroviral drug, 3'-azidothymidine (AZT), was assessed for its susceptibility to *in vitro* reduction by dithiothreitol (6), mercaptoethanol and the endogenous thiol, glutathione (7) (Handlon and Oppenheimer, 1988). As for aryl azides, this process was rapid in the presence of dithiols such as dithiothreitol (DTT) but greatly reduced in the presence of monothiols such as mercaptoethanol and glutathione (GSH).



(6) Dithiothreitol



(7) Glutathione

Glutathione, γ -L-glutamyl-L-cysteinyl-glycine is a major thiol constituent of mammalian cells. As the most important and plentiful nonprotein thiol present in animal cells (Larsson *et al*, 1983; Meister and Anderson, 1983), it is involved in number of important cellular functions including maintenance of membrane integrity and cytoskeletal organization, involvement in protein and

DNA synthesis, and modulation of protein conformation and enzyme activity (Kosower and Kosower, 1978). GSH is also utilized in the synthesis of essential metabolites such as leukotrienes and prostaglandins. In addition, as an endogenous antioxidant, it is considered to perform an important protective function, especially in the skin (Connor and Wheeler, 1987). As such, GSH may act as radical scavenger *per se*, or as a cofactor for a variety of GSH-dependent enzymes including the glutathione transferases, which are important in the detoxification of electrophilic metabolites (Moldéus and Quangan, 1987).

Many tissues actively synthesize GSH (Griffith and Meister, 1977) and relatively high intracellular concentrations (in the millimolar range) often exist. Levels of up to 12 mM may be present in hepatocytes, while concentrations of 1.21 and 1.07 mmol kg⁻¹ have been detected in normal and involved psoriatic epidermis respectively (Connor and Wheeler, 1987). These observations suggest that the potential exists for GSH to provide a route for the dermal or systemic deactivation of azides to amines.

In the current study, the dithiol DTT, was employed as a model thiol to investigate the reduction of the azido group of AZP and its corresponding alkyl esters. Although DTT is not a naturally occurring thiol reductant, there are intracellular sources of dithiols, *e.g.*, lipoamide and the active sites of enzymes including ribonucleotide reductase, lipoamide dehydrogenase, and glutathione reductase (Handlon and Oppenheimer, 1988). DTT was chosen in preference to GSH as previous studies have reported significantly faster rates of reduction with the former thiol, enabling rapid analysis and facile comparative screening between analogous azides under varying reaction conditions.

3.2 EXPERIMENTAL

3.2.1 Reduction kinetics of azidoprofen

3.2.1.1 Effect of pH on the rate of reduction.

Phosphate buffer solutions (comprising KH_2PO_4 and NaOH) were prepared in a pH range of 5.8 to 9.0 (Appendix 2). A constant ionic strength of 0.5 M was maintained by the addition of appropriate amounts of potassium chloride. A mixture comprising 41 ml of buffer and 4 ml of an aqueous stock solution containing 22.59 mg ml^{-1} DTT was incubated in a reaction vessel, surrounded by a water jacket maintained at 37°C by a Churchill thermostatic pump. The mixture was stirred magnetically and protected from light for the duration of the experiment. Once the reaction vessel contents had equilibrated at 37°C , the reaction was initiated by the addition of 5 ml of the aqueous AZP stock solution containing 2.5 mg ml^{-1} of the corresponding sodium salt (AZP-Na). The final concentration of the reaction mixture was 1.17 mM and 11.7 mM with respect to AZP and DTT; *i.e.*, a tenfold molar excess of DTT was present. The pH of the incubation mixture was monitored during the reaction, as buffers in the upper pH range afforded a lower buffering capacity and were susceptible to change. Control experiments were also included, with distilled water replacing the DTT solution.

Samples (0.5 ml) were withdrawn at appropriate time intervals throughout the course of the reaction and diluted with an equal volume of the buffer and 1 ml of internal standard solution (butyl paraben: $60 \text{ } \mu\text{g ml}^{-1}$). Aliquots ($10 \text{ } \mu\text{l}$) of this solution were assayed by HPLC as described in section 2.3.2, using system A. Peak height ratios of AZP to internal standard were measured and used to determine the percentage AZP remaining by employing a normalization procedure. Pseudo-first order rate constants were calculated by following the decrease in concentration using a first-order model.

3.2.1.2 NMR analysis.

The use of HPLC to monitor the reduction kinetics of AZP, enabled only the quantitative analysis of azide degradation. For various reasons discussed later, formation of the degradation product, AMP, could not be followed under the same conditions. In order to verify formation of AMP, an alternative analytical method using ^1H NMR spectroscopy was developed.

A buffer solution consisting of disodium hydrogen phosphate and citric acid (McIlvaine) in deuterated water with a final pD of 6.95 was prepared (Appendix 2). Individual vials containing AZP-Na (10 mg) and DTT (72.3 mg: 10 fold molar excess; 144.6 mg: 20 fold molar excess; 361.5 mg: 50 fold molar excess) were assembled. A 0.5 ml aliquot of deuterated water was introduced to both an AZP-Na and a DTT vial. The reaction was initiated by vigorously mixing the two solutions together. The resulting mixture was then immediately transferred to a NMR tube, the final reaction concentration being 10 mg ml⁻¹ in AZP-Na. For each kinetic experiment, the DTT concentration was varied. Spectra were collected at 23°C as shown in Table 3.1, using a Bruker AC 300 NMR spectrometer operating at 300 MHz.

Table 3.1 Conditions used to collect NMR spectra

Excess of DTT (M)	Number of acquisitions for each spectrum	Acquisition time (seconds)	Interval between each spectrum (seconds)
10 fold	15	3.637	variable, initially 30
20 fold	20	2.449	120
50 fold	5	2.486	4 Dummy scans {4 × (5 × 2.486 secs)} = 49.72 secs

Results were analyzed quantitatively by weighing the peak areas resulting from the *ortho* protons for both AZP and AMP. The percentage concentration of each species was derived by calculating each weight as a fraction of the total sum of areas for the two compounds.

3.2.1.3 Comparative study between NMR and HPLC analysis.

Analogous reduction experiments were followed kinetically using both NMR spectroscopy and HPLC as assay methods, in order to investigate the correlation between the two techniques. Stock solutions of AZP-Na (20 mg ml⁻¹) and DTT (144.6 mg ml⁻¹) were prepared in a disodium hydrogen phosphate - citric acid - deuterated water buffer (pD 7.05) and maintained at 23°C.

NMR analysis

Aliquots (0.5 ml) of each stock solution were thoroughly mixed together and transferred to an NMR tube. The final reactant concentrations were 10mg ml⁻¹ in AZP and 72.3 mg ml⁻¹ in DTT (10 fold molar excess). Spectra were collected at 23°C and at intervals of 60 seconds, each consisting of 15 scans of 3.637 seconds. The results were treated as in section 3.2.1.2.

HPLC analysis

Volumes of 5 ml of each stock solution were mixed together and maintained at 23°C, with constant stirring. The resulting concentrations were therefore identical to that in the NMR analysis above. Samples (100 µl) were withdrawn initially and at intervals of 2 minutes over a period of 30 minutes. Samples taken during 0 to 15 minutes were immediately treated by the addition of 2 ml of 0.1 M HCl followed by cooling to 0°C. Prior to HPLC analysis these samples were diluted with 0.9 ml of internal standard solution (butyl paraben: 800 µg ml⁻¹), resulting in a 1: 29 dilution. Samples removed after 15 minutes were treated similarly by the addition of 0.95 ml of 0.1 M HCl and 0.45 ml of IS solution, resulting in a 1: 14 dilution. 10 µl of the diluted samples were analyzed by HPLC as described in section 3.2.1.1.

3.2.2 Murine liver metabolism of azidoprofen

Male BALB/c mice (20-25g) were killed by cervical dislocation. The livers were excised rapidly and washed twice in ice-cold 0.1 M phosphate buffer, pH 7.4 (Appendix 2). Excess fluid was gently blotted off and the wet tissue weight obtained. Following dissection into small pieces, the livers were homogenized with 4 mls of the phosphate buffer per g of tissue, using a glass-Teflon homogenizer precooled to 0°C. The homogenate preparations (1 ml) were pipetted into a series of glass vials and placed on ice. Phosphate buffer, pH 7.4 (0.95 ml) and an NADPH generating system (0.50 ml) were introduced to the liver homogenates. The NADPH generating system comprised NADP (1.53 mg), glucose-6-phosphate (8.46 mg), $MgCl_2 \cdot 6H_2O$ (5.08 mg) and glucose-6-phosphate dehydrogenase (4 IU) per 0.5 ml of 0.1 M phosphate buffer, pH 7.4 (Nicholls, personal communication). A number of the vials were gassed with nitrogen and immediately sealed with airtight closures. The sample tubes were incubated at 37°C in a shaking water bath, under air or an atmosphere of nitrogen for 10 minutes prior to introduction of a 50 μ l aliquot of the substrate (25 mM AZP in methanol), in a dropwise manner. Samples (0.5 ml) were removed at 0, 30 and 60 minutes during the incubations and diluted with 1 ml of chilled methanol. The mixture was vortexed and then centrifuged at 3000 rpm for 10 minutes. The supernatants (20 μ l) were assayed for AZP, using HPLC system A. Control experiments substituting heat treated homogenate or phosphate buffer for the liver homogenate, and without cofactor solution were also performed.

3.2.3 Reduction kinetics for the alkyl esters of azidoprofen.

3.2.3.1 Preliminary studies on azidoprofen-propyl ester.

Reduction with a 10 fold molar excess of dithiothreitol.

Stock solutions for the propyl-ester (10.7 mM) and DTT (107 mM) were prepared in a solvent composed of acetonitrile: 0.05 M phosphate buffer (50: 50 v/v, final pH 7.4). An aliquot (5 ml) of the ester solution was introduced to a reaction mixture composed of 40 ml of solvent and 5 ml of the DTT stock solution. The mixture, 1.07 mM in ester and 10.7 mM in DTT, was maintained at 37°C with continuous stirring, while 0.5 ml samples were removed at

various intervals for a period of 84 hours. The samples were quenched by the addition of 1 ml of 0.1 M HCl, resulting in a final pH of approximately 1.0, and then frozen until further analysis. Prior to HPLC assay, the samples were diluted with 0.5 ml of a mixture of internal standards (ethyl salicylate: 8 $\mu\text{g ml}^{-1}$ for the amino ester; propyl salicylate: 80 $\mu\text{g ml}^{-1}$ for the azido ester). Two internal standards were necessary as the azido and amino derivatives were detected at different sensitivities and being recorded on separate charts.

Aliquots (100 μl) of the diluted solutions were analyzed using HPLC system K. Concentrations were calculated by interpolation of the peak height ratios of analyte to internal standard, onto a calibration plot prepared from standards chromatographed under the same conditions.

Reduction with a 50 fold molar excess of dithiothreitol

The reduction of the propyl-ester of AZP with a 50 fold molar equivalent of DTT was also investigated, employing a similar experimental procedure as above. The final concentrations were 1.25 mM in ester and 62.5 mM in DTT. Samples were diluted with internal standard solution (ethyl salicylate) and directly assayed by HPLC, using system E and following only the degradation of the ester. Percentage concentrations were calculated by normalization of peak height ratios to the value at the first time point (taken as 100%). A first-order kinetic model was employed to determine the rate of degradation.

Anaerobic reduction

A mixture of acetonitrile and 0.05 M phosphate buffer (50: 50 v/v, final pH 7.4) was degassed by repeated boiling and cooling under a stream of nitrogen. Stock solutions of the ester (12.5 mM) and DTT (125 mM) were prepared in this solvent. An aliquot (5 ml) of the DTT stock solution was incubated with 40 ml of the degassed solvent in a reaction vessel connected to a nitrogen supply and protected from light. The reaction was initiated by the addition of 5 ml of the ester stock solution to the reaction mixture, which was maintained at 37°C with constant stirring and purged with a stream of nitrogen. Samples (0.5 ml)

taken at appropriate intervals were suitably diluted with internal standard and solvent prior to HPLC analysis of 10 µl aliquots employing system E.

3.2.3.2 Anaerobic reduction of azidoprofen and its alkyl esters

Quantities of acetonitrile and phosphate buffer (pH 6.65) were degassed. Stock solutions for the alkyl esters of AZP (12.5 mM in acetonitrile) and DTT (125 mM in phosphate buffer) were prepared. A solvent composed of 10 ml of acetonitrile and 30 ml of phosphate buffer (pH 6.65) was degassed and equilibrated at 37°C. Aliquots (5ml) of an ester and DTT stock solution were added, with constant stirring. The reaction mixtures were 1.25 mM in ester and 12.5 mM in DTT, in a solvent composed of 30% v/v acetonitrile in buffer, final pH 7.4. The experiment was repeated for AZP-Na, reversing the choice of solvent for the azide and DTT stock solutions (i.e., AZP-Na in buffer and DTT in acetonitrile). Samples (0.5 ml) were removed at appropriate time points, suitably diluted with solvent and appropriate internal standard (Table 3.2) prior to HPLC analysis of 10µl samples using system A, C, D or E according to the azide being assayed.

Table 3.2 Analytical conditions for the assay of AZP and corresponding esters.

Compound	HPLC system	Internal standard	Sample diluent	Sensitivity (AUFS)
AZP	A	Butyl paraben 0.080 mg/ml	1.0 ml internal std 1.5 ml solvent	0.16
Methyl ester	C	Propyl salicylate 1.2 mg/ml	0.5 ml internal std 1.0 ml solvent	0.32
Ethyl ester	D	Ethyl salicylate 0.30 mg/ml	1.0 ml internal std 1.5ml solvent	0.16
Propyl ester	E	Ethyl salicylate 0.25 mg/ml	1.0 ml internal std 1.0 ml solvent	0.16

3.3 RESULTS AND DISCUSSION

Incubation of azidoprofen with dithiothreitol (DTT) results in the disappearance of the azide, as monitored by HPLC. The product was identified as 2-(4-aminophenyl)propionic acid [aminoprofen, AMP], by ^1H NMR spectroscopy and this observed reduction by DTT may be illustrated by the example chromatogram in Figure 3.1, where the peak corresponding to AZP can be seen to reduce in height with time. This conversion was not evident in control experiments in the absence of DTT.

The reduction of AZP in phosphate buffer at 37°C followed first-order kinetics over several half-lives throughout the pH range employed (pH 5.80-8.40), as illustrated in Figure 3.2. Pseudo-first order rate constants (k) for the reduction and corresponding half-lives ($t_{1/2}$) were calculated from the slopes of the linear plots of \ln (percentage AZP remaining) against time by linear regression, and are summarized in Table 3.3.

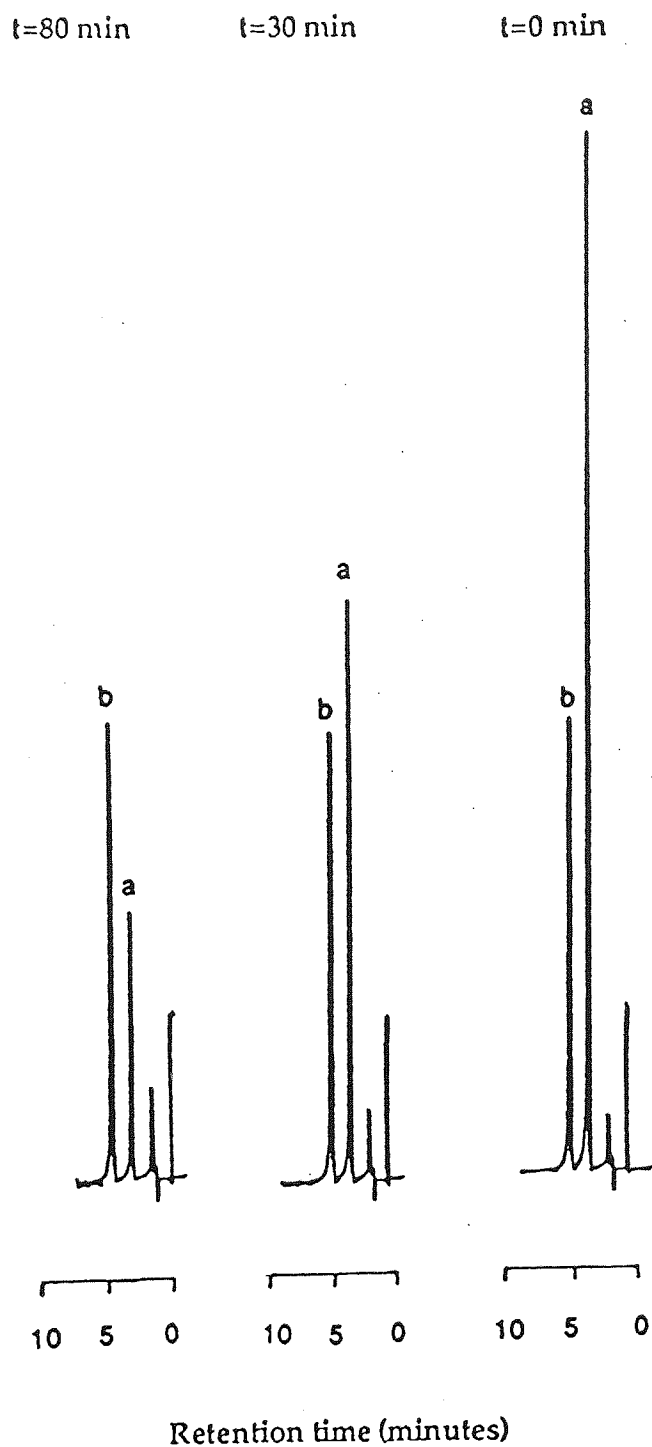


Figure 3.1 Example HPLC chromatogram for the reduction of AZP in phosphate buffer, pH 7.21 at 37°C. (a) AZP, and (b) butyl paraben (IS).

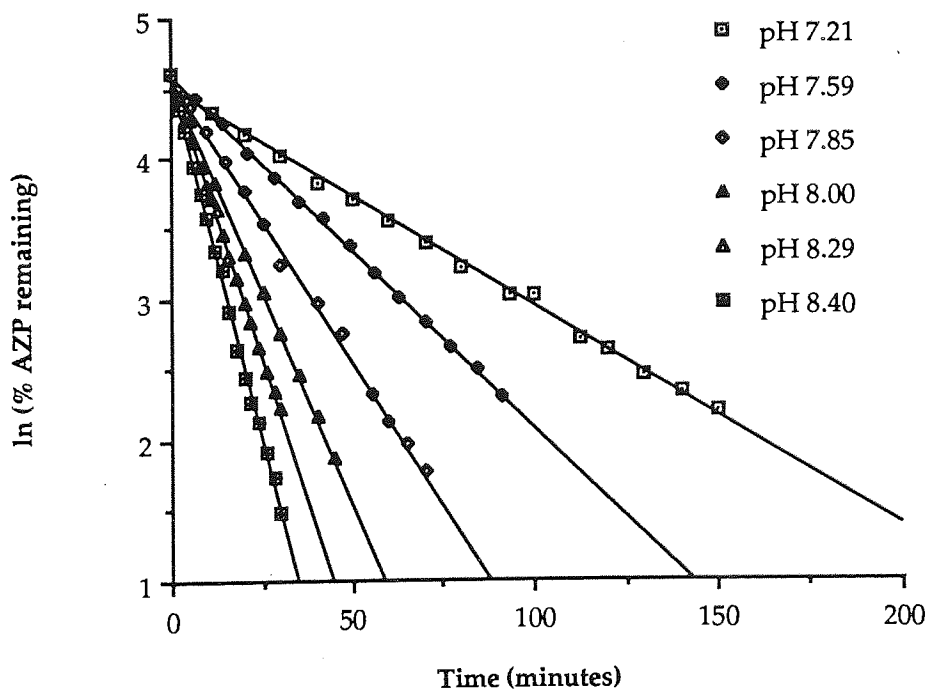
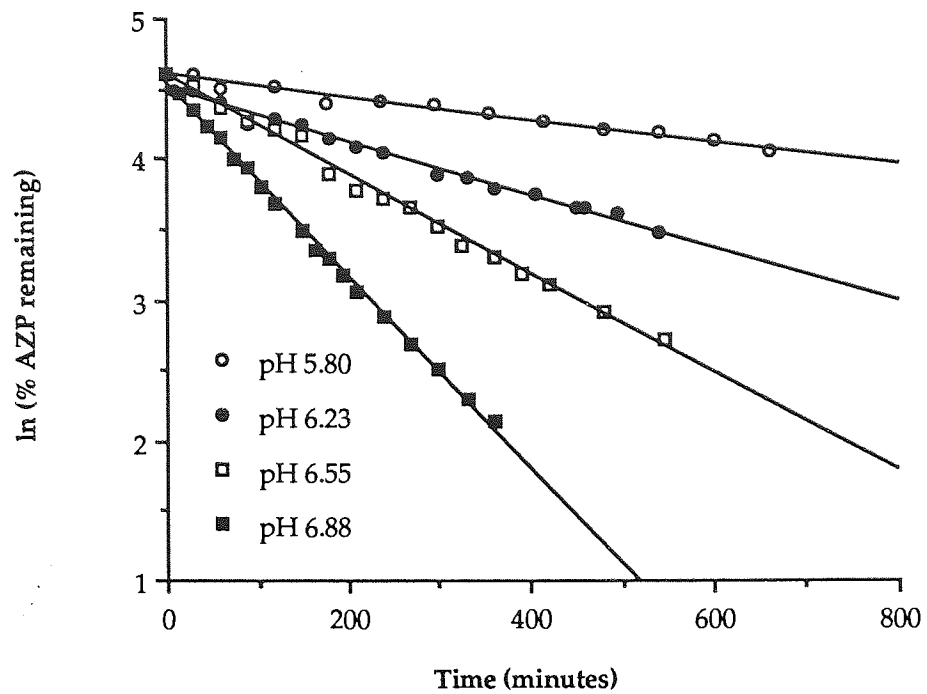


Figure 3.2 Effect of pH on the first-order reduction kinetics of azidoprofen at 37°C.

Table 3.3 Effect of pH on the rate of reduction of azidoprofen at 37°C.

pH	k (min ⁻¹ × 10 ³)	log k	t _{1/2} (minutes)
5.80	0.7518	-3.1239	921.8
6.23	1.8789	-2.7261	368.8
6.55	3.5081	-2.4550	197.5
6.88	6.8512	-2.1642	101.2
7.21	15.566	-1.8078	44.5
7.59	21.542	-1.6667	32.2
7.85	40.362	-1.3940	17.2
8.00	60.358	-1.2193	11.5
8.29	80.454	-1.0945	8.6
8.40	103.38	-0.9856	6.7

The pH-rate profile for the reduction of AZP in phosphate buffers is shown in Figure 3.3. The rate of reduction increases logarithmically with pH, indicating a base-catalyzed reaction. Cartwright *et al* (1976) observed a similar profile for the reduction of 8-azidoadenosine derivatives over this pH range, but reported a rate maxima at pH 10 with rates decreasing rapidly beyond this range.

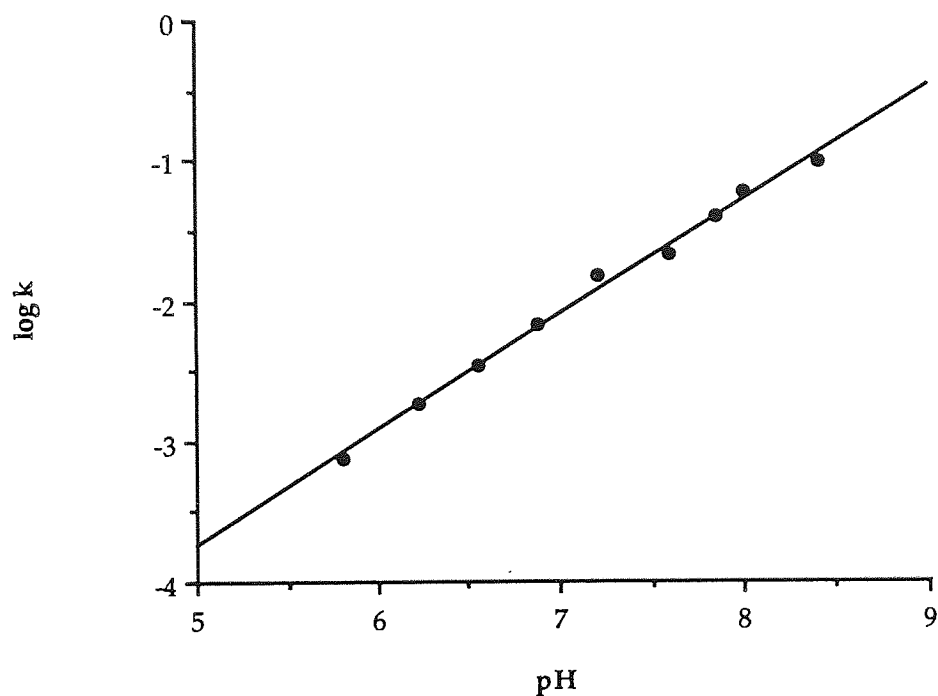


Figure 3.3 pH-rate profile for the base-catalyzed reduction of AZP in phosphate buffer at 37°C.

The observed rate constant, k_{obs} , for the hydrolysis of an ionizable, anionic substrate may be represented by the following equation:

$$k_{obs} = \left[k'_0 [\text{H}_2\text{O}] + k'_{\text{H}_3\text{O}^+} [\text{H}_3\text{O}^+] + k'_{\text{OH}^-} [\text{OH}^-] \right] \cdot \frac{[\text{H}_3\text{O}^+]}{K_a + [\text{H}_3\text{O}^+]} + \left[k_0 [\text{H}_2\text{O}] + k_{\text{H}_3\text{O}^+} [\text{H}_3\text{O}^+] + k_{\text{OH}^-} [\text{OH}^-] \right] \cdot \frac{K_a}{K_a + [\text{H}_3\text{O}^+]} \quad (3.1)$$

where k'_0 , $k'_{\text{H}_3\text{O}^+}$ and k'_{OH^-} refer to the rate constants for solvent, acid and base catalysis respectively for the undissociated species. The terms k_0 , $k_{\text{H}_3\text{O}^+}$ and k_{OH^-} are the corresponding rate constants for the ionized species. K_a is the dissociation constant for the acid and the terms $[\text{H}_3\text{O}^+]/(K_a + [\text{H}_3\text{O}^+])$ and $K_a/(K_a + [\text{H}_3\text{O}^+])$ refer to the concentration of the unionized, [HA], and ionized, [A⁻] species respectively. With a $\text{p}K_a$ of 4.294, AZP is predominantly in the ionized form over the pH range of this study, thus equation 3.1 reduces to:

$$k_{obs} = (k_0 [\text{H}_2\text{O}] + k_{\text{H}_3\text{O}^+} [\text{H}_3\text{O}^+] + k_{\text{OH}^-} [\text{OH}^-]) [A] \quad (3.2)$$

where A represents the drug undergoing degradation. In solutions of high pH, the hydrogen ion concentration is negligible relative to that of the hydroxyl ion and the $k_{\text{OH}^-} [\text{OH}^-]$ term will dictate the degradation rate. Under such conditions, if the reaction is base catalyzed and not subject to other catalytic reactions, equation (3.2) reduces to:

$$k_{obs} = k_{\text{OH}^-} [\text{OH}^-] = k_{\text{OH}^-} \cdot \frac{[K_w]}{[\text{H}_3\text{O}^+]} \quad (3.3)$$

and $\log k_{obs} = \log (k_{\text{OH}^-} \cdot K_w) + \text{pH} \quad (3.4)$

A plot of $\log k_{obs}$ against pH should therefore be linear with a slope equal to unity and intercept equal to the product of the hydroxyl ion catalytic rate constant and K_w (ionic product of water). Analysis of the data in Figure 3.3 gives a straight line ($r = 0.998$) with a positive slope of 0.8250. The value of k_{OH^-} is $1.37 \times 10^6 \text{ l mol}^{-1} \text{ min}^{-1}$. Deviation of the slope from unity implies that hydroxyl ion catalysis is not the sole catalytic reaction influencing the

reduction. Catalysis by other species such as buffer components may also be important. Indeed, phosphate ions are well known to complex with other organic and inorganic ions (Perrin and Dempsey, 1974). More importantly, as discussed below, the postulated mechanism of reduction may also help to explain this discrepancy.

For a reaction undergoing both acid and base catalysis, according to equation 3.2, the $k_{\text{H}_3\text{O}^+}[\text{H}_3\text{O}^+]$ term would also be expected to influence the rate of decomposition at pH values below 7.0. In solutions of low pH, the hydrogen ion concentration will exceed that of the hydroxyl ion. Under such conditions specific hydrogen ion catalysis will be observed if the reaction is not subject to other catalytic reactions, and equation 3.2 can be expressed as:

$$k_{\text{obs}} = k_{\text{H}_3\text{O}^+} \cdot [\text{H}_3\text{O}^+] \quad (3.5)$$

$$\text{and} \quad \log k_{\text{obs}} = \log k_{\text{H}_3\text{O}^+} - \text{pH} \quad (3.6)$$

A plot of $\log k_{\text{obs}}$ against pH should therefore give a straight line with a negative slope equal to unity. Consequently, at low pH values the rate of reduction would be expected to increase, resulting in a 'V' shaped relationship. The pH value corresponding to the minimum rate of degradation would be dependent on the relative magnitudes of k_{OH^-} and $k_{\text{H}_3\text{O}^+}$. Since the data continues to obey a linear relationship at pH values below 7.0 and there is no indication of an increased rate of reduction at lower pH's, as determined from preliminary experimental work, one may assume that the rate constant for acid catalysis is of relatively small magnitude and that the decomposition is predominantly base-dependent.

The manner in which the hydroxyl ion concentration influences the rate of reaction may be explained by a consideration of the postulated mechanism of thiol-mediated azide reduction, as proposed by Cartwright *et al* (1976).

Figure 3.4 illustrates one of the mechanisms by which the reaction is thought to proceed. An attack by the thiolate anion on the terminal nitrogen of the azide is followed by intramolecular cyclization and loss of nitrogen to produce the cyclic disulphide and the arylamine.

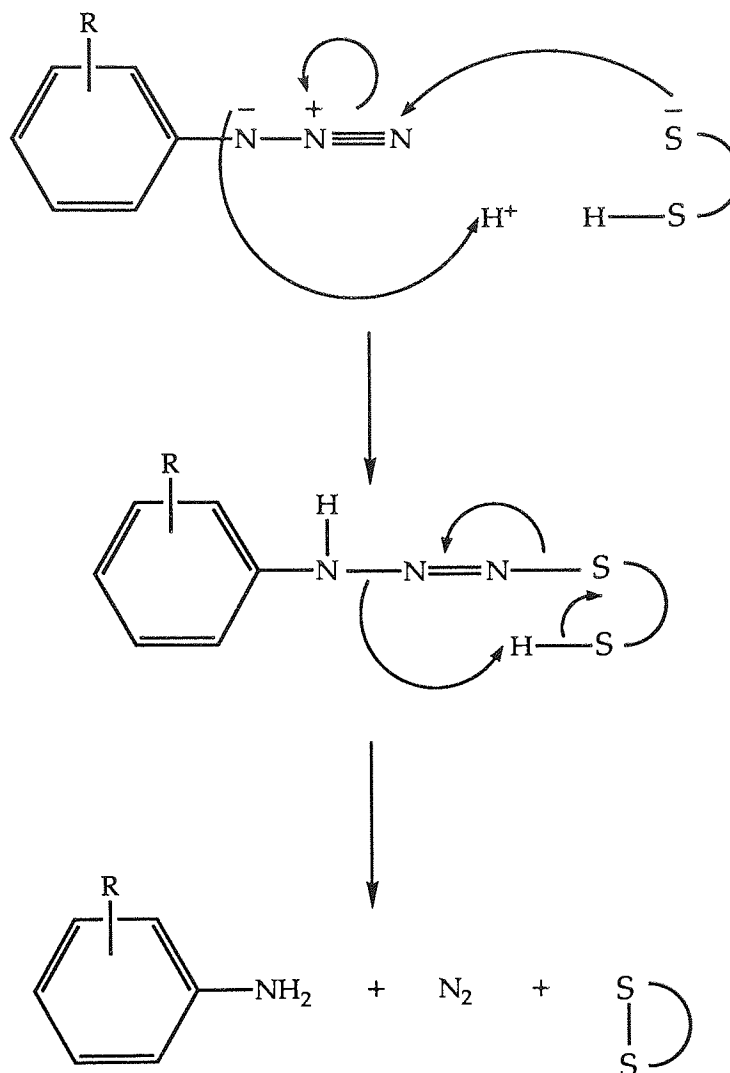


Figure 3.4 Proposed mechanism of reduction for aryl azides (Cartwright *et al*, 1976)

This suggests that in this scheme, hydroxyl ions catalyze the reaction by ionizing the thiol, rather than direct reaction with the azide group. Consequently, ionization of the thiol moiety appears to be the base-dependent step. The pK_a values of DTT are 8.3 and 9.5 (Zahler and Cleland, 1968), hence over the pH range of study (5.80-8.40), small changes in hydroxyl ion

concentration will have a great effect on the degree of ionization of DTT and the amount of thiolate ion available for nucleophilic attack. This indirect base-catalysis may also explain the deviation from unity of the slope of the linear relationship between $\log k_{\text{obs}}$ and pH, since the degree of ionization of the thiol as a function of pH will not be linear at all values.

The observation that the hydroxyl ion rate constant dictates the degradation rate even at lower pH's, lends further support to the theory that the thiolate anion is the species which reacts initially with the azide group. In summary, the rate of reduction is presumably dependent upon the concentration of the thiol anion, the rate of formation of which is in turn base-dependent.

The HPLC method employed, allowed only the quantitative analysis of AZP degradation. The decomposition product AMP, as a result of increased polarity eluted close to the solvent front, and therefore its formation could not be quantified under the the same analytical conditions. Furthermore, at a mobile phase pH of 2.5, employed such that AZP would be present in an unionized form, protonation of the amino (NH_2) residue to the NH_3^+ species occurred. The consequent modification of its UV absorbing chromophore resulted in a lower molar absorption coefficient (section 2.3.1; Table 2.1) which further complicated attempts to measure both AZP and AMP together. In contrast, ^1H NMR spectroscopy enabled kinetic analysis of both AZP degradation and AMP formation (Figures 3.5 and 3.6). As AZP was reduced to AMP, an upfield chemical shift of the *ortho* and *meta* protons (relative to the azido/amino substituent) was observed, due to a shielding effect produced by the electron-donating nature of the NH_2 group. During a kinetic run, both species could be detected by the presence of the aromatic *o* and *m* protons of AZP at 6.9 and 7.2 ppm and those of AMP at 6.7 and 7.0 ppm respectively.

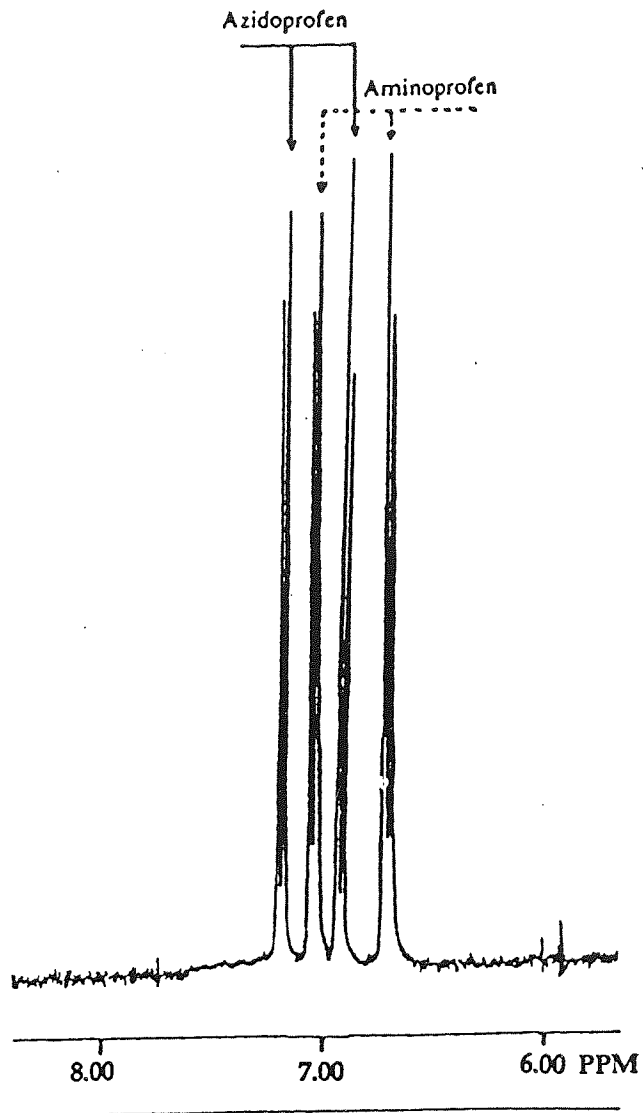
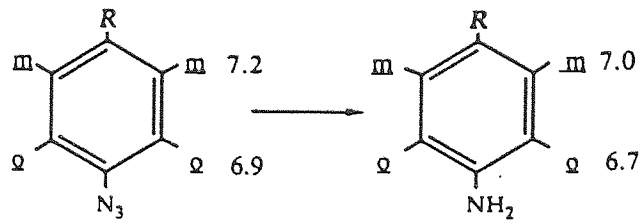


Figure 3.5 NMR spectrum illustrating the upfield shift of *ortho* and *meta* protons as AZP is reduced to AMP. R = CH(CH₃)COOH

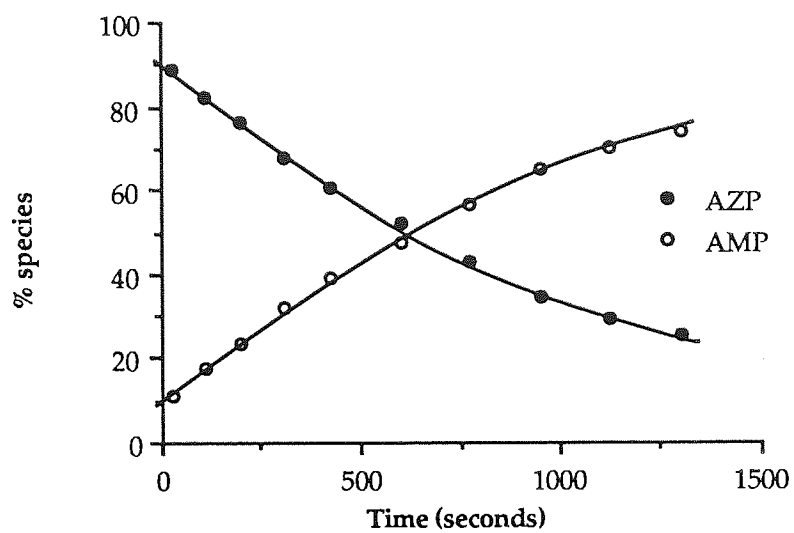


Figure 3.6 Time courses for AZP and AMP during reduction at pH 6.95 as determined by NMR spectroscopy.

The effect of thiol concentration on the rate of AZP reduction was studied utilizing NMR spectroscopy as the analytical technique. Figure 3.7 A displays typical reduction profiles for AZP, which follow pseudo-first order kinetics. As can be seen in Figure 3.7 B, the rate varies linearly with DTT concentration.

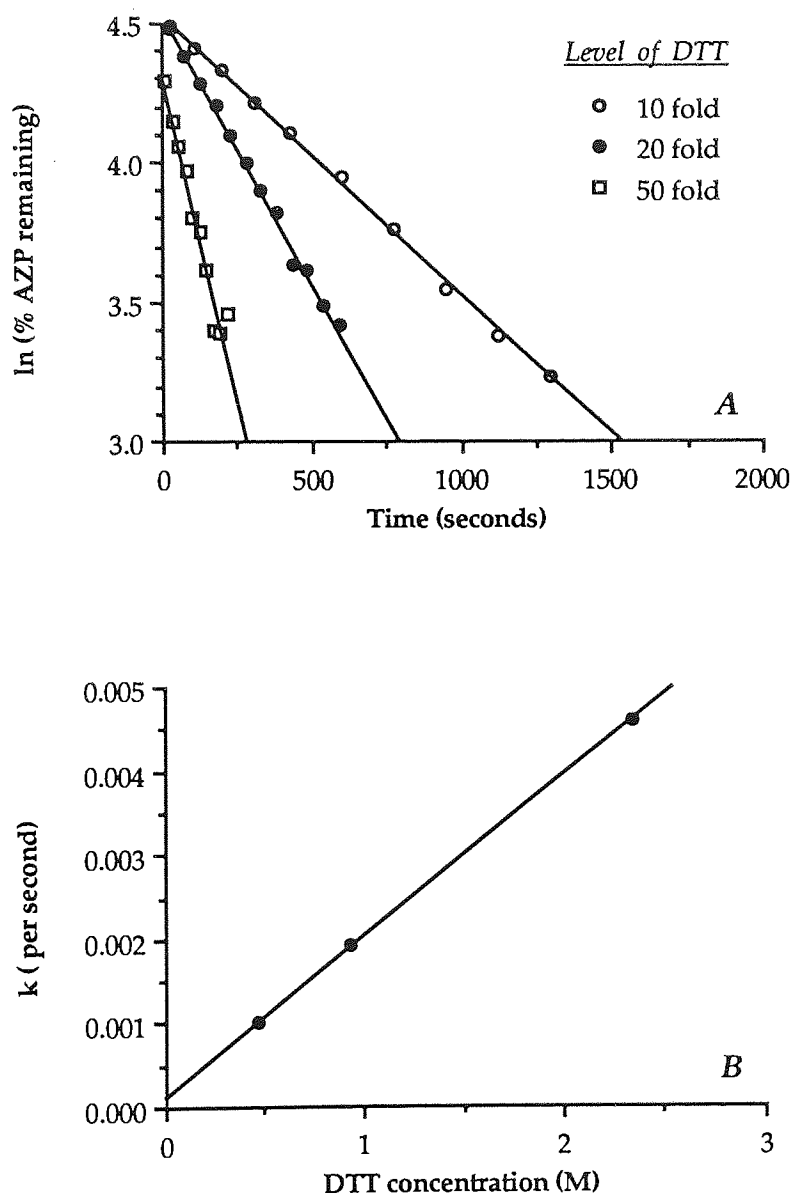


Figure 3.7 Effect of DTT concentration on the reduction of AZP at pD 6.95, as determined by NMR spectroscopy.

The validity of the quantitative method used to determine the percentage AZP remaining with time and resultant pseudo-first order rate constants required verification. Two analogous experiments, one using HPLC and the other NMR spectroscopy as methods of quantitative analysis, were conducted in order to compare the data obtained from the two individual methods. The pseudo-first order reduction profiles as determined by the two techniques, are illustrated in Figure 3.8 together with their respective rate constants. The close agreement of the two values confirms the validity of the NMR method of analysis.

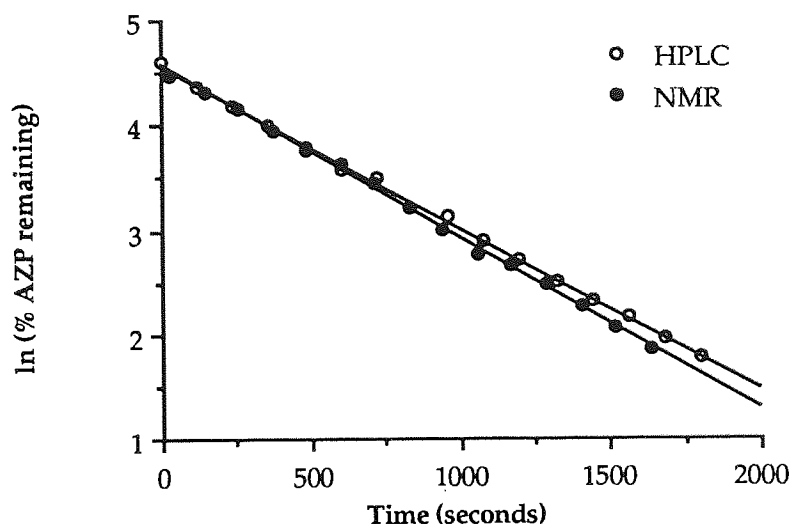


Figure 3.8 First-order plots for the reduction of AZP, determined by NMR analysis ($k = 1.64 \times 10^{-3} \pm 1.95 \times 10^{-5} \text{ sec}^{-1}$) and HPLC analysis ($k = 1.54 \times 10^{-3} \pm 1.41 \times 10^{-5} \text{ sec}^{-1}$) ($\pm \text{SE}$, $n = 15$).

Following incubation of AZP (1.25 mM) with GSH (12.5 mM) in phosphate buffer (pH 7.4) at 37°C for 24 hours, no azide degradation was observed. However, azide reduction was noticeable under more forcing reaction conditions (62.5 mM GSH, pH 8.4) over a period of 36 hours. Although reduction occurred at a much slower rate than with DTT, this preliminary study suggests that the potential does exist for intracellular conversion of azides by endogenous thiols such as glutathione.

In preliminary studies with liver homogenates, no significant loss of azide was observed following a 60 minute incubation period. A HPLC assay for AMP was not sensitive enough to adequately detect any amine, which may have been formed. Although these initial experiments suggest that AZP is not susceptible to liver metabolism, further studies are required to confirm this result. In particular, the viability of the liver homogenate preparation must be verified and an assay to monitor AMP formation improved.

Reduction of the alkyl esters of AZP using the DTT model system was also studied, in an attempt to investigate the dependence of the rate of azide conversion on structural modifications. Figure 3.9 illustrates the postulated decomposition pathways for the azido-esters. The relative importance of these degradation routes is discussed in section 4.1. However, for the purpose of the current study, it was necessary to determine whether reduction was accompanied by parallel (A to B) or consecutive (D to C) hydrolysis. In order to achieve this, HPLC methods were developed to detect three of the components in Figure 3.9 (azido-ester, amino-ester, azido-acid) for all three esters, while the fourth component (amino-acid) was determined by mass balance. In preliminary experiments, employing HPLC systems to detect products of both the reduction and potential hydrolysis, no hydrolytic decomposition was observed. Therefore, in subsequent reduction studies, only the decomposition of the azido-ester was kinetically modelled, with the assumption that reduction to the corresponding amino-ester was the only reaction occurring.

Due to the low aqueous solubility of the esters of AZP, acetonitrile was employed as a co-solvent. It became apparent that on including acetonitrile in the solvent system, the rate of degradation was reduced significantly (pseudo-first order rate constants for AZP in phosphate buffer, pH 7.4: $1.74 \times 10^{-2} \text{ min}^{-1}$; in 30% MeCN-buffer, pH 7.4: $3.64 \times 10^{-3} \text{ min}^{-1}$). The consequent increased reaction times necessitated the introduction of an additional experimental precaution; that of performing the studies in the absence of oxygen.

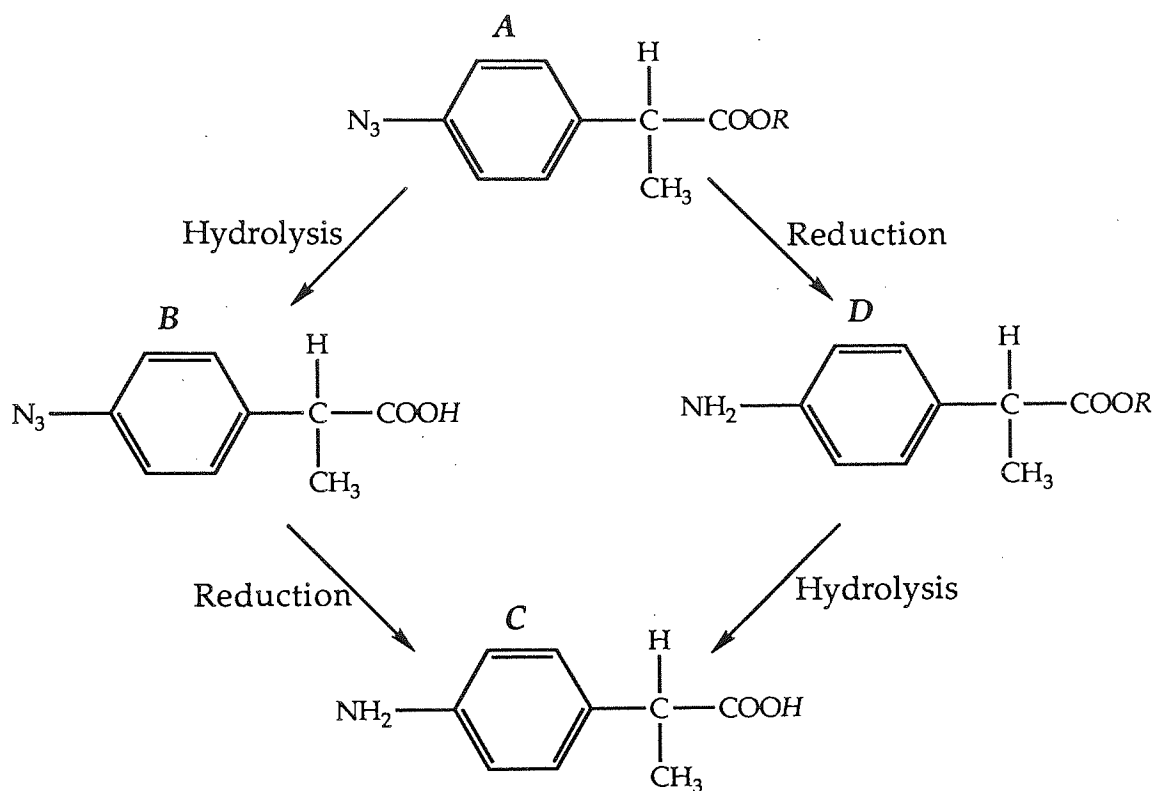


Figure 3.9 Schematic illustration of decomposition pathways for the alkyl esters of AZP. $R = C_nH_{2n+1}$

Thiols are known to undergo oxidation on exposure to air (Capozzi and Modena, 1974). Disulphides are the dominant product, although prolonged reaction times cause oxidation beyond the disulphide level in aqueous solutions. Both the rate (Wallace and Schriesheim, 1963a) and extent (Wallace and Schriesheim, 1963b) of oxidation are increased in dipolar-aprotic solvents under mild conditions. As the mechanism of reduction of the azido group is dependent on the presence of the un-oxidised thiolate anion, it is plausible that depletion of this species *via* aerobic oxidation during the course of the reaction results in a reduced rate of reduction. Furthermore, the presence of acetonitrile, a dipolar-aprotic solvent, may accelerate this process.

This possibility was supported by the observation made when following the reduction of the propyl-ester, in the presence of oxygen for a period of 84 hours. As Figure 3.10 A shows, the pseudo-first order rate of reduction appears to gradually decrease, becoming constant after approximately 35 hours, indicating a cessation of the reaction process. One other possible explanation was that the residual material, which did not reduce any further was an impurity in the propyl-ester. However, NMR analysis and the magnitude of the residual concentration (~20% of initial level) did not support this.

DTT concentration is another factor governing the rate of reduction. A ten-fold molar ratio had been used as for the reduction of the parent acid AZP, where the reaction had approached completion. The initial DTT concentration used for the ester was therefore sufficient to allow complete reduction. Reaction with a 50 fold molar excess of DTT followed first-order kinetics over several half-lives as shown in Figure 3.10 B, and suggested that the initial observations were associated with DTT availability.

That DTT depletion resulting from aerial oxidation was responsible for the unusual reaction profile, was confirmed by repeating the reduction with a 10 fold molar equivalent of DTT in the absence of oxygen. Figure 3.10 C shows that the reaction now follows first order kinetics with a reduction rate constant of 0.0978 hr^{-1} and $t_{1/2}$ of 7.14 hours.

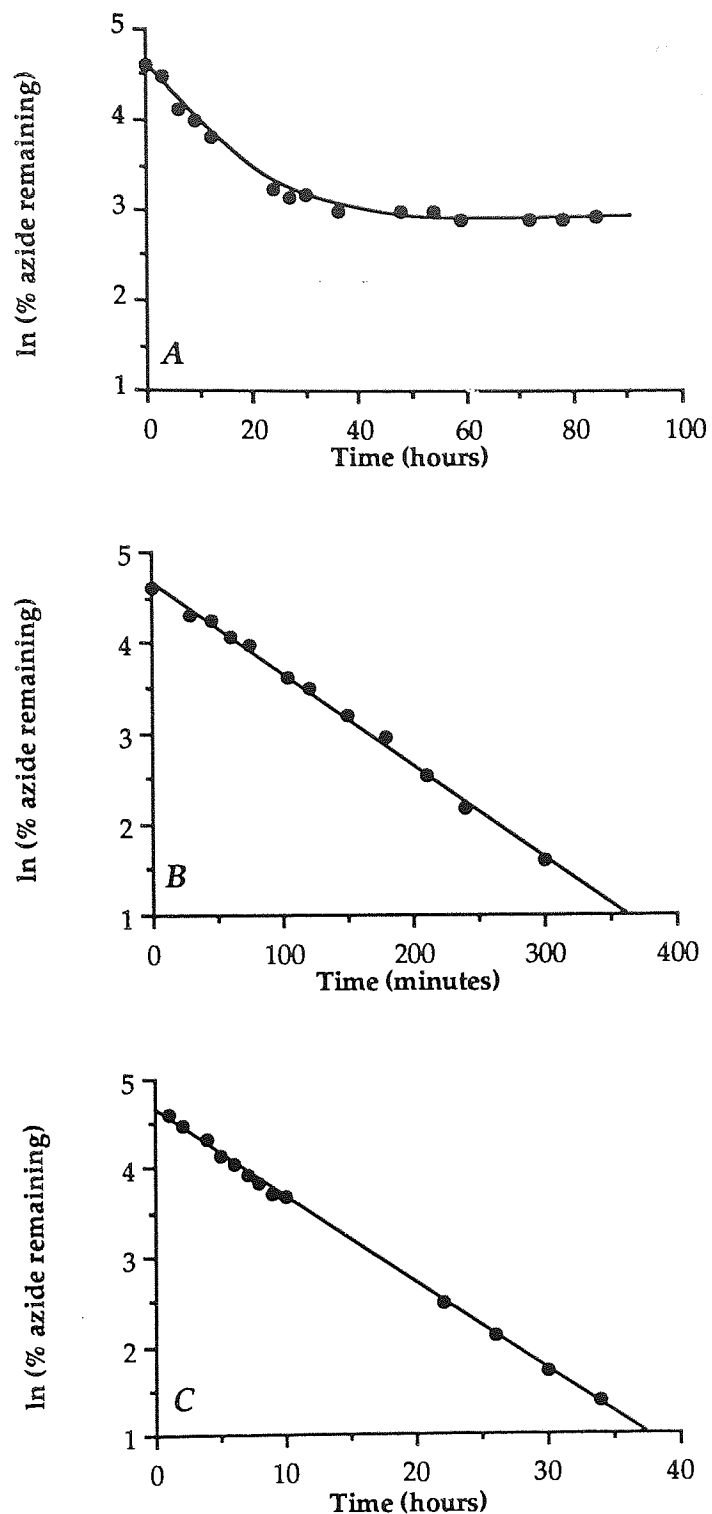


Figure 3.10 Reduction of the propyl ester of AZP in 50% acetonitrile-buffer, pH 7.4 at 37°C.

A: aerobic reduction with 10-fold molar excess of DTT;

B: aerobic reduction with 50-fold molar excess of DTT ($k = 0.0102 \text{ min}^{-1}$);

C: anaerobic reduction with 10-fold molar excess of DTT ($k = 0.0978 \text{ hr}^{-1}$).

Thiol depletion by aerobic oxidation should therefore be regarded as an important phenomenon, particularly over prolonged reaction times. Subsequent reduction studies for the esters of AZP were performed under anaerobic conditions.

Example HPLC chromatograms and first-order plots illustrating the reduction kinetics for AZP and its methyl, ethyl and propyl esters are displayed in Figure 3.11 and 3.12 respectively. The latter data show that there is little difference in the pseudo-first order rate constants for the different esters, although the rank order of reduction rates (Table 3.4) is comparable to that of normal ester hydrolysis rates (Isaacs, 1987). AZP is reduced much more slowly and this may be a consequence of its ionization state. At a pH of 7.4 AZP would be expected to be completely ionized. The electron-donating nature of the carboxylate anion may be responsible for stabilizing the N₃ moiety and rendering it less susceptible to nucleophilic attack by the thiolate ion. Alternatively, charge repulsion between the two ionized species may also hinder reaction. In contrast, the unionized esters would be expected to be more labile. This would be consistent with the findings of Staros *et al* (1978) and Baker *et al* (1989) who reported faster rates of reduction for electron-deficient aryl azides, supporting a pathway involving rate-limiting nucleophilic addition to the azide group.

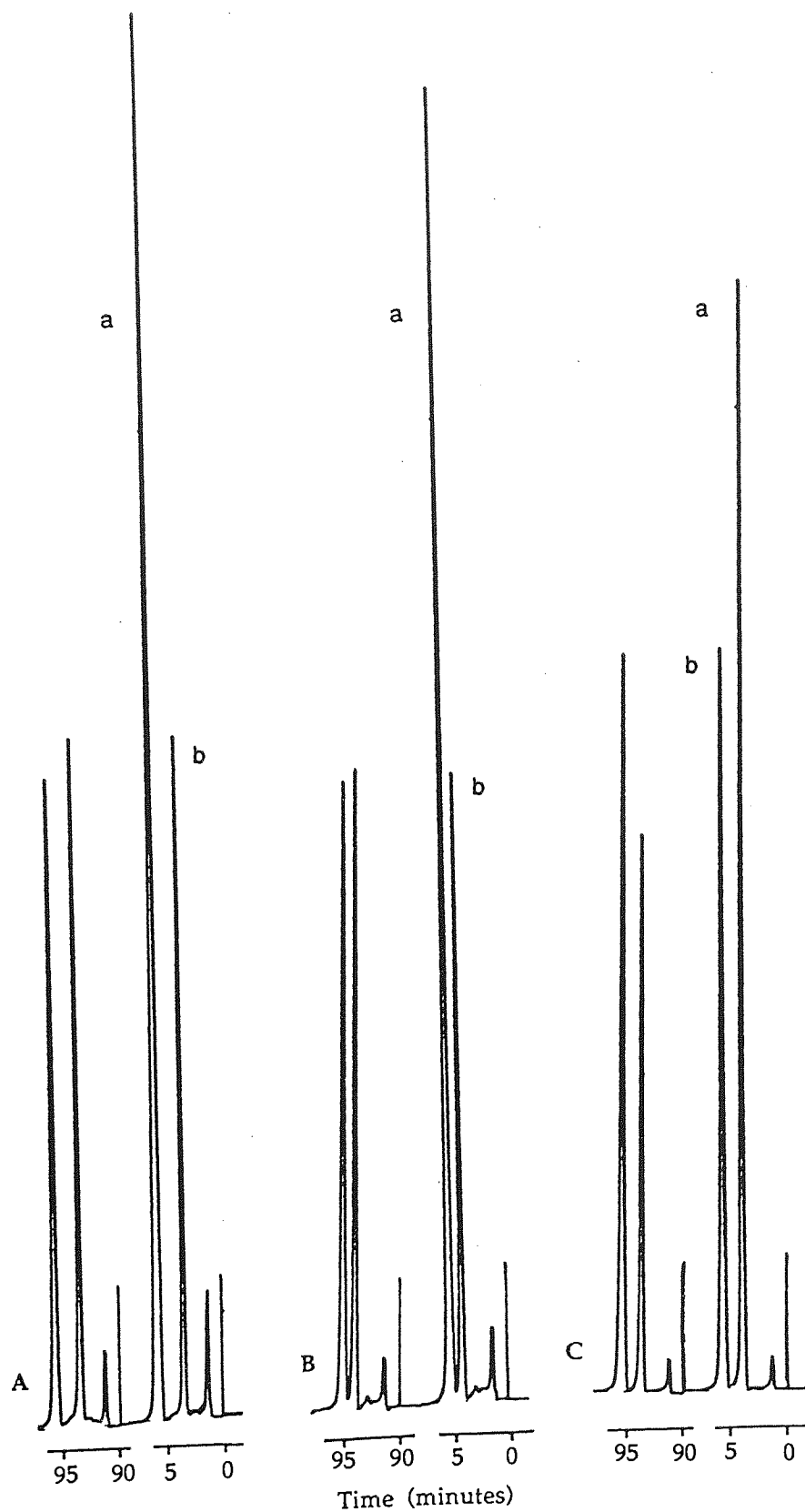


Figure 3.11 Example HPLC chromatograms for the methyl (A), ethyl (B) and propyl (C) esters of AZP. a = ester, b = internal standard; propyl salicylate in A and ethyl salicylate in B and C.

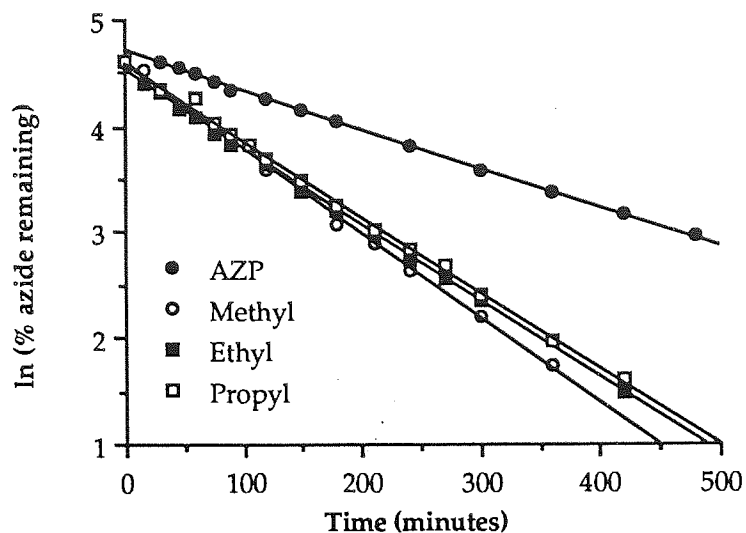


Figure 3.12 First-order reduction profiles for AZP and its alkyl esters in 30% acetonitrile-buffer, pH 7.4 at 37°C.

Table 3.4 Reduction data for AZP and its alkyl esters in 30% acetonitrile-buffer, pH 7.4 at 37°C.

Compound	k ($\text{min}^{-1} \times 10^3$)	$t_{1/2}$ (minutes)
AZP	3.6416	190.3
Methyl ester	8.0491	86.1
Ethyl ester	7.2420	95.7
Propyl ester	7.1982	96.3

3.4 SUMMARY

AZP undergoes a rapid, base-catalyzed reduction by DTT *in vitro*, in aqueous solution at physiological temperature. The base-dependence of the reaction lends support to the view that the nucleophilic thiolate ion (RS^-) is the predominant reducing species. Thiol-mediated reduction may be proposed as an intracellular detoxification mechanism for aryl azides, where sources of endogenous thiols including glutathione may be utilized as suitable *in vivo* reducing agents. The conditions of the *in vitro* model with respect to DTT concentration and pH, may be modified to facilitate kinetic modelling, permitting comparison between analogous compounds. This model *in vitro* system may therefore be useful in conducting a preliminary assessment of the relative potentials for the *in vivo* metabolism of azides.

CHAPTER FOUR
METABOLIC TRANSFORMATION OF AZIDOPROFEN ESTERS

4.1 INTRODUCTION

The "soft-drug" approach to drug design, as discussed earlier (chapter one, section 1.3), involves the predictable *in vivo* detoxification of an active drug after therapeutic activity, in order to minimize systemic toxicity. In contrast, the "prodrug" concept involves the controlled *in vivo* bioactivation of a previously inactive species, prior to eliciting a pharmacological response. A prodrug may therefore be defined as a pharmacologically inactive derivative of a parent drug molecule, which requires chemical or enzymatic *in vivo* transformation to regenerate the active drug (Bundgaard, 1985).

Prodrug modification is a valuable tool for manipulation of the physicochemical properties of a parent drug. Such an approach has been used to improve solubility, lipophilicity, chemical and enzymatic stability, taste and reduce irritability; thereby enhancing its biopharmaceutical profile with respect to delivery, efficacy and patient acceptability. In recent years, NSAIDs have been the focus of bioreversible derivatization in order to depress their gastrointestinal side-effects (Jones, 1985). Temporary masking of the carboxylic acid function *via* esterification, for example, has been proposed as a promising means of reducing gastro-intestinal irritation (Whitehouse and Rainsford 1977).

Esterification is also a useful means of modifying the lipophilicity of drug derivatives, thereby furnishing a prodrug which has ideal characteristics for partitioning into the stratum corneum and which therefore permeates the skin more readily than the parent compound. Reversion to the parent drug is facilitated by enzyme-catalyzed ester cleavage, a process which can exploit the significant metabolic capacity of the skin (Bucks, 1984; Hadgraft, 1985). The predominance of carboxylic acid and hydroxyl groups in drug molecules together with the abundance of cutaneous hydrolytic enzymes makes esterification an excellent prodrug type for dermal delivery.

Although esterification is perhaps the most common form of prodrug derivatization, it is by no means exhaustive. The skin is recognized as a highly active metabolic organ and cutaneous enzymes other than esterases, which can metabolize a wide range of endogenous and exogenous substances have been identified (Table 4.1) (Kappus, 1989; Noonan and Wester, 1985; Pannatier *et al*, 1978). Consequently, enzyme-labile derivatives other than esters, which are able to utilize this vast range of cutaneous enzyme activities for bioactivation have also been considered (Chan and Li Wan Po, 1989). A variety of topical drugs have been the subject of such prodrug modifications in order to improve their penetration profile and/or localize drug action within the skin (Table 4.2).

In the context of present definitions of prodrugs and soft drugs, ester derivatives of AZP may be regarded as "pro-soft drugs", designed to enhance the topical bioavailability of the parent drug. Figure 4.1 illustrates a simplified scheme for the postulated decomposition of the azido-ester.

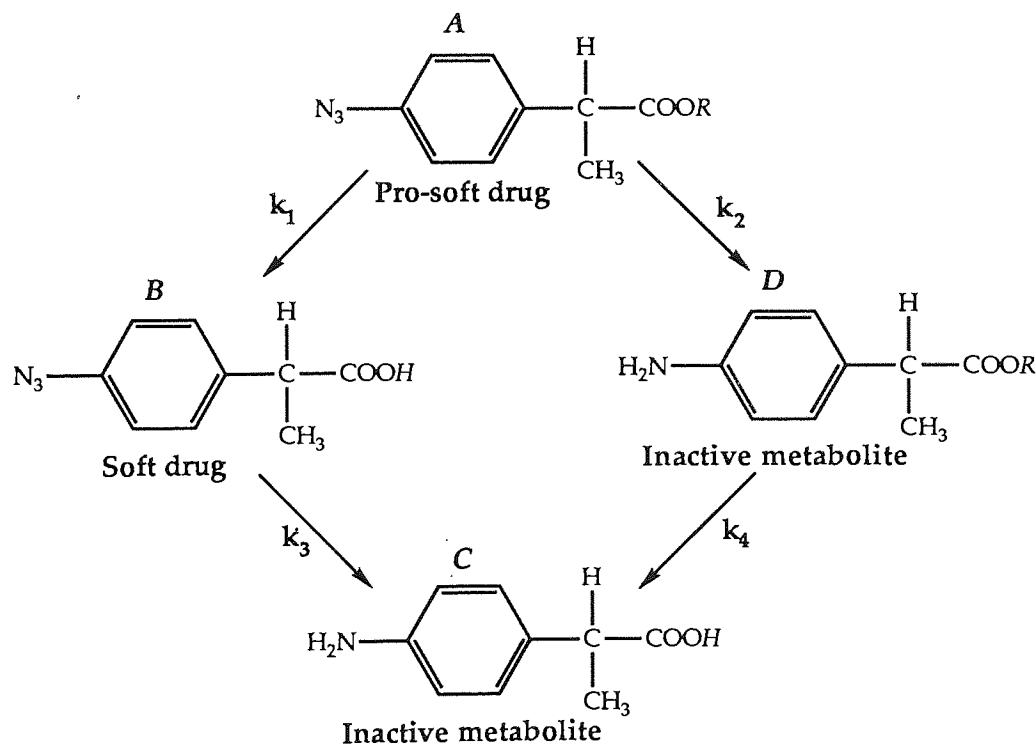


Figure 4.1 Postulated decomposition pathways for esters of AZP.

Table 4.1 Example biotransformation reactions in the skin (Täuber, 1982)

Reaction	Enzyme(s) involved	Example substrate
<u>Phase I functionalization</u>		
<i>Oxidation</i>		
aliphatic C-atoms	mixed function oxidase	dimethylbenz(a)anthracene
alicyclic C-atoms	mixed function oxidase	dehydroepiandrosterone
aromatic rings	hydroxylases	3,4-benzopyrene
alcohols	dehydrogenases	cortisol
deamination	monoamine oxidases	norepinephrine
dealkylation	dethylase, demethylase	7-ethoxycoumarin aminopyrine
<i>Reduction</i>		
carbonyl groups	ketoreductase	cortisol progesterone oestrone androstanedione
C=C bonds	5 α -reductase	testosterone progesterone
<i>Hydrolysis</i>		
esters	esterases	glucocorticoid esters e.g., fluocortin-butylester diflucortolone-21-valerate
epoxides	epoxidehydratase	styrene oxide
<u>Phase II conjugation</u>		
glucuronidation	UDPG-transferase	hydroxybenzopyrene
sulphation	sulpho-transferases	dehydroepiandrosterone aminophenol
methylation	catechol O-methyl transferases	norepinephrine
glutathione conjugation	glutathione-S-transferases	styrene glycol

Table 4.2

Examples of prodrugs developed for topical use.

Bioconversion mechanism/ Parent drug	Prodrug derivative	Intended therapeutic area	Reference
Chemical hydrolysis			
5-Fluorouracil	N-Mannich bases	Psoriasis	Sloan <i>et al</i> , 1984b Sloan <i>et al</i> , 1988
Indomethacin	N,N-Dialkylhydroxylamine derivatives	Anti-inflammatory	Sloan <i>et al</i> , 1984a
6-Mercaptopurine	N-Mannich bases	Psoriasis	Siver and Sloan, 1988
Theophylline	N-Mannich bases	Psoriasis	Sloan <i>et al</i> , 1984b
Enzymic hydrolysis			
Aspirin and salicylic acid	Methylthiomethyl and methylsulfinylmethyl esters	Anti-inflammatory	Loftsson and Bodor, 1981a & b
Difluocortolone	Valerate ester	Anti-inflammatory Anti-proliferative	Täuber and Toda, 1976; Täuber, 1982
Dithranol	Triacetate esters	Psoriasis	Wiegrebbe <i>et al</i> , 1984
5-Fluorouracil	N-Acyloxymethyl derivatives	Psoriasis	Møllgaard <i>et al</i> , 1982
Hydrocortisone	Spirothiazolidine derivative	Anti-inflammatory Anti-proliferative	Bodor <i>et al</i> , 1982
6-Mercaptopurine	Bisacyloxymethyl derivatives	Psoriasis	Waranis and Sloan, 1987
	Acyloxymethyl derivatives	Psoriasis	Waranis and Sloan, 1988
Metronidazole	Aliphatic esters	Anti-bacterial	Johansen <i>et al</i> , 1986
Vidarabine	5'-Valerate ester	Anti-viral	Yu <i>et al</i> , 1979, 1980a & b
	5'-Monoesters	Anti-viral	Higuchi <i>et al</i> , 1983
Enzymic oxidation			
Theophylline	Acyloxymethyl derivatives	Psoriasis	Sloan and Bodor, 1982
Enzymic reduction			
Cromolyn	Pivaloyloxymethylnitrate ester	Anti-inflammatory	Bodor <i>et al</i> , 1980

To meet our design approach, the pro-soft drug (A) is required to undergo hydrolysis to the soft drug (B) after penetrating the epidermal barrier; a bioactivation process which should be facilitated in the presence of skin esterases. Metabolism of the active entity to the inactive species (C) subsequent to exerting a pharmacological response is the next requirement.

For this strategy to be satisfied, k_1 must be greater than k_2 , such that the dominant pathway follows the following kinetic model.



The complexity of this series of events, progression of which is dependent upon a multitude of pharmacokinetic and physicochemical parameters involving drug (prodrug, soft drug, metabolite), vehicle and membrane is self-evident. Theoretical studies, mathematically modelling the concurrent penetration and metabolism of drugs in the skin (Ando et al, 1977; Guy and Hadgraft, 1982 and 1984) could serve to facilitate the rational evaluation of topical prodrug delivery in such instances. A prior understanding of the factors governing the transport and metabolism of biologically labile compounds is, however, a prerequisite.

In the current study, a series of ester prodrugs of AZP with a range of lipophilicities were investigated for susceptibility to enzymatic and chemical hydrolysis using *in vitro* models, namely isolated enzyme systems and skin homogenates, in order to assess their prodrug potential.

4.2 EXPERIMENTAL

4.2.1 Enzymatic hydrolysis

Porcine liver esterase

The porcine liver esterase used in the metabolic studies was a commercially available purified carboxylic ester hydrolase (Sigma Chemicals), suspended in 3.2 M ammonium sulphate solution adjusted to pH 8. Each mg of protein was

equivalent to 260 units, where each unit was capable of hydrolyzing 1 μ l of ethyl butyrate per minute at pH 8 and at a temperature of 25°C. The esterase solution contained 10.5 mg of protein per ml of solution and was diluted as appropriate with distilled water, prior to use.

Concentrated Tris buffer solution

Concentrated Tris buffer solutions (0.5 M; pH 7.5 and 8.2) were prepared according to Appendix 2, using a tenfold salt concentration, such that a constant ionic strength would be maintained on dilution.

4.2.1.1 Porcine liver esterase studies

In Propylene Glycol

A reaction mixture consisting of (a) 5 ml of concentrated Tris buffer (pH 8.23), (b) 5 ml of propylene glycol (PG), (c) 34 ml of distilled water and (d) 1 ml of porcine esterase solution (11 units per ml) was incubated in a reaction vessel at 37°C with constant stirring and protection from light. The reaction was initiated by the addition of 5 ml of an AZP-methyl ester stock solution (5 mM in PG). The final composition of the mixture was 20% propylene glycol and 80% Tris buffer solution with a final pH of 8.02. The concentrations of esterase and ester were 22 units % (22 units per 100 ml) and 0.5 mM respectively. Control experiments, substituting distilled water for the esterase solution, were also conducted.

Samples (0.5 ml) withdrawn at appropriate intervals during the experiment were diluted with 0.5 ml of IS solution (butyl paraben: 40 μ g ml⁻¹ in 20% PG) prior to analysis of 10 μ l aliquots using system A. Concentrations of both the ester and AZP (hydrolysis product) were calculated by interpolation of peak height ratios (phrs) onto a calibration line prepared from standards chromatographed under the same conditions.

In alcohols

Concentrated pH 8.23 Tris buffer (2 ml), distilled water (15.8 ml) and porcine esterase solution (0.2 ml; 55 units/ml) were mixed together and equilibrated at 37°C. An aliquot (2 ml) of the ester stock solution (5 mM in 95% ethanol) was introduced to initiate the hydrolysis. The final composition was 0.5 mM in ester and 55 units % in esterase, in a solvent comprising 10% v/v ethanol (95%) with a pH of 8.06. Experiments were performed in duplicate together with controls, omitting the esterase solution.

Samples of 0.5 ml, removed during the course of the reaction, were diluted with an equal volume of solvent (10% aqueous EtOH) and 1 ml of IS solution (butyl paraben: 20 µg ml⁻¹ in 10% EtOH). After HPLC analysis employing system A, concentrations of the reactant, the intermediate (in case of transesterification) and the product (AZP) were determined by measurement of phrs in relation to those of standards assayed under identical conditions.

Enzymatic hydrolysis of the methyl, ethyl and glycolamide esters of AZP was similarly studied in aqueous methanolic solutions consisting of a concentration of methanol, equivalent in molar terms, to the ethanol content in the above studies. The composition of the reaction mixture was therefore 6.5% v/v MeOH in Tris buffer (final pH 8.02) with a final ester concentration of 0.5 mM and esterase level of 55 units %. Samples (0.5 ml) were quenched by the addition of 1 ml of acetonitrile (to denature enzyme) and stored at 0°C prior to analysis, at which time they were diluted with 1 ml of IS solution (butyl paraben: 25 µg ml⁻¹ for methyl and ethyl esters; methyl paraben: 12.5 µg ml⁻¹ for glycolamide ester). HPLC systems A and F were employed for the assay of the alkyl and glycolamide esters respectively.

In acetonitrile

The alkyl, THF, THP and GA esters of AZP were investigated for hydrolytic decomposition in a solvent system composed of 10% acetonitrile in Tris buffer (final pH 7.44), such that kinetic data could be compared without interference from transesterification reactions. The final concentrations of esterase and

ester were 55 units % and 0.5 mM respectively. HPLC analysis was performed with system B with the exception of the GA ester, where system F was employed.

4.2.1.2 Hairless mouse skin homogenate studies

Two male hairless mice (type MF1/hr/hr/01a, supplied by Olac Ltd), each weighing approximately 20 g, were sacrificed by cervical dislocation and the skin immediately dissected. Any underlying subcutaneous tissues were gently removed before macerating the skin into fine pieces with scissors. The skin was weighed prior to suspension in iced phosphate buffered saline (PBS) (Appendix 2) to give approximately 100 mg tissue per ml of buffer. The suspension was then homogenized with a french press (Aminco), which had been precooled to -4°C in order to minimize heat-induced denaturation of the cutaneous enzymes during processing. This was followed by centrifugation of the homogenate at 4000 rpm for 20 minutes to separate the solid matter. The supernatant was removed and an aliquot assayed for protein content according to a colorimetric method by Bradford (1976). This assay involves monitoring the magnitude of the UV absorption at 595 nm, resulting from the binding of a dye, Coomassie Brilliant Blue to the protein. A calibration curve was prepared from a series of concentrations of bovine serum albumin and used to determine the protein content of unknown samples. The supernatant from the homogenate was then diluted with iced PBS to yield a protein concentration of 1.6 mg ml^{-1} , and either used immediately or stored at -15°C overnight.

A series of sample tubes containing either skin homogenate prepared as above or PBS pH 7.4 (9.5 ml) together with 0.3 ml methanol was incubated at 37°C . A 0.2 ml aliquot of the ester stock solution (25 mM in methanol) was dispensed into each of the reaction vessels to initiate the reaction. Samples (0.5 ml) withdrawn periodically were vortexed with 1 ml of MeOH for 1 minute. Samples of the homogenate incubations were also followed by centrifugation at 2500 g for 5 minutes. A 0.5 ml aliquot of the supernatant was diluted with an equal volume of IS solution (butyl paraben: $20\text{ }\mu\text{g ml}^{-1}$ in DW) and assayed

directly by HPLC. All incubations were performed in triplicate and protected from light for the duration of the experiment.

4.2.2 Chemical hydrolysis

Non-enzymatic hydrolyses were conducted in solutions containing 10% acetonitrile and 90% Tris buffer (final pH 7.44) at 37°C and 70°C. Due to the stability of the majority of esters under these conditions, experiments were repeated at a pH of 9.0 and temperature of 70°C, in order to obtain comparative kinetic data for the series of esters.

4.3 RESULTS AND DISCUSSION

Bioactivation of the azido-ester *prodrug* to the azido-acid *soft drug* was assessed by investigating the susceptibility of a series of ester derivatives of AZP to *in vitro* enzymatic hydrolysis. Initial studies were conducted with a commercially available, purified porcine liver carboxylic ester hydrolase since purified cutaneous esterase was unavailable.

In preliminary studies, enzymatic hydrolysis of the methyl ester was followed in a solvent composed of 20% propylene glycol (PG), employed as a cosolvent due to the poor aqueous solubility of the esters. Figure 4.2 shows a typical HPLC chromatogram for the decay of the substrate (methyl ester), formation of the hydrolysis product (AZP), and the appearance of an unidentified peak, which is not completely resolved. This latter intermediate was not apparent in the control experiment, in the absence of esterase, suggesting that its formation was enzyme-mediated. That this species was not the amino-methyl ester or AMP was confirmed by chromatography conducted with the authentic compound. This peak was also absent when hydrolysis was performed in a solvent replacing PG with acetonitrile. Figure 4.3 shows that complete mass balance was achieved in acetonitrile, in contrast to the profile observed with PG.

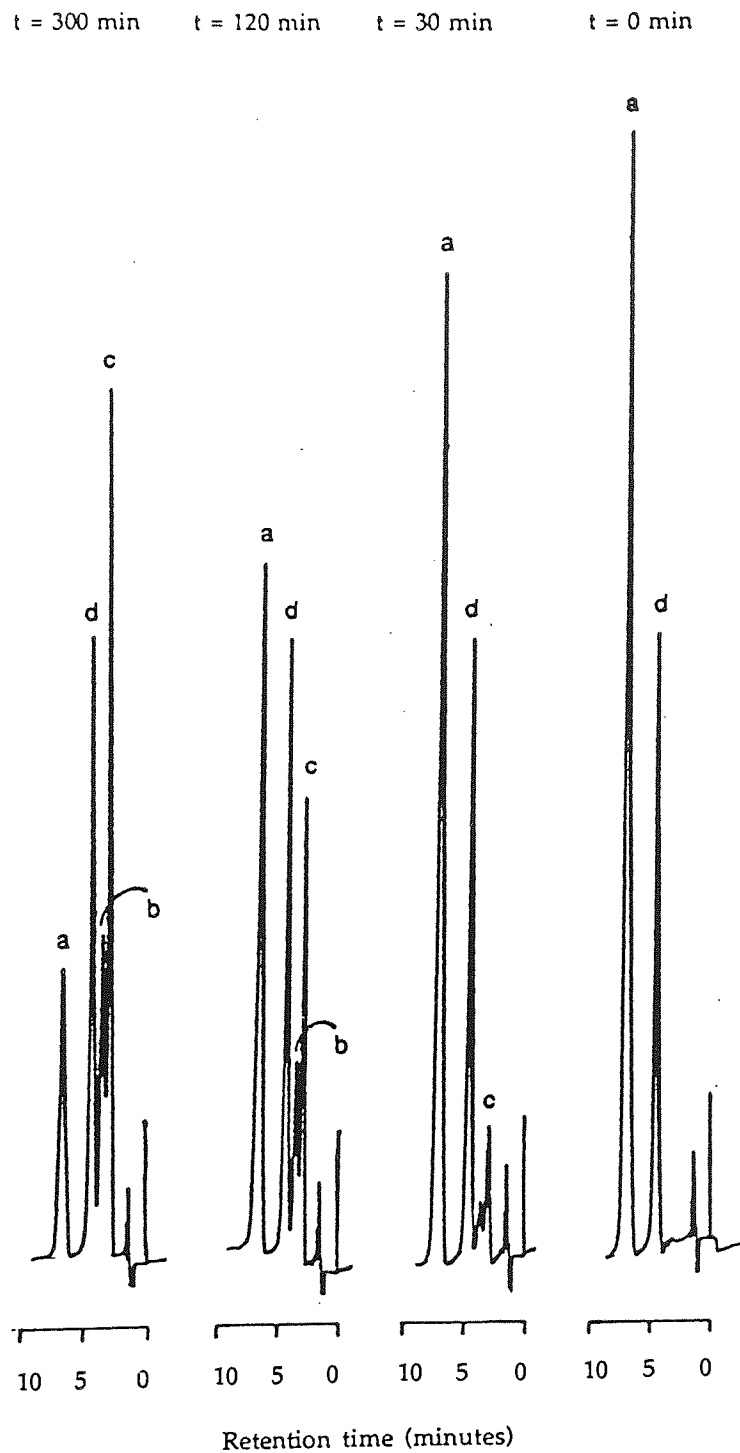


Figure 4.2 Example chromatogram for the enzymic degradation of AZP-methyl ester in 20% propylene glycol at 37°C. a: methyl ester; b: intermediate; c: AZP; d: butyl paraben (IS).

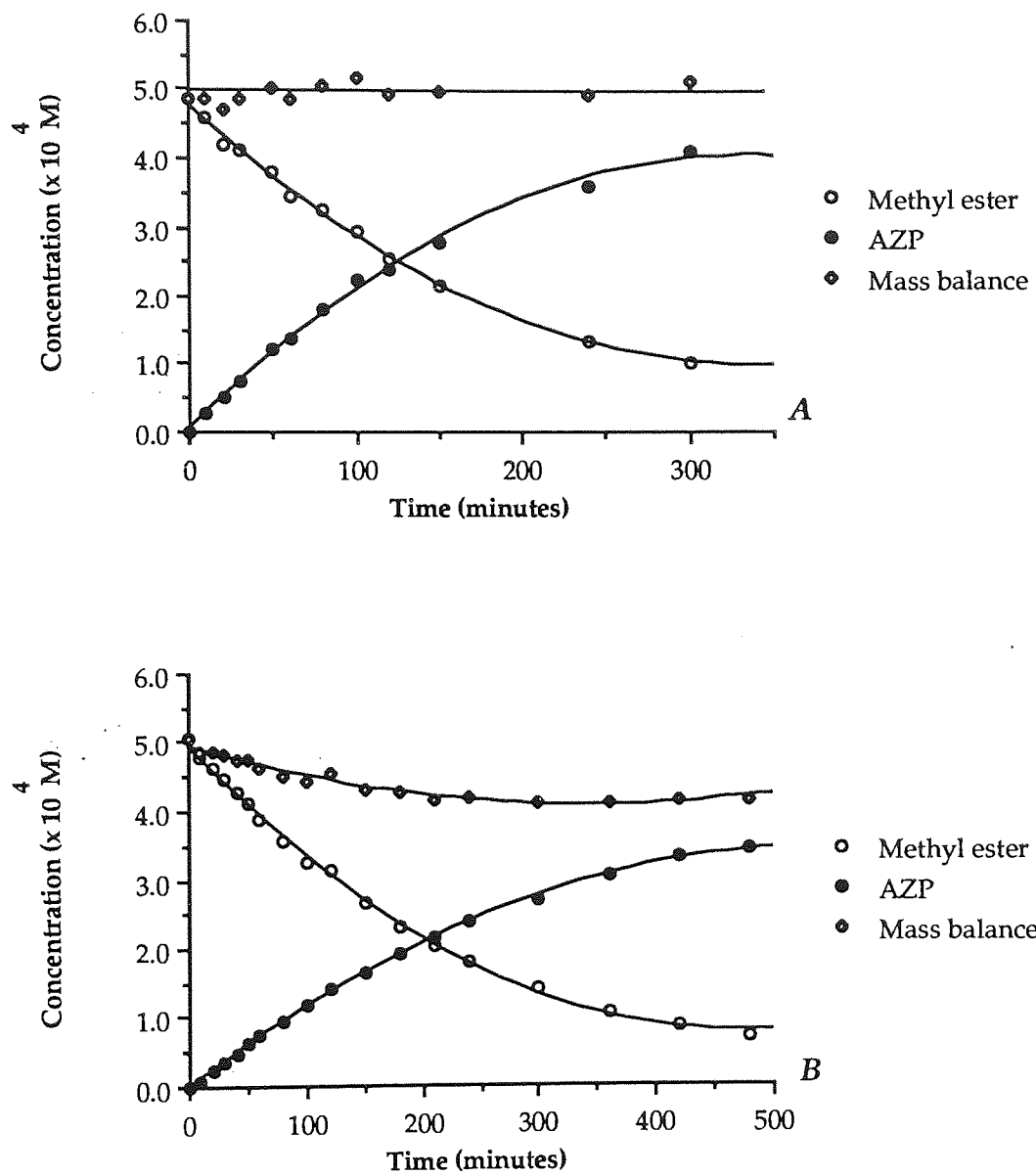


Figure 4.3 Reaction profiles for the enzymatic hydrolysis of AZP-methyl ester in (A) 10% acetonitrile and (B) 20% propylene glycol at 37°C.

A possible explanation which could be put forward to account for the presence of this intermediate was that of a transesterification reaction; occurring between the methyl ester and propylene glycol, and resulting in the formation of a glycol ester of AZP. The possibility of transesterification was investigated by monitoring the stability of the methyl and ethyl esters in hydro-alcoholic solvents, where the alcohol function differed from the alkyl group of the ester. Figure 4.4 illustrates a HPLC chromatogram following the fate of the methyl-ester in 10% ethanol-buffer (pH 8.06), in the presence of esterase. The initial trace (t=0 mins) indicates the presence of the ester and IS alone. After 30 minutes, traces of the hydrolysis product (AZP) can be detected, but a fourth peak is also present. The ethyl-ester of AZP was found to co-elute with this peak and suggests that transesterification is occurring under these conditions. The methyl-ester remained unchanged in the absence of esterase. Formation of the ethyl-ester intermediate can be clearly seen in Figure 4.5., which displays the reaction profile showing the fate of the reactants and products. Both the esters eventually undergo hydrolysis to AZP. A similar profile was evident for the analogous transesterification of the ethyl ester in aqueous methanolic solution.

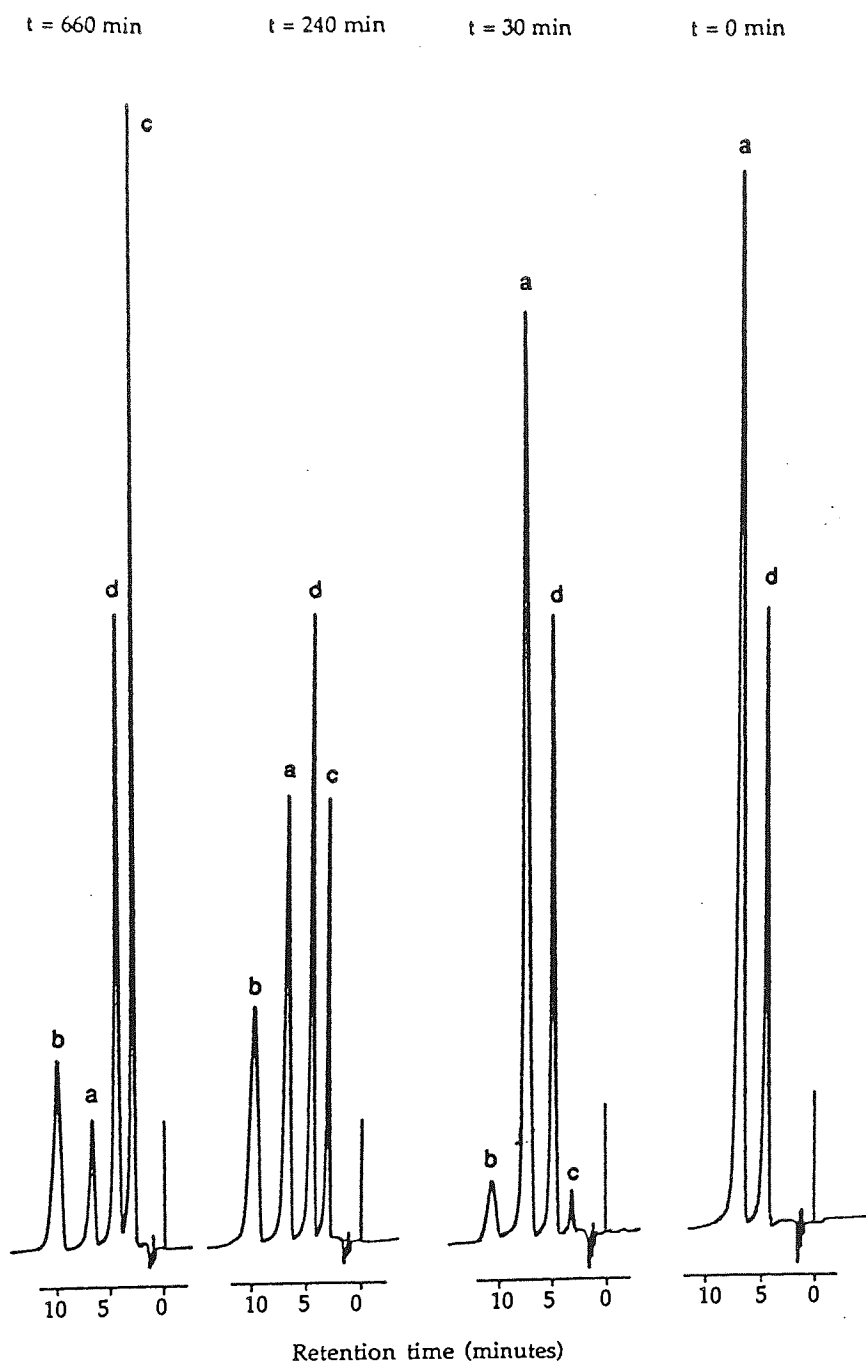


Figure 4.4 Example chromatogram for the enzymic degradation of AZP-methyl ester in 10% ethanol at 37°C. a: methyl ester; b: ethyl ester; c: AZP; d: butyl paraben (IS).

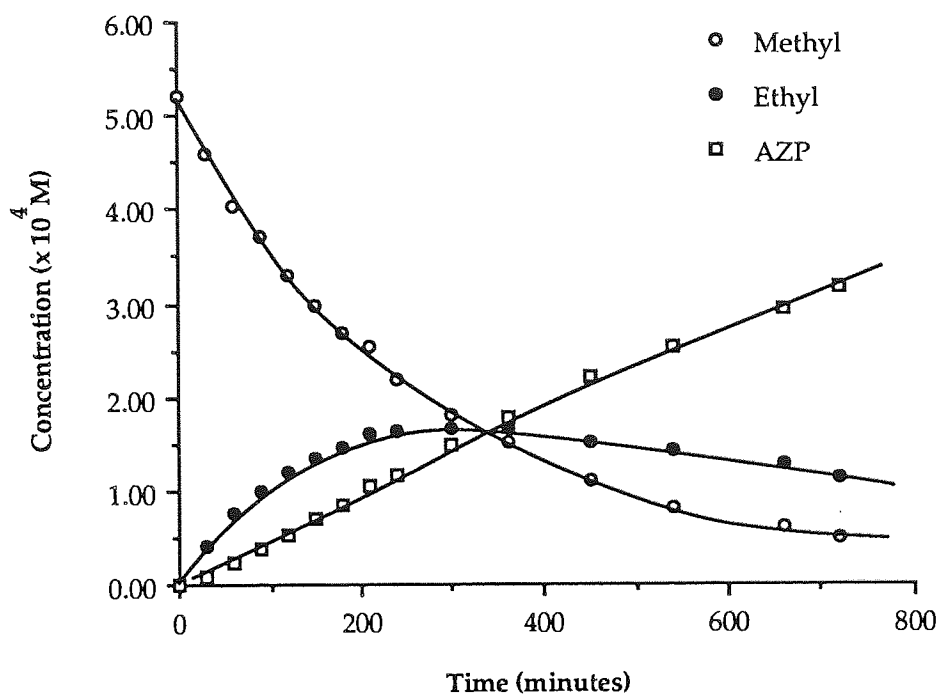


Figure 4.5 Reaction profile for the enzymatic decomposition of AZP-methyl ester in 10% ethanol-Tris buffer, pH 7.44, by 55 units % esterase at 37°C.

In the event of transesterification of the methyl ester with propylene glycol two intermediates may be expected as shown in Figure 4.6. Ester II would be expected to predominate due to less steric hindrance during attack from the primary alcohol.

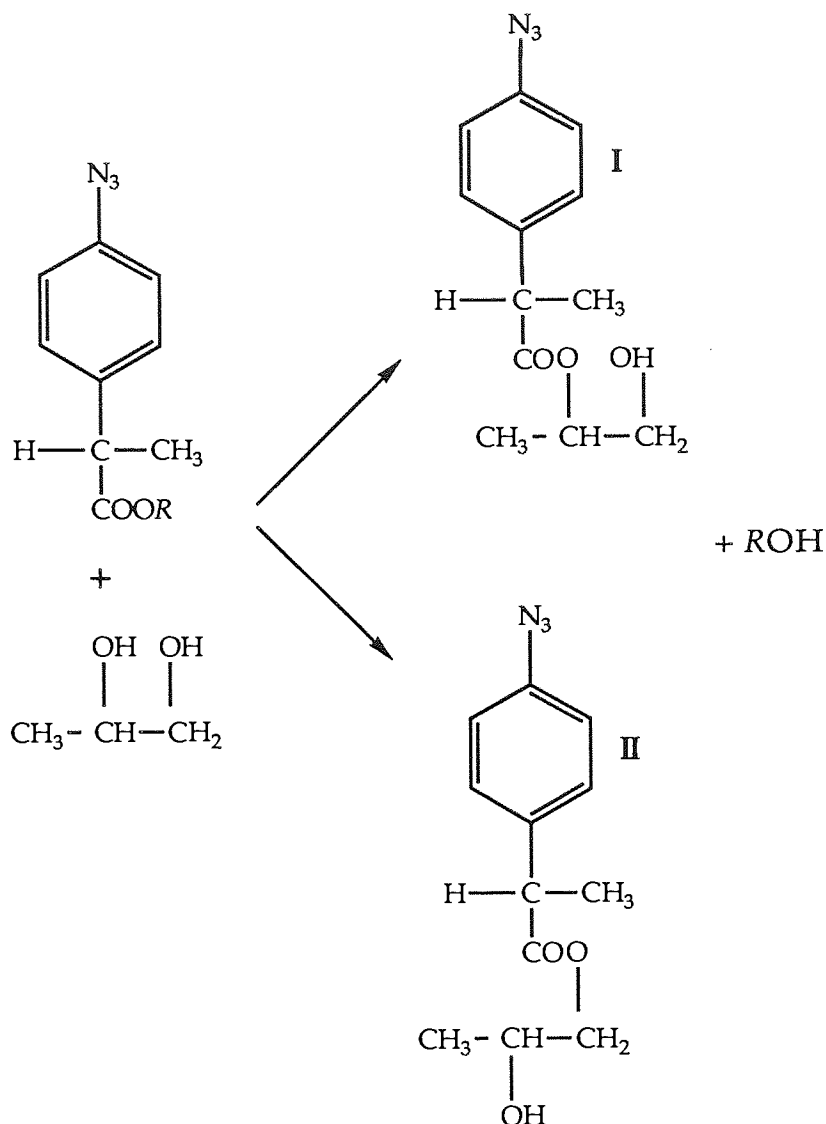
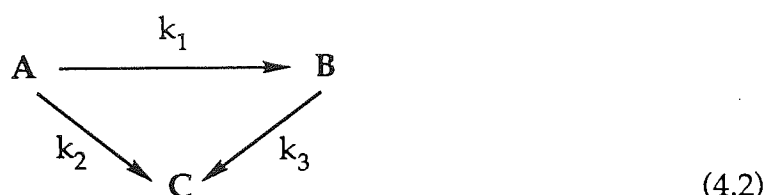


Figure 4.6 Scheme illustrating the possible transesterification intermediates from reaction between AZP esters and propylene glycol. ($R = CH_3$)

These glycol esters of AZP were synthesized (by Dr R J Griffin) in order to investigate whether one of these compounds was indeed the intermediate detected in earlier studies monitoring the hydrolysis of the AZP-methyl ester in a solvent comprising propylene glycol. The experiment was repeated and the

composition of the HPLC eluent adjusted to completely separate the unidentified peak. Co-elution of the 'unidentified' species with one of the authentic samples suggested that the intermediate was a glycol ester of AZP, formed as a result of enzyme-mediated transesterification between the methyl ester and the co-solvent.

These events may be represented by the following kinetic model, proposed to describe the hydrolysis of an ester in a hydro-alcoholic solution, where the alcohol does not correspond to the ester function:



where A represents the original ester undergoing transesterification to a second ester B. Both esters undergo hydrolysis to C (AZP). A reversible model may be proposed but unless a mixed alcohol system is used, reversibility may be excluded. The rates of change in concentration of species A, B and C are given by:

$$\frac{dA}{dt} = -A(k_1 + k_2) \tag{4.3}$$

$$\frac{dB}{dt} = k_1A - k_3B \tag{4.4}$$

$$\frac{dC}{dt} = k_2A + k_3B \tag{4.5}$$

Integration of these equations between time zero and the current time, according to Irwin *et al* (1984), enables expressions for the concentrations of each species at time t to be determined.

$$A_t = A_0 \cdot \exp[-(k_1 + k_2) t] \quad (4.6)$$

$$B_t = A_0 \cdot k_1 \cdot \left\{ \frac{\exp(-k_3 t)}{(k_1 + k_2 - k_3)} + \frac{\exp[-(k_1 + k_2) t]}{(k_3 - k_1 - k_2)} \right\} \quad (4.7)$$

$$C_t = A_0 \cdot \left\{ \frac{1 - k_1 \cdot \exp(-k_3 t) + (k_2 - k_3) \cdot \exp[-(k_1 + k_2) t]}{(k_1 + k_2 - k_3)} \right\} \quad (4.8)$$

Rate constants for the transesterification reactions may be estimated by fitting the measured reaction profiles to these equations by non-linear regression (Irwin, 1990; Metzler and Weiner, 1986). The data are summarized in Table 4.3 and show that the theoretical degradation rate constants $(k_1 + k_2)$ are generally in close agreement with the observed data, derived from linear regression of the plots of \ln (percentage ester remaining) as a function of time. Transesterification proceeds at a significantly faster rate than the corresponding hydrolysis reaction, and both these reactions are favoured by the ethyl ester, compared to the methyl ester. On this basis, longer chain esters may be expected to undergo rapid enzyme-mediated hydrolysis, perhaps due to a more favourable interaction with the enzyme. Experiments to investigate this possibility with a homologous series of esters under universal conditions, proved unsuccessful at this stage although preliminary studies indicated that the propyl ester of AZP was more vulnerable to enzymatic hydrolysis than its methyl and ethyl counterparts.

Table 4.3 Transesterification and hydrolysis rates for AZP esters at 37°C.

Methyl ester in ethanol ($k \text{ min}^{-1} \times 10^3$)				
	k_1	k_2	k_3	$(k_1 + k_2)$
Theoretical ¹	2.667	0.666	2.426	3.333
Observed ²	–	–	2.214 [†]	3.2235
Ethyl ester in methanol ($k \text{ min}^{-1} \times 10^3$)				
	k_1	k_2	k_3	$(k_1 + k_2)$
Theoretical ¹	40.719	7.994	5.739	48.713
Observed ²	–	–	5.885 [‡]	58.300

¹ from non-linear regression analysis

² first-order rates from linear regression analysis of ester hydrolysis

[†] first-order hydrolysis rate constant for methyl ester in methanol

[‡] first-order hydrolysis rate constant for ethyl ester in ethanol

Transesterification is a commonly occurring and well documented reaction between esters and alcohols, where the ester radical differs from that of the alcohol. These reactions are invariably acid or base-catalyzed, occurring in aqueous and organic reaction media. Enzyme-catalyzed transesterification, on the other hand, has only recently begun to generate interest. The majority of literature existing in this field is concerned with this process in anhydrous organic solvents (Bevinakatti and Banerji, 1988; Kirschner *et al*, 1985). Non-aqueous enzymology has been investigated with a view to mechanistic elucidation of the dependence of enzymatic properties on the nature of the solvent. Since the process of transesterification does not require water (hydrolytic enzymes may utilize alcohols as nucleophiles instead of water) it represents a model enzyme-mediated reaction for study in organic solvents (Zaks and Klibanov, 1988).

According to a detailed review on the physiological roles of carboxylic ester hydrolases by Leinweber (1987), information on the reversible nature of esterase action appears to be limited. Although isolated examples exist, the

involvement of esterases in the *synthesis* of esters from acid and alcohol seems to be of minor physiological importance.

The pharmaceutical implications of non-enzymatic transesterification reactions were inherent in a report by Irwin *et al* (1984) who observed the reversible, base-catalyzed transesterification of salicylate esters in hydro-alcoholic solutions. These esters are widely used as topical analgesics, preparations of which are commonly formulated with hydroxylic vehicles such as glycols. Formation of glycol esters may therefore be expected to affect the integrity of the pharmaceutical formulation. Similarly, in view of the esterase activity and drug metabolizing capacity of the skin (Taüber and Rost, 1987), the potential of cutaneous transesterification, which may affect the availability and activity of the original ester should be considered. Furthermore, Bodor and Sloan (1983) have reported the improved topical delivery of hydrocortisone prodrugs into which solubilizing groups of the penetration enhancers dimethylsulphoxide and dimethylformamide had been incorporated. Loftsson and Bodor (1981b) have also shown such an approach to be effective with respect to the delivery of NSAIDs. The possibility therefore exists that glycol esters may also function as carriers of this solubilizing group and consequently enhance percutaneous penetration.

A comparative examination of chemical and enzymatic stability between the various esters necessitated the use of a universal solvent system. As a result of the transesterification reaction, alcohols could not be used. After preliminary studies with a range of solvents, a reaction medium consisting of 10% acetonitrile in buffer was employed. The alkyl, THF and THP esters were found to be hydrolyzed quantitatively to the parent acid in the presence of porcine liver esterase, in 10% acetonitrile-buffer (pH 7.44) at 37°C as exemplified by Figure 4.7. Under the experimental conditions used, hydrolysis followed first-order kinetics over several half-lives as illustrated in Figure 4.8. Pseudo-first order rate constants (k) and corresponding half-lives ($t_{1/2}$), which were calculated from the slopes of these linear plots are summarized in Table 4.4.

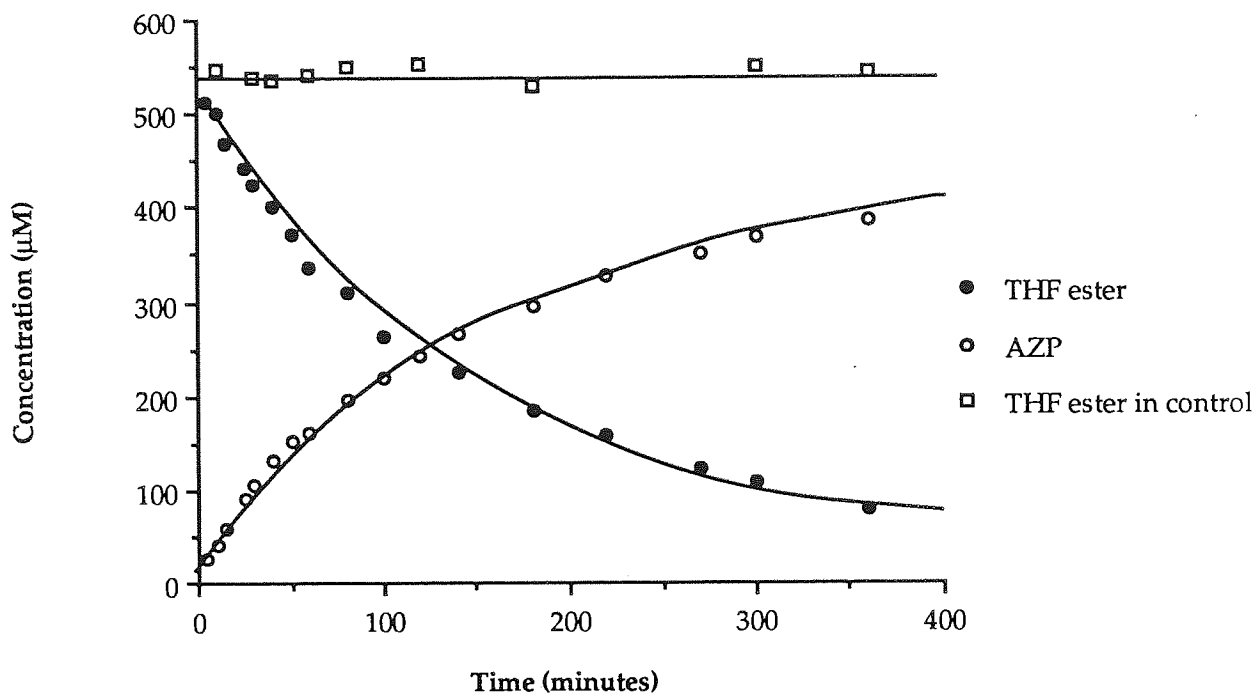


Figure 4.7 Reaction profile for enzymatic hydrolysis of the AZP-THF ester in 10% acetonitrile-Tris buffer, pH 7.44, by 55 units % esterase at 37°C.

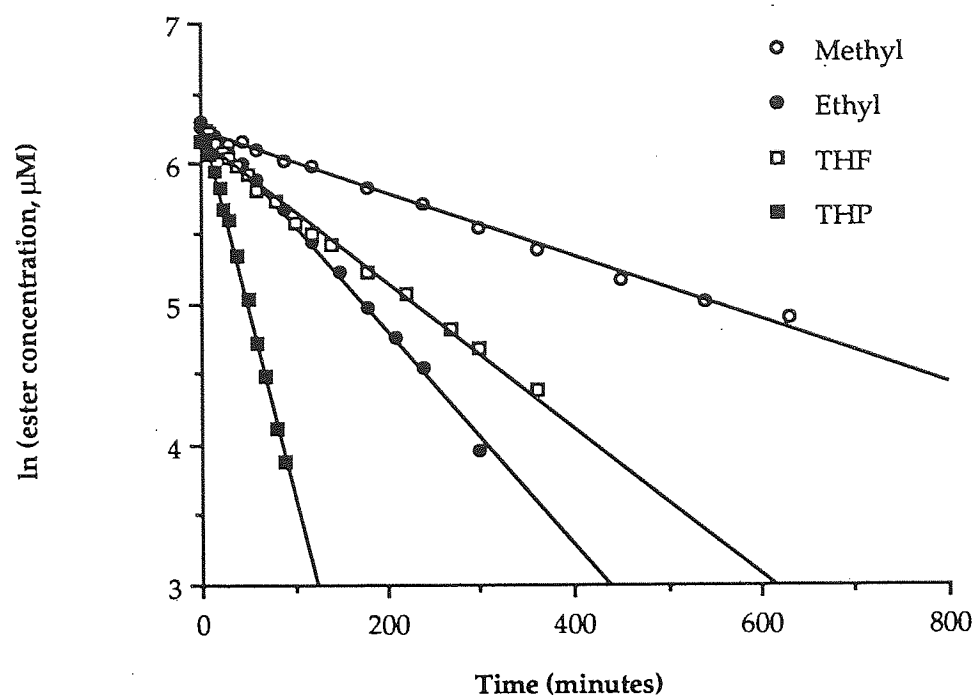


Figure 4.8 First-order plots for the enzymatic hydrolysis of various esters of AZP in 10% acetonitrile-Tris buffer, pH 7.44, by 55 units % esterase at 37°C.

Table 4.4 Kinetic data for the enzymatic hydrolysis of various esters of AZP in 10% acetonitrile-Tris buffer, pH 7.44, by 55 units % esterase at 37°C.

Ester	k (min^{-1}) ($\times 10^3$)	$t_{1/2}$ (minutes)
Methyl	2.5830	268.29
Ethyl	7.5978	91.21
THF	5.1683	134.09
THP	26.769	25.89

In agreement with the rate data for hydrolysis in alcoholic media (Table 4.3), the process was favoured by the ethyl ester, compared to the methyl derivative. The enzymatic lability of the THP ester was some 5 fold greater than the corresponding THF ester, and much higher than the simple alkyl esters.

Under analogous non-enzymatic conditions, these esters proved to be highly stable, indicating their potential ability to fulfill one of the criteria for an ideal prodrug (*i.e.*, metabolic lability versus good chemical or aqueous stability). Kinetic data for comparative purposes were thus derived from a study of chemical hydrolysis under accelerated conditions, at pH 9.0 and 70°C. The progress of the reaction followed first-order kinetics as shown in Figure 4.9; kinetic data are tabulated in Table 4.5. Amongst the limited number of esters studied, the methyl ester shows the greatest instability under these conditions, in contrast to its stability towards enzymatic hydrolysis. The reactivities of the THF and THP esters were not significantly different, in contrast to their capacities for enzymatic degradation. More importantly, if the ratios of the enzymatic/chemical hydrolysis rate constants are compared for the series of esters (bearing in mind the vigorous reaction conditions for the latter process), the THP derivative exhibits the greatest promise as a potential prodrug.

The glycolamide ester, conversely, was significantly more susceptible to chemical hydrolysis and less labile to enzymatic hydrolysis than the corresponding alkyl, THF and THP esters (data not shown). In 10% MeCN-buffer, pH 7.4 and 37°C, the GA ester was not subject to enzymatic hydrolysis yet underwent non-enzymatic degradation during the same period of study.

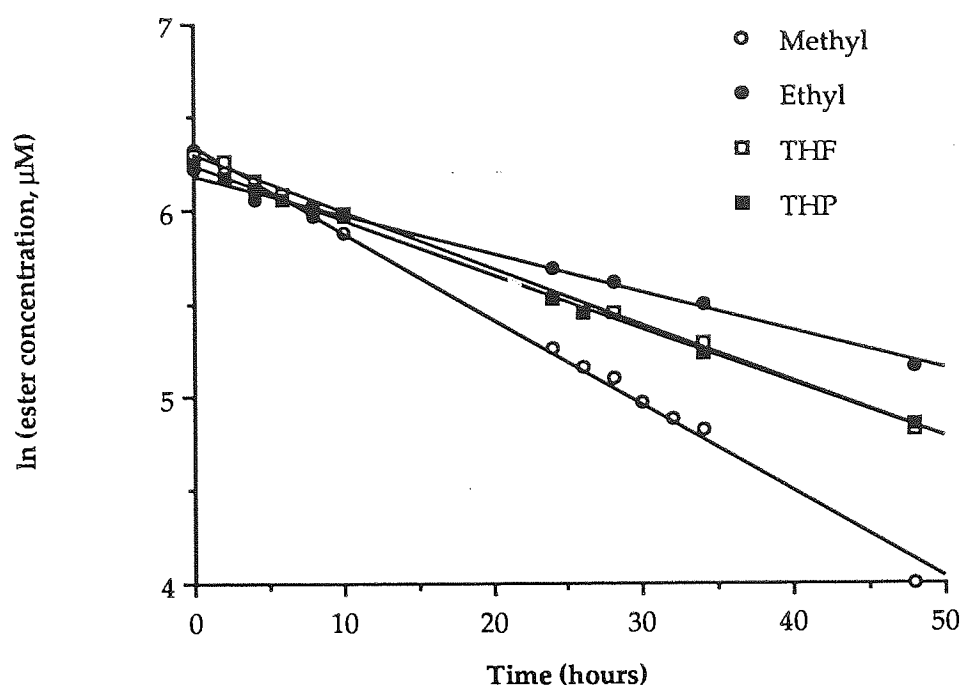


Figure 4.9 First-order plots for the chemical hydrolysis of various esters of AZP in 10% acetonitrile-Tris buffer, pH 9.0 at 70°C.

Table 4.5 Kinetic data for the chemical hydrolysis of various esters of AZP in 10% acetonitrile-Tris buffer, pH 9.0 at 70°C.

Ester	k (min ⁻¹) ($\times 10^2$)	$t_{1/2}$ (minutes)
Methyl	4.6323	14.96
Ethyl	2.0712	33.46
THF	3.0304	22.87
THP	2.9137	23.78

Bundgaard and Nielsen (1988) have suggested glycolamide esters as useful prodrug functions for NSAIDs with carboxylic acid groups, combining high stability in aqueous solution together with a high susceptibility towards enzymatic hydrolysis. The most important structural requirement for this profile appears to be the presence of two substituents on the amide nitrogen, *N,N*-disubstituted glycolamide esters being much more readily hydrolyzed in plasma than either mono- or unsubstituted GA esters (Nielsen and Bundgaard, 1987 and 1988). The unsubstituted nature of the GA ester of AZP in the present study may therefore explain its stability to enzymatic attack.

The metabolic degradation of the methyl ester in the presence of a cutaneous homogenate was also investigated, in order to assess its potential for reconversion to the parent acid during topical delivery. The resulting reaction profile is presented in Figure 4.10. First-order rate constants for the ester degradation and AZP formation were derived from linear transformation of this data (over 0 to 12 hours) and were 0.095 hr^{-1} and 0.0816 hr^{-1} respectively. The formation of AZP was not observed in control experiments, where the skin homogenate was replaced by phosphate buffered saline. However, there was significant loss of the ester, possibly due to adsorption on to the reaction vessel; this was not evident in the skin experiment where good mass balance was achieved. These experimental difficulties therefore need to be overcome prior to conducting further studies with additional ester analogues.

During these initial skin homogenate studies, reduction of the azido moiety was not apparent, suggesting that such a process is unlikely to occur during the delivery of AZP across the skin.

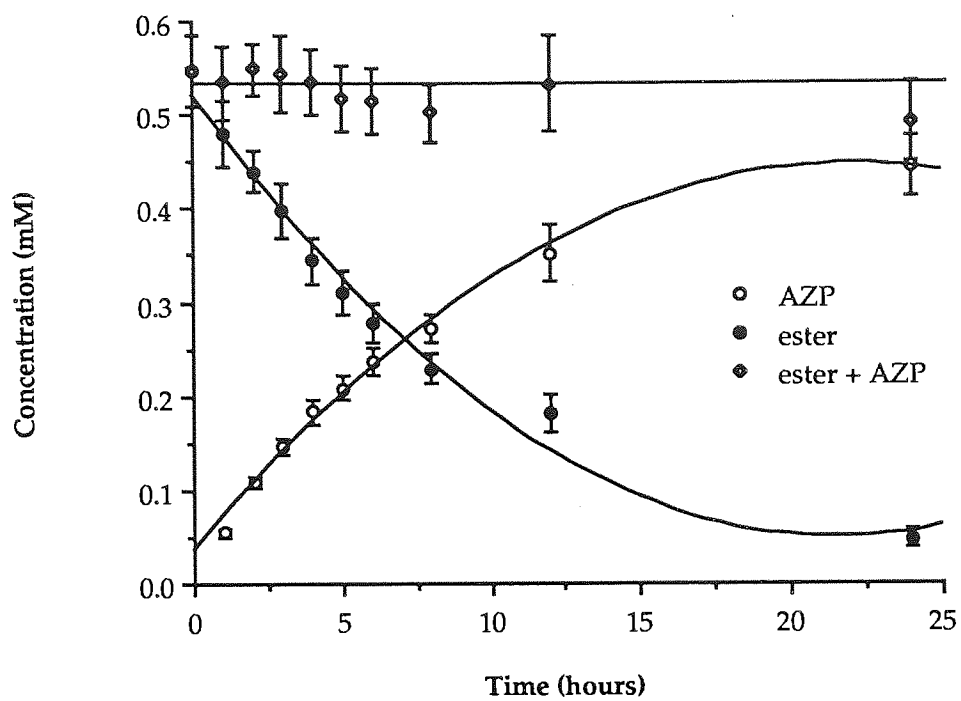


Figure 4.10 Reaction profile for the cutaneous metabolism of AZP-methyl ester at 37°C.

4.4 SUMMARY

A series of esters providing a range of lipophilicities, which may enable modification of their percutaneous transport, were investigated for their susceptibilities towards *in vitro* chemical and enzymatic hydrolysis. This hydrolytic cleavage regenerates the parent acid AZP; the rate and extent of the process being dependent on the nature of the ester moiety. The majority of esters studied exhibited greater lability towards enzyme-mediated hydrolysis compared to chemical decomposition. The THP ester showed the largest difference in sensitivities towards these two processes. This is an important requirement for an ideal prodrug, demonstrating the potential capacity to undergo rapid metabolic activation, while exhibiting stability towards chemical decomposition under conditions such as those encountered during formulation and storage. That the skin may be capable of activating these pro-drugs was shown by the ability of the methyl ester, to undergo hydrolysis on incubation with a hairless mouse skin homogenate. On the basis of the isolated enzyme studies, the remainder of the esters may be expected to undergo cutaneous activation at faster rates. Whether these prodrugs are capable of being metabolized by intact skin, mimicking the *in vivo* situation, remains to be ascertained.

These kinetic studies also demonstrated that alkyl esters are capable of undergoing enzyme-mediated transesterification reactions in the presence of appropriate solvents. This may have important implications for the pharmaceutical integrity and bioavailability of topical formulations of ester derivatives comprising alcoholic solvents.

CHAPTER FIVE
PERCUTANEOUS ABSORPTION STUDIES

5.1 INTRODUCTION

5.1.1 NSAIDs and topical delivery

The use of NSAIDs, most notably salicylates, for inflammatory conditions dates back to antiquity, as does the treatment of a range of ailments, both dermatological and systemic, by the application of medicaments to the skin. Ancient topical remedies to soothe pain and inflammation included poultices and decoctions made from various plants and barks of tree. As an active ingredient of willow bark, salicylic acid is regarded as the forerunner of contemporary synthetic NSAIDs, a group of drugs which has attracted considerable interest in the field of topical delivery.

Since inflammation is a major component of many skin diseases, NSAIDs have potential as important therapeutic agents in dermatology (Greaves, 1987; Lichtenstein *et al*, 1987). Additionally, the ability of topically applied drugs to penetrate local subcutaneous structures such as muscle and synovial fluid (Guy and Maibach, 1983; Marty *et al*, 1985) offers the possibility of a delivery system capable of targeting these anti-arthritic drugs to affected tissues without significant systemic distribution of the drug. A number of studies showing preferential accumulation of NSAIDs in deeper tissues, compared to blood and plasma, following dermal delivery have been reported (Panse *et al*, 1974; Rabinowitz *et al*, 1982; Reiss *et al*, 1986; Wada *et al*, 1982). In those evaluations, examining drug levels in subcutaneous structures following both topical and oral administration, the former achieved greater levels in these deeper tissues. Several topical formulations of NSAIDs, indicated for musculo-skeletal and joint disease, have also recently been marketed. These include Traxam® (felbinac), Proflex® (ibuprofen) and Feldene® (piroxicam) gel or cream.

For the treatment of diseased skin, the aim of topical drug delivery is to elicit a therapeutic response by achieving an adequate drug level at the site of action. The onset, duration and magnitude of this response is dependent on the relative efficiency of three sequential events: release of medicament from the topical vehicle, penetration through the skin barriers and induction of a pharmacological response by the active moiety (Barry, 1983; Guy *et al*, 1986; Hadgraft, 1989). Optimization of topical performance therefore aims to facilitate the transport of a potentially pharmacologically active substance to its local site of action. This may be achieved through the simultaneous manipulation of physicochemical properties of the drug and vehicle, a strategy which is consequently at the forefront of studies investigating the feasibility of topical delivery systems for NSAIDs. Hadgraft (1989) has recently addressed the issues of formulation confronting this category of drugs in the light of much of the current literature in this area.

Several texts offer excellent treatises on the fundamental principles of skin permeation, dealing with methodology, mechanisms, optimization and applications of this highly complex process (Barry, 1983; Bronaugh and Maibach, 1985; Schaefer *et al*, 1982). The complexity of the series of events underlying this process, which is initiated by the release of the drug from the formulation and culminates in a therapeutic response at the local site of action is represented in Figure 5.1. The processes of diffusion and partitioning dominate the course of absorption, and any factor, biological or physicochemical, which may influence this sequence of events will have a bearing on the overall bioavailability of a topically applied drug.

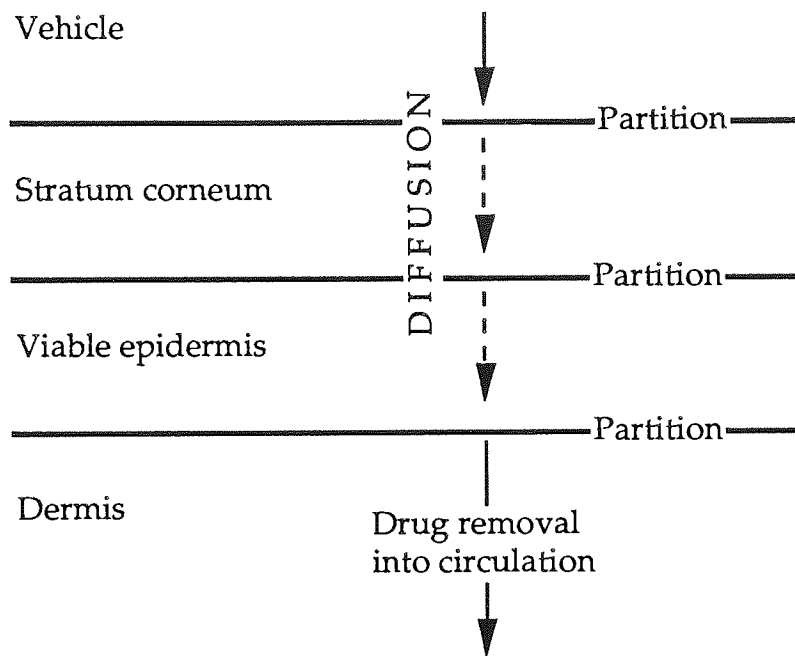


Figure 5.1 Schematic representation of percutaneous absorption.

5.1.2 Properties influencing percutaneous absorption

The predominant physiological factors which influence percutaneous absorption are the age, condition, regional site, metabolic potential, species variation and vascularization of the treated skin (Barry, 1983; Siddiqui, 1989). Some of these factors are briefly discussed in section 5.1.3 with respect to their role as determinants in the choice of a skin membrane for *in vitro* experiments. In clinical practice, it is usually not possible to exercise any control over these biological variables. Optimization of topical delivery is, therefore, most frequently achieved by the manipulation of physicochemical parameters of the dosage form. The main characteristics of the permeant which influences its absorption are its partition coefficient, diffusivity and concentration (see section 5.1.3.1). Thus, various formulatory or vehicular factors capable of modifying these properties through interactions with the penetrant and skin, and hence of influencing percutaneous absorption, are important considerations in the design of a topical dosage form. A number of these are discussed briefly in the following section. For detailed treatises, the reader is referred to publications by Barry (1983), Idson (1983), Katz and Poulsen (1971) and Poulsen (1972).

5.1.2.1 Formulation factors

The nature of the solvent or vehicle is a major factor influencing the percutaneous absorption of drugs. A combination of parameters, which modify this process, may be dependent on the vehicle: relative affinity of the solute for the vehicle and skin affecting drug partitioning into the skin; drug solubility and therefore concentration in the vehicle; potential interactions between vehicle and skin, which may alter the barrier properties.

A change in solvent character is usually accompanied by an alteration in the degree of affinity of the permeant for the solvent. As a result, partitioning into the membrane and consequently, the absorption rate will be modified. This is exemplified by the dependence of permeability of a series of alkanols on their lipophilicity and solubilizing vehicle (Scheuplein, 1978a). With water as the solvent, an increase in carbon number and thus lipophilicity, resulted in an

increased partitioning into the skin, which is largely lipophilic in nature, and hence enhanced permeability. However, when the less polar isopropyl palmitate was employed, the trend was reversed; an increase in carbon number enhanced solute affinity for the vehicle and concomitantly reduced the absorption rate.

The affinity of the relatively lipophilic stratum corneum for the penetrant will also be dependent on the chemical nature of the solute; penetration being facilitated for drugs with high lipid-water partition coefficients. Most drugs are weak acids or bases and therefore, according to the pH-partition theory, the relative fraction of unionized and ionized species will determine the degree of absorption. According to the pH-partition hypothesis (Shore *et al*, 1957), only the unionized moiety can permeate lipoidal membranes, such as the stratum corneum, in significant amounts. Absorption may therefore be improved by adjustment of vehicle pH of aqueous solutions to ensure that drug remains predominantly in the undissociated form. This is exemplified by NSAIDs, many of which are carboxylic acids. Indomethacin has a pK_a of 4.5; penetration will therefore be favoured from solutions maintained below this pH. Inagi *et al* (1981) reported the effect of pH on indomethacin absorption *in vivo* in guinea pigs. Below the pK_a value, the amount of indomethacin absorbed percutaneously correlated well with the fraction unionized, indicating that only the neutral form penetrates the skin. The flux decreased with increasing pH as expected, however at pH 6.2 it was observed to be greater than the calculated value (from the unionized component) suggesting that the anionic form of the drug was also transferred across the skin, possibly by ion-pair complexation.

The pH at the surface of the skin is quoted as ranging from 4.2-6.5 (Katz and Poulsen, 1971). Although topical preparations ranging from pH 4-10 have been reported not to damage the barrier properties of the skin (Matoltsy *et al*, 1968), Katz and Poulsen (1971) recommended the use of topical formulations of pH values greater than 4.5, above the iso-electric point of keratin, in order to promote keratin hydration. Thus, it may not always be cosmetically or

pharmaceutically desirable to apply drug in a predominantly unionized form. In such instances it may be advantageous to provide a counter-ion with which the charged species can ion-pair, thereby improving lipophilicity and facilitating transport. Barker and Hadgraft (1981) showed that a series of bis(2-hydroxypropyl)amines which were incorporated in an IPM-impregnated membrane, were capable of facilitating the transport of the anionic permeant methyl orange across such a membrane, against its own concentration gradient. This was achieved by utilizing a pH gradient of 5.0 to 7.4, from the 'dermal' surface to the receiver phase, analogous to the *in vivo* situation, to provide the driving force for the carrier mediated transport. A similar phenomenon has been suggested to exist between salicylate ions and the penetration enhancer, Azone (Hadgraft *et al*, 1985).

The rate of penetration of a drug is proportional to the applied concentration under steady-state conditions. As only dissolved drug is capable of diffusing from the vehicle phase and penetrating the skin, flux is expected to increase linearly with concentration until saturation is achieved. Such a profile was exhibited by fluocinolone acetonide from solutions in aqueous propylene glycol (Poulsen *et al*, 1978). Maximal flux is likely to be achieved with vehicle compositions which just solubilize the amount of permeant that is present (Poulsen, 1972). In such a situation, the drug will be at saturated solubility and exhibit maximum thermodynamic activity. This latter phenomenon has been described as the "escaping" tendency of a molecule from a vehicle (Barry, 1985). Higuchi (1960) derived the following equation:

$$J = \frac{a D}{\gamma \delta} \quad (5.1)$$

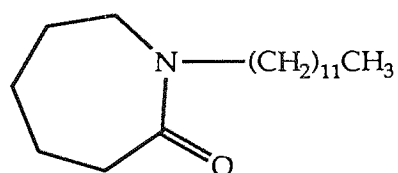
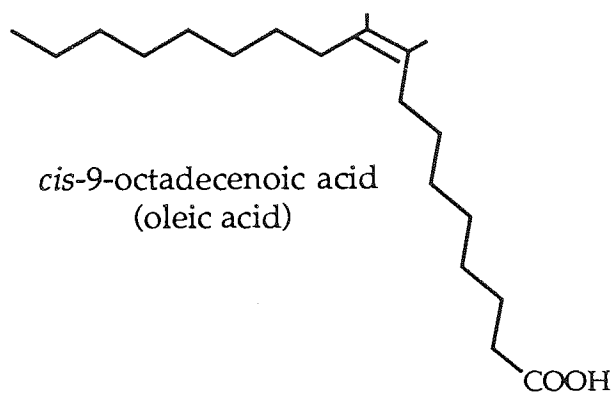
where J is the penetrant flux (see equation 5.2), D is the drug diffusivity, a is the thermodynamic activity, δ is the membrane thickness and γ is the activity coefficient of the drug in the skin. This predicts that under ideal conditions, the drug flux through the skin should be directly proportional to the drug activity in the vehicle, provided D , γ , and δ remain constant. Furthermore, for

maximum flux, the penetrant should be at maximal thermodynamic activity (*ie.*, at saturated solubility), thereby promoting interfacial drug transfer into the stratum corneum. Poulsen *et al* (1968) studied the effect of solubility and concentration of fluocinolone acetonide and its acetate ester on their *in vitro* release rates from binary mixtures of aqueous propylene glycol. Maximum release was achieved with propylene glycol concentrations just sufficient to solubilize the steroid. Excess cosolvent lowered the thermodynamic activity of the steroid and therefore the release rate. Similar trends were also observed with skin penetration experiments studying fluocinolone acetonide and fluocinonide (Ostrenge *et al*, 1971) and hydrocortisone (Shahi and Zatz, 1978).

Once the drug has partitioned into the skin, it will diffuse through the stratum corneum as a result of the existing concentration gradient. The potential routes of penetration comprise (i) the transappendageal (transecrine and transfollicular) and (ii) the transepidermal (transcellular and intercellular) pathways. Although the transepidermal route across the intact stratum corneum is acknowledged as the major penetration pathway, the precise route is under considerable debate. Both routes may be of importance, depending on the physicochemical characteristics of the penetrant (Wiechers, 1989), however, increasing evidence suggests that the major route is through the lipid-laden intercellular channels (Guy and Hadgraft, 1988; Houk and Guy, 1988). Partitioning from the stratum corneum into the largely aqueous viable epidermis is favoured by a hydrophilic drug character. This directly contradicts the prerequisite for entry into the stratum corneum, and consequently optimal penetration is achieved for drugs with balanced hydrophilic-lipophilic properties. The design of a lipophilic prodrug favouring partitioning into the skin, but undergoing biotransformation to a more hydrophilic moiety to optimize the second partitioning step, as it traverses the stratum corneum (Hadgraft, 1989) is also an interesting concept. Yano *et al* (1986) investigated the skin permeabilities of a series of NSAIDs as a function of their oil-water partition coefficients and reported a parabolic relationship, indicating that drugs with extremes of hydrophilic or lipophilic nature were not well absorbed. The optimal value of log P for maximal flux appeared to be around 2.5.

Solvent composition and pH of a topical formulation are usually chosen to ensure that the drug has maximum tendency to leave the vehicle and partition into the skin. In addition, solvents may themselves exert specific interactive effects on the stratum corneum thus modifying its resistance to diffusion. They may alter the state of skin hydration, influence the stratum corneum-viable epidermis partition coefficient mentioned above, and thus modify absorption particularly for lipophilic compounds. It has also been suggested that permeation of the solvent itself may affect drug solubility within the skin, thus influencing partitioning behaviour and penetration (Møllgaard and Hoelgaard, 1983).

Alternatively, excipients (penetration enhancers) may be included in the formulation which temporarily diminish the impermeability of the stratum corneum, thus promoting drug penetration. These compounds have recently been the subject of considerable research with respect to percutaneous absorption, and may reflect the recent interest in transdermal delivery systems and their need to deliver substantial amounts of drug systemically, following topical application. Several comprehensive reviews have been published in this field (Barry, 1983; Walters, 1989; Woodford and Barry, 1986), which also illustrate the diversity of chemical structures that have been employed as penetration enhancers. No single agent is likely to possess the spectrum of attributes desirable of an enhancer, nor is any singular mechanism of action likely to be responsible for their effect. Based on extensive biophysical research such as that described by Ward and Tallon (1990) and Potts (1989), several theories accounting for the molecular nature of their interactions have been proposed (Walters, 1989). Figure 5.2 depicts several of these compounds; those generating most interest at present are perhaps Azone® and oleic acid, which have also been assessed for their effect on the penetration of NSAIDs (Akhter and Barry, 1984; Catz and Friend, 1989; Green *et al*, 1988; Hadgraft *et al*, 1985; Ogiso *et al*, 1986; Tzuzuki *et al*, 1988).



1-Dodecylazacycloheptan-2-one
(Azone)

Figure 5.2 Structures of some penetration enhancers.

The potential value of penetration enhancers in the treatment of chronic psoriasis was demonstrated by Kaidbey (1976). The author showed that the sequential application of dimethyl sulphoxide and topical steroids produced remission of the lesions previously resistant to treatment with the latter agents. Efficacy declined with decreasing DMSO concentration, suggesting that inadequate penetration may have been responsible for resistance to treatment.

5.1.3 Permeation studies

The effect on the topical bioavailability of many of the physiological and physicochemical factors discussed in section 5.1.2, may be assessed by a variety of percutaneous penetration experiments. In addition, they may seek to answer questions regarding the route of penetration, drug binding, and skin metabolism (Barry, 1983). The experimental approaches available to make this evaluation may be broadly divided into *in vivo* and *in vitro* methods. The former category employs a range of techniques to assess the penetration of a drug across the skin of human or animal subjects *in situ*, generally by monitoring the appearance of the drug in body compartments and/or the disappearance of drug from a surface depot following topical application. These methods are discussed further in chapter 6. An alternative approach is to study the process *in vitro*, using isolated human or animal skin, or an artificial membrane mounted in a diffusion cell.

The stratum corneum, recognized as the principal barrier to drug penetration (Blank and Scheuplein, 1969), is a multicellular layer of metabolically inactive tissue residing on the outermost surface of the epidermis. Hence, the main justification for using *in vitro* models centres on the assumption that the diffusional resistance of the stratum corneum, which is a *dead* tissue *in vivo*, cannot be significantly altered in the *in vitro* situation. Much of our current understanding about the fundamental nature of the percutaneous absorption process is derived from *in vitro* studies, which may be performed under a controlled environment. Elucidation of structure-dependent parameters which characterize skin permeation, such as diffusivities and partition coefficients, provide mechanistic insights into the permeation process and may

be used to predict potential drug permeability. In the development of topical dosage forms, the *in vitro* approach enables a rapid, convenient and efficient screening facility with respect to formulation variables and structural modifications. Whilst clearly a valuable technique, disadvantages centre upon the fact that such a system does not exactly mimic the behaviour of the living tissue *in situ*. Excised skin may not retain full enzymatic activity due to the compromised viability of the epidermis, a factor which may also impact on the otherwise dynamic state of renewal of the stratum corneum. In addition, the absence of a substantial microvasculature may modify the clearance and therefore the flux of the penetrant. Despite these drawbacks, favourable correlations between *in vivo* and *in vitro* models have been reported (Bronaugh *et al*, 1982a; Franz, 1975, 1978), suggesting that well designed *in vitro* methodology can provide useful data, predictive of the *in vivo* situation.

A variety of diffusion cells, of different styles and configurations, may be employed for conducting *in vitro* permeation experiments (Barry, 1983). Most are based on the simple design of Franz (1975), where a membrane (skin or synthetic) is mounted, separating a donor and receptor chamber. The passage of drug, across the membrane, from the donor to the receiver compartment is then monitored by radiochemical, spectrophotometric or chromatographic (*e.g.* HPLC) analytical techniques. The latter is particularly suitable for the determination of degradation products or metabolites. The horizontal orientation of the membrane means that the donor chamber may be exposed to ambient temperature and humidity, while the lower chamber can be maintained at physiological temperature, thus mimicking *in vivo* conditions. Refinements to this basic design include flow-through diffusion cells (Bronaugh and Stewart, 1985a; Martin *et al*, 1989), which offer the advantage of continuous and automated sample collection. This is more representative of the *in vivo* milieu in terms of blood flow and permits a facile maintenance of sink conditions. Automated apparatus, comprising of small scale flow-through cells have the combined advantages of automation, *in vivo* simulation and need for very small samples of skin (Akhter *et al*, 1984). Inter-specimen

variation may therefore be eliminated by reducing the number of donors required for any investigation.

The nature of the membrane used for *in vitro* studies falls into three main categories; human skin, animal skin and synthetic model membranes. Human skin, being most representative of the *in vivo* barrier, is the membrane of choice, although by no means an ideal one (Skelly *et al*, 1987). Physiological factors such as skin age, site and condition contributing to large inter and intra-specimen variabilities in the barrier properties of human skin cannot be strictly controlled, especially when availability is often limited. In contrast, use of animal skin which is easier to obtain, imparts greater control over many of these parameters, thus reducing variability.

The relevance of animal models to human data appears to be dependent on both the animal species and the nature of the permeant (Bronaugh *et al*, 1982b; Bronaugh and Maibach, 1985). In general, pig and monkey skin appear to be good models for human skin, whilst rat, rabbit and mouse skin tend to be more permeable. Hairless mice represent a popular, easily obtainable and reproducible source of skin. A further advantage is that preparatory shaving, clipping or depilation is unnecessary; the smaller number of hair follicles relative to other more hirsute animals makes it more comparable to human skin in this respect. Although generally more permeable than human skin, several studies have reported similarities in permeation characteristics between the two skin types, for a selected number of alcohols and steroids (Durrheim *et al*, 1980; Stoughton, 1975). This partly reflects the nature of the compound and is not a universal observation. Hairless mouse stratum corneum is less substantial than its human counterpart (Bronaugh *et al*, 1982b) and this fragility may compromise its barrier properties in certain circumstances encountered in *in vitro* percutaneous penetration studies. Long-term hydration in excess of 24 to 48 hours leads to degeneration of the stratum corneum and a subsequent increase in permeability (Bond and Barry, 1988a; Hinz *et al*, 1989), thus restricting the use of this model. Reservations concerning the use of this model to predict the effect of penetration enhancers on human skin have also

been expressed, based on the greater susceptibility of the murine barrier to chemical impairment (Bond and Barry, 1988b; Rigg and Barry, 1990).

Many investigations have also utilized artificial systems such as silastic and eggshell membranes, zeolites and cellulose filters impregnated with oils or lipids to simulate the dermal barrier (Houk and Guy, 1988). The *in vitro* use of shed snake skin has also generated interest (Rigg and Barry, 1990). As with all model membranes, comparative studies with human skin are continually required to assess their utility.

The major barrier to the penetration of drugs across the skin is considered to reside in the stratum corneum. Hence, any change in this barrier function would be expected to influence the bioavailability of a topically applied drug. Most topical agents are designed for the treatment of diseased skin; a factor which may result in considerable modification of the rate-limiting barrier. Skin disorders such as psoriasis, characterized by a parakeratotic epidermal hyperproliferation are prime examples, and evaluation of drug permeation across normal skin may not be an adequate index of their behaviour in diseased skin (Schalla and Schaefer, 1985). The percutaneous absorption of hydrocortisone in psoriatic patients, as determined by urinary excretion, was similar to that in healthy subjects in a study by Wester *et al* (1983). However, Schaefer *et al* (1977) found significantly higher levels of triamcinolone acetonide within the involved skin, compared to uninvolved skin, of psoriatic patients. This may reflect an increased binding or reservoir function for corticosteroids, possibly due to the accompanying hyperkeratosis (thickened horny layer). Increased permeation of other steroids (Schalla *et al*, 1980), salicylic acid (Arnold *et al*, 1979) and hydroxyurea (Shrewsbury *et al*, 1980) in psoriatic skin has also been reported. The barrier function of psoriatic skin, therefore, appears to be compromised and may result in an increased local bioavailability, being dependent on the nature of the permeant and possibly the extent of the disease.

Impairment of barrier properties in man, due for example, to tape-stripping, results in enhanced skin permeability of a similar magnitude to that of psoriatic skin (Schaefer *et al*, 1977). Not surprisingly, animal models where the stratum corneum has been compromised in some way, have been proposed for damaged or diseased skin (Bronaugh and Stewart, 1985b; Scott and Dugard, 1981). Techniques to simulate dermatoses include tape-stripping, UV irradiation and chemical or thermal perturbation. A number of other studies investigating the effect of a damaged barrier on the absorption of chemicals have been published (Feldmann and Maibach, 1965; Flynn *et al*, 1981). The relevance of these studies, particularly *in vitro* investigations, to the clinical situation, however, remains to be determined.

5.1.3.1 Mathematical analysis of skin permeation

Mathematical relationships describing the permeation of drugs through the stratum corneum are an important consideration in identifying the basic principles which govern this process, evaluation of the pharmacokinetics and subsequent optimization of topical dosage forms and ultimately, the quantitative prediction of percutaneous absorption of drugs.

The theoretical diffusion profile of a drug through the skin, from an 'infinite' or effectively unchanging source, is illustrated in Figure 5.3. It is characterized by a period of non-steady state diffusion (non-linear portion of curve) while the amount of penetrant in the epidermis achieves equilibrium, followed by steady-state penetration (linear portion of curve) corresponding to a net balance in the rate of entry and exit of drug into and out of the epidermis.

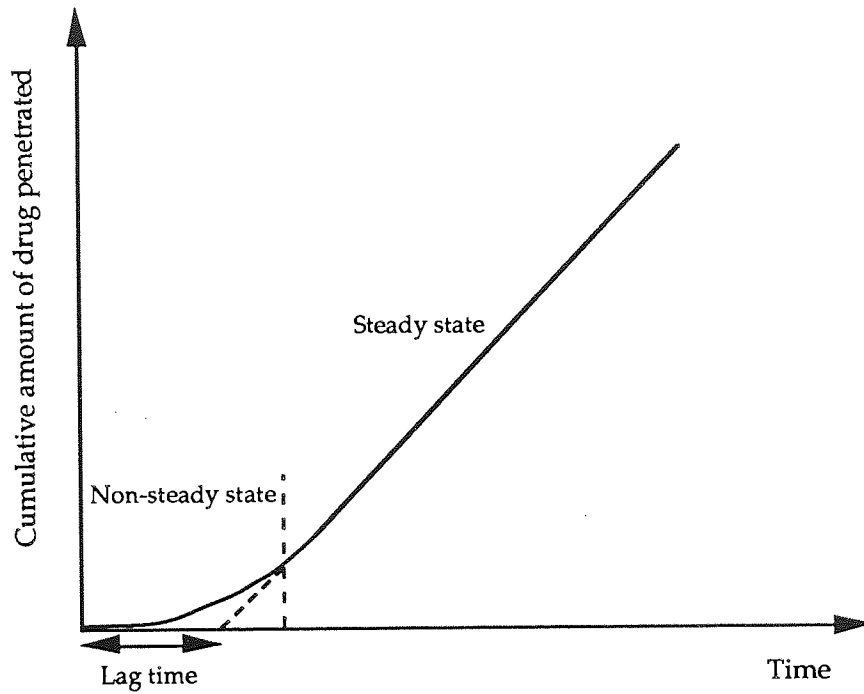


Figure 5.3 Schematic representation of a typical penetration profile through a membrane, using a two-compartment diffusion cell.

The most simple way of modelling the process of skin absorption is to apply Fick's first law of diffusion to this steady-state phase, which states that the rate of absorption is proportional to the concentration difference across the membrane:

$$J = -D \frac{dc}{dx} \quad (5.2)$$

where J is the amount absorbed through a unit area of membrane in unit time (penetrant 'flux'), dc/dx is the concentration gradient across the membrane and D is the diffusion coefficient or diffusivity of the drug in the membrane. The flux of the penetrant corresponds to the slope of the steady-state diffusion curve in Figure 5.3.

However, the stratum corneum is not simply an inert structural barrier to diffusion but one with an affinity for the applied solute. Hence, the drug concentration at the skin surface will not be the same as in the formulation but will be related to it according to the membrane-vehicle partition coefficient, P , which is defined as an index of the relative affinity of the solute for the stratum corneum and vehicle. Equation 5.2 can therefore be expressed as:

$$J = \frac{D P \Delta C_v}{\delta} \quad (5.3)$$

where J is the steady-state flux of the solute, D is the membrane diffusivity of the solute, ΔC_v is the concentration difference across the membrane, and δ is the membrane thickness.

If P, D and δ are combined into a single proportionality constant:

$$K_p = \frac{P D}{\delta} \quad (5.4)$$

where K_p represents the permeability coefficient, substitution into equation 5.3 gives:

$$J = K_p \Delta C_v \quad (5.5)$$

Provided that depletion in the donor compartment is negligible and sink conditions apply, ΔC_v approximates to C_v , since the applied concentration is essentially constant and the drug concentration in the receptor phase remains effectively zero, thus:

$$J = K_p C_v \quad (5.6)$$

The establishment of steady-state diffusion, described by the equations above, is preceded by a period (non-steady state) where the flux of the drug gradually increases as it equilibrates within the membrane (Figure 5.3). By extrapolating the linear region of this plot to the x-axis, a lag time (τ) can be defined, which is dependent upon the membrane diffusion coefficient (D) and the thickness of the membrane (δ):

$$\tau = \frac{\delta^2}{6D} \quad (5.7)$$

The lag time, therefore, allows an estimation of the diffusion coefficient, providing there is no skin binding. The time taken to achieve steady-state diffusion is considered to be approximately 2.7 times the lag time (Barry, 1983). As values of τ for different penetrants can vary from a few minutes to a many hours, this early phase of absorption is clearly of clinical relevance.

Equations 5.2-5.6 are only applicable to the steady-state phase of absorption provided there are no significant interactions, such as binding, between the drug and components of the skin (Katz and Poulsen, 1971). Such analysis of *in vitro* experiments, which enable steady state or quasi-steady state conditions to be achieved, have contributed significantly to an understanding of the inter-relationships between the drug, vehicle and skin and their influence on the absorption process. Although, Fick's first law of diffusion may be a valid approximation for such *in vitro* experiments, it is unlikely to be a true assumption *in vivo* (Guy and Hadgraft, 1985). This is because in most practical situations, it is unusual for skin to be in contact with a penetrant (i) of a constant concentration or 'infinite dose' and (ii) for periods long enough to establish steady-state conditions.

Equations used to model *in vivo* absorption profiles, which do not normally establish steady-state kinetics, are derivations of Fick's second law of diffusion:

$$\frac{dc}{dt} = D \frac{d^2c}{dx^2} \quad (5.8)$$

The resulting solutions which model the complete penetration profile rather than just the steady-state portion are complex, depending on boundary conditions for the experiment, and may require computer analyses (Dyer *et al*, 1984). They may be further complicated by the inclusion of terms to address events such as cutaneous metabolism (Guy and Hadgraft, 1982), dermal transport (Albery *et al*, 1983) and epidermal binding (Hadgraft, 1979).

The theoretical curve in Figure 5.3 may be described by the following simplified equation, provided that permeation is from an infinite dose (Scheuplein, 1978b):

$$M = CK \left\{ \frac{Dt}{h} - \frac{h}{6} - \frac{2h}{\pi^2} \sum_{n=1}^{\infty} \frac{(-1)^n}{n^2} \exp \left[\frac{-D n^2 \pi^2 t}{h^2} \right] \right\} \quad (5.9)$$

where M is the cumulative amount of drug in the receptor phase, C is the concentration of drug in the donor compartment, D is the diffusion coefficient of the drug in the skin, K is the skin-vehicle partition coefficient, h is the thickness of the skin and t is the time elapsed. Equation 5.7 may also be applied to determine D from the lag time.

The objectives of the present study were to assess the influence of a range of formulation parameters on the *in vitro* percutaneous penetration of azidoprofen, and to correlate these observations with physicochemical drug-vehicle-membrane inter-relationships governing this process. Much of the work employed excised hairless mouse skin as a model membrane to study the transport of AZP from aqueous solutions and suspensions. Experiments to examine the effect of vehicle pH, permeant concentration, and inclusion of penetration enhancers on penetration were conducted. In order to correlate observed fluxes with physical variables, solubility, partition coefficients and ionization constants were determined under the conditions of the penetration studies. Preliminary studies also compared the absorption profiles of ibuprofen and AZP across an artificial membrane.

5.2 EXPERIMENTAL

5.2.1 Preparation of membranes

Skin was obtained from male hairless mice (type MF1, supplier Olac Ltd.), 2-6 months old and weighing 20-30g. The mice were sacrificed by cervical dislocation and whole thickness intact skin carefully excised and placed in ice-cold phosphate buffered saline (PBS; Appendix 2). After removal of any subcutaneous fat or visceral debris from the undersurface, the membranes were washed with PBS and either used immediately or stored in the frozen state, between sheets of aluminium foil for up to 12 hours (until commencement of the permeation study at a suitable time). Each epidermal specimen generally provided sufficient skin for three or four diffusion cells, each portion measuring approximately 2.5-3.0 cm in diameter. These samples were distributed amongst the experiments, which were designed such that each set of replicate permeability values was obtained from at least two and usually three donors, thus minimizing inter-specimen variation between comparative determinations.

A series of experiments also utilized a silicone rubber membrane (Silastic® Medical grade 500-3, Dow Corning, 0.010 in. thick). The membrane was rinsed in distilled water to remove surface chemicals deposited during their manufacture and subsequently cut into rectangular sections of appropriate size, prior to mounting on to diffusion cells.

5.2.2 Diffusion cell design

Franz-type diffusion cells (Franz, 1975) as shown in Figure 5.4, were employed during the course of the permeation studies. The membrane was mounted (epidermis uppermost, in the case of skin) between the two halves of the diffusion cell, comprising an upper donor chamber and a lower receptor chamber, thereby offering a surface area of approximately 2.0 cm² for diffusion. The two halves of the cell were secured with Nescofilm and held together by a spring clamp. The receptor compartment, which had a capacity to hold 20 to 30 ml of fluid, could be sampled *via* a side arm. This sampling port was sealed

with a small rubber stopper in between sampling to prevent evaporation of the receptor solution. Uniform mixing of the drug in the receiver phase was achieved by a small teflon coated magnetic stirring bar driven by an external motor. The receptor cell was maintained at 37°C by a thermostatic water pump which circulated water through a jacket surrounding the cell body. This resulted in donor phase (and skin surface) temperature of $32 \pm 1^\circ\text{C}$. The donor chamber could be sealed with a perspex lid to minimize evaporation of the donor fluid during the permeation study.

5.2.3 Preparation of test vehicles

A range of non-buffered (10-50% v/v PG in water) and buffered aqueous propylene glycol mixtures (10% v/v PG in water; pH 3.50-7.40) were used as test vehicles during the permeation studies. To prepare the latter vehicles, concentrated citric acid-phosphate (McIlvaine) buffers of constant ionic strength (pH 3.0-7.0) were initially prepared according to Appendix 2. These were then diluted by a factor of 10, incorporating propylene glycol to a concentration of 10% v/v. pH measurements were adjusted as required with sodium hydroxide or phosphoric acid to reproduce values used in different experiments; pH values quoted are those of the final mixture. Donor phases consisted of either solutions, saturated solutions or suspensions in the appropriate vehicle. Saturated solutions and suspensions were prepared by stirring an appropriate excess (3-4 times saturated solubility) of AZP (free acid) in vehicle (10 ml) in a sealed container, protected from light, for 24 hours at 32°C. To produce a saturated solution, the resulting suspension was filtered using a 0.2 µm membrane filter (Millipore GS). Suspensions of caffeine in 10% PG-buffer were prepared similarly. Penetration enhancer pretreatment solutions were prepared by dissolving the enhancer to the required concentration (% v/v or % w/v) in the appropriate solvent. Enhancers used were 3% v/v azone in PG, 3% v/v azone with 0.1% Tween 20 in normal saline (T/S), 5% v/v oleic acid in PG, 15% w/v decyl methyl sulphoxide (DCMS) in PG, 0.5% w/v dodecylamine (DCA) in PG. Control experiments using propylene glycol and 0.1% Tween 20 in normal saline as pretreatment solutions were also conducted.

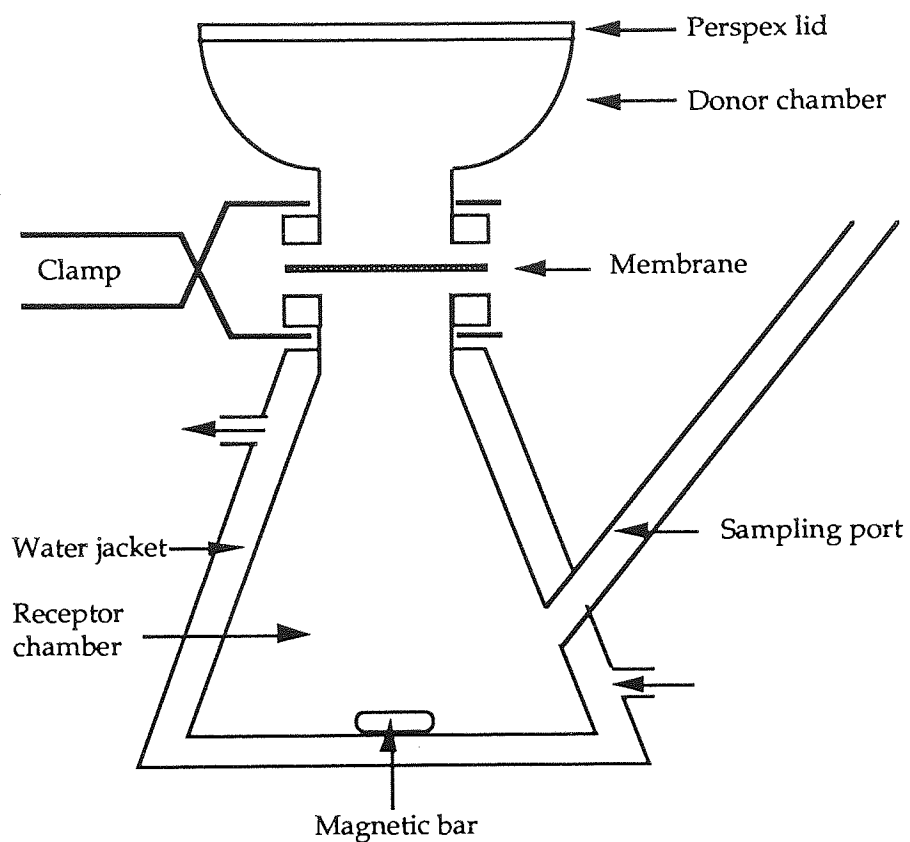


Figure 5.4 Schematic representation of a Franz-type diffusion cell.

5.2.4 Permeation procedure

For all permeation studies, receptor phase solutions were chosen so as to correspond to the donor phase vehicle, *i.e.*, if the donor phase consisted of an AZP suspension in 10% PG-buffer (pH 4.50), then the corresponding drug-free vehicle was employed as the receiver fluid. Subsequent to mounting the membrane and assembling the diffusion cell as described in section 5.2.2, receptor chambers were filled with the chosen vehicle (20-30 ml; accurately measured), which had been maintained at 37°C and de-gassed by sonication to minimize volume changes and prevent accumulation of air bubbles at the skin-receptor fluid interface. The membrane was allowed to equilibrate with the receptor solution for 1 hour, at which time any air bubbles which had collected in the vicinity of the membrane were removed *via* the sampling port by carefully rocking the cell assembly. An aliquot (5 ml for solutions; 3 ml for suspensions) of the formulation under study was introduced into the donor chamber. During initial permeation studies with AZP and IBP, across silastic membrane, a donor volume of 15 ml was used.

Samples of the receptor phase (1 ml) were removed at appropriate intervals (usually hourly) after addition of the donor phase and assayed by HPLC (section 2.3.2) following suitable dilution. After the withdrawal of each sample the receptor fluid was replenished with an aliquot of the drug-free vehicle. As this resulted in progressive dilution of the receptor phase, it was necessary to adjust each successive sample concentration for the dilution attending all previous sampling. This was accomplished by applying the following correction factor:

$$C_t = C_{mt} + \left[V_s \cdot \frac{\sum_{t=1}^{t=n-1} C_m}{V_r} \right] \quad (5.10)$$

where C_t is the current concentration of permeant in the receptor phase at time t , C_{mt} is the current *measured* concentration of permeant in the receptor chamber, V_s is the volume of sample removed for analysis, V_r is the volume of

the receptor medium, and ΣC_m is the summed total of the previous measured concentrations ($t = 1$ to $n-1$).

For studies involving pretreatment procedures, the pretreatment solution (1 ml) was applied to the epidermal surface of the skin for 1 or 12 hours, according to the experimental protocol, prior to introduction of the test formulation. At the end of this period, the application was removed by gently blotting with a paper tissue. The skin surface was then briefly rinsed with distilled water and blotted dry prior to addition of the donor medium.

All permeation studies were performed in triplicate and were protected from light for the duration of the study. The concentration of permeant in the receptor phase at each sampling point was determined by HPLC and corrected for preceding dilutions as described. The amount of drug penetrating the membrane per unit area was calculated by accommodating the volume of the receptor solution and the area of the membrane available for diffusion, which varied for each cell. A plot of the cumulative amount penetrated per unit area as a function of time yielded the steady-state flux (slope of linear portion of profile), the permeability coefficient (flux (J)/saturated concentration (C_v) of permeant in the donor phase) and the lag time (x-axis intercept of extrapolated linear regression line).

5.2.5 Solubility determinations

The solubility of AZP in each vehicle employed was determined in triplicate as follows. An excess of AZP (25-50 mg) was suspended in the appropriate solvent system (5 ml) in a stoppered glass sample tube at 32°C. These suspensions were stirred for 48 hours after which time they were allowed to stand for 2-3 hours. An aliquot of the supernatant fluid was withdrawn and filtered through a 0.2 μm membrane filter (Millipore GS), which was initially diluted to yield a propylene glycol (PG) concentration of 50% v/v. All further dilutions were performed with the latter solvent (50% v/v PG). Concentrations of AZP were determined by assaying 10 μl aliquots of the resulting filtrate by HPLC (system

A; section 2.3.2). A temperature of 32°C was chosen for the study as this was representative of the conditions in the donor chamber of the diffusion cells.

5.2.6 Partition coefficient measurements

Isopropyl myristate/water

Oil-water partition coefficients for AZP between equal volumes of isopropyl myristate (IPM) and aqueous buffer were determined at 37°C over a pH range of 3.20-7.40. Citric acid-phosphate buffers of constant ionic strength (0.5 M) were prepared according to Appendix 2. The buffers were presaturated with IPM by being agitated overnight at 37°C, before separation by centrifugation after standing in a separating funnel. A quantity of IPM was similarly presaturated with distilled water.

Stoppered sample tubes containing equal volumes (5 ml) of aqueous buffer and a solution of AZP in IPM (100 µg ml⁻¹) were shaken mechanically in a water bath at 37°C for 12 hours. After centrifugation (500 g, 10 min) to ensure separation of the two phases, an aliquot of the aqueous phase was diluted with internal standard solution (butyl paraben; 10 µg ml⁻¹ in IPM saturated DW) and assayed for AZP content by HPLC (system A). The concentration of AZP in the IPM phase was estimated by the difference between the initial and final drug concentration in the aqueous phase. The experiments were performed in triplicate for each buffer solution.

Partition coefficient measurements for the alkyl esters of AZP were also attempted by determining the distribution of the esters between equal volumes of IPM and aqueous buffer (pH 7.4). The greater lipophilicity of these esters, however, favoured partitioning into the oily phase which made it extremely difficult to accurately detect the relatively low levels in the aqueous phase. Use of volume differentials (small volumes of non-polar solvent relative to polar) to ensure retention of larger amounts of sample in the aqueous phase did not completely resolve the problem.

Octanol-water

To partially overcome difficulties presented by the lipophilic esters, the IPM phase was replaced by *n*-octanol, enabling HPLC analysis of both the aqueous and non-aqueous phases. Further modifications incorporated the use of volume differentials, conducting the experiment at room temperature and for short equilibration periods to minimize adsorption onto glass and the inclusion of a cosolvent (PG) in the aqueous phase to enhance partitioning into this layer. Although this latter precaution would not provide a true octanol/water partition coefficient, it was expected to allow a comparative assessment of lipophilicity amongst the congeneric series of esters.

Solutions of 20% PG in distilled water and octanol were presaturated with each other in the ratio 40:1 at room temperature. A quantity of 20% PG in 0.1 M HCl was similarly presaturated with octanol. Presaturation was performed with these volume ratios as they conformed to those used in the actual partitioning experiment. It was necessary to replicate these conditions in order to control and maintain the distribution of PG between the two immiscible solvents (which would in turn influence partitioning of the compounds under study). Stock solutions of the esters (4 mg ml⁻¹) were prepared in appropriately presaturated octanol. Stoppered flasks consisting of 200 ml of 20% PG in DW, 4.5 ml of octanol and 0.5 ml of ester stock solution were manually inverted at frequent intervals for a period of 1 hour, at room temperature, to establish equilibrium. After separation of the two phases by centrifugation, both layers were analyzed by HPLC (system B) following dilution with methanol and internal standard. All experiments were performed in triplicate.

AZP was assessed similarly, replacing the aqueous (PG-DW) phase with either (a) a solution of 20% PG in 0.1 M HCl or (b) 0.1 M HCl, to maintain the azide in an unionized form.

The apparent octanol-water partition coefficient of AZP, over a range of pH's, was also determined as follows. Citric acid-phosphate buffers were prepared in the pH range 4.20-7.40 (Appendix 2). Both buffer and octanol were presaturated

with each other at 37°C. Stoppered sample tubes containing 5ml of aqueous buffer and 5 ml of octanol containing AZP (400 µg ml⁻¹) were magnetically stirred in a jacketed beaker maintained at 37°C by a Churchill circulating thermostatic pump for 12 hours. The two phases were separated by centrifugation (500 g, 10 min) and appropriately diluted with methanol to yield a final MeOH concentration of 75% v/v. Both phases were then diluted with internal standard solution (butyl paraben) prior to HPLC analysis.

A similar experiment was also conducted at 20 ± 1°C, where only the aqueous phase was assayed for AZP. All determinations were performed in triplicate. The partition coefficient (P) between two phases was calculated using:

$$P = \frac{C_{\text{org}}}{C_{\text{aq}}} \quad (5.11)$$

where C_{org} and C_{aq} are the solute concentrations in the organic and aqueous phases after partitioning respectively. Where only the aqueous phase was assayed, C_{org} was calculated by subtracting the concentration in the aqueous phase after partitioning (C_t) from that initially (C_o), and correcting for the volumes of the aqueous (V_{aq}) and organic (V_{org}) phases:

$$C_{\text{org}} = \frac{V_{\text{aq}} (C_o - C_t)}{V_{\text{org}}} \quad (5.12)$$

Skin/vehicle

Partitioning of AZP between various vehicles employed during the permeation studies and hairless mouse skin, either untreated or pretreated with appropriate penetration enhancers, was estimated as follows.

Hairless mouse skin was obtained as described in section 5.2.1. Adherent subcutaneous fat and tissue were carefully removed before separation of the dermis and epidermis. This was achieved by immersing the membrane in water at 55°C for 30 seconds followed by ice cold phosphate buffered saline (PBS). The dermis was then removed with a sharp scalpel blade. Quantities of

skin were then pretreated with vehicle systems employed in the permeation studies by immersing in the vehicle for an appropriate period of time (1 or 12 hours) followed by rinsing in distilled water and PBS. Segments of skin (pretreated or untreated as required) were then blotted dry on filter paper and accurately weighed (150-200 mg) into glass sample tubes. Aliquots (1 ml) of AZP solution (200 μ M) in the appropriate vehicle was introduced into the sample tube and the contents gently mixed in a water bath at 37°C for 60 hours.

Samples of the aqueous layer were diluted with solvent and internal standard solution prior to HPLC analysis. The amount of AZP taken up by the skin was estimated by calculating the difference between the initial and final concentration in the aqueous layer. Densities of the AZP solutions were determined using 25 ml density bottles so that partition coefficients could be calculated on the basis of weight as opposed to volume (equation 5.13). All determinations were performed in triplicate and controls (without skin) included to assess any loss due to uptake by glass.

$$P = \frac{\text{mass of solute per g of skin}}{\text{mass of solute per g of vehicle}} \quad (5.13)$$

5.2.7 pK_a determinations

Ionization constants for AZP, both in aqueous media and 10% propylene glycol-water were obtained by potentiometric methods (Albert and Serjeant, 1984). The accuracy of this methodology was assessed by ascertaining the pK_a value of a standard, benzoic acid, using the same procedure. Stock solutions of 0.05 M sodium hydroxide in DW, 0.0025 M AZP in DW and 10% PG-DW and 0.005 M benzoic acid in DW were prepared using cooled boiled distilled water (free from CO₂) and stored at 25°C.

Figure 5.5 represents a schematic diagram of the apparatus employed. An aliquot (10 ml) of the drug solution was introduced to the jacketed titration cell, which was maintained at 25°C by a Churchill circulating thermostatic pump. This was then titrated by the addition of 0.05 M sodium hydroxide (50 μ l).

aliquots; end-point 0.5 ml for AZP, 1.0 ml for benzoic acid). The solutions were stirred for ~30 secs in between each addition and allowed a further 30 secs to equilibriate before a pH measurement was obtained. Each determination was repeated 5 times. Data were subjected to computer analysis in order to calculate pK_a values.

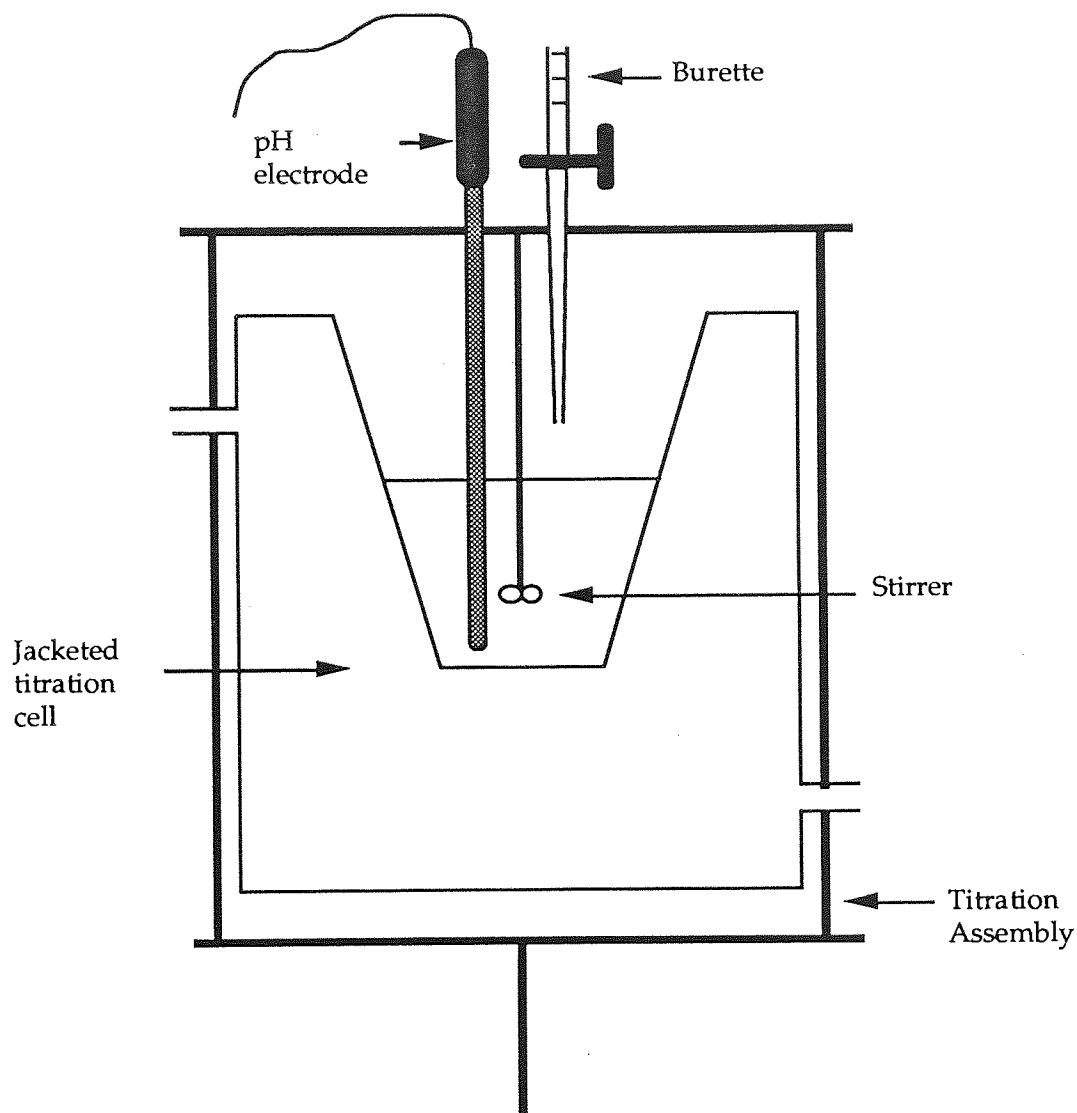


Figure 5.5 Schematic representation of a titration assembly used to determine ionization constants

5.3 RESULTS AND DISCUSSION

5.3.1 Measurement of physicochemical parameters

Measurements of solubilities, partition coefficients and ionization constants (pK_a) for AZP were conducted, where possible and/or deemed appropriate, to reflect the conditions of the percutaneous absorption experiments to which they were to be correlated. For example, solubilities were determined at 32°C, a temperature representative of the donor chamber.

Ionization constant

The pK_a for AZP was determined potentiometrically in (a) water, and (b) 10% propylene glycol-water. The obtained values are summarized in Table 5.1. The accuracy of this methodology was assessed by determining the pK_a for the aryl acid, benzoic acid, values for which are well documented in the literature. The result shows that the experimental value is within 5% of those quoted in the literature, suggesting a similar range of accuracy for AZP.

Table 5.1 Example ionization constants.

Compound	Solvent	Experimental value (\pm sem)	Literature value
AZP	water	4.294 (9.24×10^{-3})	—
	10% PG-water	4.357 (8.83×10^{-3})	—
Benzoic acid	water	4.113 (8.69×10^{-3})	4.199 ^a
			4.205 ^b
Ibuprofen	water	—	4.4 ^c

Measurements carried out at 25°C.

^a Brockman and Kilpatrick (1934)

^b King and Prue (1961)

^c Albert and Serjeant (1984)

Solubilities

Solubility determinations were performed for those solvent systems employed during the penetration experiments. These generally utilized propylene glycol as a cosolvent in order to facilitate inclusion of penetration enhancers in later studies. The same protocol was therefore adopted for investigations in the absence of enhancers to aid comparison. Incorporation of propylene glycol into aqueous buffers at a level of 10% v/v enabled the solvent mixture to remain essentially aqueous and thus less susceptible to pH modification due to addition of cosolvent.

The solubility of AZP was determined in (a) 10% v/v propylene glycol/buffer mixtures of varying pH and (b) propylene glycol/buffer mixtures of varying cosolvent concentration but constant pH (4.50). Due to a limited supply of AZP, measurements in only those vehicle systems of direct relevance to permeation experiments were performed and hence, do not represent a comprehensive solubility profile amenable to detailed mathematical analysis.

The mean saturated solubilities in these systems are summarized in Tables 5.2 and 5.3. The solubility of AZP increases with increasing pH. The degree of dissolution in this case will be determined by the fraction of ionized species in the system, with the anionic form being more soluble. For a weakly acidic molecule such as AZP, a rise in pH results in an increase in the percentage ionization, thus rendering the molecule more soluble. Similarly, the solubility of AZP increases in tandem with the increasing solubilizing capacity of the vehicle. Since the pH is maintained at a constant value, any influence of this parameter on the solubility is eliminated.

Table 5.2 Effect of pH on the saturated solubility of AZP in 10% propylene glycol-buffer at 32°C.

pH	AZP solubility \pm sem ($\mu\text{mol ml}^{-1}$)	Percentage ionization*
3.50	11.502 \pm 0.925	12.20
4.00	16.438 \pm 0.416	30.53
4.50	20.731 \pm 0.375	58.16
5.00	29.549 \pm 0.678	81.47
5.50	39.203 \pm 0.979	93.29
6.50	54.640 ¹	99.29
7.40	123.093 ¹	99.91

* calculated using equation 5.15; pKa value of 4.357.

¹ n=2

Table 5.3 Effect of propylene glycol (PG) concentration on the saturated solubility of AZP in buffered vehicles (pH 4.50), at 32°C.

Percentage PG in water	AZP solubility \pm sem ($\mu\text{mol ml}^{-1}$)
0	17.253 \pm 0.499
10	20.731 \pm 0.375
20	28.088 \pm 0.233
30	39.242 \pm 3.605
40	76.787 \pm 4.623
50	159.312 \pm 3.178

Partition coefficients

Partition coefficients for AZP were determined between

- (a) Octanol and buffers of varying pH at 20°C and 37°C.
- (b) Isopropyl myristate and buffers of varying pH at 37°C.
- (c) Hairless mouse skin and
 - (i) 10% propylene glycol-buffer vehicles of varying pH.
 - (ii) propylene glycol-water mixtures.
- (d) Hairless mouse skin pretreated with various enhancer treatments and 10% propylene glycol-buffer systems.

Determinations were also made for the methyl, ethyl and propyl esters of AZP between octanol and 20% propylene glycol-water. Propylene glycol was included in the aqueous phase to favour partitioning of the highly lipophilic esters into this phase. This was necessary as preliminary studies were unable to detect, within the limits of analytical sensitivity, adequate levels of drug in the aqueous phase. Although not providing true oil/water partition coefficients, they were expected to enable a comparative examination of lipophilicity. The data are presented in Table 5.4. Figure 5.6 illustrates the linear relationship between log P and increasing alkyl chain length of the esters.

The dependence of the apparent oil/water partition coefficient of AZP on pH is illustrated by Figures 5.7-5.8. Partitioning into the aqueous phase increases with increasing pH, as a result of enhanced dissociation and consequently the presence of a larger fraction of charged species with a greater affinity for the aqueous phase. For a weak acid or base, both the unionized and ionized species will contribute to the observed distribution between the two phases, although to varying extents; partitioning into the oily phase being favoured by the undissociated form. Hence, the observed or apparent partition coefficient (P_{app}) of an ionizable species will be dependent on the individual partition coefficients of the unionized (P_u) and the ionized form (P_i), and the degree of dissociation.

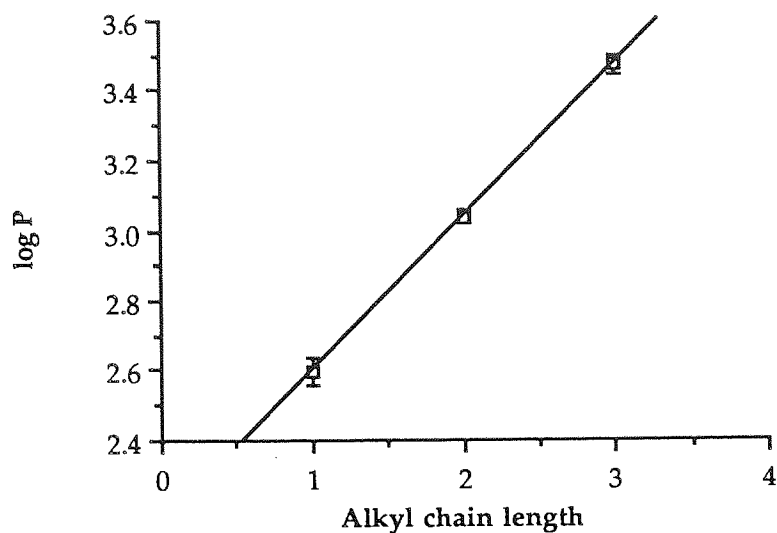


Figure 5.6 Plot of log octanol/20% propylene glycol-water partition coefficient against alkyl chain length for alkyl esters of AZP. Points are the mean \pm sem of three determinations.

Table 5.4 Partitioning data for AZP and corresponding alkyl esters between octanol and 20% propylene glycol in water at 20°C.

Compound	Log P (\pm sem)
AZP	2.437 (\pm 0.010)
Methyl ester	2.596 (\pm 0.037)
Ethyl ester	3.037 (\pm 0.019)
Propyl ester	3.473 (\pm 0.028)

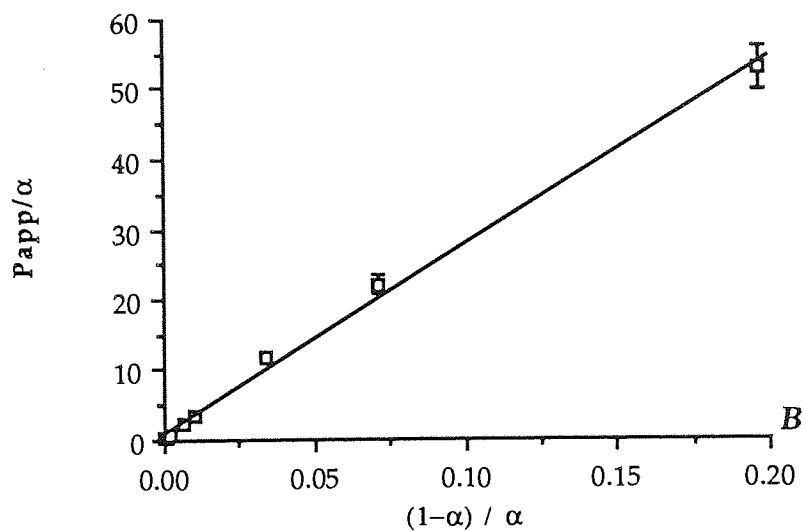
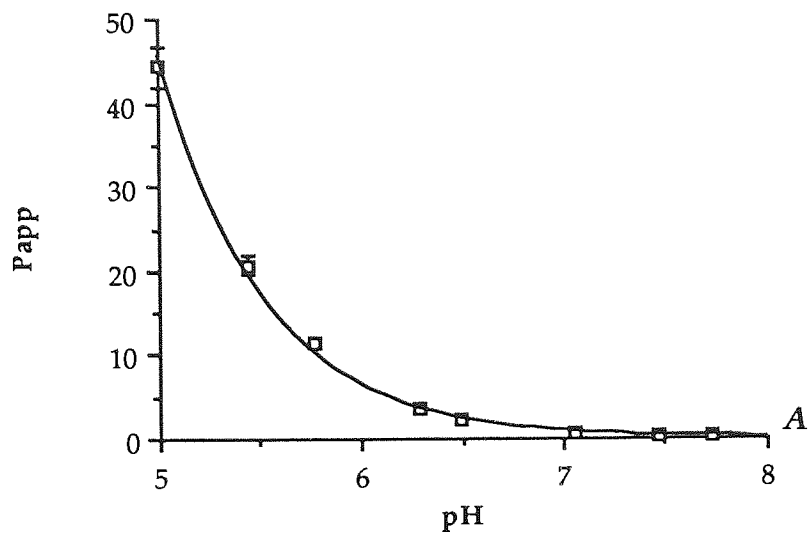


Figure 5.7 Effect of pH on the apparent partition coefficient of AZP between octanol and McIlvaine buffer at 20°C.

(A) Plot of P_{app} against pH. (B) Plot of P_{app}/α against $(1-\alpha)/\alpha$ to determine P_u and P_i (see text).

Points are the mean \pm sem of three determinations.

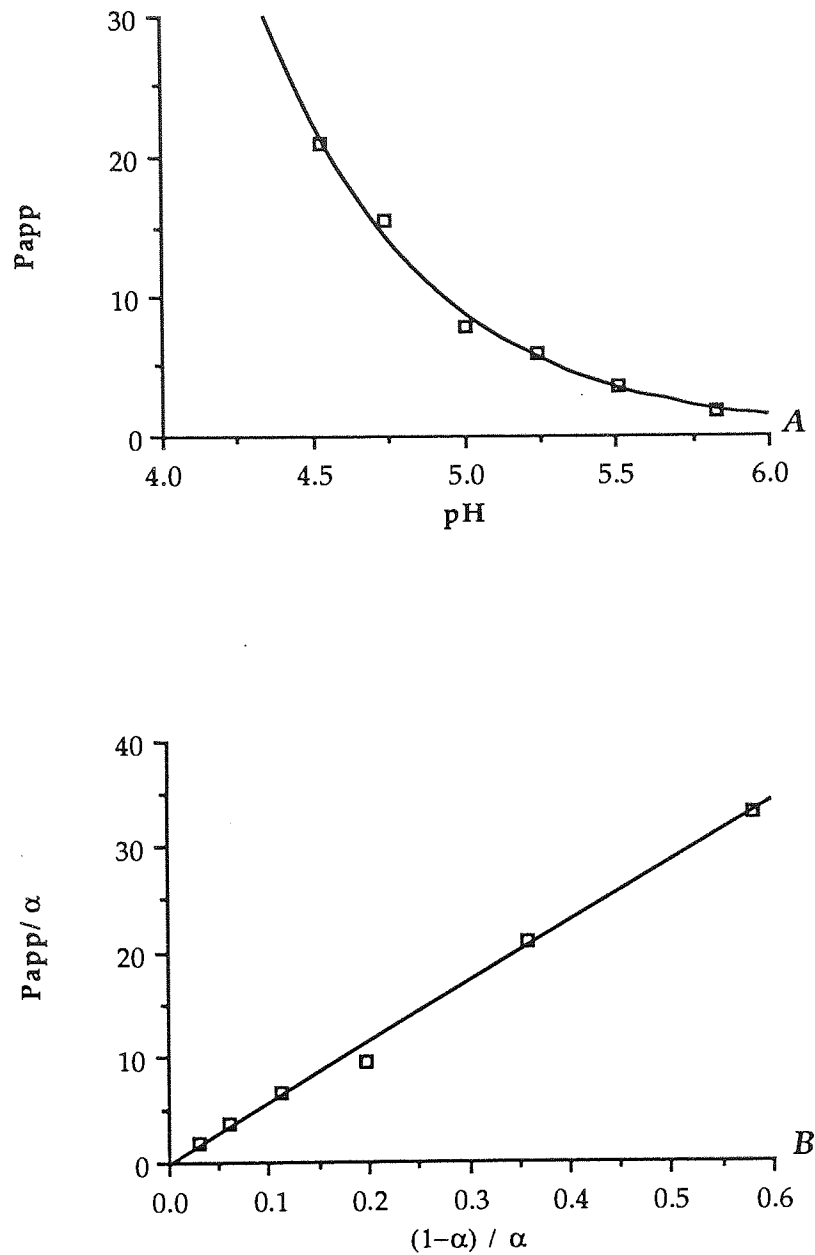


Figure 5.8 Effect of pH on the apparent partition coefficient of AZP between IPM and McIlvaine buffer at 20°C.
 (A) Plot of P_{app} against pH. (B) Plot of P_{app}/α against $(1-\alpha)/\alpha$ to determine P_u and P_i (see text).
 Points are the mean \pm sem of three determinations.

For a weak acid, the degree of dissociation at any pH may be calculated by using the Henderson-Hasselbalch equation (Florence and Attwood, 1988):

$$\text{Fraction ionized } (\alpha) = \frac{1}{1 + \text{antilog}(pK_a - \text{pH})} \quad (5.14)$$

Irwin and Li Wan Po (1979) derived a mathematical relationship between P_{app} , P_u , P_i and the degree of dissociation for a weak base, thus enabling a determination of P_u and P_i from experimental data. Following similar treatment for a weak acid (Sanderson, 1986), the following equations may be derived:

$$P_{app} = \alpha P_i + (1 - \alpha) P_u \quad (5.15)$$

or

$$\frac{P_{app}}{\alpha} = P_i + \frac{(1 - \alpha) P_u}{\alpha} \quad (5.16)$$

A plot of P_{app}/α against $(1 - \alpha)/\alpha$ should, therefore, yield a straight line of slope P_u and intercept P_i . This analysis was applied to the data obtained from a study of the octanol/water and IPM/water partitioning for AZP (Figures 5.7 B-5.8 B). The results are presented in Table 5.5.

Partitioning data for AZP between hairless mouse skin and 10% v/v propylene glycol-buffer vehicles (pH 3.5-7.4) are presented in Figure 5.9. As with the oil/water distribution data discussed above, partitioning into the lipid phase increases with decreasing pH, as the proportion of neutral molecules rises.

Table 5.5 Partitioning data for AZP between various systems.

Organic phase	Aqueous phase	Temp. (°C)	P_u	P_i
Octanol	Buffer	20	269.27	0.975
		37	380.16	4.179
Isopropyl myristate	Buffer	37	57.37	-0.156*
Hairless mouse skin	10% PG in buffer	37	6.84	1.112
Hairless mouse skin (pretreated with 3% azone for 12 hrs)	10% PG in buffer	37	37.42	1.333

* negative value indicates nil penetration into the organic phase.

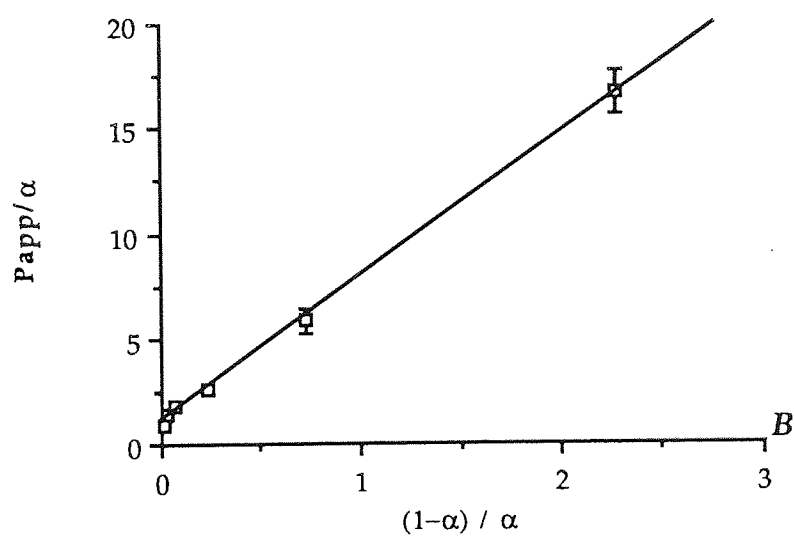
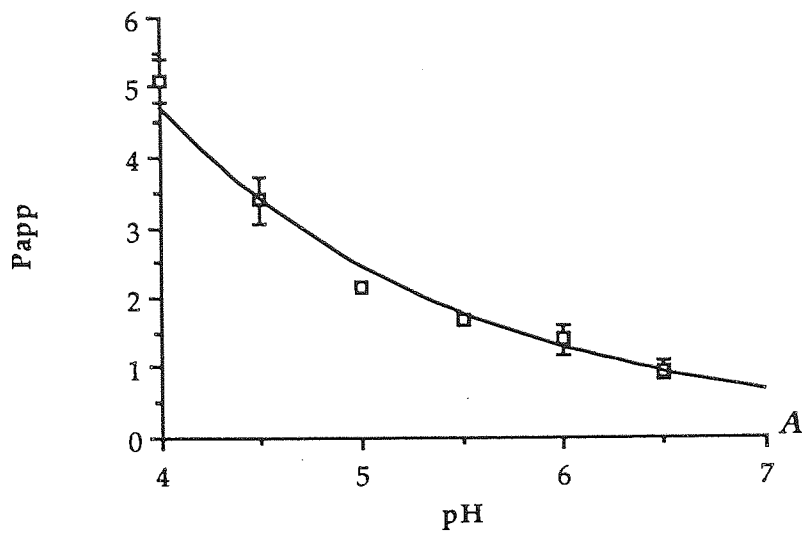


Figure 5.9 Effect of pH on the partitioning of AZP between hairless mouse skin and 10% propylene glycol-buffer at 37°C. (A) Plot of P_{app} against pH. (B) Plot of P_{app}/α against $(1-\alpha)/\alpha$ in order to determine P_u and P_i (see text). Points are the mean \pm sem of three determinations.

Figure 5.10 illustrates the partition data for AZP between hairless mouse skin and propylene glycol-water mixtures. The effect of increasing propylene glycol concentration in the aqueous phase is less interpretive, showing no significant influence on the partitioning behaviour. As the fraction of propylene glycol and therefore the affinity of the solute for the aqueous layer increases, one would expect a decrease in the P_{app} . This effect is probably not observed since only a limited concentration range of propylene glycol was studied, over which the solubility increases only moderately; observation of any subtle changes may have been precluded by the inherent errors of this methodology.

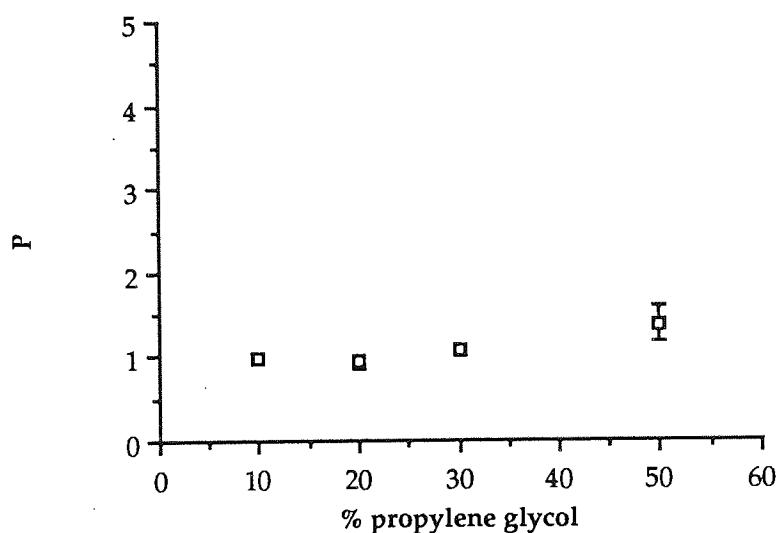
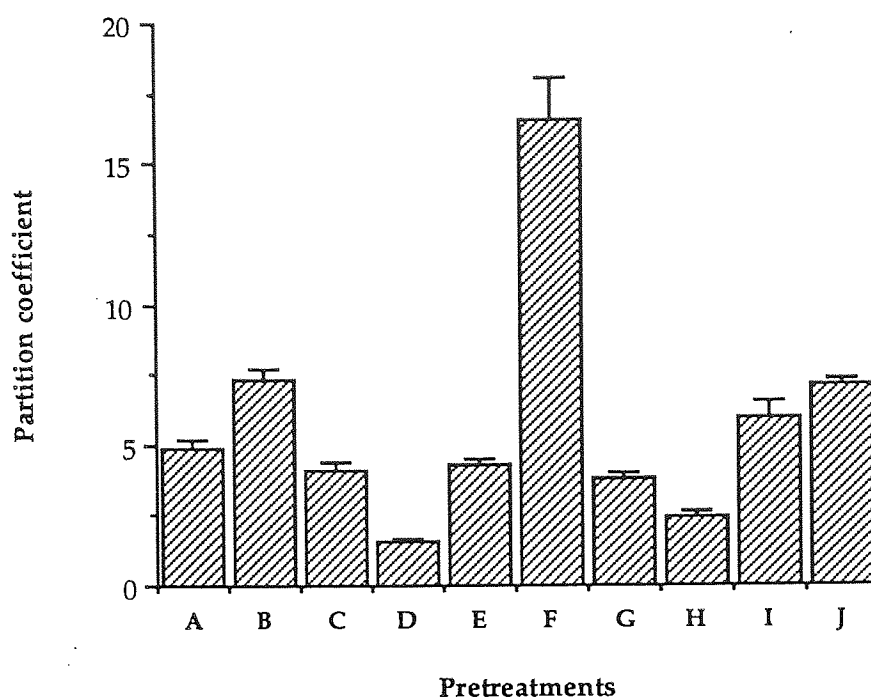


Figure 5.10 Effect of propylene glycol concentration on the partitioning of AZP between hairless mouse skin and propylene glycol-water mixtures.

The technique employed was subject to inaccuracies and difficulty in interpretation for a number of reasons. Since only the aqueous phase was monitored for AZP, the amount taken up by the membrane could only be estimated. A direct measurement, by radiochemical analysis for example, would improve accuracy and precision. The use of isolated stratum corneum would provide a better index of SC-vehicle partition coefficient by eliminating variation due to binding and dissolution in the remainder of the skin layers.

To remedy this situation, at least in part, an attempt was made to use epidermal membranes throughout, however the success of the separation technique could not always be assessed. Drug binding to stratum corneum components may also provide misleading results, since this proportion of the drug although not contributing to the permeation process, may result in high partition coefficients. Immersion of skin samples in a solvent for lengthy periods of time leading to alteration in the state of skin hydration or dissolution of drug in vehicle entrapped within the skin do not resemble the *in vivo* situation and pose further difficulties in interpretation (Barry, 1983). Despite these limitations, it represents the only realistic partitioning measurement which can be correlated directly with skin permeation (Katz and Poulsen, 1971).

Figure 5.11 presents the data for AZP partitioning between 10% propylene glycol-buffer (pH 4.50 or 6.50) and hairless mouse skin pretreated with an enhancer or control regimen (for 1 or 12 hours as stated). The pretreatment procedure was analogous to that performed in subsequent permeation experiments. Similarly, the distribution data for AZP between hairless mouse skin (pretreated with 3% azone in PG) and 10% PG-buffers (pH 4.50 to 6.50) are presented in Figure 5.12. These data will be discussed with reference to the permeation studies, where appropriate, at a later stage.



KEY

Code	Pretreatment	pH of aqueous phase	Length of treatment (hours)
A	0.1% v/v tween 20 in normal saline (TS)	4.50	12
B	3% azone in TS	4.50	12
C	Propylene glycol	4.50	1
D	Propylene glycol	6.50	12
E	Propylene glycol (PG)	4.50	12
F	3% azone in PG	4.50	12
G	0.5% dodecylamine in PG	4.50	1
H	0.5% dodecylamine in PG	6.50	12
I	0.5% dodecylamine in PG	4.50	12
J	5% oleic acid in PG	4.50	12

Figure 5.11 Partitioning data for AZP between hairless mouse skin, pretreated with various regimens, and 10% PG-buffer. Error bars are the sem of three determinations.

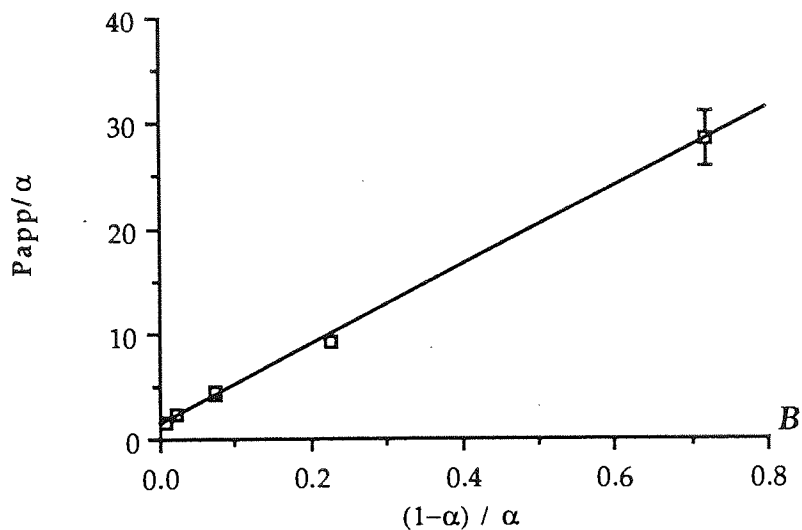
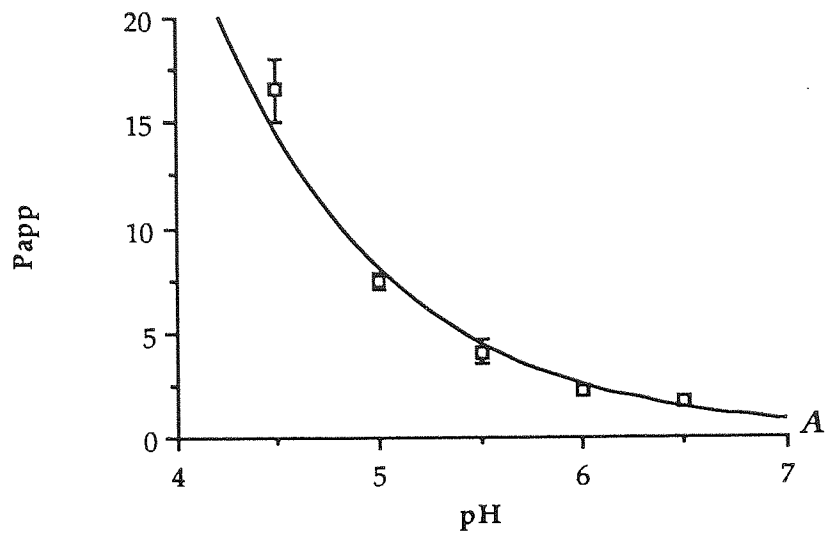


Figure 5.12 Effect of pH on the partitioning of AZP between hairless mouse skin pretreated with 3% v/v azone in PG for 12 hours and 10% PG-buffer.

(A) Plot of P_{app} against pH. (B) Plot of P_{app}/α against $(1-\alpha)/\alpha$ in order to determine P_u and P_i .

Points are the mean \pm sem of three determinations.

5.3.2 Percutaneous absorption studies

Experimental design

Before examining the results of the *in vitro* permeation studies undertaken with AZP, it is appropriate to discuss the choice of certain experimental parameters pertaining to these studies.

The selection of an appropriate membrane to model human skin is one of the most important considerations; permeation being largely dependent on the nature of this membrane. An overview of the choice available and its relevance to *in vivo* conditions was presented in section 5.1.3. Much of the current experimental work was performed using isolated hairless mouse skin, which although much more permeable than human skin, is a reasonably good and increasingly popular model. Reservations concerning the use of this murine membrane with respect to the duration of such studies (Bond and Barry, 1988a; Hinz *et al*, 1989) and the investigation of penetration enhancement (Bond and Barry, 1988b) were taken into consideration. Studies were conducted for a period of less than 48 hours, and usually for 12 to 24 hours, well below the recommended limits (< 2-3 days), thereby minimizing effects of prolonged hydration on barrier integrity. Evaluations of penetration enhancement were performed using the same membrane for comparative purposes, thus enabling a preliminary screening of putative enhancer treatments, whilst recognizing the limitations of this model when making any extrapolations to human skin.

Several comparative permeation studies of AZP and ibuprofen were also undertaken. These employed an artificial dimethyl polysiloxane model membrane, otherwise known as silastic. The largely lipoidal nature of the stratum corneum has implications for the use of simple lipid membranes such as silastic to mimic skin, which have found widespread use in permeation studies (Houk and Guy, 1988). Of a range of synthetic membranes used to study the permeation of salicylic acid, silastic yielded a flux closest to that of excised human skin (Nacht and Yeung, 1985). A composite (cellulose acetate/silastic/cellulose acetate) membrane, reflecting the multilamellar organization

of stratum corneum lipids with alternating hydrophilic and hydrophobic regions, produced values almost identical to that of human skin.

The choice of a suitable receptor medium is also important. A range of vehicles have been employed (Jones *et al*, 1989). Isotonic saline or pH 7.4 buffer are commonly used to simulate the *in vivo* milieu, but selection may also depend on factors such as the need to maintain skin viability for metabolism studies (Collier *et al*, 1989) or the lipophilicity of the permeant and its ability to partition into the receiver phase. For the duration of these permeation studies, the receptor phase employed was chosen to resemble the drug-free donor vehicle. This was most commonly a vehicle composed of 10% propylene glycol in buffer (pH 3.50 to 7.40). The prime objective of a receptor medium is to provide an effective sink for the penetrant and thus maintain a favourable driving force for absorption. This criteria is considered to be met, provided the concentration of the penetrant in the receptor phase does not exceed 10% of its saturated solubility in the donor medium. All measurements during the course of these experiments complied with this requirement. Replication of vehicle composition on either side of the membrane enabled a facile assessment of the influence of donor variables, without complications of pH gradients etc., in this preliminary investigation.

5.3.2.1 Permeation studies with azidoprofen and ibuprofen

As discussed in section 1.3.3, the chemical structure of AZP (5) is based on the simple skeleton of the arylpropionic acid group of NSAIDs. Ibuprofen (IBP; 3) may be regarded as the simplest of these, bearing a hydrophilic α -propionic acid and hydrophobic isobutyl side chain. In order to compare the permeation characteristics of both AZP and IBP, their transport across silastic membrane from (a) equimolar solutions, and (b) saturated solutions was studied. The use of solutions in the donor phase results in a progressive decrease in thermodynamic activity of the drug as the source is depleted and gives rise to a gradual plateauing in the rates of penetration.

The initial linear portions of these rate curves are however amenable to zero-order analysis (Figures 5.13 and 5.14). No significant lag time is evident, indicating little resistance to diffusion from the artificial lipoidal membrane. The values of fluxes and permeability coefficients are presented in Table 5.6, together with solubility and partitioning data for the two permeants. The relative permeability of the two compounds may be assessed by considering their permeation from the saturated solutions, where initially they are both at equivalent and maximal thermodynamic activity. The duration of the steady-state phase implies that this maximal thermodynamic activity is maintained for a considerable period of time, *i.e.*, donor depletion is of a relatively small magnitude in this early phase. Under these conditions, although AZP exhibits a higher flux, the permeability coefficient of IBP is ~ 5 times greater than that of AZP due to the lower solubility and therefore the presence of a smaller amount of IBP in the donor phase at saturation. The greater permeability of IBP also reflects its larger log octanol/water partition coefficient (IBP: 3.51 (Dunn, 1973); AZP: 2.43).

As for permeation from dilute equimolar solutions, IBP is present at a higher thermodynamic activity, compared to AZP, as a result of its lower solubility in the same vehicle, and therefore exhibits a greater flux. The discrepancies in the values of K_p obtained from the dilute and saturated solutions (Table 5.6), particularly for AZP, is probably a result of the large difference in the degree of saturation of the two media. This suggests that extrapolation from very dilute solutions to saturated solutions should be performed with due caution.

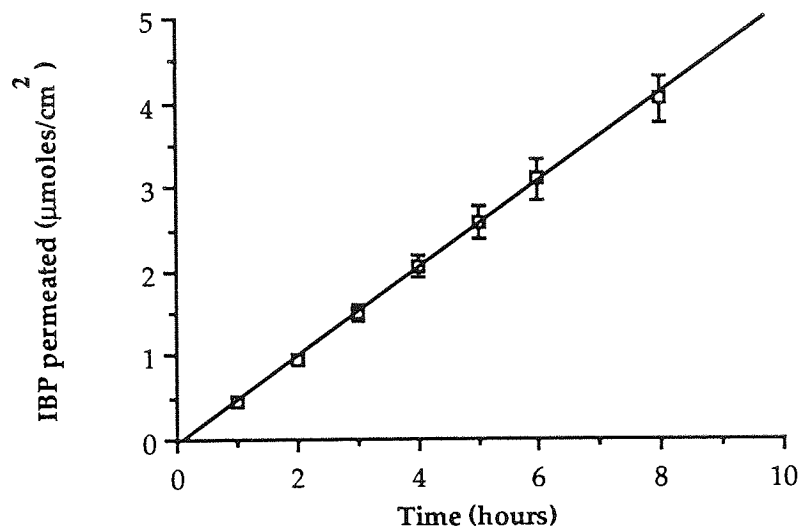
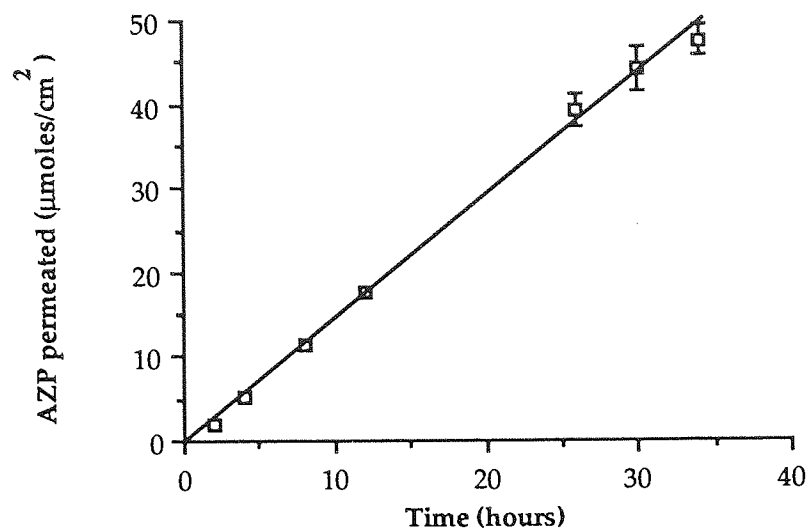


Figure 5.13 Steady-state phases of the permeation profiles for AZP and IBP across silastic membrane from saturated solutions in 10% PG-buffer, pH 5.50.

Points are the mean \pm sem of three determinations.

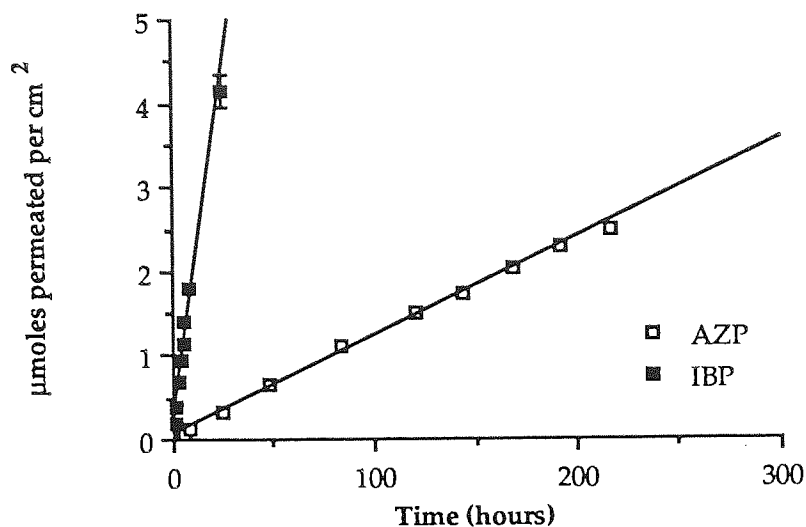


Figure 5.14 Steady-state phases of the permeation profiles for AZP and IBP across silastic membrane from 1mM solutions in 10% PG-buffer, pH 5.50.

Points are the mean \pm sem for three determinations.

Table 5.6 Permeation data for AZP and IBP across silastic membrane from dilute and saturated solutions in 10% PG-buffer, pH 5.50.

Permeant	Saturated solubility ($\mu\text{moles cm}^{-3}$)	$\log P$ (octanol/water)	Donor	Flux \pm sem ($\mu\text{mol cm}^{-2} \text{hr}^{-1}$)	$K_p \pm$ sem (cm hr^{-1})
AZP	39.203 ± 0.979	2.43	1mM solution	$1.664 \times 10^{-2} \pm 1.990 \times 10^{-4}$	$1.664 \times 10^{-2} \pm 1.990 \times 10^{-4}$
			saturated solution	1.463 ± 0.090	$0.0373 \pm 2.305 \times 10^{-3}$
IBP	$2.497 \pm 0.107^\ddagger$	3.51*	1mM solution	0.2594 ± 0.0217	0.2594 ± 0.0217
			saturated solution	0.5187 ± 0.0391	0.2077 ± 0.0157

‡ from Sanderson (1986)

* from Dunn (1973)

5.3.2.2 Effect of pH on the percutaneous absorption of AZP

A series of experiments were conducted to assess the effect of pH on the percutaneous absorption of AZP. In initial investigations the permeation of AZP from *equimolar* solutions in buffered 10% PG-buffer vehicles across hairless mouse skin was examined. Steady-state fluxes, permeability coefficients and lag times were determined from the initial linear portions of the resulting rate curves and are summarized in Table 5.7. Typical permeation profiles are illustrated in Figure 5.15. These clearly illustrate the pH-dependency of these parameters. Both the flux and the permeability coefficients increase with decreasing pH. On the other hand, lag times increase with increasing pH.

Table 5.7 Permeation data for AZP across hairless mouse skin from a series equimolar (15 mM) solutions in 10% PG-buffer.

pH	Flux $\mu\text{moles cm}^{-2} \text{hr}^{-1}$	K_p cm hr^{-1}	Lag time (hours)
4.00	1.0335 ± 0.0261	$0.0689 \pm 1.738 \times 10^{-3}$	1.83 ± 0.160
4.50	0.6488 ± 0.0373	$0.0433 \pm 2.488 \times 10^{-3}$	2.78 ± 0.065
5.00	0.3617 ± 0.0025	$0.0241 \pm 1.638 \times 10^{-4}$	3.39 ± 0.211

Values are the mean \pm sem of three determinations

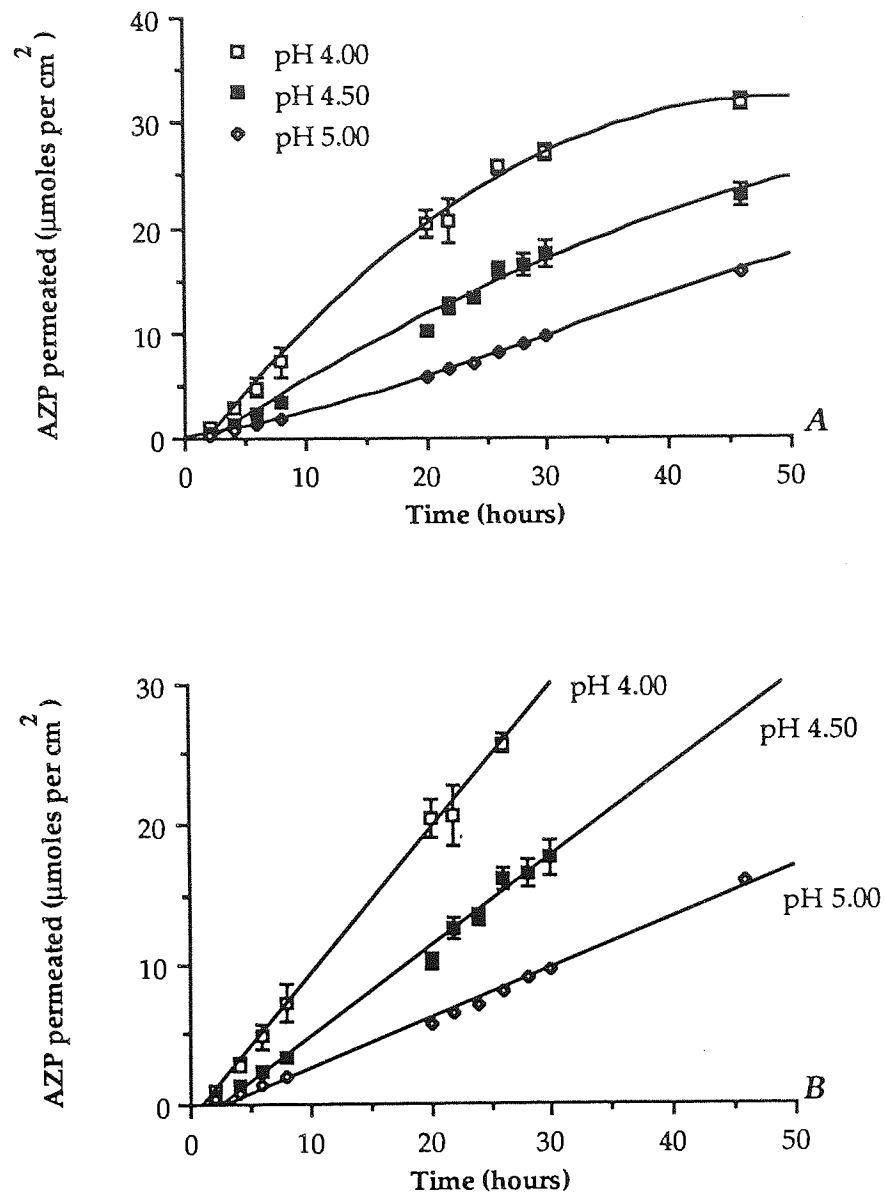


Figure 5.15 Effect of pH on the permeation of AZP across hairless mouse skin from 15 mM solutions in 10% PG-buffer vehicles. Plots in (B) represent the initial steady-state phase of the complete profiles seen in (A). Points are the mean \pm sem of three determinations.

A plot of the observed flux against the fraction of unionized drug in the donor solution reveals a linear relationship (Figure 5.16), indicating one possible means by which pH may influence penetration. Partitioning into skin is favoured by the undissociated form of the drug (Table 5.5), the ratio of which increases with decreasing pH for an acidic drug such as AZP. The increase in lag times with increasing donor vehicle pH may be due to greater resistance from the largely lipophilic membrane towards the resultant increased level of the ionized form of the permeant.

The relative rates of percutaneous absorption (fluxes) of the unionized and ionized forms of a permeant may be estimated from equation 5.17. If the partitioning term P_{app} , in equation 5.16 is replaced by k_{obs} , the observed rate of absorption at a particular pH, then the fluxes of both the undissociated (k_u) and dissociated (k_i) species may be calculated:

$$\frac{k_{obs}}{\alpha} = k_i + \frac{(1-\alpha) \cdot k_u}{\alpha} \quad (5.17)$$

A plot of k_{obs}/α against $(1-\alpha)/\alpha$ for the data from this study provides a linear relationship (Figure 5.17) with the equation:

$$y = -9.9262 \times 10^{-2} + 1.421 \frac{(1-\alpha)}{\alpha} \quad (r^2 = 1.000) \quad (5.18)$$

The negative intercept suggests that the ionized form does not penetrate the membrane, thus supporting the pH-partition theory. A flux of $1.421 \mu\text{moles cm}^{-2} \text{ hr}^{-1}$ is predicted from a 15 mM solution at a pH where the drug is totally unionized. The experimentally obtained flux at pH 4.00 is $1.0335 \pm 0.0261 \mu\text{moles cm}^{-2} \text{ hr}^{-1}$, where the drug is ~70% unionized. This corresponds to ~70% of the theoretical value and is thus in accordance with this model.

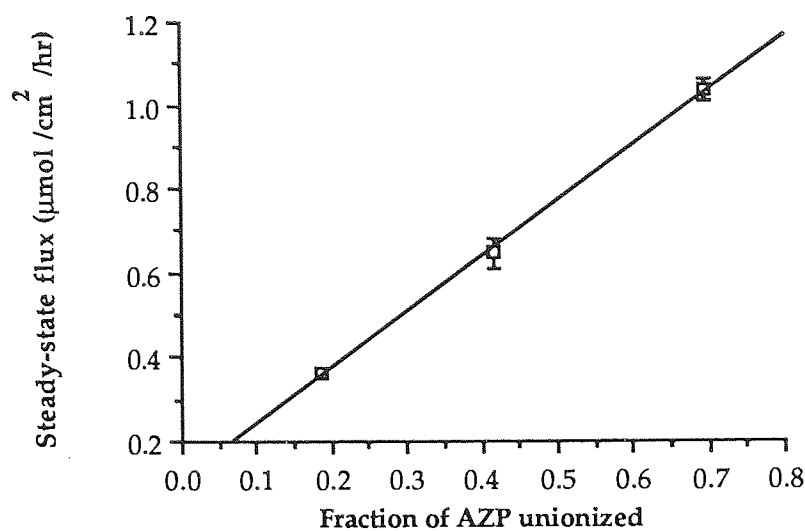


Figure 5.16 Plot of the steady-state flux of AZP across hairless mouse skin from solutions of differing pH, as a function of degree of ionization.

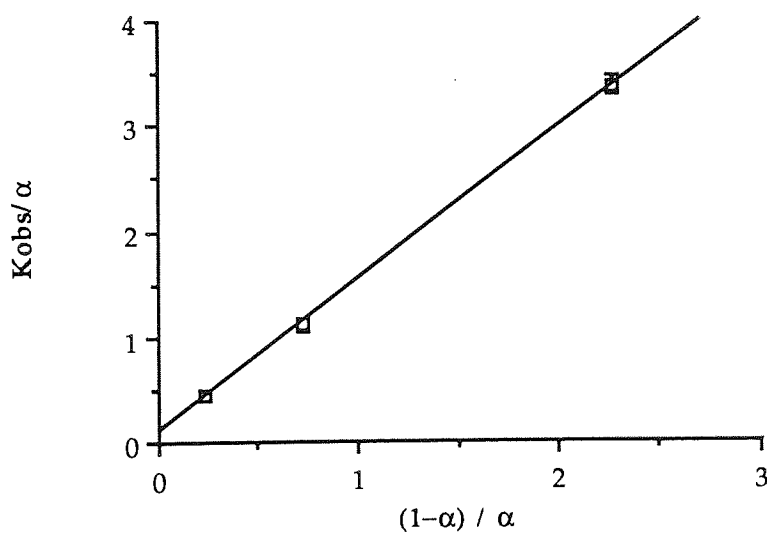


Figure 5.17 Plot of the observed flux of AZP (k_{obs}/α) as a function of $(1-\alpha)/\alpha$, in order to determine k_u and k_i .

Since this study utilized equimolar donor solutions, a further variable which may impact on the observed trend in the rates of penetration is the varying thermodynamic activity of each vehicle. The solubility of AZP varies with pH (Table 5.2), hence when using equimolar solutions, each vehicle will be saturated to a different degree according to the pH and will therefore exhibit varying thermodynamic activities. This effect is demonstrated by plotting the observed flux against the degree of saturation (Figure 5.18). A linear relationship is evident:

$$J = -0.49865 + 1.6513 FS \quad (r^2 = 0.985) \quad (5.19)$$

where FS = fraction of saturation. The predicted steady-state flux for a saturated solution, from this equation, is $1.1527 \mu\text{moles cm}^{-2} \text{hr}^{-1}$.

Penetration of AZP across silastic membrane, as opposed to hairless mouse skin, from dilute equimolar solutions of varying pH, was also investigated. The initial linear regions of the resulting permeation profiles are illustrated in Figure 5.19. Steady-state fluxes (J) and permeability coefficients (K_p), derived from these plots are summarized in Table 5.8. Of particular interest are the values of K_p obtained at pH 4.00 and 4.50, which may be directly compared to those obtained with hairless mouse skin. The close agreement of these data lends further support to the use of silastic as a model membrane for this series of experiments.

The data also suggest that the pH dependency of the penetration profile across skin is not a result of a direct insult to the barrier properties of the membrane, from for *e.g.*, a non-physiological formulation pH range, since a similar profile is also observed with the relatively inert silastic membrane.

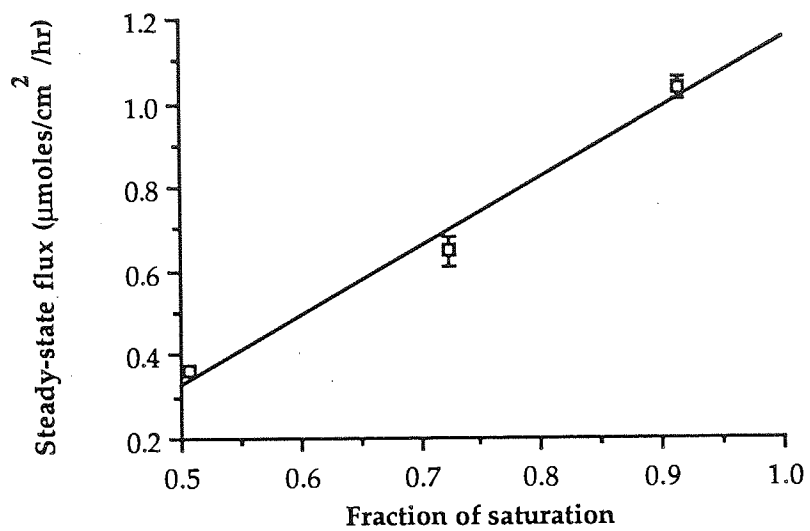


Figure 5.18 Plot of the steady-state flux of AZP across hairless mouse skin from solutions of differing pH, as a function of fraction of saturation.

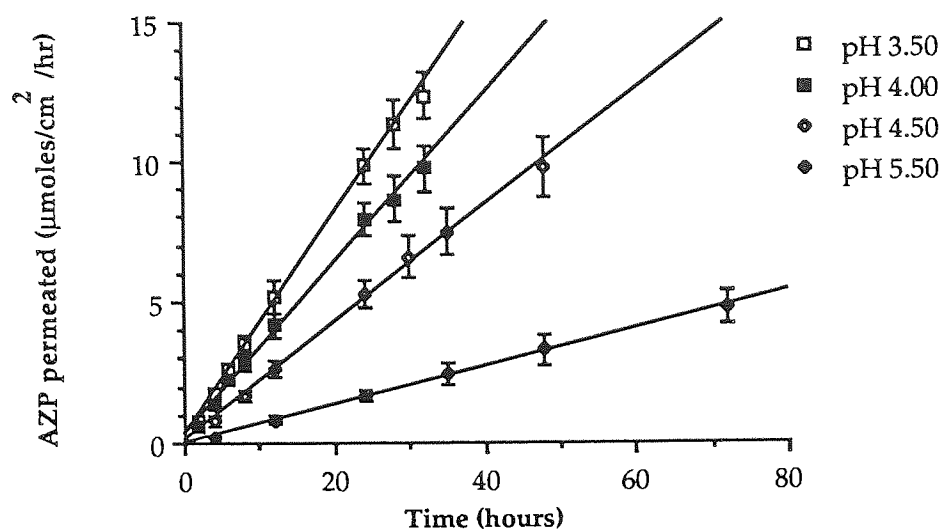


Figure 5.19 Effect of pH on the penetration of AZP across silastic membrane from 5 mM solutions in 10% PG-buffer. Points are the mean \pm sem of three determinations.

Table 5.8 Permeation data for AZP across silastic membrane from a series of equimolar (5 mM) solutions in 10% PG-buffer.

pH	Flux $\mu\text{moles cm}^{-2} \text{hr}^{-1}$	K_p (silastic) cm hr^{-1}	K_p (hms) cm hr^{-1}
3.50	0.3914 ± 0.0211	$0.0783 \pm 4.229 \times 10^{-3}$	
4.00	0.3053 ± 0.0191	$0.0610 \pm 3.819 \times 10^{-3}$	$0.0689 \pm 1.738 \times 10^{-3}$
4.50	0.2080 ± 0.0175	$0.0416 \pm 3.495 \times 10^{-3}$	$0.0433 \pm 2.488 \times 10^{-3}$
5.50	0.0676 ± 0.0075	$0.0135 \pm 1.499 \times 10^{-3}$	

hms; hairless mouse skin

Values are the mean \pm sem of three determinations.

Relationships between steady-state flux and (a) degree of ionization, and (b) extent of saturation of the donor vehicle, analogous to those with hairless mouse skin were obtained. These data are shown in Figure 5.20. A plot of flux as a function of the fraction of drug in the unionized form (Figure 5.20 A) yields the following equation:

$$J = 4.0854 \times 10^{-2} + 0.39303 \text{ FU} \quad (r^2 = 0.998) \quad (5.20)$$

This predicts a flux of $0.4339 \mu\text{moles cm}^{-2} \text{ hr}^{-1}$ from a 5 mM solution where all the drug is in the undissociated form.

Similarly, the following relationship is obtained from a plot of flux against fraction of saturation (Figure 5.20 B):

$$J = -5.2615 \times 10^{-2} + 1.0678 \text{ FS} \quad (r^2 = 0.969) \quad (5.21)$$

This predicts a flux of $1.0152 \mu\text{moles cm}^{-2} \text{ hr}^{-1}$ for a completely saturated solution and correlates very well with the experimentally obtained value of $1.0333 \pm 0.0261 \mu\text{moles cm}^{-2} \text{ hr}^{-1}$, across *hairless mouse skin*, from a ~90% saturated solution, at pH 4.00 (Table 5.7).

The above pH profiles indicate that a combination of two variables, namely; the degree of ionization and saturation, which reflect the pH of the donor vehicle, affect the penetration of AZP from *dilute solutions*. A series of analogous experiments were therefore conducted utilizing *saturated suspensions* as the donor vehicle, thus maintaining the degree of saturation essentially constant at any pH, and consequently helping to elucidate the true effect of pH on penetration.

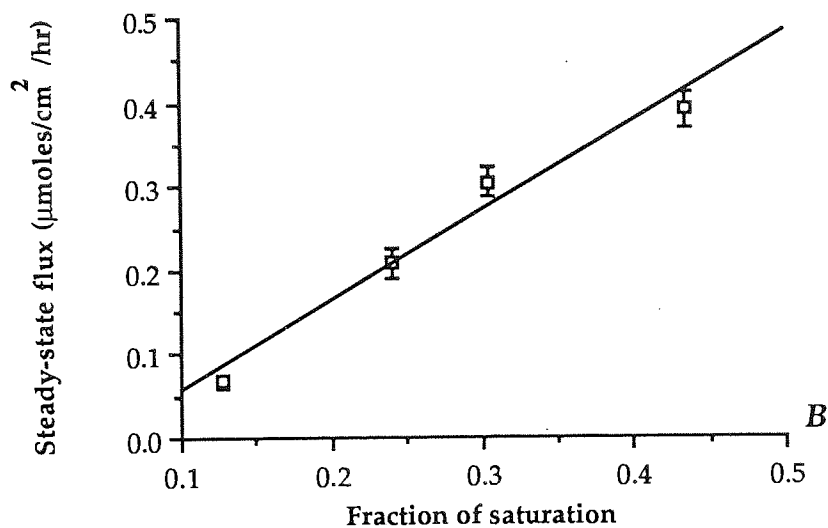
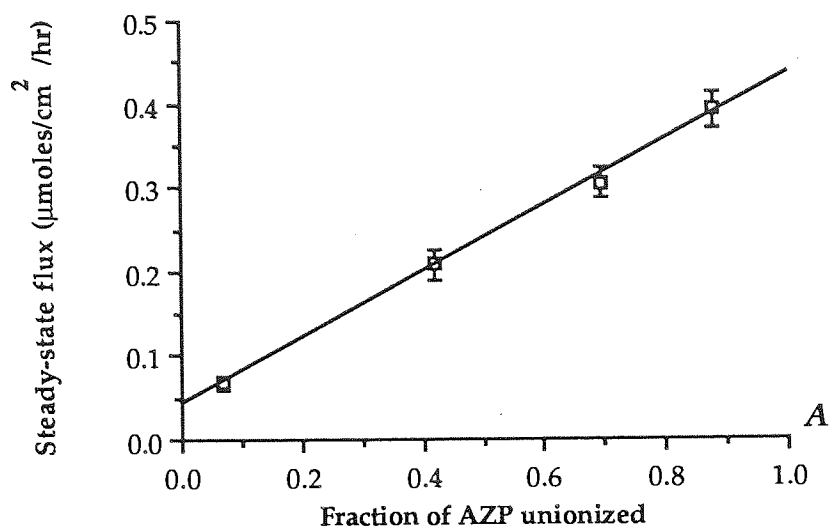


Figure 5.20 Effect of pH on the penetration of AZP across silastic membrane from 5 mM solutions in 10% PG-buffer. Plots of steady-state flux as a function of (A) fraction of unionized drug and (B) fraction of saturation of donor vehicle.

The resulting permeation data are summarized in Table 5.9. These show that the penetration rates of AZP from suspensions do not vary significantly as pH increases from 3.50 to 7.40. Figure 5.21 shows that the steady-state flux from suspensions is generally independent of the degree of ionization. By employing suspensions as the donor vehicle, the amount of unionized drug in solution is held constant at any pH, and hence the degree of saturation and thermodynamic activity is maintained at unity. Since permeation through skin is predominantly a function of neutral drug concentration, this results in penetration rates (fluxes) which are essentially independent of pH.

Table 5.9 Permeation data for AZP across hairless mouse skin from a series of suspensions in 10% PG-buffer.

pH	Flux ($\mu\text{moles cm}^{-2} \text{hr}^{-1}$)	K_p (cm hr^{-1})	Lag time (hours)	Percentage unionized
3.50	1.8941 ± 0.5096	0.1647 ± 0.0044	1.63 ± 0.228	87.80
4.00	2.0324 ± 0.1987	1.2364 ± 0.0012	1.70 ± 0.158	69.47
4.50	1.9735 ± 0.0500	0.0952 ± 0.0024	2.14 ± 0.077	41.80
5.00	2.0305 ± 0.0674	0.0687 ± 0.0023	2.08 ± 0.180	18.53
5.50	2.6577 ± 0.1667	0.0678 ± 0.0043	1.90 ± 0.146	6.71
6.50	1.9795 ± 0.0931	0.0362 ± 0.0017	0.82 ± 0.163	0.71
7.40	2.6090 ± 0.0745	0.0021 ± 0.0061	1.62 ± 0.099	0.09

Values are the mean \pm sem of three determinations

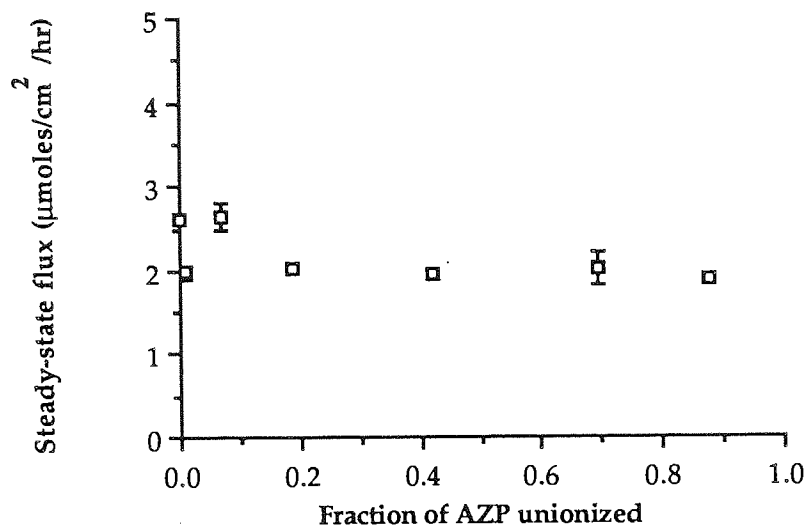


Figure 5.21 Effect of pH on the penetration of AZP across hairless mouse skin from suspensions in 10% PG-buffer. Plot of steady-state flux as a function of fraction of drug unionized.

The mean flux across hairless mouse skin from suspensions was calculated to be $2.1818 \pm 0.0781 \mu\text{moles cm}^{-2} \text{hr}^{-1}$, compared to $1.1527 \mu\text{moles cm}^{-2} \text{hr}^{-1}$, predicted from the solution data (equation 5.20). The difference may be attributed to the continual depletion of donor phase concentration when solutions are employed, which although of a small magnitude (as indicated by a significant linear region of the permeation profile), may result in an overall reduction of the penetration rate.

Permeability coefficients, on the other hand, decrease with increasing pH (Table 5.9), since progressively larger amounts of the non-diffusible species are present at saturation as a result of increasing solubility, while fluxes remain essentially constant. Figure 5.22 illustrates the following linear relationship between log permeability coefficient (K_p) and pH:

$$\log K_p = -4.3347 \times 10^{-3} - 0.22297 \text{ pH} \quad (r^2 = 0.988) \quad (5.22)$$

This correlation may be explained on the basis of the dependency of K_p on solubility and the latter parameter upon pH, as discussed earlier.

These relationships serve to emphasize the dependence of skin permeability on vehicle composition and hence drug partitioning. This dependence is further demonstrated by Figure 5.23, which illustrates the linear relationship between log K_p and the log apparent partition coefficient (P_{app}) for AZP between hairless mouse skin and vehicle (10% PG-buffer), described by the equation:

$$\log K_p = -1.3379 + 0.36280 \log P_{app} \quad (r^2 = 0.936) \quad (5.23)$$

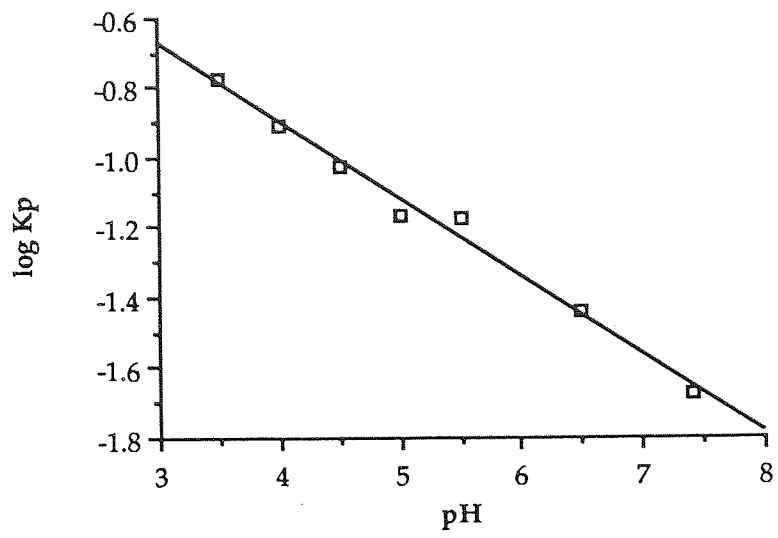


Figure 5.22 Plot of log permeability coefficient (K_p) for AZP across hairless mouse skin against pH of donor formulation.

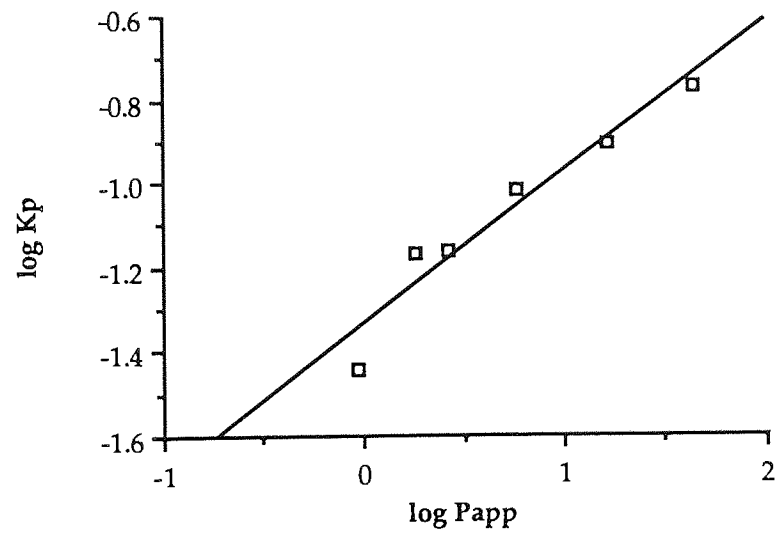


Figure 5.23 Plot of log K_p of AZP against the apparent log skin/aqueous propylene glycol partition coefficient.

5.3.2.3 Effect of drug concentration on the percutaneous absorption of AZP

The dependence of penetration rate on solute concentration has already been alluded to in the above section with respect to the influence of pH on the effective concentration. This was further investigated, more directly, by studying the permeation of AZP from a series of solutions in 10% PG-buffer (pH 4.50) of varying drug concentration.

The resulting penetration profiles and corresponding data are presented in Figure 5.24 and Table 5.10 respectively, and reinforce the observations made in previous studies. The rate of penetration increases, as expected, with increasing concentration, as the donor phase approaches saturation and hence maximal thermodynamic activity (Figure 5.25). In contrast, the values of permeability coefficients remain essentially constant, in accordance with their role as proportionality constants. The permeability coefficient is a value which is uniquely dependent on (a) the chemical structure of the drug, (b) the physicochemical nature of the formulation, and (c) the physicochemical nature of the membrane. The invariability of the K_p value (mean \pm sem: $0.0406 \pm 1.538 \cdot 10^{-3} \text{ cm hr}^{-1}$) reflects the constancy of these parameters and the reproducibility of the experimental procedure.

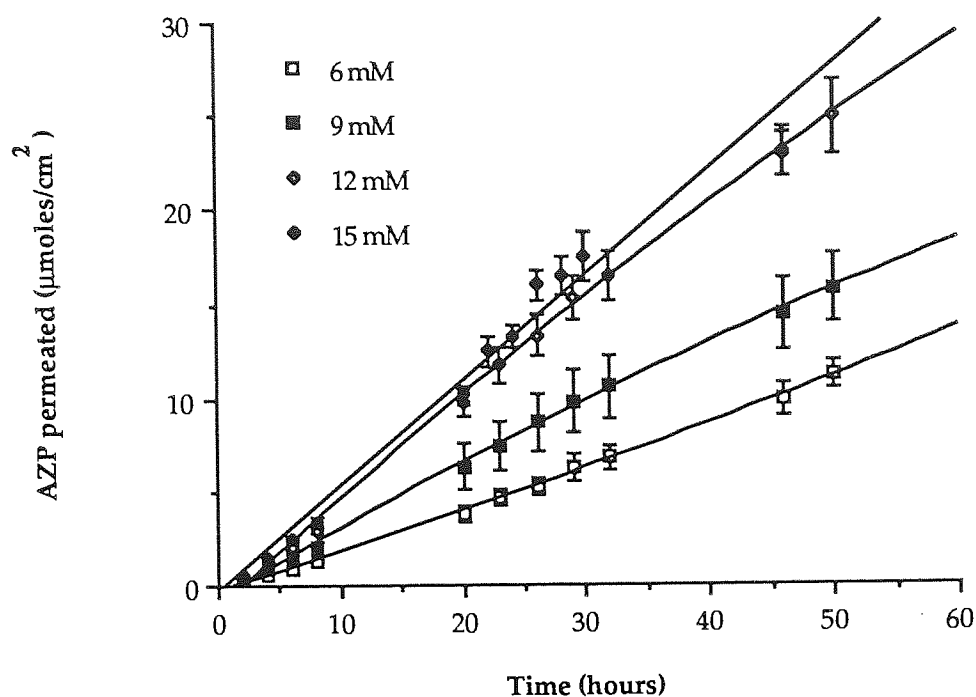


Figure 5.24 Effect of solute concentration on the penetration of AZP across hairless mouse skin from solutions in 10% PG-buffer (pH 4.50). Points are the mean \pm sem of three determinations.

Table 5.10 Permeation data for AZP across hairless mouse skin from solutions of varying concentration in 10% PG-buffer.

[AZP] ($\mu\text{moles cm}^{-3}$)	Flux ($\mu\text{moles cm}^{-2} \text{hr}^{-1}$)	K_p (cm hr^{-1})	Lag time (hours)
6.0	0.2364 ± 0.0154	0.0394 ± 0.0026	3.29 ± 0.65
9.0	0.3295 ± 0.0358	0.0366 ± 0.0040	1.70 ± 0.41
12.0	0.5178 ± 0.0341	0.0432 ± 0.0028	0.81 ± 0.24
15.0	0.6488 ± 0.0373	0.0433 ± 0.0025	2.78 ± 0.07

Values are the mean \pm sem of three determinations.

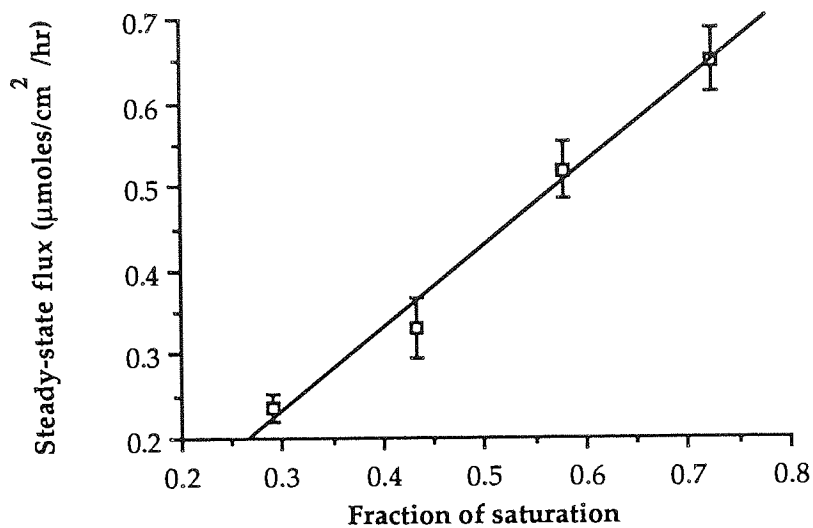


Figure 5.25 Effect of the degree of donor phase saturation on the penetration rate of AZP across hairless mouse skin from solutions in 10% PG-buffer (pH 4.50).

Points are the mean \pm sem of three determinations.

5.3.2.4 Effect of cosolvent concentration on the percutaneous absorption of AZP

Typical penetration profiles for AZP across hairless mouse skin from a series of buffered propylene glycol suspensions (pH 4.50) are shown in Figure 5.26. Corresponding permeation data are presented in Table 5.11. According to these results, values of flux remain fairly constant as the fraction of propylene glycol in the vehicle increases, whereas permeability coefficients decrease to accommodate the increasing AZP concentration in the donor phase due to the greater solubilizing capacity of the vehicle. The uniformity of the flux with respect to cosolvent level reflects the corresponding partitioning data (Figure 5.10), which was also independent of propylene glycol concentration over this range. One would expect the skin/vehicle partition coefficient, flux and K_p to decrease with further increases in cosolvent level as a result of increased affinity of the solute for the vehicle. However, an extended study was not possible at this time due to a limited supply of AZP.

5.3.2.5 Effect of penetration enhancers on the percutaneous absorption of AZP

The effect of a number of established penetration enhancers on the permeation of AZP through hairless mouse skin was investigated. These included formulations of oleic acid in propylene glycol, azone in propylene glycol and as an emulsion in 0.1% (w/v) Tween 20 in normal saline, and DCMS in propylene glycol. These enhancer regimes been used extensively to study their effect on the percutaneous penetration of a wide variety of drugs at concentrations similar to those chosen for this study (Barry and Bennett, 1987; Bond and Barry, 1988b; Goodman and Barry, 1986; Loftsson, 1989; Sugibayashi *et al*, 1985). Also investigated was the lipophilic amine, dodecylamine, for potential penetration enhancement properties. Barker and Hadgraft (1981) reported the facilitated transport of anionic drugs by ion-pairing with a series of N-substituted bis(2-hydroxypropyl)amines. Dodecylamine (pK_a 10.63; Albert and Serjeant, 1984) was therefore chosen as a model amine to provide a counter-ion, which was expected to ion-pair with dissociated AZP and thus potentially enhance skin permeation of AZP.

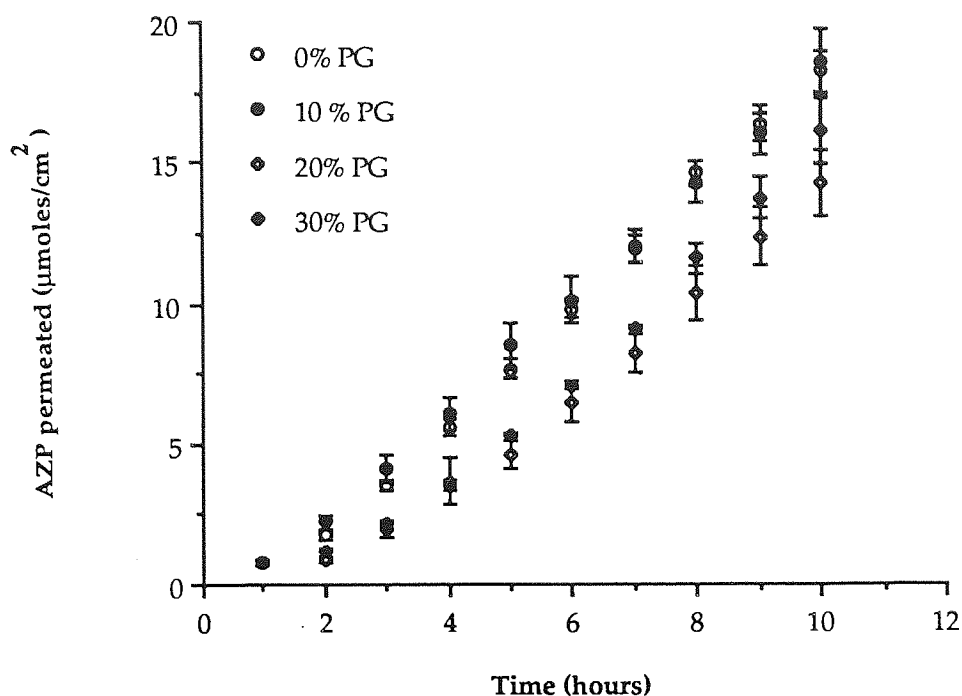


Figure 5.26 Effect of propylene glycol concentration on the penetration of AZP across hairless mouse skin from buffered suspensions (pH 4.50).

Table 5.11 Permeation data for AZP across hairless mouse skin from buffered propylene glycol suspensions (pH 4.50).

PG (% v/v)	Flux ($\mu\text{moles cm}^{-2} \text{hr}^{-1}$)	K_p (cm hr^{-1})	Lag time (hours)
0	2.1107 ± 0.0732	0.1223 ± 0.0042	1.30 ± 0.039
10	1.9735 ± 0.0500	0.0952 ± 0.0024	2.14 ± 0.077
20	1.8845 ± 0.1365	0.0671 ± 0.0049	2.52 ± 0.096
30	2.1146 ± 0.1660	0.0539 ± 0.0042	2.51 ± 0.157

Hairless mouse skin was pretreated with the penetration enhancer formulation for a duration of 1 or 12 hours, prior to studying the absorption of AZP from a suspension in a buffered 10% propylene glycol vehicle. Control pretreatments comprised of the solvent upon which the enhancer solutions were based to test for enhancement effects of the solvent itself. The use of such pretreatment periods to assess the effect of penetration enhancers have been used by other investigators (Goodman and Barry, 1988; Sherertz *et al*, 1987) in an attempt to separate the true enhancer action from its effect on the SC/vehicle partitioning of the permeant.

The flux values obtained from these experiments are presented in Table 5.12. Example permeation profiles are shown in Figure 5.27. The majority of enhancer pretreatments produced an approximate 2 fold enhancement. Although the penetration enhancement reflects, to some extent, the increased skin/vehicle partitioning under analogous conditions (Figure 5.11), the nature of the partitioning experiment impedes any direct correlation. Moreover, disruption of the SC lipids, the proposed mechanism of penetration enhancement for some enhancers, may not dictate partitioning, but rather influence diffusivity, which would not be reflected in the latter data. On the other hand, since pretreatment procedures were used for both the permeation and partitioning experiments, any thermodynamic effect of the enhancer, *i.e.*, influence on the SC/vehicle partitioning should theoretically be eliminated.

Propylene glycol has also been reported to promote skin penetration, of for instance, metronidazole and oestradiol (Møllgaard and Hoelgaard, 1983a and 1983b). In the current study, no such effect was observed following pretreatment of skin with propylene glycol, in comparison to penetration of AZP across skin which had been allowed to equilibrate for the same period of time without treatment. This was shown for both 1 and 12 hour pretreatment periods (Table 5.12).

Table 5.12 Permeation data for AZP across hairless mouse skin from suspensions in 10% PG-buffer (pH 4.50) following a 1 or 12 hour pretreatment with various penetration enhancers.

Pretreatment	Flux ($\mu\text{moles cm}^{-2} \text{ hr}^{-1}$)	K_p (cm hr^{-1})	Flux ratio ²
3% azone in PG	5.3177 \pm 0.2215	0.2565 \pm 0.0107	1.89
3% azone in TS	4.4765 \pm 0.2980	0.2159 \pm 0.0144	1.18
5% oleic acid in PG	7.0092 \pm 0.1831	0.3381 \pm 0.0088	2.49
15% DCMS in PG	6.1714 \pm 0.2745	0.2977 \pm 0.0132	2.19
0.5% DCA in PG	4.5429 \pm 0.4787	0.2191 \pm 0.0231	1.61
0.5% DCA in PG ¹	3.0445 \pm 0.2834	0.1469 \pm 0.0137	1.74
PG	2.8206 \pm 0.2707	0.1361 \pm 0.0131	-
PG ¹	1.7525 \pm 0.0773	0.0845 \pm 0.0037	-
TS ²	3.7808 \pm 0.2667	0.1824 \pm 0.0129	-
No pretreatment, 12 hour equilibration	2.7121 \pm 0.1377	0.1308 \pm 0.0066	-
No pretreatment, 1 hour equilibration	1.9735 \pm 0.0500	0.0952 \pm 0.0024	-

¹ 1 hour pretreatment. All other pretreatments were for 12 hours.

² 0.1% v/v Tween 20 in normal saline

³ Flux ratio = flux following pretreatment with enhancer/flux following pretreatment with appropriate vehicle (i.e., TS or PG)

Values are the mean \pm sem for three determinations.

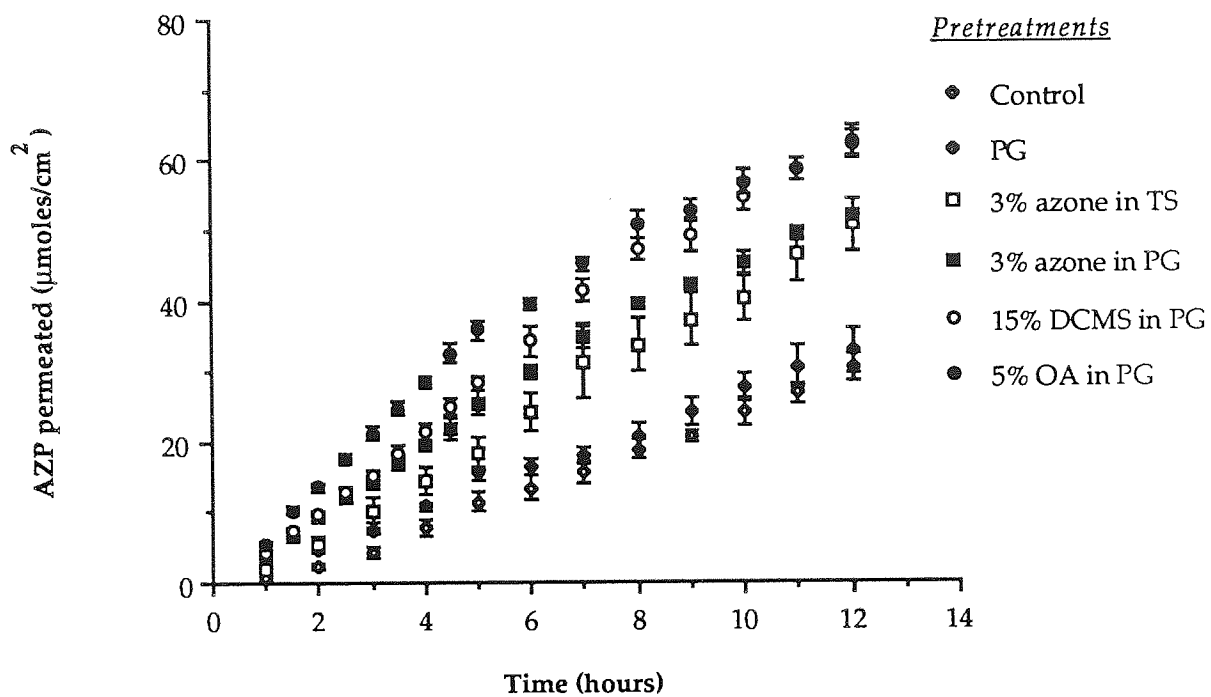


Figure 5.27 Example permeation profiles of AZP across hairless mouse skin from suspensions in 10% PG-buffer (pH 4.50) following various 12 hour pretreatments. The control protocol represents a 12 hour equilibration period without chemical pretreatment. Points are the mean \pm sem of three determinations.

The evidence regarding the role of propylene glycol as an accelerant appears to be conflicting and suggests that in most cases, is due to a modification of the thermodynamic status of the formulation through its solubilizing properties (Woodford and Barry, 1986). The activity of other enhancers may, however, be significantly improved when applied in combination with propylene glycol (Cooper, 1984; Wotton *et al*, 1985) indicating a synergistic effect.

Although 12 hour pretreatment periods were employed for the study, a shorter duration of treatment may be sufficient. This was demonstrated by studying the penetration of AZP following a 1 and 12 hour treatment with 0.5% DCA in PG. The two protocols produced a similar enhancement (Table 5.12). A shorter duration of pretreatment would be desirable in view of the vulnerability of hairless mouse stratum corneum to degradation following prolonged hydration and enhancer treatment (Bond and Barry, 1988a and 1988b).

Inclusion of dodecylamine (DCA) in the donor formulation failed to produce flux levels higher than those with a vehicle without DCA (Table 5.13). In fact, the flux ratio suggests a suppression of penetration, although this difference may not be statistically significant. The possibility exists that a large ion-pair may be associated with a lower diffusivity. Increasing the pH of the donor vehicle, which would theoretically promote ion-pairing due to the increased ionization of AZP, also failed to increase penetration compared to that from a vehicle of lower pH. It should be noted that previous studies investigating the carrier facilitated transport of anionic drugs (Hadgraft and Wotton, 1985) have generally employed a pH gradient across the skin. The absence of such a gradient in this study may have some bearing on the present observations. These data together with the observation that pretreatment with DCA does enhance penetration, suggest that barrier impairment as opposed to ion-pairing may be responsible for the observed enhancement.

Table 5.13 Effect of dodecylamine on the permeation of AZP across hairless mouse skin from a suspension in buffered 10% PG.

Treatment	pH of donor vehicle	Flux ($\mu\text{moles cm}^{-2} \text{hr}^{-1}$)	Flux ratio
0.5% DCA in donor formulation	4.50	1.4712 ± 0.2054	0.75
0.5% DCA in donor formulation	6.50	1.7611 ± 0.2864	0.89
1 hour pretreatment with 0.5% DCA in PG	4.50	3.0445 ± 0.2834	1.74
12 hour pretreatment with 0.5% DCA in PG	4.50	4.5429 ± 0.4787	1.61
1 hour pretreatment with PG	4.50	1.7525 ± 0.0733	-
12 hour prertreatment with PG	4.50	2.8206 ± 0.2707	-
No pretreatment	4.50	1.9735 ± 0.0500	-
No pretreatment	6.50	1.9795 ± 0.0931	-

Permeation experiments utilizing the weak base caffeine were performed in order to separate the two postulated modes of enhancer action. Caffeine has a pK_b value of 13.4 (Florence and Attwood, 1988) and is therefore expected to exist in the unionized form at the pH of study (4.50). Any potential for ion-pairing is thus eliminated. Skin was pretreated for a period of 1 hour with a 0.5% w/v solution of DCA in propylene glycol prior to following the permeation of caffeine from a suspension in 10% propylene glycol in buffer. A control experiment studying the diffusion of caffeine across skin pretreated with propylene glycol alone was also conducted. The resulting permeation profiles are presented in Figure 5.28. The penetration enhancement of caffeine, a neutral molecule, following pretreatment with a DCA regime suggests that a reduction of barrier resistance, as opposed to ion-pair transport, is the predominant mechanism of enhancement. Ionic surfactants, particularly those of a cationic nature such as amines, are reputed to induce skin irritation (Walters, 1989). It is therefore possible that these agents promote penetration by causing damage to the skin's integrity rather than through a genuine enhancement action.

The permeation of AZP from donor suspensions of various pH values was investigated following 12 hour pretreatment with 3% azone in propylene glycol. Example permeation profiles are shown in Figure 5.29. Permeation data are summarized in Table 5.14. These results demonstrate an increase in flux as pH increases and are in contrast to the observations regarding the influence of pH without enhancer treatment (Table 5.9), where flux was independent of pH. These data therefore suggest that the penetration is favoured by the ionized species, possibly as a result of an ion-pairing mechanism as proposed by Hadgraft *et al* (1985). These authors have suggested that azone may be capable of forming ion-pairs with anionic drugs, based on the observed promotion of sodium salicylate transport across an artificial lipid membrane in the presence of azone.

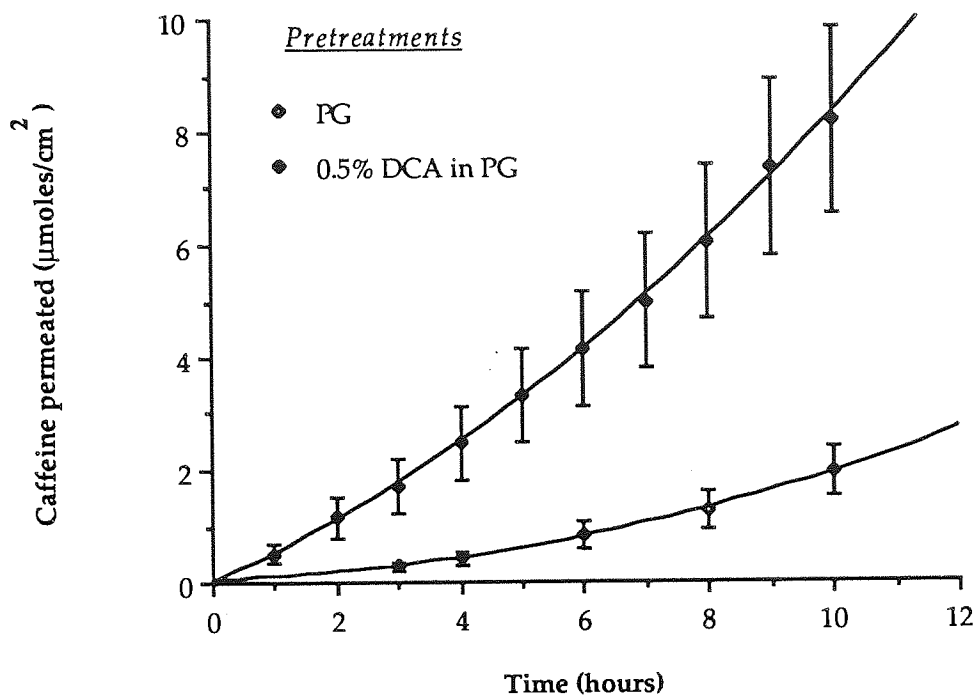


Figure 5.28 Permeation profile for caffeine across hairless mouse skin with and without a 1 hour pretreatment with 0.5% DCA in PG. The donor phase was a suspension in 10% PG-buffer (pH 4.50)

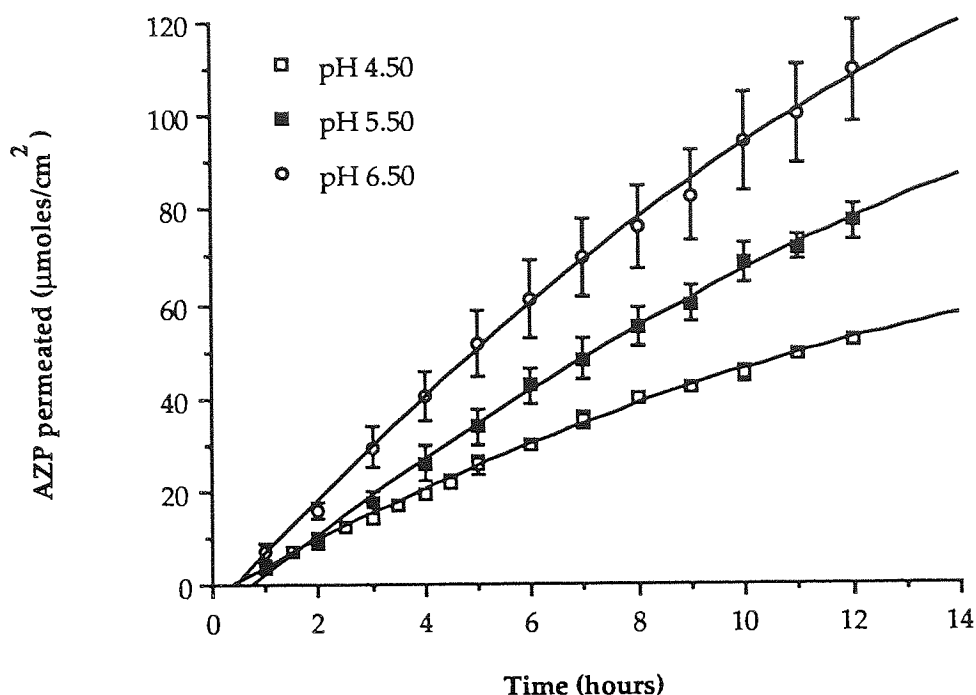


Figure 5.29 Example permeation profiles of AZP across hairless mouse skin from suspensions in buffered 10% PG vehicles (pH 4.50-6.50) following pretreatment with 3% azone in PG for 12 hours. Points are the mean \pm sem of three determinations.

Table 5.14 Permeation data for AZP across hairless mouse skin from suspensions in buffered 10% PG (pH 4.50-6.50) following 12 hour pretreatment with 3% azone in PG.

pH of donor vehicle	Flux ($\mu\text{moles cm}^{-2} \text{hr}^{-1}$)	K_p (cm hr^{-1})
4.50	5.3177 ± 0.2215	0.2565 ± 0.0107
5.00	6.6959 ± 0.4471	0.2266 ± 0.0151
5.50	7.2713 ± 0.3113	0.1855 ± 0.0079
6.00	7.8718 ± 0.3711	
6.50	10.226 ± 1.1817	0.1872 ± 0.0216

Values are the mean \pm sem of three determinations.

It should however be noted that a pH gradient, providing a driving force for ion-pair transport, was not employed in these experiments as in the above mentioned study. Enhanced penetration by the ionized species following azone pretreatment is also not supported by the appropriate partitioning data (Figure 5.12). Ratios of partition coefficients following azone treatment to those without treatment do not show a maxima at pH values where the drug exists predominantly in the anionic form and hence, where ion-pairing is most effective. These observations therefore do not entirely support the theory of enhancement by ion-pairing. Before any conclusions can be derived, it would be important to examine the effect of vehicle pH on the penetration of AZP following pretreatment with propylene glycol alone. This solvent is known to penetrate the stratum corneum (Møllgaard and Hoelgaard, 1983a and 1983b; Polano and Ponec, 1976), a process promoted by azone (Wotton *et al*, 1985), and may therefore result in a modified solubilizing capacity for the permeant within the site (Barry, 1987), although once again, this should theoretically be evident in the partition data.

Elucidation of the precise mechanism by which penetration enhancers exert their effect remains largely unresolved. In recent years, this area of research has attracted considerable interest, various theories having been proposed. The activity of DCMS appears to be limited to the penetration enhancement of polar or ionic molecules and may reflect its characteristics as a non-ionic surfactant and its potential ability to interact with epidermal proteins (Cooper, 1982). Alkyl sulphoxides may also be expected to disrupt the structural lipids in the intercellular channels of the SC (Hadgraft, 1984). This largely lipoidal pathway has been proposed as presenting a significant route for the percutaneous penetration of drugs, the structural modification of which has been implicated as the mechanism of enhancement for several penetration promoters. Both azone and oleic acid may exert their action by increasing lipid fluidity and consequently decreasing the resistance of the barrier to permeation (Walters, 1989). In particular, oleic acid is thought to alter the mode of packing of the SC lipids as a result of insertion into the membrane of this *cis*-9-octadecenoic molecule with a "kinked" alkyl chain (Figure 5.2). Recently a model of

permeation enhancement involving solid-fluid phase separation of lipids was proposed for oleic acid (Francoeur *et al*, 1990). This has been suggested to facilitate the penetration of ionized species, as was shown by studying the permeation of piroxicam at various levels of dissociation. It would therefore be interesting to see if a similar interfacial defect was associated with azone, which may also shed some light on the increased permeation of ionized AZP observed, following pretreatment with azone.

5.4 SUMMARY

The penetration of AZP through excised hairless mouse skin and silastic membrane was investigated. Formulation factors influencing skin permeation, such as pH, solute and cosolvent concentration were studied in order to correlate these parameters to drug-vehicle-membrane interrelationships governing the penetration of AZP. In addition, the effect of a range of penetration enhancers on the transport of AZP was also assessed.

Permeation studies utilizing skin and silastic membrane as model barriers, resulted in similar penetration rates for AZP, indicating the suitability of the latter model. Comparative permeation studies for AZP and the related arylalkanoic acid ibuprofen yielded permeability coefficients within the same order of magnitude; the increased permeability of the latter reflecting its greater lipophilicity.

When studying the permeation of AZP from solution formulations, the flux was found to be dependent on vehicle pH and permeant concentration. The effect of pH was related to the degree of ionization of the solute and consequently its solubility, extent of saturation and thermodynamic activity in the vehicle. Similarly, increased permeant concentration in the vehicle resulted in a greater level of saturation and hence, a higher rate of penetration. Flux from suspensions was independent of pH, since the level of unionized drug, the predominant diffusing species, was maintained at saturated solubility at any pH. It was not possible to fully evaluate the effect of cosolvent

concentration on the penetration of AZP at this stage. A suspension formulation in 10% v/v propylene glycol-McIlvaine buffer (pH 4.50) was found to deliver AZP to a suitable extent and rate, and was used for the majority of studies.

As discussed in section 4.1, ester prodrugs may modify skin partitioning and subsequent penetration of the parent compound, by manipulation of physicochemical properties such as lipophilicity. The increased octanol/water partition coefficients of a series of alkyl esters compared to the parent drug AZP, were noted (Table 5.4), and may be expected to enhance skin partitioning and/or penetration relative to AZP, provided that partitioning into the viable epidermis does not become the rate-determining step as lipophilicity increases. The transport of these ester prodrugs across silastic membrane was demonstrated in preliminary studies (data not shown). However, quantification of permeation data and subsequent comparative analysis proved difficult due to significant adsorption of the lipophilic esters to both the membrane and glassware. Silanization of diffusion cells to remedy the latter situation did not prove successful. It would therefore be important to overcome these limitations prior to investigating the penetration potential of these compounds as well as their ability to undergo cutaneous metabolic activation.

Pretreatment of the skin with a range of enhancer formulations was found to moderately promote the permeation of AZP, although none was found to be superior. Pretreatment with azone in propylene glycol appeared to facilitate penetration of the ionized species, contrary to the pH partition hypothesis, however further studies are required to confirm this observation.

CHAPTER SIX
MEASUREMENT OF PERCUTANEOUS ABSORPTION *IN VIVO* BY ATTENUATED TOTAL
REFLECTANCE FOURIER TRANSFORM INFRARED SPECTROSCOPY

MEASUREMENT OF PERCUTANEOUS ABSORPTION *IN VIVO* BY ATTENUATED TOTAL REFLECTANCE FOURIER TRANSFORM INFRARED SPECTROSCOPY

6.1 INTRODUCTION

The local and systemic bioavailability of topically applied drugs is most frequently assessed by a study of the kinetics and extent of the percutaneous absorption process. These skin penetration experiments, which seek to examine the multitude of factors governing the transport of drugs across the dermal barrier, may be classified into *in vitro* and *in vivo* techniques, and have been reviewed by several authors (Barry, 1983; Guy *et al*, 1986; Wester and Maibach, 1983 and 1986). The aims of these studies, together with the methodology of *in vitro* procedures utilizing excised skin or artificial model membranes have been addressed in chapter 5. Here, *in vivo* methods available for studying percutaneous absorption, will be discussed briefly as a preface to an account of the principles and development of attenuated total reflectance Fourier transform infrared (ATR-FTIR) spectroscopy, which has been used to monitor this process *in vivo* in man, during the present investigation.

Whilst *in vitro* studies have been an invaluable tool in understanding the processes by which substances traverse the skin, there is little doubt that *in vivo* investigations in suitable animal models and particularly humans are preferable and more relevant to the final clinical situation. Some of the limitations imposed by human studies may be overcome by the use of animal models, various species having been employed. Their suitability and the relevance of animal data to humans has been reviewed by several investigators (Wester and Maibach, 1986; Wester and Noonan, 1980). The following section will deal with techniques of general applicability, with particular reference to human studies.

6.1.1 *In vivo* percutaneous absorption studies

The skin's impressive barrier properties to the ingress of foreign compounds means that most compounds are poorly absorbed through the skin.

Consequently, drug levels in body fluids and tissues following topical application are usually extremely low, requiring very sensitive assay techniques for detection. The most widespread method for studying *in vivo* penetration which offers this level of sensitivity is the use of radiolabelled tracers. Following topical application of a radiolabelled compound, usually ^{14}C or ^3H , the rate and extent of penetration is evaluated from the cumulative urinary (and sometimes faecal) excretion of the radiolabel over the next 5 to 10 days. Correction for the percentage of dose transported across the skin, but retained in the body or excreted by some route not assayed, is made by measuring the amount of radioactivity excreted following slow intravenous administration (Feldmann and Maibach, 1969 and 1970). This correction procedure relies on the principle that following absorption through the skin, a chemical directly enters the bloodstream. Thus, the disposition of the fraction of topical dose which reaches the general circulation is mimicked by an intravenous injection, whose elimination profile is assumed to be identical. Blood plasma analysis will also give a measure of percutaneous penetration by consideration of the ratio of the areas under the plasma concentration versus time profiles following topical and intravenous administration. One clear limitation of this technique is that the radioactivity data do not distinguish between the parent compound and its metabolites and thus give no indication of the rate and extent of cutaneous or systemic metabolism. In addition, only the fraction of dose absorbed is estimated; the fate of the remainder of the applied radioactivity remains unknown. Simple modifications of this standard radiochemical methodology has, however, led to improved "mass balance" and dose accountability (Bucks *et al* , 1985, 1987, 1988).

A measurement of the rate of disappearance of a compound from the surface as it penetrates the skin should also, in principle, enable an estimation of percutaneous penetration. However, since only a small amount of chemical will be absorbed from a relatively large surface depot, the sensitivity of the technique must be very high. This approach is therefore largely used to monitor the disappearance of a radiolabel at the skin surface by placing a counter directly above the application site (Ainsworth, 1960; Wahlberg, 1965).

Overestimation of absorption due to epidermal quenching of radioactivity as well as loss of surface material by sweating, surface desquamation or stratum corneum reservoir formation also limits the usefulness of the technique. However, some of these difficulties have been overcome by a refinement of the experimental procedure (Guy *et al*, 1987a).

One of the main objections against using *in vitro* methods is that such a system does not truly mimic the *in vivo* situation especially with respect to an efficient blood supply which removes the penetrant at various rates. This is of particular relevance in the case of topical corticosteroids, a group of drugs which cause vasoconstriction of the capillaries and may decrease their own clearance; a process which cannot occur *in vitro*. Induction of such a pharmacological response, if easily measurable, can be exploited to study the *in vivo* penetration of a compound (McKenzie and Stoughton, 1962). Thus, the "vasoconstrictor" or "blanching assay" for topical corticosteroids has found widespread application in assessing the relative potencies of different steroids and in examining the effect of formulation changes on activity (Barry, 1983). It should however be noted that the assay is primarily a qualitative one and does not provide information regarding the absolute quantities of steroid penetrating. Nicotines, which cause erythema as a result of dilatation of blood vessels at the dermal-epidermal interface have been studied in a similar fashion.

Other qualitative methods of estimating *in vivo* percutaneous absorption include histological techniques such as those which aim to reveal structural changes caused by the penetrant, *e.g.*, keratolysis induced by salicylic acid (Strakosch, 1943), autoradiography, where radioactivity is visualized by photographic development (Zesch and Schaefer, 1975) and fluorescence microscopy. These methods cannot, however, provide accurate information relating to rates or routes of absorption.

The ultimate aim of topical drug delivery to diseased skin is the induction of a local therapeutic response by achieving an appropriate drug level at the affected site. Thus, measurements in compartments other than the skin provide only indirect evidence of availability in the target organ. A number of methods enabling the localization and distribution of substances within the skin or specific tissue layers have been reviewed by Schalla and Schaefer (1985), and include histological techniques mentioned above. The concentration and distribution of drug in the stratum corneum also has the potential to provide an indication of the amount available to penetrate the deeper layers and an insight into the likely kinetics of the substance in the skin (Zesch, 1981).

Rougier *et al* (1983, 1985, 1986, 1987) and Dupuis *et al* (1984, 1986) have recently described an elegant series of experiments in humans and animal models which correlate the amount of radiolabelled drug within the stratum corneum, 30 minutes post-application, to the total amount penetrating in a 4 day period, after an identical drug exposure. This relationship was found to be independent of factors such as animal species, vehicle, dose, contact time, physicochemical nature of penetrant and anatomical site of application, all of which influence the rate of absorption. The amount in the stratum corneum was determined by sequential tape-stripping of the application site. The results suggest that it is possible to predict the percutaneous absorption of a compound from a simple measurement of the stratum corneum reservoir. Although radiolabelled compounds were used for the purposes of these studies, the relatively large amounts of material present in the stratum corneum at the end of the application, should enable the use of non-radioactive analytical techniques in many instances with this "stripping" method. The legal and ethical limitations posed by the use of radiolabels in humans may therefore be circumvented to some extent by such procedures.

6.2 ATTENUATED TOTAL REFLECTANCE FOURIER TRANSFORM INFRARED SPECTROSCOPY

An alternative method, which may be used to acquire similar information concerning the distribution of a substance in the stratum corneum *in vivo* is attenuated total reflectance Fourier transform infrared (ATR-FTIR) spectroscopy. The title of this technique simply describes the phenomenon whereby an infrared spectrum is obtained using attenuated total reflectance in conjunction with Fourier transform spectroscopy.

6.2.1 Principles of ATR-FTIR.

6.2.1.1 Infrared spectroscopy

The infrared region of the electromagnetic spectrum corresponding to the energy of most molecular vibrations lies at wavelengths between 2.5 and 15 μm (4000 to 650 cm^{-1}). In the absorption process, only selected frequencies of IR radiation which precisely match the natural stretching and bending vibrational energies of the molecule are absorbed. Since these vibrational frequencies are characteristic of a particular functional group and influenced by the local environment, they represent a simple and rapid means of identifying molecular structure. Although the technique is most commonly associated with the analysis of simple organic molecules, it has in recent years found an increasingly important role in the structural evaluation of biological molecules. This application has expanded rapidly with the introduction of sophisticated methods of data acquisition, analysis and sample handling (Lee and Chapman, 1986). Amongst these is the Fourier transform (FT) algorithm, which allows conversion of an interferogram (the normal output of an FT interferometer) into a conventional intensity versus wavenumber spectrum. The advantages of FT-IR over the traditional dispersive IR technique include increased speed and resolution, higher signal to noise ratio and excellent frequency precision, allowing data manipulations such as spectral subtraction.

6.2.1.2 Attenuated Total Reflectance

The technique of attenuated total reflectance is sometimes also referred to as total or multiple internal reflection, although each term has a defined usage according to the nature of the phenomenon (Harrick, 1967). In ATR, an infrared beam is transmitted to an IR transparent crystal whose geometry permits it to be internally reflected until it exits from the opposite face, from where it is directed back to the detector of the spectrophotometer (Figure 6.1). During transit through the crystal (the internal reflection element; IRE), the radiation penetrates slightly beyond the surface of the IRE before returning. Consequently, any material in contact with the IRE will absorb energy at wavelengths corresponding to its normal absorption spectrum during each successive reflection, producing a conventional IR spectrum.

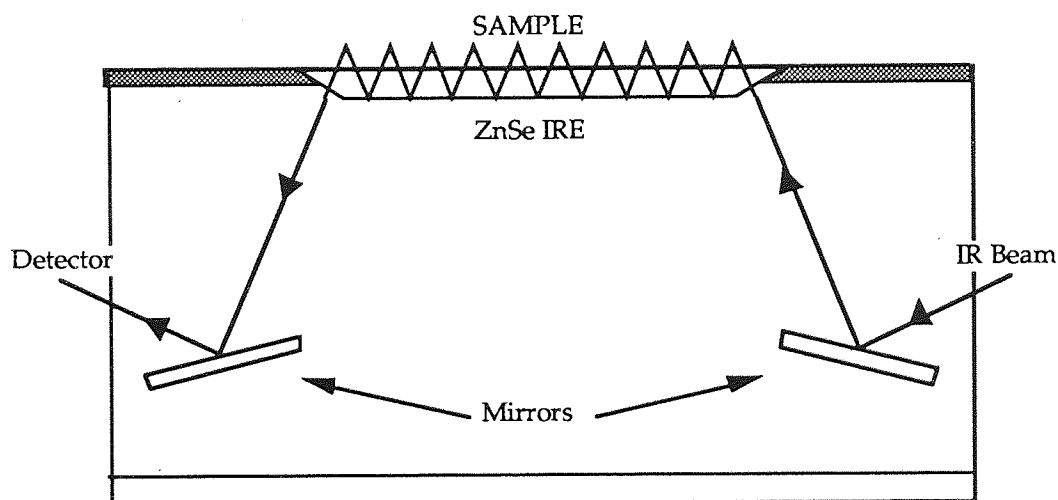


Figure 6.1 A schematic diagram of an ATR-FTIR sampling device.

The origins of this design (Harrick, 1960; Fahrenfort, 1961) lie in the observations made by Isaac Newton over 250 years ago, who discovered in his studies of the total reflection of light at the interface between two media of different refractive indices, the existence of an evanescent wave which extended into the rarer medium beyond the reflecting interface. This phenomenon is based on the principle that if radiation travelling through a medium of refractive index n_1 (e.g., IRE) strikes the interface of a second

medium of lower refractive index n_2 (e.g., sample) at an angle that is greater than the critical angle θ , defined as;

$$\theta = \sin^{-1} \frac{n_2}{n_1} \quad (6.1)$$

it will penetrate slightly into the second medium (*i.e.*, sample in contact with the IRE, such as stratum corneum) as it is being totally reflected (Figure 6.1). If the first medium is IR transparent, each penetration will result in energy loss due to absorption by the second medium, the effect being amplified by successive reflections within the IRE. The sensitivity of the technique is dependent on the magnitude or strength of coupling of the evanescent wave to the absorbing medium. Coupling may be increased by improving the 'index matching' of the two mediums, *i.e.*, choosing an IRE with a refractive index close to, but greater than, the sample ($n_2/n_1 \rightarrow 1$) and by increasing the depth of penetration which may be achieved by choosing an incident angle close to, but greater than, the critical angle, θ (equation 6.1).

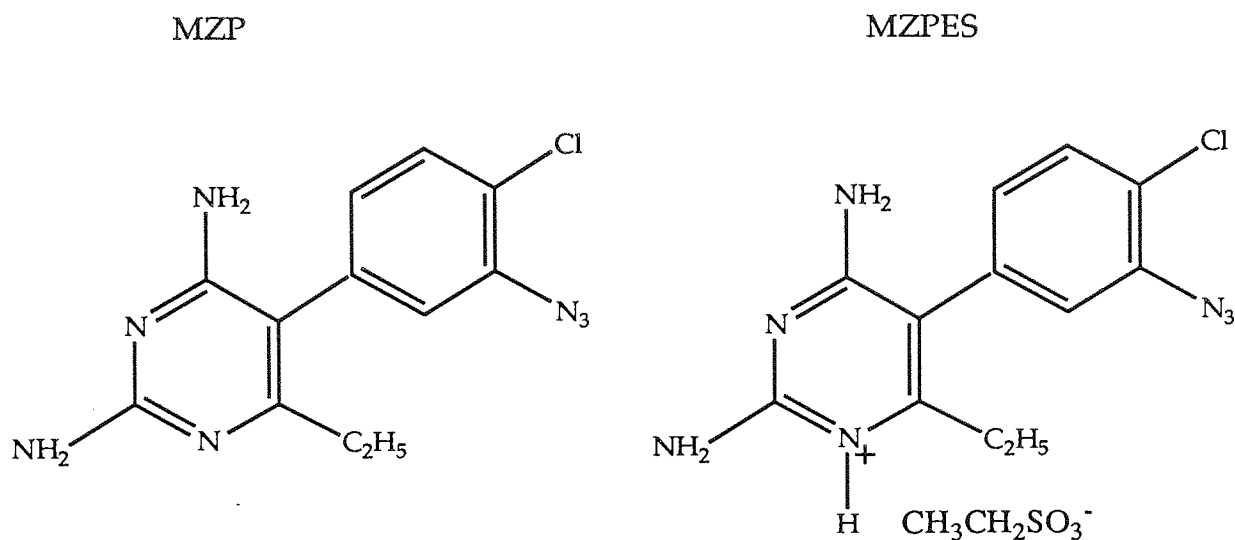
A number of investigators (Baier, 1978; Comaish, 1968; Puttnam, 1972; Puttnam and Baxter, 1967) have utilized the technique of ATR-IR spectroscopy to characterize human skin *in vivo*. However, only recently has its use been extended to investigate the biophysical nature of the skin's barrier function and to support deductions concerning the mechanism of penetration enhancement, previously made *in vitro*. In one of these studies (Mak *et al*, 1990a), the technique also enabled an estimation of the level of enhancer within the SC as a function of time. Subsequent to these studies, the authors demonstrated the application of ATR-FTIR to monitor non-invasively the enhanced percutaneous absorption *in vivo* of a model permeant cyanophenol, in man, in the presence of a chemical enhancer (Mak *et al*, 1990b). Higo *et al* (1990), have further quantified the distribution of this penetrant *in vivo* by correlating the amount of penetrant removed by tape-stripping with that determined spectroscopically.

The choice of cyanophenol as a model permeant in these studies was a function of its characteristic IR absorbance, attributable to the cyano (CN) substituent, which was distinct from that of the SC and other vehicle components. Thus the potential exists for other topically applied drugs to be similarly assessed, provided they possess the appropriate spectral features; most notably an IR absorbance in the region where the SC is IR transparent (between about 1700cm^{-1} and 2700cm^{-1}) and remote from absorbances of other components of the delivery system.

The azido functional group satisfies these constraints, possessing a characteristic IR absorbance at approximately 2115 cm^{-1} , which may serve as a highly diagnostic marker for the detection of compounds possessing this moiety. This suggests therefore that ATR-IR could enable an evaluation of the percutaneous penetration of azidoprofen and its analogues in a similar manner to cyanophenol. The elegance of this technique clearly lies in the ability to monitor this process *in vivo*; however, our currently limited knowledge concerning the toxicity of these compounds prevents this evaluation at the present time.

A parallel project to assess the role of the azido substituent in the control of topical delivery has been concerned with the evaluation of a novel lipophilic dihydrofolate reductase (DHFR) inhibitor as a potential topical anti-psoriatic agent (Baker, 1989). This antifolate, *m*-Azidopyrimethamine (2,4-diamino-5-(3-azido-4-chlorophenyl)-6-ethylpyrimidine; MZP), was designed to incorporate the DHFR inhibitory activity of agents such as pyrimethamine and metoprin, also known to possess potential topical anti-psoriatic activity, whilst curtailing the prolonged biological half-life which contributed to their toxicity (Bliss *et al*, 1987). The essence of this design was the inclusion of an azido moiety, which was expected to provide a means of biotransformation to more polar metabolites (Stevens *et al*, 1987), as in the case of azidoprofen.

The ethanesulphonate salt (MZPES) was synthesized to overcome problems of low aqueous solubility, and was the formulation of choice in Phase I and II clinical trials to investigate its antitumour activity as a short-acting lipophilic DHFR inhibitor (Stuart *et al*, 1989). The compound is also under investigation for anti-psoriatic activity *via* the topical route in human subjects. Therefore, in light of this background and the pharmacokinetic, metabolic and toxicological data available for MZPES from human studies, this compound, which also possesses the characteristic azido-substituent was chosen as a model penetrant for the *in vivo* ATR-FTIR studies.



The objectives of this study were firstly, to monitor the distribution of MZPES in the SC, in the presence and absence of a penetration enhancer (oleic acid) and secondly, to investigate whether the penetration of solvent (propylene glycol) and enhancer could also be determined. As a result, it was hoped to (a) complement the studies of Higo *et al* (1990) in examining the potential of ATR-FTIR to measure percutaneous penetration enhancement *in vivo* using a novel permeant and (b) to assess the potential utility of the azido group as a probe to study the topical delivery of compounds possessing this functionality.

6.3 EXPERIMENTAL

These studies were conducted at the Department of Pharmaceutical Chemistry, University of California, San Francisco, USA.

6.3.1 Attenuated Total Reflectance Fourier Transform Infrared Spectroscopy

Infrared spectra of the subject's forearms were recorded using an Analect FX-6200 Fourier transform infrared (FTIR) spectrophotometer (Laser Precision Devices, Irvine, CA, USA) equipped with an ATR skin analyzer accessory (Spectra-Tech, Stamford, CT, USA) and a liquid nitrogen cooled mercury-cadmium-telluride detector. The skin analyzer supported a trapezoidal zinc selenide (ZnSe) internal reflection element (dimensions: $7.5 \times 1 \times 0.2$ cm; incident angle: 60° ; refractive index, n_1 : 2.89), allowing the IR beam to penetrate the SC ($n_2 \cong 1.6$) to a depth of approximately $0.8 \mu\text{m}$. Spectra thus obtained, represent an average of 40 scans acquired over a period of about 70 seconds. All measurements were performed at ambient laboratory conditions (temperature: $21 \pm 1^\circ\text{C}$; relative humidity: 30-40%). Determination of changes in IR peak frequency maxima of C-H stretching absorbances required a greater precision than that allowed by the instrument (2.7 cm^{-1}). These measurements were therefore performed using a centre-of-gravity algorithm which allowed a precision of 0.1 cm^{-1} to be obtained (Cameron *et al*, 1982).

6.3.2 *In vivo* measurements

The participants in this study were healthy volunteers (aged 19-35 years) with no history of dermatological disease and were not receiving any medication. The region of skin used for the investigation was the midventral forearm. Two sites, one on each arm, were studied for each subject. These sites were gently cleansed with a water-soaked cotton swab (Q-tips[®]) followed by a dry one, prior to the experiment. An IR spectrum was then recorded which served as a pre-treatment control. This procedure was also performed prior to admittance of the subject to the study in order to deduce suitability, by examining the control spectrum for any irregularities.

The subjects were treated topically with either a 5% (w/v) solution of MZPES¹ in propylene glycol or an identical solution also containing 5% (w/v) oleic acid. The formulations (1 ml) were applied *via* a gauze pad (2 x 8 cm) which was affixed to the skin with a non-occlusive dressing (Tegaderm®, 3M, St. Paul, MN, USA). The application time was 1, 2 or 3 hours during which the volunteers pursued their normal activities, keeping the treated areas protected from light. At the end of the treatment period the pad was removed, and the skin surface gently cleansed 5 times with ethanol-soaked cotton swabs, followed by once with water before finally wiping with a dry cotton-swab.

After this post-treatment cleaning procedure, the treatment site on the forearm was positioned on the IRE and an IR spectrum recorded as described above. Following this initial spectral acquisition, the site was tape stripped once, using Scotch® Book tape no. 845 (3M, St. Paul, MN, USA) and a further IR spectrum immediately obtained. This latter procedure of tape-stripping followed by IR spectrum acquisition was repeated up to a maximum of 20 times, the IRE being wiped clean with ethanol in between successive measurements. In most cases, the frequency of spectrum recording was reduced after the first 6 tape-strips, *i.e.*, subsequent to this, a spectrum was obtained after every 2 strips. The outline of the treatment site was defined with a marker pen in order to ensure reproducible repositioning of the subject's forearm for each spectral measurement. At the end of this experimental regimen, subjects were advised to wash the application site with soap and water. In order to quantify the amount of SC removed by the tape-stripping procedure the tape strips were weighed before and after this routine.

6.3.3 Calibration

Solutions of MZPES in propylene glycol were prepared in the concentration range 0.25% to 2.0% (w/v). An aliquot (5 µl) was pipetted, dropwise, onto a glass microscope slide, centrally and along the length of the slide using a disposable glass pipette (Drummond-Wiretrol). The slide was then carefully

¹ synthesized by Dr R J Griffin, Pharmaceutical Sciences Institute, Aston University, Birmingham, U.K.

inverted over the IRE and positioned to ensure even spreading of the MZPES solution. An IR spectrum was recorded. This was repeated 4 times for each concentration.

6.4 RESULTS AND DISCUSSION

6.4.1 Spectral analysis

Figure 6.2 A illustrates a typical *in vivo* ATR-IR spectrum of untreated human stratum corneum obtained over the frequency range of 800 to 4000 cm^{-1} . The membrane biophysics literature can be used to assign the resulting major absorption bands to corresponding molecular vibrations, some of which are tabulated in Table 6.1. Subtle changes in the absorbance frequencies of these vibrations can be diagnostic of changes in membrane integrity. The use of infrared spectroscopy for the biophysical characterisation of the SC has been recently reviewed by Potts (1989). Of importance to our present studies however, is the existence of the IR transparent "window", principally between 1700 and 2700 cm^{-1} . Figure 6.2 shows IR spectra of MZPES (B) and human SC (C) following application of a 5% (w/v) solution of MZPES in propylene glycol, in comparison with untreated human SC (A). The spectra clearly show that the absorbance at $\sim 2115 \text{ cm}^{-1}$, arising from the cumulated double bond stretching of the $-\text{N}_3$ group in MZPES, rests in this window region, distinct from other SC absorbances and can thus easily be identified in the spectrum of SC following treatment. Consequently, the magnitude of this absorbance at 2115 cm^{-1} was used to indicate the relative amounts of MZPES present in the SC during the course of the experiment.

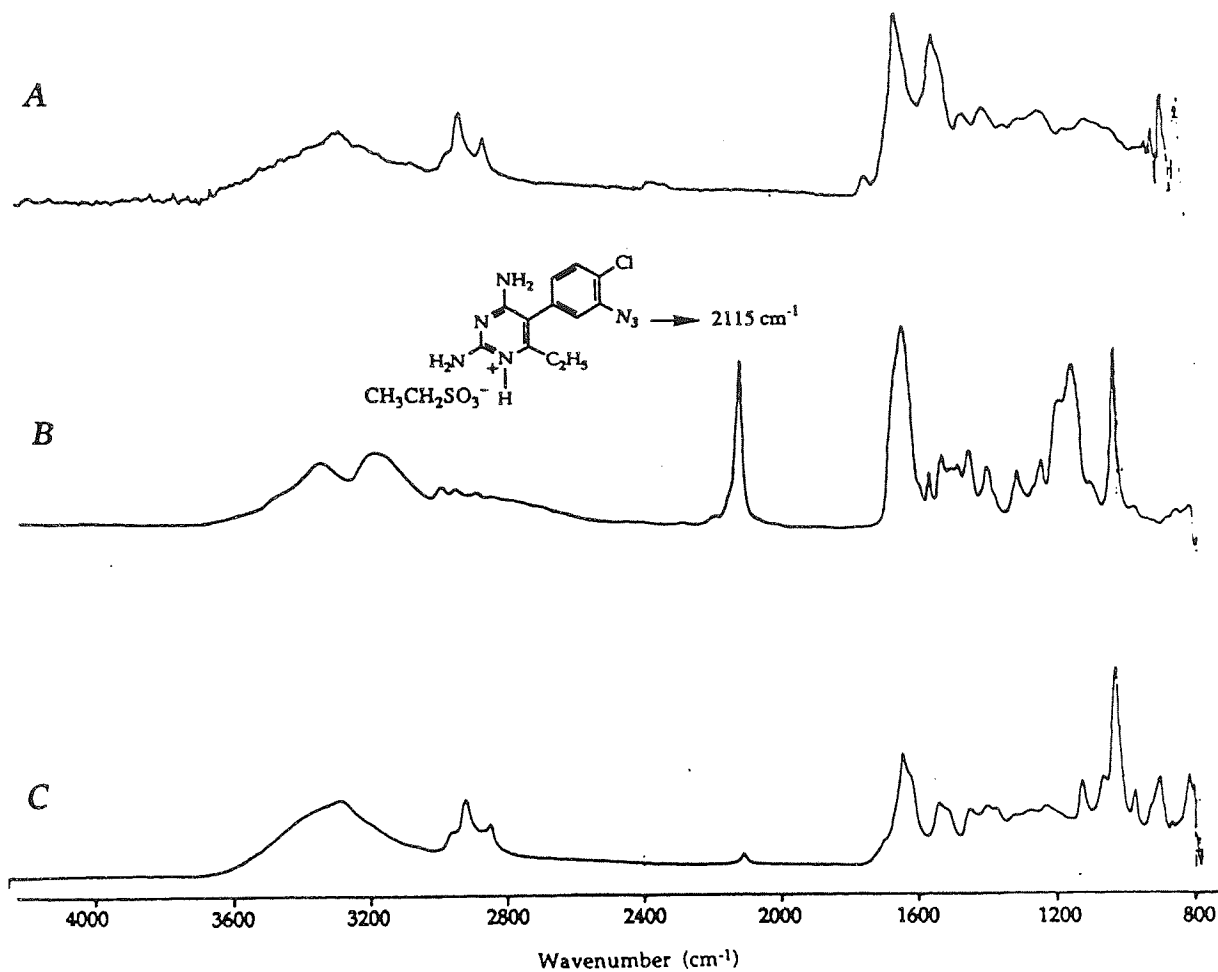


Figure 6.2 Example IR spectra of (A) untreated human SC, (B) MZPES, and (C) human SC following application of a 5% (w/v) solution of MZPES in propylene glycol.

Table 6.1 Infrared band assignments for stratum corneum constituents.

Vibrational motions	Origin	Frequency (cm ⁻¹)
O-H stretching	water	3500 - 3400
N-H stretching	protein, lipid	3400 - 3300
C-H stretching, asymmetric	lipid (CH ₂ acyl side chain)	2920
C-H stretching, symmetric	lipid (CH ₂ acyl side chain)	2850
C=O stretching	lipid	1740
C=O stretching, (Amide I)	protein, lipid (amide linkage)	1640
N-H bending, (Amide II)	protein, lipid (amide linkage)	1565
C-H bending and twisting	lipid, protein	1470-1400

adapted from Knutson *et al* (1985).

The amount of absorbing species may be quantified by determining the integrated intensity or area under the curve of the absorbance, which is directly proportional to this concentration (Byler and Susi, 1986; Keighley, 1976). An inherent difficulty with this method is that, in ATR, the intensity of an absorbance is dependent on the degree of contact between the sample and IRE. With *in vivo* measurements, there are inevitably both intra- and inter-subject variabilities in the level of contact established. This may be overcome by employing a normalization procedure, described by Potts *et al* (1985). Figure 6.3 shows that the IR spectrum of the absorbing species is superimposed upon a background absorbance due to scattered radiation. Increased sample/IRE contact leads to enhanced light scattering, with a resultant amplification of the area between the signal and zero baseline. If two baseline points on either side of the absorbance peak are connected, then both the areas A and B are proportional to the degree of skin/IRE contact. The ratio A/B (IR absorbance ratio) is, however, independent of this degree of contact and used to quantify the absorbing species.

For MZPES, the limits of 2091.1 cm^{-1} and 2144.1 cm^{-1} were chosen as baseline values on either side of the absorbance peak. The integrated intensity between these frequencies together with the corresponding area 'B' due to light scattering were computed for each spectral measurement and the resultant normalized ratios used for data analysis. The quality of certain spectra occasionally necessitated altering these limits by $\pm 2.7\text{ cm}^{-1}$, which was the minimum digital resolution of the equipment.

The correlation between the IR absorbance ratio and the concentration of MZPES was verified experimentally by performing an *in vitro* calibration with a series of concentrations. Figure 6.4 illustrates the linear relationship between these two parameters.

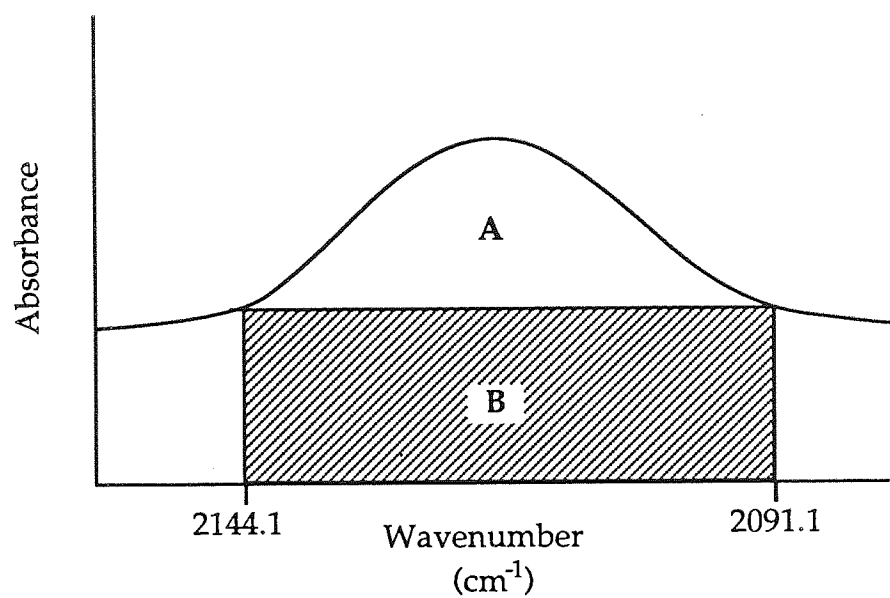


Figure 6.3 Normalization of an IR absorbance to correct for variations in skin/IRE contact. IR absorbance ratio = area A/area B.

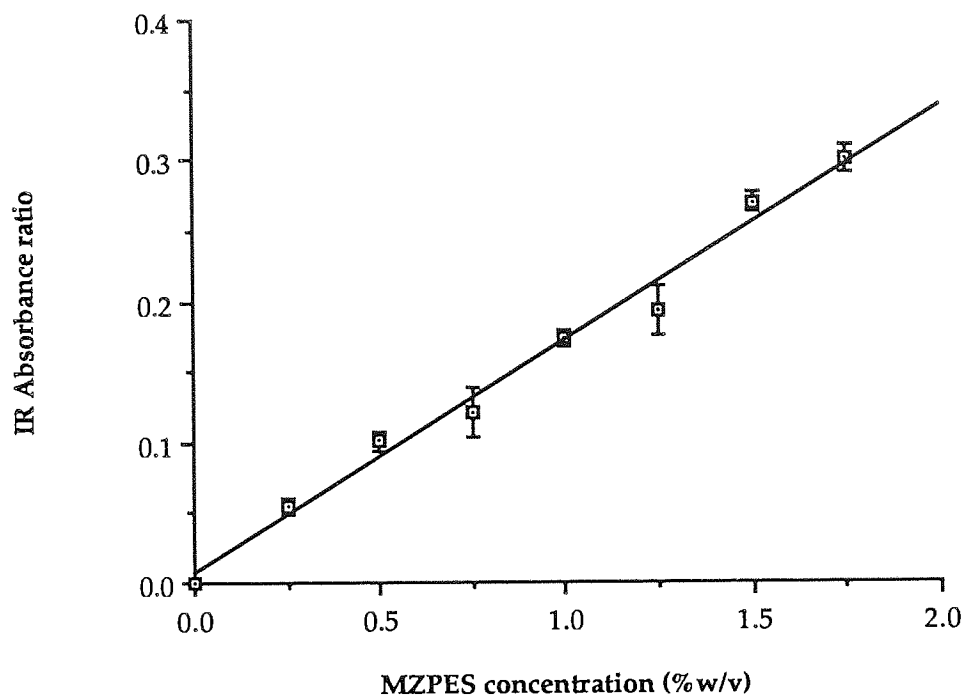


Figure 6.4 Calibration plot for MZPES, illustrating the linear relationship between MZPES concentration and IR absorbance ratio. The data represents the mean \pm sem ($n = 4$).

6.4.2 Removal of Stratum Corneum

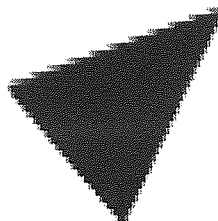
During the course of this discussion, the distribution of MZPES in the layers of the SC will be expressed in the form of 'MZPES absorbance' as a function of 'SC depth'. Having discussed the 'absorbance' parameter above, it is appropriate to comment on the relevance of the second variable, before proceeding to discuss the results. The average thickness of the SC layer is usually quoted as $\sim 20 \mu\text{m}$, with each cellular layer occupying 0.5 to 1.5 μm (Barry, 1983; Guy *et al*, 1987b; Siddiqui, 1989). The magnitude of these dimensions impedes any direct, routine measurement of the depth of SC penetration produced with each tape stripping. The depth may, however, be approximated to the weight of SC removed by this process, on account of the following reasoning. The mass of skin removed by each tape strip will be equivalent to the product of its volume (area \times depth) and density. The density of the SC should remain fairly constant, as will the area of SC removed, since it is a function of the dimensions of the tape strip, which remain constant. Consequently, the depth of penetration achieved at any stage can be considered to be proportional to the cumulative mass of SC removed.

In previous studies measuring drug concentrations in different layers of the SC (Schaefer *et al*, 1978 and 1982), data has most commonly been presented in the form of 'concentration' versus 'tape strip number', which yielded logarithmic concentration gradients as shown in Figure 6.5. The linear scale of the x-axis (tape strip no.) assumes that each stripping procedure extracts a constant mass of SC, and therefore penetrates the SC by a constant depth. Although, this may be the case for non-hydrated or untreated skin (Bommannan *et al*, 1990), the present studies indicate that the amount of SC adhering to each consecutive tape strip is variable, depending on the conditions of the experiment.



Aston University

Illustration removed for copyright restrictions



Aston University

Illustration removed for copyright restrictions

Figure 6.5 Distribution of radioactivity in the SC after topical application of 4-chlortestosterone acetate. (A) Linear plot. (B) Semilogarithmic plot. (From Schaefer *et al*, 1982).

Figure 6.6 shows plots of the cumulative weight of SC removed per unit area as a function of tape strip number, treatment time and regimen. Plateauing of the curves clearly illustrates that the amount of SC removed by each consecutive strip decreases; greater amounts being removed by the earlier tape-strips. This may be a consequence of the reduced cohesiveness of the outermost few layers of the SC, which are in the process of desquamating and therefore offer less resistance to removal. For the controls, the net amount of SC removed, increases with increasing treatment times. This increase is also evident in the presence of oleic acid as compared to the controls. However, in this case, the length of treatment does not appear to have any further effect. These results are consistent with the observations of Weigand and Gaylor (1973), who reported the facilitation of SC removal by prior hydration, such that each strip removed a larger quantity of SC from wet than from dry skin. Treatment with a solution of propylene glycol, which is often used as a humectant in topical preparations (Lorenzetti, 1979), would be expected to increase SC hydration; a process which may be enhanced with increasing period of application. The presence of oleic acid appears to compromise the membrane integrity even further. Hence, if one compares the same data set of drug distribution across the SC plotted as a function of (a) tape strip number and (b) cumulative SC weight (or "depth"), as in Figure 6.7, the influence of this disproportionality on the concentration profiles becomes apparent (refer to section 6.4.3 for origin of data). Drug distribution data were therefore generally described as a function of cumulative SC weight during this study.

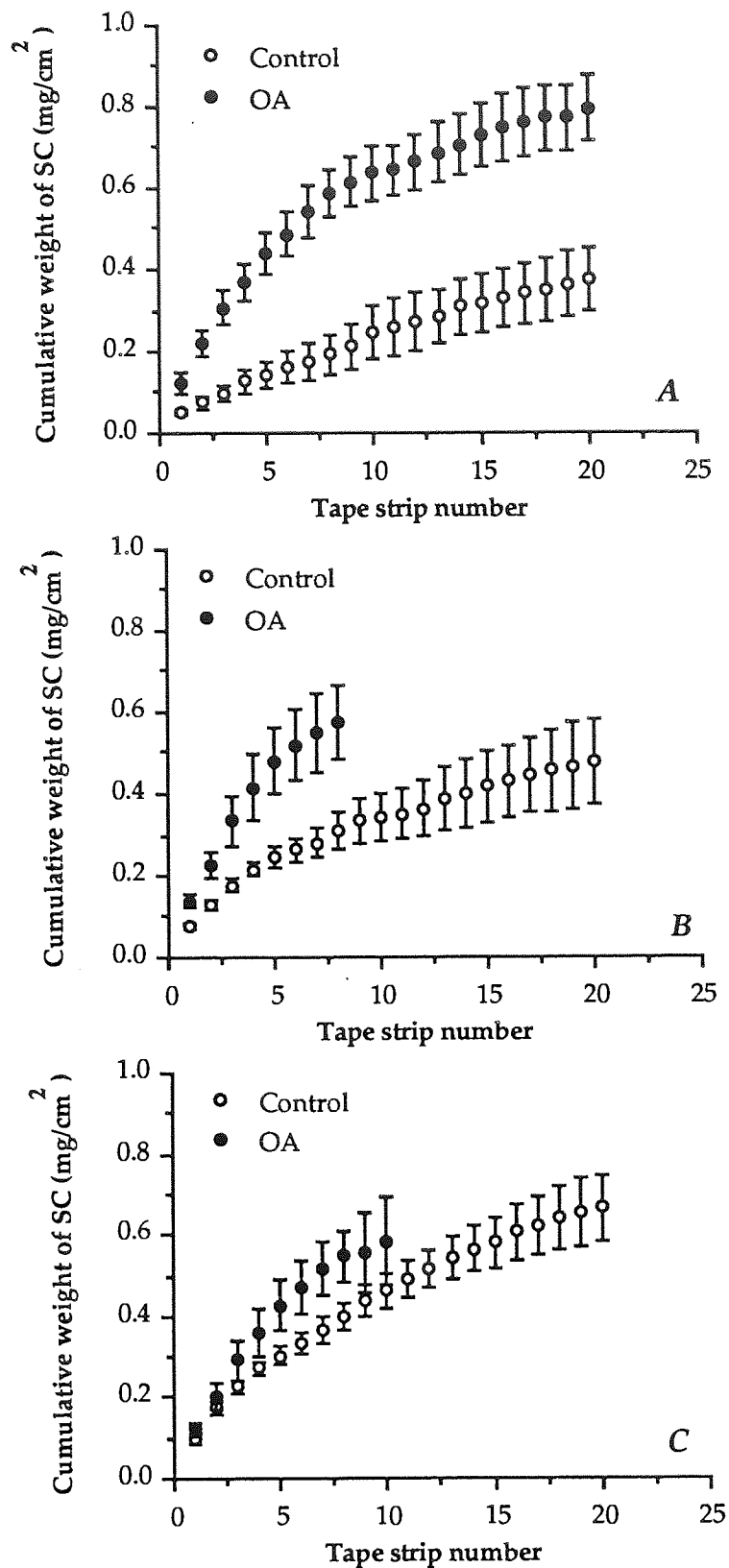


Figure 6.6 Cumulative weight per unit area of SC removed by sequential tape-stripping following treatment for (A) 1 hour, (B) 2 hours, and (C) 3 hours with either a 5% (w/v) solution of MZPES in propylene glycol (control) or the identical solution containing 5% (w/v) oleic acid (OA). The data represent the mean \pm sem for 4 subjects.

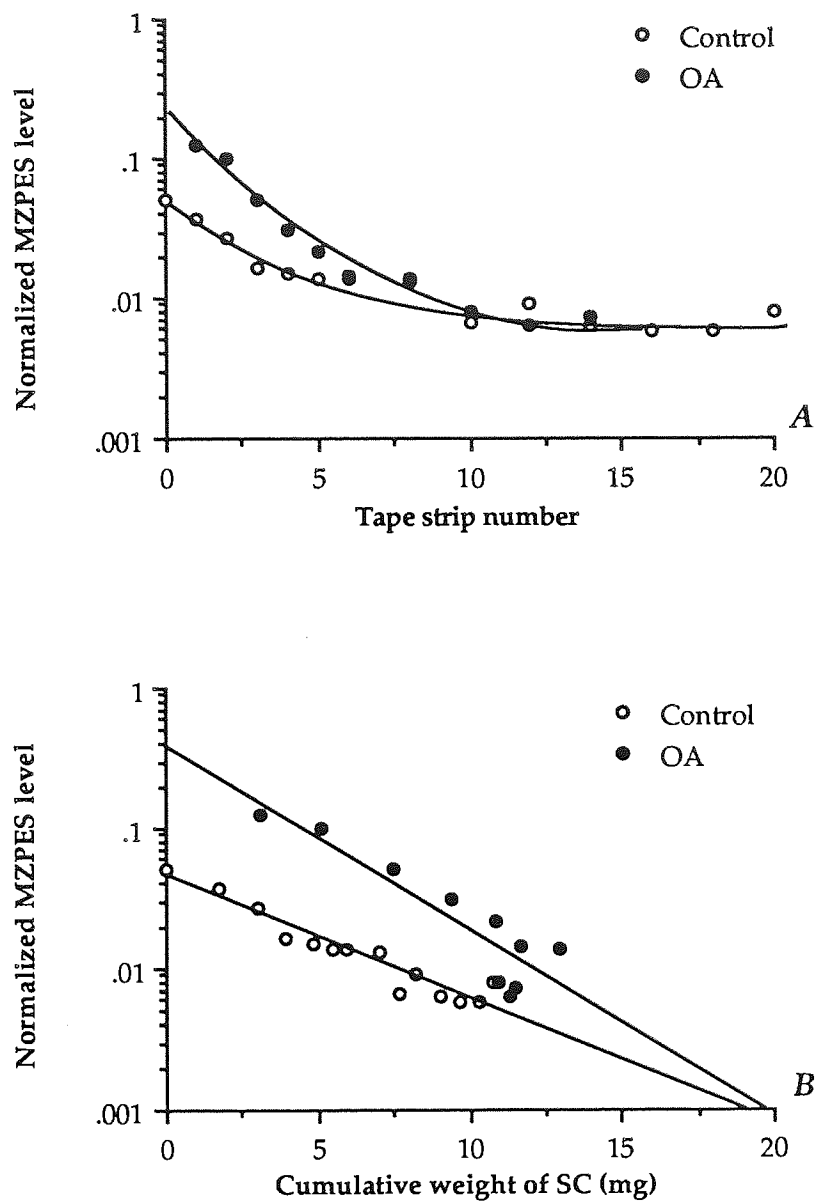


Figure 6.7 Semi-logarithmic plots of the normalized MZPES level as a function of (A) tape-strip number and (B) cumulative weight of SC removed. The data represent the mean for 4 subjects.

6.4.3 Distribution of MZPES

Figures 6.8-6.10 show plots of the normalized integrated intensity of the MZPES absorbance at 2115 cm^{-1} as a function of the cumulative weight of SC removed by repeated tape strippings, following a 1, 2 and 3 hour application of either a 5% (w/v) solution of MZPES in propylene glycol (Control) or the same solution including 5% (w/v) oleic acid (OA treatment). Semi-logarithmic transformation of the data in Figures 6.8 B-6.10 B, illustrate a linear decrease in drug concentration with increasing depth, for the oleic acid treatments. These profiles are consistent with the observations of Schaefer *et al* (1978), who described the logarithmic concentration gradient with a mathematical expression of a convergent geometric series. When applied to the SC, this mathematical treatment implied that each single layer offered the same resistance to penetration, with a cumulation of effect through the layers. A similar transformation for the controls, however, does not lead to linearization in all cases and reveals a biphasic profile. Penetration profiles of triamcinolone acetonide in the horny layer of normal and psoriatic skin (Schaefer *et al*, 1977) display similar behaviour. This may again reflect the loosely packed nature of the upper few layers of the SC, which by offering decreased resistance to penetration, are able to take up much greater amounts of drug than the deeper, more compact layers (Zesch *et al*, 1974). Additionally, once in the deeper layers, there may be a tendency for MZPES to accumulate prior to partitioning into the more aqueous viable phase. The presence of oleic acid, on the other hand, facilitates penetration throughout the layers and may serve to eliminate this difference in permeability possibly by disruption of the lipids across the SC. Whether it is able to alter the stratum corneum-viable epidermis partition coefficient for lipophilic drugs such as MZPES remains uncertain.

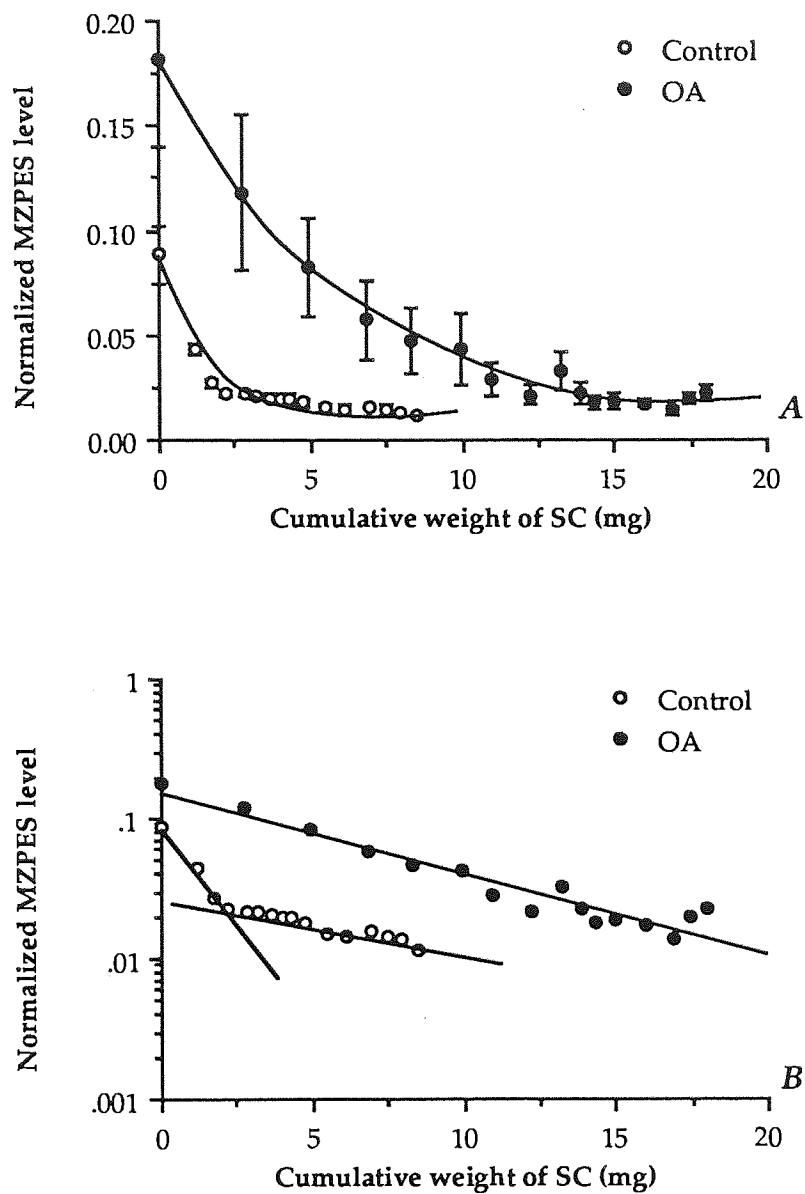


Figure 6.8 Normalized MZPES level as a function of SC 'depth' following treatment for 1 hour with either a 5% (w/v) solution of MZPES in propylene glycol or the identical solution containing 5% (w/v) oleic acid. (A) Linear plot and (B) Semi-logarithmic transformation. The data represent the mean \pm sem for 4 subjects.

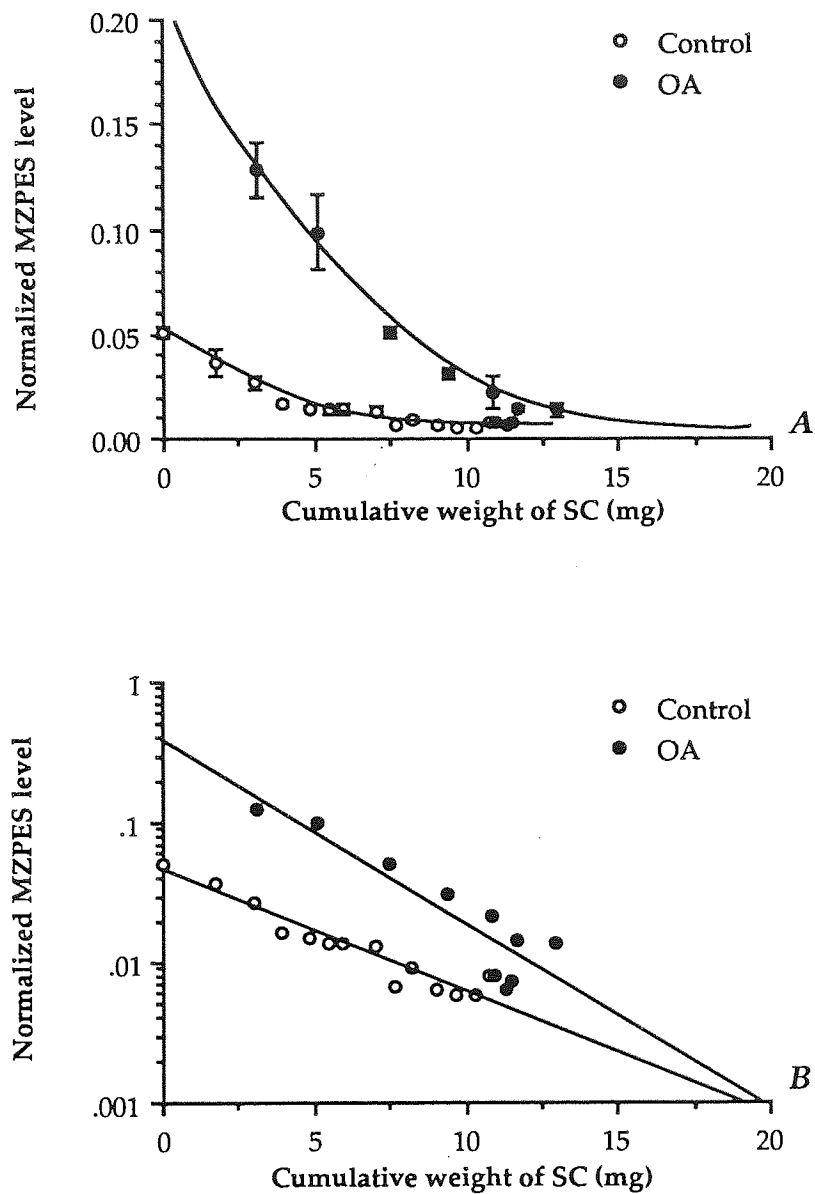


Figure 6.9 Normalized MZPES level as a function of SC 'depth' following treatment for 2 hours with either a 5% (w/v) solution of MZPES in propylene glycol or the identical solution containing 5% (w/v) oleic acid. (A) Linear plot and (B) Semi-logarithmic transformation. The data represent the mean \pm sem for 4 subjects.

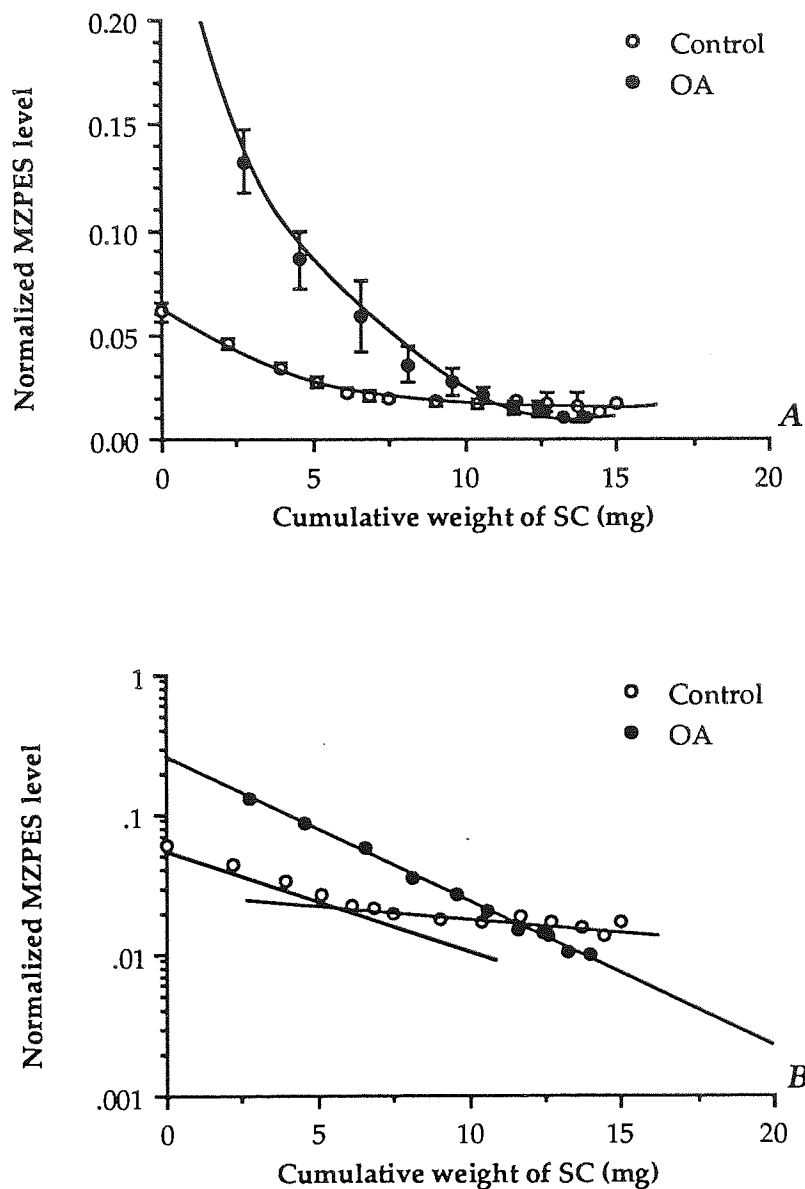


Figure 6.10 Normalized MZPES level as a function of SC 'depth' following treatment for 3 hours with either a 5% (w/v) solution of MZPES in propylene glycol or the identical solution containing 5% (w/v) oleic acid. (A) Linear plot and (B) Semi-logarithmic transformation. The data represent the mean \pm sem for 4 subjects.

The total amount of drug present in the various layers of the stratum corneum, reflecting the extent of penetration, can be estimated by calculating the area under each curve. These results are tabulated in Table 6.2 and show that increasing treatment time from 1 to 3 hours progressively enhances the delivery of MZPES into the SC from the control formulations. This is also illustrated by Figures 6.8-6.10, which show that MZPES can be located in the deeper layers at higher concentrations after a 3 hr application, compared to shorter treatment periods. The effect of including oleic acid in the vehicle may also be observed from these data. For all application times, the presence of oleic acid significantly increases the amount of MZPES in the SC. However, this enhancement appears to be independent of the length of application. This may reflect a saturation of oleic acid effect on SC or an uptake limitation. Further studies therefore need to address this issue.

Table 6.2 Relative amounts* of MZPES in the SC following various treatment protocols.

	Treatment period (hours)		
	1	2	3
i. without oleic acid	0.213	0.228	0.401
ii. with oleic acid	1.111	1.053	0.997
Ratio ii/i	5.217	4.620	2.486

* from AUC of data in Figures 6.8-6.10

The nature of the oleic acid induced enhancement is also uncertain. Is it a true enhancer effect, *i.e.*, does oleic acid facilitate skin penetration by reducing the SC barrier permeability, or does it simply aid partitioning of MZPES into the SC? These two effects can be difficult to separate, but an attempt may be made by considering some of the available *in vitro* penetration data. Baker (1989) reported that inclusion of oleic acid in the donor medium failed to enhance flux levels of MZPES through hairless mouse skin when compared to an equivalent medium without oleic acid. This was however, in contrast to the

results from experiments where skin was pretreated with 5% (w/v) oleic acid in propylene glycol for 12 hours prior to commencement of permeation; here, a 17-fold rise in flux was observed. This suggests that any thermodynamic effect of oleic acid on the SC/vehicle partitioning of the permeant is not predominantly responsible for the enhancement, since an increased partitioning phenomenon would have been demonstrated by the former experiment.

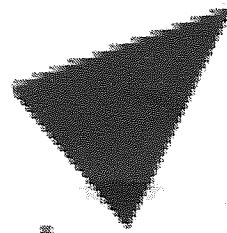
Oleic acid has also been shown to facilitate the permeation of cationic β -blockers across a lipoidal membrane (Green and Hadgraft, 1987) and may enhance permeation through a dual mechanism involving disruption of the SC lipids as well as ion-pair facilitation (Green *et al*, 1988). This latter effect would be expected to increase the lipophilicity of the permeant by the formation of an ion-pair complex between the carboxylate anion of the fatty acid and the cationic drug. A dual mechanism for oleic acid enhancement has been similarly proposed for cationic MZPES, in the light of *in vitro* penetration and partitioning data (Baker, 1989).

Despite the usefulness of these *in vitro* data in ascertaining the role of oleic acid in the penetration enhancement of MZPES, one should recognize the inherent limitations of extrapolating observations from these *in vitro* studies to the present *in vivo* investigations, which have been performed under very different conditions.

6.4.4 Stratum Corneum lipids

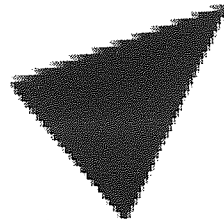
The role of ATR-FTIR in the biophysical characterization of the SC has already been briefly mentioned. Its ability to provide valuable information concerning the intercellular lipid domains also has the potential to aid understanding of the mode of action of penetration enhancers, the effect of which appears to be primarily mediated *via* modification of these lipids (Barry, 1987; Francoeur *et al*, 1990).

The C-H symmetric and asymmetric stretching vibrations of methylene (-CH₂) groups of the lipid hydrocarbon chains absorb near 2850 and 2920 cm⁻¹ respectively, at room temperature, and are attributed to a predominantly all planar *trans* conformation of the acyl chains. Introduction of *gauche* conformers into the chains as a result of their increased flexing and twisting, due, for example, to thermal perturbation, causes these infrared absorbances to shift to higher frequencies (Figure 6.11) (Casal and Mantsch, 1984, Golden *et al*, 1986). These "blue shifts" can therefore be used to indicate the introduction of *gauche* conformers accompanying lipid phase transitions, a process also described as fluidization or lipid disordering of the SC. Several investigators have related this thermally induced lipid disordering to increased murine (Knutson *et al*, 1985 and 1987) and porcine (Golden *et al*, 1987a and 1987b) skin permeability. Interestingly, oleic acid, a well documented penetration enhancer, has been shown to lower SC lipid phase transition temperatures, as demonstrated by differential scanning calorimetry (Francoeur *et al*, 1990; Golden *et al*, 1987b), suggesting a mode of action based upon disruption of the SC lipid matrix. Subsequent *in vitro* and *in vivo* IR studies of SC demonstrated C-H stretching frequency shifts to higher wavenumbers in the presence of oleic acid (Figure 6.11), implicating the enhancer as a cause of lipid fluidization and thereby presenting a possible mechanism of action. Further investigations have however, clearly shown that these changes in C-H stretching frequencies reflected vibrational conformations of both endogenous SC lipids and the exogenously applied oleic acid (Ongpipattanakul *et al*, in press). Using deuterated oleic acid, these investigators were able to differentiate between the C-H and C-D stretching frequencies of the SC lipids and oleic acid respectively, and hence conclude that oleic acid was not responsible for lipid fluidization at physiological temperature. Additionally, whilst the endogenous lipids were shown to exist in a highly ordered state at 37°C, oleic acid exists in a disordered fluid phase.



Aston University

Illustration removed for copyright restrictions



Aston University

Illustration removed for copyright restrictions

Figure 6.11 IR spectra of human SC in the C-H stretching region.

(A) Transmission IR spectra obtained at 30°C (—) and 115°C (----). (From Golden *et al*, 1986).

(B) ATR-IR spectra before (—) and after (----) 0.5 hour treatment with a 1% solution of oleic acid in ethanol. (From Mak *et al*, 1990).

The peak frequency shifts of the C-H asymmetric stretching vibrations from the present studies have been summarized in Figure 6.12. The data is presented as a function of tape-stripping (up to a total of 5 such procedures), with a shift of zero assigned to the background, pre-treatment measurement. These data clearly show a displacement of absorbances towards higher wavenumbers for treatments with the oleic acid-containing formulations compared to the controls. The aforementioned *in vitro* observations of Ongpipattanakul *et al* (in press), however, caution against a direct inference since these shifts undoubtedly reflect the physical state of both the SC lipids and the oleic acid. In addition, their results from porcine SC demonstrated the existence of highly ordered endogenous lipids at physiological temperature. If this finding is extrapolated to the present investigation, it suggests that the higher wavenumber absorbance shifts are purely a contribution from the exogenous oleic acid and not the endogenous SC lipids. In this instance, the absorbance displacement is indicative of the presence of oleic acid and may therefore provide information regarding the distribution of the enhancer across the SC layers.

The data show a shift to *lower* wavenumbers for the control treatments. Such *red* shifts indicate an increase in structural order of the lipids. This is consistent with the observations of Bommannan *et al* (1990) who reported an increase in order, but decrease in the amount, of intercellular lipid per layer, with increasing depth of SC. In contrast, treatment with oleic acid results in *blue* shifts over a similar depth. These may be attributed to the enhancer and therefore substantiate its presence throughout the upper layers. Any inference from data beyond 5 tape-strips is difficult due the superimposition of diminishing blue shifts (decreasing concentration of oleic acid) upon fairly constant red shifts. It is appropriate to point out that data in Figure 6.12 is presented as a function of tape-strip number. Since each tape-strip generally removes a larger mass of enhancer treated skin compared to the corresponding control (see section 6.4.2), each tape-stripping results in a slightly different depth of penetration for the control compared to the OA treated skin.

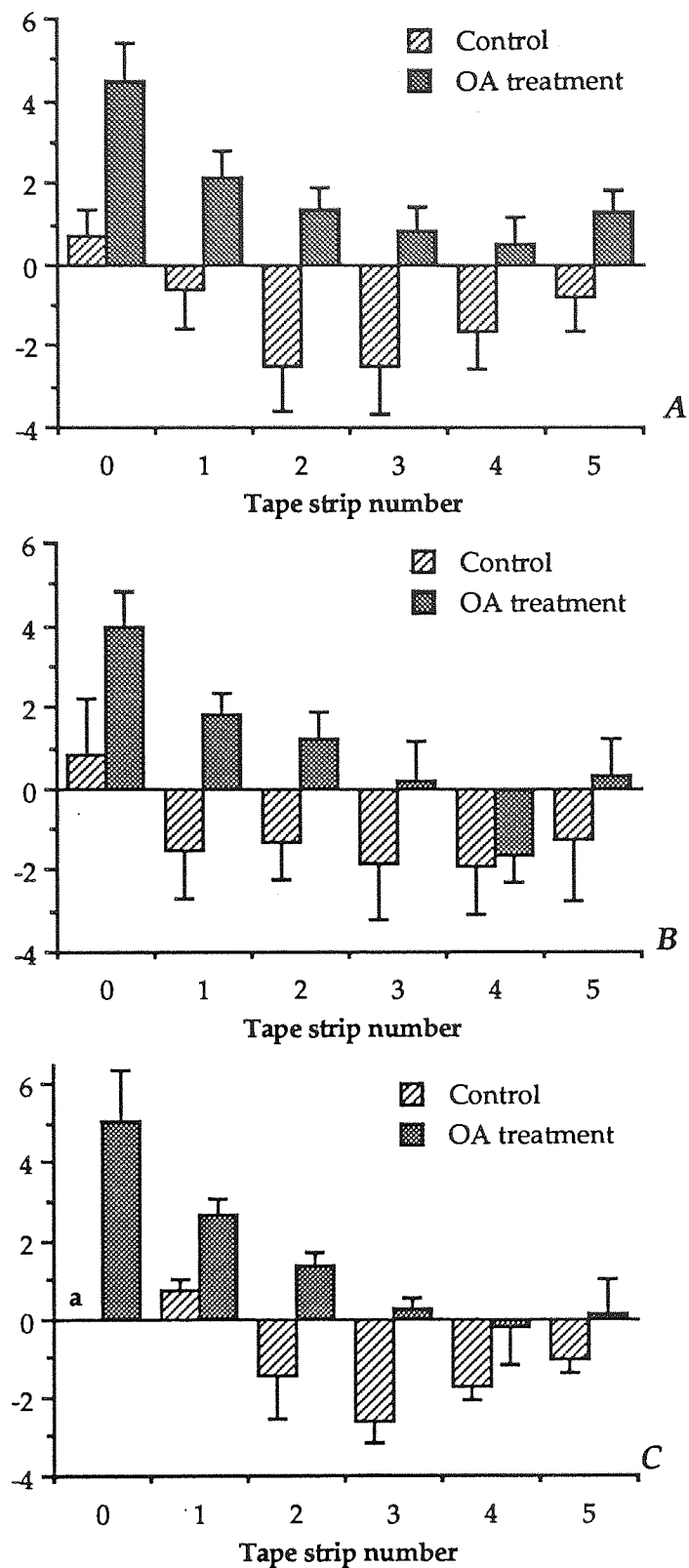


Figure 6.12 Frequency shift of the C-H asymmetric stretching absorbance as a function of tape-strip number following (A) 1 hour, (B) 2 hour and (C) 3 hour treatment with either a 5% (w/v) solution of MZPES in propylene glycol (control) or an identical solution containing 5% (w/v) oleic acid (OA treatment). The data are the mean \pm sem for 4 subjects. (a; data not available).

Therefore, following any number of tape-strips, C-H stretching absorbance measurements will not be at precisely the same SC depth with respect to the OA and non-OA treated skin.

Previous studies have shown that it is also possible to monitor the relative distribution of propylene glycol (vehicle) in the SC (Mak *et al*, 1990). An intense IR absorbance at 1040 cm^{-1} , resulting from C-O stretching vibrations of the glycol, may be used to follow this vehicle component. However, it has not been possible to do so in the present investigation due to a potential overlapping absorbance in the same region from MZPES, attributable to the S=O group of the ethanesulphonate. This would be apparent in the event of MZP penetrating the SC as an ion-pair with the ethanesulphonate ion; although this possible outcome needs to be investigated. In theory, if necessary, it should be possible to 'subtract' the contribution of MZPES to this absorbance, therefore permitting an estimate of the relative amount of propylene glycol. The intensity of absorbance at 1040 cm^{-1} arising from MZPES should be proportional to its concentration, which is known (in terms of IR absorbance ratio at 2115 cm^{-1}) at each measurement. Unfortunately, preliminary attempts to correlate these values have proven unsuccessful.

A further limitation of this study includes the determination of *relative* amounts of MZPES in the SC as opposed to *absolute* concentrations. An *in vitro* calibration verified the linear relationship between MZPES concentration and the parameter of IR absorbance ratio. Absorbance measurements *in vivo*, however, could not be quantified accurately with respect to concentration using this method during the initial investigation.

6.5 SUMMARY

The technique of ATR-FTIR spectroscopy has enabled a non-invasive examination of the *in vivo* percutaneous penetration of a model drug in man. It has permitted the penetration enhancement achieved by oleic acid to be monitored and allowed the presence of this enhancer in the outermost layers of the SC to be followed spectroscopically. The azido functionality by virtue of its characteristic IR absorbance thus offers the potential for azido-substituted compounds, of which many pharmaceutical examples exist, to be assessed in a similar manner.

CHAPTER SEVEN
GENERAL SUMMARY

GENERAL SUMMARY

The therapeutic potential of NSAIDs in the treatment of inflammatory dermatoses such as psoriasis may be restricted by their undesirable toxicity profiles, as illustrated by the example of benoxaprofen. Inclusion of an azido group into a drug molecule has been proposed as a promising strategy for the design of soft drugs (Stevens *et al*, 1987), an approach aimed at optimizing the therapeutic efficacy of drugs by controlling their degradation and subsequent elimination (Bodor, 1984). In view of this, azidoprofen [2-(4-azidophenyl) propionic acid] was synthesized as a model azido-substituted agent, incorporating both potential anti-inflammatory activity and metabolic instability.

This candidate molecule was assessed for susceptibility to bioreduction in various *in vitro* chemical and enzymatic model systems, using either reversed-phase HPLC or ^1H NMR to monitor the transformation (Chapter three). Incubation with dithiothreitol, a model reducing agent, resulted in a base-dependent conversion to the corresponding amine, hence supporting the postulated mechanism of thiol-mediated azide reduction. Although dithiothreitol is not a naturally occurring thiol, the presence of other endogenous thiols such as glutathione has implications for the intracellular conversion of azido-substituted drugs.

No reduction was observed in the presence of murine skin homogenates (Chapter four), indicating the unlikelihood of epidermal bioreduction *in vivo*. However, this cutaneous stability may not be representative of its metabolic fate in other tissues, as demonstrated by Baker (1989) and Kamali *et al* (1988) for the aryl azide, *m*-azidopyrimethamine (MZP). Although AZP did not undergo reduction in preliminary studies with murine hepatic tissue preparations, further experiments are required to confirm these observations. The reductive susceptibility of aromatic azides may be predictably varied by molecular modification (Baker *et al*, 1989), providing a potential means of optimizing the rate of soft drug inactivation.

Chapter five focused on the penetration of AZP through excised hairless mouse skin and silastic membrane. The achievement of similar penetration rates through both types of membrane during initial studies was indicative of the suitability of the latter model. Comparative permeation studies for AZP and ibuprofen yielded permeability coefficients within the same order of magnitude for the two permeants; the increased permeability of the latter reflecting its higher oil/water partition coefficient. Topical preparations of ibuprofen, delivering therapeutically effective concentrations of drug percutaneously, have recently been marketed. The comparable *in vitro* results therefore suggest that it may also be possible to deliver similar levels of AZP across human skin *in vivo*, however, the experimental nature of this model drug does not at present enable the confirmation of such a supposition.

The effect of pH, drug and cosolvent concentration, on the percutaneous absorption of AZP were investigated. The influence of pH on the penetration rate was mediated through its effect on the degree of drug ionization and consequently solubility and thermodynamic activity when solutions were used. In contrast, flux was largely independent of pH when suspensions were employed in the donor phase. These results emphasize the significance of formulation pH with respect to the anionic nature of the permeant. As expected, flux was dependent on solute concentration, with suspensions facilitating the rate of penetration. The effect of cosolvent concentration on flux could not be fully evaluated during this study.

Additionally, the effect on permeation of skin pretreatment with various penetration enhancers was studied. All enhancer treatments employed promoted penetration, although none was found to be superior. Pretreatment with azone appeared to facilitate penetration of the ionized species, contrary to the pH-partition hypothesis. Further studies are required to address the mechanism of this apparent phenomenon.

Prodrug modification is a useful means of manipulating the physicochemical properties of a parent drug in order to enhance partitioning into and subsequent diffusion through the stratum corneum. A series of ester derivatives of AZP, providing a range of lipophilicities, were assessed for their susceptibility towards chemical and enzymatic hydrolysis, which regenerates the parent acid, AZP (Chapter four). This activation was also demonstrated in homogenates of hairless mouse skin for selected esters, indicating the capacity of the skin to metabolize topical prodrugs in the vicinity of their site of action. Although, the transport of these ester prodrugs across silastic membrane was demonstrated during initial preparatory studies, quantification of permeation data and subsequent comparative analysis proved difficult due to significant adsorption to the membrane. Future studies therefore need to overcome these limitations prior to investigating the possibility of concurrent prodrug permeation and metabolism through excised skin.

The process of enzyme-mediated transesterification between alkyl ester prodrugs and alcoholic cosolvents was observed during the course of studies examining their hydrolytic activation. The frequent use of excipients containing alcoholic functions in topical formulations and the prevalence of various hydrolytic enzymes within the epidermis, may therefore have implications for such a process to occur *in vivo*, thereby modifying bioavailability of the topically applied drug. Such assumptions, however, need to be experimentally validated.

An ideal topical preparation for cutaneous therapy may be expected to target drug delivery to the affected site with minimal systemic absorption. Topical availability in this instance may only be adequately assessed by monitoring the drug level within the cutaneous layers. In any event, the concentration of drug in the stratum corneum, the rate-limiting barrier to percutaneous absorption, is the only true reflection of the amount available to penetrate the deeper layers, measurement of which can provide valuable kinetic information (Zesch, 1982). The use of a novel, non-invasive technique to determine such a distribution *in vivo* in man was addressed in Chapter six. An intense infrared absorption due

to the azide group serves as a highly diagnostic marker, enabling azido-compounds to be detected in the outer layers of the stratum corneum following their application to skin, using attenuated total reflectance Fourier transform infrared spectroscopy. The antifolate agent with potential antipsoriatic activity, *m*-azidopyrimethamine, was used as a candidate azido-substituted permeant for these *in vivo* investigations, permitting an examination of its percutaneous penetration enhancement in the presence of oleic acid.

The complex aetiology of psoriasis continues to be unravelled while novel treatment modalities, none curative or completely safe, continue to enter and exit the dermatologist's vast armamentarium for this chronic disorder. Whether the most effective future treatment will be antiproliferative, antiinflammatory, immunomodulatory or a combination of these remains to be seen. Effective lipoxygenase and cyclooxygenase inhibitors to regulate the biochemical abnormalities thought to be responsible for the inflammatory symptoms continue to be screened, and may find application not only in psoriasis but various other inflammatory disorders, cutaneous and otherwise. Their therapeutic success is dependent not only on their pharmacological potency but also their toxicity potential; successful separation of these two counteractive parameters is therefore crucial to the design of safe and effective drugs and is the ultimate aim of the soft drug approach.

REFERENCES

Abel EA, DiCicco LM, Orenberg EK, Fraki JE, Farber EM, Drugs in exacerbation of psoriasis. *J Am Acad Dermatol*, 15 (1986) 1007-1022

Abele DC, Dobson RL, Graham JB, Heredity and psoriasis: study of a large family. *Arch Dermatol*, 88 (1963) 38-47

Ainsworth M, Methods for measuring percutaneous absorption. *J Soc Cosmet Chem*, 11 (1960) 69-74

Akhter SA, Barry BW, Penetration enhancers in human skin - effect of oleic acid and azone on flurbiprofen penetration. *J Pharm Pharmacol*, 36 S (1984) 7

Akhter SA, Bennett SL, Waller IL, Barry BW, An automated diffusion apparatus for studying skin penetration. *Int J Pharm*, 21 (1984) 17-26

Albert A, Serjeant EP, *The determination of ionization constants*, 3rd edn. Chapman and Hall, London, (1984)

Albery WJ, Guy RH, Hadgraft J, Percutaneous absorption: transport in the dermis. *Int J Pharm*, 15 (1983) 125-148

Allen BR, Littlewood SM, Benoxaprofen: effect on cutaneous lesions in psoriasis. *Br Med J*, 285 (1982) 1241

Allen BR, Littlewood SM, The aetiology of psoriasis: clues provided by benoxaprofen. *Br J Dermatol*, 109S (1983) 126-129

Ananthakrishnan R, Eckes L, Walter H, On the genetics of psoriasis: An analysis of Hellgren's data for a model of multifactorial inheritance. *Arch Dermatol Forsch*, 247 (1973) 53-58

Ananthakrishnan R, Eckes L, Walter H, On the genetics of psoriasis II: An analysis of Lomholt's data from Faroe Islands for a multifactorial mode of inheritance. *J Genet*, 61 (1974) 142-146

Ando HY, Ho NFH, Higuchi WI, Skin as an active metabolizing barrier I: Theoretical analysis of topical bioavailability. *J Pharm Sci*, 66 (1977) 1525-1528

Arnold Von W, Trinnes F, Schroeder I, Zur hautresorption von salicylsäure bei psoriatikern und hautgesunden. *Beitrage zur Gerichtlichen Medizin*, 37 (1979) 325-328

Ashton RE, Andre P, Lowe NJ, Whitefield M, Anthralin: Historical and current perspectives. *J Am Acad Dermatol*, 9 (1983) 173-192

Baier RE, Noninvasive, rapid characterisation of human skin chemistry in situ. *J Soc Cosmet Chem*, 29 (1978) 283-306

Bakalayer SR, Bradley MPT, Honganen R, The role of dissolved gases in high-performance liquid chromatography. *J Chromatography*, 158 (1978) 277-293

Baker BS, Swain AF, Fry L, Valdimarsson H, Epidermal T lymphocytes and HLA-DR expression in psoriasis. *Br J Dermatol*, 110 (1984) 555-564

Baker H, Ryan TJ, Generalised pustular psoriasis. A clinical and epidemiological study of 104 cases. *Br J Dermatol*, 80 (1968) 771-793

Baker ND, *Lipophilic antifolates as potential antipsoriatic agents*. Ph.D thesis, Aston University, Birmingham, (1989)

Baker ND, Griffin RJ, Irwin WJ, Slack JA, The reduction of aryl azides by dithiothreitol: a model for bioreduction of aromatic azido-substituted drugs. *Int J Pharm*, 52 (1989) 231-238

Barker N, Hadgraft J, Facilitated percutaneous absorption: a model system. *Int J Pharm*, 8 (1981) 193-202

Barr RM, Black AK, Francis DM, Koro O, Numata T, Greaves MW, Release of prostaglandin D₂ (PGD₂) from human skin in vivo during cutaneous anaphylaxis. *Br J Pharmacol*, 88 (1986) 394P

Barr RM, Brain S, Camp RDR, Cilliers J, Greaves MW, Mallet A, Misch K, Levels of arachidonic acid and its metabolites in the skin in human allergic and irritant contact dermatitis. *Br J Dermatol*, 111 (1984) 23-28

Barry BW, *Dermatological formulations: percutaneous absorption*. Marcel Dekker, New York (1983)

Barry BW, Optimizing percutaneous absorption. In: Bronaugh RL, Maibach HI (eds), *Percutaneous Absorption. Mechanisms - Methodology - Drug Delivery*. Marcel Dekker, New York, (1985) pp 489-511

Barry BW, Mode of action of penetration enhancers in human skin. *J Control Rel*, 6 (1987) 85-97

Barry BW, Bennett SL, Effect of penetration enhancers on the permeation of mannitol, hydrocortisone, and progesterone through human skin. *J Pharm Pharmacol*, 39 (1987) 535-546

Bauer FW, Cell kinetics. In: Mier PD, van de Kerkhof PCM (eds) *Textbook of Psoriasis*. Churchill Livingstone, Edinburgh, (1986) pp 100-112

Bayley H, Standring DN, Knowles JR, Propane-1,3-dithiol: a selective reagent for the efficient reduction of alkyl and aryl azides to amines. *Tetrahedron Lett*, 39 (1978) 3633-3634

Bechet PE, Psoriasis, a brief historical review. *Arch Dermatol Syphil*, 33 (1936) 327-334

Beckman L, Bergdahl B, Cedergren B, Liden S, Genetic markers in psoriasis. *Acta Dermatovenereol*, 57 (1977) 247-251

Bedford CJ, Young JM, Wagner BM, Anthralin inhibition of mouse epidermal arachidonic acid lipoxygenase *in vitro*. *J Invest Dermatol*, 81 (1982) 566-571

Bertrams J, Lattke C, Kuwert E, Correlation of antistreptolysin-O-titre to HL-A 13 in psoriasis, *N Engl J Med*, 291 (1974) 631

Bevinakatti HS, Banerji AA, Lipase catalysis: factors governing transesterification. *Biotechnology Lett*, 10 (1988) 397-398

Blank IH, Scheuplein RJ, Transport into and within the skin. *Br J Dermatol*, 81 (1969) 4-10

Bliss EA, Brown TB, Stevens MFG, Wong CK, The biological and chemical properties of 4-azidobenzenesulphonamide ('Azidosulphanilamide'). *J Pharm Pharmacol*, 31 (1979) 66P

Bliss EA, Griffin RJ, Stevens MFG, Structural studies on bio-active compounds. Part 5. Synthesis and properties of 2,4-diaminopyrimidine dihydrofolate reductase inhibitors bearing lipophilic azido groups. *J Chem Soc Perkin Trans I*, (1987) 2217-2228

Bodor N, "Designing safer drugs based on the soft drug approach." *Trends in Pharmacol Sci*, 3 (1982) 53-58

Bodor N, Sloan KB, Improved delivery through biological membranes. XII. The effect of the incorporation of biphasic solubilizing groups into prodrugs of steroids. *Int J Pharm*, 15 (1983) 235-250

Bodor N, Sloan KB, Little RJ, Selk SH, Caldwell L, Soft drugs 4. 3-Spirothiazolidines of hydrocortisone and its derivatives. *Int J Pharm*, 10 (1982) 307-321

Bodor N, Zupan J, Selk S, Improved delivery through biological membranes VII. Dermal delivery of cromoglycic acid (Cromolyn) via its prodrugs. *Int J Pharm*, 7 (1980) 63-75

Bokoch GM, Reed RW, Evidence for the inhibition of leukotriene A₄ synthesis by 5,8,11,14-eicosatetraenoic acid in guinea pig polymorphonuclear leukocytes. *J Biol Chem*, 256 (1981) 4156-4159

Bommaman D, Potts RO, Guy RH, Examination of stratum corneum barrier function *in vivo* by infrared spectroscopy. *J Invest Dermatol*, 95 (1990) 403-408

Bond JR, Barry BW, Limitations of hairless mouse skin as a model for *in vitro* permeation studies through human skin: hydration damage. *J Invest Dermatol*, 90 (1988a) 486-489

Bond JR, Barry BW, Hairless mouse skin is limited as a model for assessing the effects of penetration enhancers in human skin. *J Invest Dermatol*, 90 (1988b) 810-813

Bos JD, The pathomechanisms of psoriasis; the skin immune system and cyclosporin. *Br J Dermatol*, 118 (1988) 141-155

Bradford MM, A rapid and sensitive method for the quantitation of microgram quantities of protein utilizing the principle of protein-dye binding. *J Biol Chem*, 272 (1976) 248-254

Brain SD, Camp RDR, Leigh IM, Ford-Hutchinson AW, The synthesis of leukotriene B₄-like material by cultured human keratinocytes (abstract). *J Invest Dermatol*, 78 (1982a) 328

Brain SD, Camp RDR, Dowd PM, Kobza Black A, Woollard PM, Mallet AI, Greaves MW, Psoriasis and leukotriene B₄. *Lancet*, 2 (1982b) 762-763

Brain SD, Camp RDR, Dowd PM, Kobza Black A, Greaves MW, The release of leukotriene B₄-like material in biologically active amounts from the lesional skin of patients with psoriasis. *J Invest Dermatol*, 83 (1984a) 70-73

Brain SD, Camp RDR, Cunningham FM, Dowd PM, Greaves MW, Kobza Black A, Leukotriene B₄-like material in scale of psoriatic skin lesions. *Br J Pharmacol*, 83 (1984b) 313-317

Braun-Falco O, Schmoeckel C, The dermal inflammatory reaction in initial psoriatic lesions. *Arch Dermatol Res*, 258 (1977) 9-16

Bray M, Retinoids are potent inhibitors of the generation of rat leukocyte leukotriene B₄-like activity *in vitro*. *Eur J Pharmacol*, 98 (1984) 61-67

Brockman FG, Kilpatrick M, The thermodynamic dissociation constant of benzoic acid from conductance measurements. *J Amer Chem Soc*, 56 (1934) 1483-1486

Bronaugh RL, Maibach HI, *In vitro* models for percutaneous absorption. In: Maibach HI, Lowe NJ (eds), *Models in Dermatology*. Karger, Basel, (1985) pp 178-188

Bronaugh RL, Stewart RF, Congdon ER, Giles AR, Jr, Methods for *in vitro* percutaneous absorption studies. I. Comparison with *in vivo* results. *Toxicol Appl Pharmacol*, 62 (1982a) 474-480

Bronaugh RL, Stewart RF, Congdon ER, Methods for *in vitro* percutaneous absorption studies. II. Animal models for human skin. *Toxicol Appl Pharmacol*, 62 (1982b) 481-488

Bronaugh RL, Stewart RF, Methods for *in vitro* percutaneous absorption studies IV: the flow-through diffusion cell. *J Pharm Sci*, 74 (1985a) 64-67

Bronaugh RL, Stewart RF, Methods for *in vitro* percutaneous absorption studies V: permeation through damaged skin. *J Pharm Sci*, 74 (1985b) 1062-1066

Bucks DAW, Skin structure and metabolism: Relevance to the design of cutaneous therapeutics. *Pharm Res*, 1 (1984) 148-153

Bucks DAW, Maibach HI, Guy RH, Percutaneous absorption of steroids: effect of repeated applications. *J Pharm Sci*, 74 (1985) 1337-1339

Bucks DAW, McMaster JR, Maibach HI, Guy RH, Percutaneous absorption of phenols *in vivo* (abst). *Clin Res*, 35 (1987) 672

Bucks DAW, McMaster JR, Maibach HI, Guy RH, Bioavailability of topically administered steroids: a "mass balance" technique. *J Invest Dermatol*, 90 (1988) 29-33

Bundgaard H, Design of prodrugs: bioreversible derivatives for various functional groups and chemical entities. In: Bundgaard H (ed), *Design of Prodrugs*. Elsevier, Amsterdam, (1985) pp 1-92

Bundgaard H, Nielsen NM, Glycolamide esters as a novel biolabile prodrug type for non-steroidal anti-inflammatory carboxylic acid drugs. *Int J Pharm*, 43 (1988) 101-110

Byler DM, Susi H, Examination of the secondary structure of proteins by deconvolved FTIR spectra. *Biopolymers*, 25 (1986) 469-487

Cameron DG, Kauppinen JK, Moffatt DJ, Mantsch HH, Precision in condensed phase vibrational spectroscopy. *Appl Spectrosc*, 36 (1982) 245-250

Camp RDR, Role of arachidonic acid metabolites in psoriasis and other skin diseases. In: Lewis A (ed) *Advances in Inflammation Research*, Vol 12. Raven Press, New York, (1988) pp 163-172

Camp RDR, Greaves MW, Inflammatory mediators in the skin. *Br Med Bull*, 43 (1987) 401-414

Camp RDR, Russell Jones R, Brain SD, Woollard PM, Greaves MW, Production of intraepidermal microabscesses by topical application of leukotriene B₄. *J Invest Dermatol*, 82 (1984) 202-204

Camp RDR, Kobza Black A, Cunningham F, Mallet A, Greaves MW, Pharmacological effects of topical lonapalene in psoriasis. *J Invest Dermatol*, 90 (1988) 550

Capozzi G, Modena G, Oxidation of thiols. In: Patai S (ed) *The Chemistry of Functional Groups: The Chemistry of the Thiol Group*, Part 2. John Wiley and Sons Ltd, London, (1974) pp 785-841

Cartwright IL, Hutchinson DW, Armstrong VW, The reactions between thiols and 8-azidoadenosine derivatives. *Nuc Acids Res*, 3 (1976) 2331-2339

Casal HL, Mantsch HH, Polymorphic phase behaviour of phospholipid membranes studied by infrared spectroscopy. *Biochim Biophys Acta*, 779 (1984) 381-401

Cashin CH, Dawson W, Kitchen EA, The pharmacology of benoxaprofen (2-[4-chlorophenyl]- α -methyl-5-benzoxazole acetic acid), LRCL 3794, a new compound with anti-inflammatory activity apparently unrelated to inhibition of prostaglandin synthesis. *J Pharm Pharmacol*, 29 (1977) 330-336

Catz P, Friend DR, Alkyl esters as skin permeation enhancers for indomethacin. *Int J Pharm*, 55 (1989) 17-23

Chan C, Dubois L, Young V, Effects of two novel 5-lipoxygenase inhibitors in a guinea-pig model of epidermal hyperproliferation. In: Farber EM (ed) *Psoriasis: Proceedings of the Fourth International Symposium*. Elsevier, New York, (1987) pp 538-539

Chan SY, Li Wan Po A, Prodrugs for dermal delivery. *Int J Pharm*, 55 (1989) 1-16

Chowaniec O, Jablonska S, Beutner EH, Proniewska M, Jarzabek-Chorzelska M, Rzeska G, Earliest clinical and histological changes in psoriasis. *Dermatologica*, 163 (1981) 42-51

Church MK, Benyon RC, Clegg LS, Holgate ST, Immunopharmacology of mast cells. In: Greaves MW, Shuster S (eds), *Handbook of Experimental Pharmacology, Vol 87/1. Pharmacology of the Skin I*. Springer Verlag, Berlin, (1989) pp 129-166

Collier SW, Sheikh NM, Sakr A, Lichtin JL, Stewart RF, Bronaugh RL, Maintenance of skin viability during *in vitro* percutaneous absorption/metabolism studies. *Toxicol Appl Pharmacol*, 99 (1989) 522-533

Comaish S, Infra-red studies of human skin *in vivo* by multiple internal reflection. *Br J Derm*, 80 (1968) 522-528

Connor MJ, Wheeler LA, Depletion of cutaneous glutathione by ultraviolet radiation. *Photochem Photobiol*, 46 (1987) 239-245

Convit J, Investigation of the incidence of psoriasis among Latin American Indians. In: Pillsbury, Livingwood (eds) *Proceedings of the XII International Congress of Dermatology*. Excerpta Medica Fdtn, New York, (1963) pp 196-199

Coombs RV, Danna RP, Denzer M, Hardtmann GE, Huegi B, Koletar G, Koletar J, Ott H, Jukniewicz E, Perrine JW, Takesue EI, Trapold JH, Synthesis and antiinflammatory activity of 1-alkyl-4-aryl-2(1H)-quinazolinones and quinazolinethiones. *J Med Chem*, 16 (1973) 1237-1245

Cooper ER, Effect of decylmethyl sulfoxide on skin penetration. In: Mittal KL, Fendler EJ (eds) *Solution behaviour of surfactants*. Plenum Press, New York, (1982) p 1505

Cooper ER, Increased skin permeability for lipophilic molecules. *J Pharm Sci*, 73 (1984) 1153-1156

Corey EJ, Shir C, Cashman JR, Docasohexaenoic acid is a strong inhibitor of prostaglandin but not leukotriene biosynthesis. *Proc Natl Acad Sci USA*, 80 (1983) 3581-3584

Cunningham FM, Greaves MW, Woollard PM, Chemokinetic activity of 12(S) and 12(R) hydroxyeicosatetraenoic acid (12-HETE) for human polymorphonuclear leukocytes. *Br J Pharmacol*, 87 (1986) 107P

Czarnetzki B, Increased monocyte chemotaxis towards leukotriene B₄ and platelet activating factor in psoriasis. *Clin Exp Immunol*, 54 (1983) 486-492

Dale HH, Progress in autopharmacology. A survey of present knowledge of the chemical regulation of certain functions by natural constituents of the tissues. *Bull Johns Hopkins Hosp*, 53 (1934) 297-347

Degreef H, Dockx, P, De Doncker P, De Beule K, Cauwenbergh G, A double-blind vehicle-controlled study of R 68 151 in psoriasis: a topical 5-lipoxygenase inhibitor. *J Am Acad Dermatol*, 22 (1990) 751-755

Dolan JW, LC troubleshooting. Shortcuts for LC measurements. *LC-GC International*, 1 (1988) 18-22

Dowd PM, Kobza Black A, Woollard PM, Camp RDR, Greaves MW, Cutaneous responses to 12-hydroxy-5,8,10,14-eicosatetraenoic acid (12-HETE). *J Invest Dermatol*, 84 (1985) 537-541

Duell EA, Ellis CN, Voorhees JJ, Determination of 5, 12, and 15-lipoxygenase products in keratomed biopsies of normal and psoratic skin. *J Invest Dermatol*, 91 (1988) 446-450

Duller P, van Veen-Vietor, Psychosocial aspects. In: Mier PD, van de Kerkhof PCM (eds) *Textbook of Psoriasis*. Churchill Livingstone, Edinburgh, (1986) pp 84-95

Dunn WJ, Binding of certain nonsteroid antiinflammatory agents and uricosuric agents to human serum albumin. *J Med Chem*, 16 (1973) 484-486

Dupuis D, Rougier A, Roguet R, Lotte C, Kalopissis G, In vivo relationship between horny layer reservoir effect and percutaneous absorption in human and rat. *J Invest Dermatol*, 82 (1984) 353-356

Dupuis D, Rougier A, Roguet R, Lotte C, The measurement of the stratum corneum reservoir. A predictive method for in vivo percutaneous absorption studies. *Br J Dermatol*, 115 (1986) 233-238

Durrheim H, Flynn G, Higuchi W, Behl CR, Permeation of hairless mouse skin I: Experimental methods and comparison with human epidermal permeation by alkanols. *J Pharm Sci*, 69 (1980) 781-786

Dyer A, Hayes GG, Wilson JG, Catterall R, The interpretation of rate curves arising from membrane permeation studies. *Int J Cos Sci*, 6 (1984) 123-130

Elias PM, Epidermal lipids, barrier function, and desquamation. *J Invest Dermatol*, 80 (1983) 44S-49S

Elias PM, Structure and function of the stratum corneum permeability barrier. *Drug Dev Res*, 13 (1988) 97-105

Ellis CN, Fallon JD, Heezen JL, Voorhees JJ, Topical indomethacin exacerbates lesions of psoriasis. *J Invest Dermatol*, 80 (1983) 362

Ellis CN, Goldfarb MT, Roenigk HH, Rosenbaum M, Wheelr S, Voorhees JJ, Effects of oral meclufenamate therapy in psoriasis. *J Am Acad Dermatol*, 14 (1986a) 49-52

Ellis CN, Gorsulowsky DC, Hamilton TA, Billings JK, Brown MD, Headington JD, Cooper KD, Baadsgaard O, Duell EA, Annesly TM, Turcotte JG, Voorhees JJ, Cyclosporin improves psoriasis in a double-blind study. *J Am Med Assoc*, 256 (1986b) 3110-3116

Eyre RW, Krueger GP, Response to injury of skin involved and uninvolved in psoriasis, and its relation to disease activity. *Br J Dermatol*, 106 (1982) 153-159

Fahrenfort J, Attenuated total reflection. A new principle for the production of useful infra-red spectra of organic compounds. *Spectrochim Acta*, 17 (1961) 698

Farber EM, Nall ML, The natural history of psoriasis in 5,600 patients. *Dermatologica*, 148 (1974) 1-18

Farber EM, Nall ML, Epidemiology in psoriasis research. *Hawaii Med J*, 41 (1983) 430-442

Farber EM, Nall ML, An appraisal of measures to prevent and control psoriasis. *J Am Acad Dermatol*, 10 (1984) 511-517

Farber EM, Nall L, Charuworn A, The epidemiology of severe psoriasis. In: Kukita A, Siji M (eds) *Proceedings of the XVI International Congress of Dermatology*. Tokyo University Press, Tokyo, (1983) pp 81-85

Farber EM, Nall L, Strefling A, Psoriasis: A disease of the total skin. *J Am Acad Dermatol*, 12 (1985) 150-156

Farber EM, Roth EJ, Aschheim E, Role of trauma in isomorphic response in psoriasis. *Arch Dermatol*, 91 (1969) 390-400

Fauci AS, Immunosuppressive and anti-inflammatory effects of glucocorticoids. In: Baxter JD, Rousseau GG (eds) *Glucocorticoid hormone action*. Springer, Berlin, (1979) pp 449-465

Feldmann RJ, Maibach HI, Penetration of ¹⁴C-hydrocortisone through normal skin. The effect of stripping and occlusion. *Arch Dermatol*, 91 (1965) 661-666

- Feldmann RJ, Maibach HI, Percutaneous penetration of steroids in man. *J Invest Dermatol*, 52 (1969) 89-94
- Feldmann RJ, Maibach HI, Absorption of some organic compounds through the skin in man. *J Invest Dermatol*, 54 (1970) 399-404
- Fenton DA, Wilkinson JD, Benoxaprofen: effect on cutaneous lesions in psoriasis. *Br Med J*, 285 (1982) 1420-1421
- Fincham NJ, Camp RDR, Gearing AJH, Bird CR, Cunningham F, Neutrophil chemoattractant and interleukin-1-like activity in samples from psoriatic skin lesions: further characterisation. *J Immunol*, 140 (1988) 4294-4299
- Fisher LB, Maibach HI, The effect of corticosteroids on human epidermal mitotic activity. *Arch Dermatol*, 103 (1971) 39-44
- Florence AT, Attwood D, *Physicochemical Principles of Pharmacy*. The Macmillan Press Ltd, London, (1988)
- Flynn GL, Durrheim H, Higuchi WI, Permeation of hairless mouse skin II: membrane sectioning techniques and influence on alkanol permeabilities. *J Pharm Sci*, 70 (1981) 52-56
- Foster S, Ilderton E, Norris JFB, Summerly R, Yardley HJ, Characterization and activity of phospholipase A₂ in normal human epidermis and in lesion-free epidermis of patients with psoriasis or eczema. *Br J Dermatol*, 112 (1985) 135-147
- Francoeur ML, Golden GM, Potts RO, Oleic acid: its effect on stratum corneum in relation to (trans)dermal drug delivery. *Pharm Res*, 7 (1990) 621-627
- Franz TJ, Percutaneous absorption. On the relevance of in vitro data. *J Invest Dermatol*, 64 (1975) 190-195
- Franz TJ, The finite dose technique as a valid *in vitro* model for the study of percutaneous absorption in man. *Curr Prob Dermatol*, 7 (1978) 58-68

Fry L, Psoriasis. *Br J Dermatol*, 119 (1988) 445-461

Golden GM, Guzek DB, Harris RR, McKie JM, Potts RO, Lipid thermotropic transitions in human stratum corneum. *J Invest Dermatol*, 86 (1986) 255-259

Golden GM, Guzek DB, Kennedy AH, McKie JE, Potts RO, Stratum Corneum lipid phase transitions and water barrier properties. *Biochemistry*, 26 (1987a) 2382-2388

Golden GM, McKie JE, Potts RO, Role of stratum corneum lipid fluidity in transdermal drug flux, *J Pharm Sci*, 76 (1987b) 25-28

Goodman M, Barry BW, Action of skin permeation enhancers azone, oleic acid and decylmethyl sulphoxide: permeation and DSC studies. *J Pharm Pharmacol*, 38 S (1986) 71

Goodman M, Barry BW, Action of penetration enhancers on human skin as assessed by the permeation of model drugs 5-fluorouracil and estradiol. I. Infinite dose technique. *J Invest Dermatol*, 91 (1988) 323-327

Grabbe J, Czarnetski BM, Mardin M, Release of lipoxygenase products of arachidonic acid from freshly isolated human keratinocytes. *Arch Dermatol Res*, 276 (1984) 128-130

Greaves MW, Pharmacology and significance of nonsteroidal anti-inflammatory drugs in the treatment of skin diseases. *J Am Acad Dermatol*, 16 (1987) 751-764

Greaves MW, Inflammation and mediators. *Br J Dermatol*, 119 (1988) 419-426

Greaves MW, McDonald-Gibson W, Prostaglandin biosynthesis by human skin, and its inhibition by corticosteroids. *Br J Pharmacol*, 46 (1974) 172-175

Greaves MW, Shuster S (eds), *Handbook of Experimental Pharmacology, Vol 87/1. Pharmacology of the skin I*. Springer Verlag, Berlin, (1989)

Green CA, Shuster S, Lack of effect of topical indomethacin on psoriasis. *Br J Clin Pharmacol*, 24 (1987) 381-384

Green PG, Hadgraft J, Facilitated transfer of cationic drugs across a lipoidal membrane by oleic acid and lauric acid. *Int J Pharm*, 37 (1987) 251-255

Green PG, Guy RH, Hadgraft J, In vitro and in vivo enhancement of skin permeation with oleic and lauric acids. *Int J Pharm*, 48 (1988) 103-111

Griffith OW, Meister A, Glutathione: interorgan translocation, turnover and metabolism. *Proc Natl Acad Sci USA*, 76 (1979) 5606-5610

Griffiths CEM, Leonard JN, Fry L, Dermatitis herpetiformis exacerbated by indomethacin. *Br J Dermatol*, 112 (1985) 443-445

Griffiths CEM, Powles AV, Leonard JN, Fry L, Baker BS, Valdimarsson H, Clearance of psoriasis with low dose cyclosporin. *Br Med J*, 293 (1986) 731-732

Gund P, Jensen NP, Nonsteroidal antiinflammatory and antiarthritic drugs. In: Topliss JG (ed) *Quantitative Structure-Activity Relationships of Drugs*. Academic Press, New York, (1983) pp 285-327

Guy RH, Hadgraft J, Percutaneous metabolism with saturable enzyme kinetics. *Int J Pharm*, 11 (1982) 187-197

Guy RH, Hadgraft J, Pharmacokinetics of percutaneous absorption with concurrent metabolism. *Int J Pharm*, 20 (1984) 43-51

Guy RH, Hadgraft J, Mathematical models of percutaneous absorption. In: Bronaugh RL, Maibach HI (eds), *Percutaneous Absorption. Mechanisms - Methodology - Drug Delivery*. Marcel Dekker, New York, (1985) pp 3-15

Guy RH, Hadgraft J, Physicochemical aspects of percutaneous penetration and its enhancement. *Pharm Res*, 5 (1988) 753-758

Guy RH, Maibach HI, Drug delivery to local subcutaneous structures following topical administration. *J Pharm Sci*, 72 (1983) 1375-1380

Guy RH, Guy AH, Maibach HI, Shah VP, The bioavailability of dermatological and other topically administered drugs. *Pharm Res*, 3 (1986) 253-262

Guy RH, Bucks DAW, McMaster JR, Villaflor DA, Roskos KV, Hinz RS, Maibach HI, Kinetics of drug absorption across human skin *in vivo*. In: Shroot B, Schaefer H (eds), *Pharmacology of the skin*, Vol 1. Karger, Basel, (1987a), pp 70-76

Guy RH, Hadgraft J, Bucks DAW, Transdermal drug delivery and cutaneous metabolism. *Xenobiotica*, 17 (1987b) 325-343

Hadgraft J, The epidermal reservoir: a theoretical approach. *Int J Pharm*, 2 (1979) 265-274

Hadgraft J, Penetration enhancers in percutaneous absorption. *Pharm Int*, 5 (1984) 252-254

Hadgraft J, Prodrugs and skin absorption. In: Bundgaard H (ed), *Design of Prodrugs*. Elsevier, Amsterdam, (1985) pp 271-289

Hadgraft J, Formulation of anti-inflammatory agents. In: Hensby C, Lowe NJ (eds), *Pharmacology and the Skin, Vol 2. Nonsteroidal Anti-inflammatory Drugs*. Karger, Basel, (1989) pp 21-43

Hadgraft J, Wotton PK, Facilitated percutaneous absorption of anionic drugs. In: Bronaugh RL, Maibach HI (eds), *Percutaneous Absorption. Mechanisms - Methodology - Drug Delivery*. Marcel Dekker, New York, (1985) 87-95

Hadgraft J, Walters KA, Wotton PK, Facilitated transport of sodium salicylate across an artificial lipid membrane by Azone. *J Pharm Pharmacol*, 37 (1985) 725-727

Hammarstrom S, Hamberg M, Samuelsson B, Duel EA, Stawiski M, Voorhees JJ, Increased concentrations of nonesterified arachidonic acid, 12-L-hydroxy-5,8,10,14-eicosatetraenoic acid, prostaglandin E₂, and prostaglandin F_{2α} in epidermis of psoriasis. *Proc Natl Acad Sci USA*, 72 (1975) 974-983

Handlon AL, Oppenheimer NJ, Thiol reduction of 3'-azidothymidine to 3'-aminothymidine: kinetics and biomedical implications. *Pharm Res*, 5 (1988) 297-299

Harrick NJ, Surface chemistry from spectral analysis of totally internally reflected radiation. *Phys Rev Lett*, 4 (1960) 224

Harrick NJ, *Internal reflection spectroscopy*. John Wiley & Sons, U.S.A., (1967)

Harvey J, Parish H, Ho PPK, Boot JR, Dawson W, The preferential inhibition of 5-lipoxygenase product formation by benoxaprofen. *J Pharm Pharmacol*, 35 (1983) 44-45

Herz-Hübner U, Täuber U, Metabolisierung von fluocortin-butyl ester in der haut von meerschweinchen und mensch. *Arzneim Forsch*, 27 (1977) 2226-2229

Higo N, Bommaman D, Potts R, Guy RH, Measurement of percutaneous penetration *in vivo* : spectroscopic and radiochemical methodologies. *Proceed Intern Symp Control Rel Bioac Mater*, 17 (1990) 413-414

Higuchi T, Physical chemical analysis of percutaneous absorption process from creams and ointments. *J Soc Cosmet Chem*, 11 (1960) 85-97

Higuchi WI, Gordon NA, Fox JL, Ho NFH, Transdermal delivery of prodrugs. *Drug Dev Ind Pharm*, 9 (1983) 691-706

Hindson C, Lawlor F, Wacks H, Benoxaprofen for nodular acne. *Lancet*, 1 (1982a) 1415

Hindson C, Lawlor F, Wacks H, Treatment of nodular prurigo with benoxaprofen. *Br J Dermatol*, 107 (1982b) 369-372

Hinz RS, Hodson CD, Lorence CR, Guy RH, In vitro percutaneous penetration: evaluation of the utility of hairless mouse skin. *J Invest Dermatol*, 93 (1989) 87-91

Hirata AA, Terasaki PI, Cross-reactions between streptococcal M proteins and human transplantation antigens. *Science*, 168 (1970) 1095-1096

Hong SL, Levine L, Inhibition of arachidonic acid release from cells as the biochemical action of anti-inflammatory corticosteroids. *Proc Natl Acad Sci USA*, 73 (1976) 1730-1734

- Houk J, Guy RH, Membrane models for skin penetration studies. *Chem Rev*, 88 (1988) 455-47
- Idson B, Vehicle effects in percutaneous absorption. *Drug Metab Rev*, 14 (1983) 207-222
- Inagi T, Muramatsu T, Nagai H, Terada H, Influence of vehicle composition on the penetration of indomethacin through guinea-pig skin. *Chem Pharm Bull*, 29 (1981) 1708-1714
- Irwin WJ, *Kinetics of Drug Decomposition: BASIC Computer Solutions*. Elsevier, Amsterdam, (1990) pp 175-181
- Irwin WJ, Li Wan Po A, The dependence of amitriptyline partition coefficients on lipid phase. *Int J Pharm*, 4 (1979) 47-56
- Irwin WJ, Scott DK, Hplc in pharmacy. *Chemistry in Britain*, 18 (1982) 708-718
- Irwin WJ, Masuda QN, Li Wan Po A, Transesterification of salicylate esters used as topical analgesics. *Int J Pharm*, 21 (1984) 35-50
- Isaacs NS, Substitution reactions at carbon. In: *Physical Organic Chemistry*. Longman Scientific and Technical, (1987) pp 375-492
- Johansen M, Møllgaard B, Wotton P, Larsen C, Hoelgaard A, In vitro evaluation of dermal prodrug delivery - transport and bioconversion of a series of aliphatic esters of metronidazole. *Int J Pharm*, 32 (1986) 199-206
- Jones G, Decreased toxicity and adverse reactions via pro-drugs. In: Bundgaard H (ed), *Design of Prodrugs*. Elsevier, Amsterdam, (1985) pp 199-241
- Jones GH, Venuti MC, Young JM, Krishna Murthy DV, Loe BE, Simpson RA, Berks AH, Spires DA, Maloney PJ, Kruseman M, Rouhafza S, Kappas KC, Beard CC, Unger SH, Cheung PS, Topical nonsteroidal antipsoriatic agents. 1. 1,2,3,4-tetraoxygenated naphthalene derivatives. *J Med Chem*, 29 (1986) 1504-1511

Jones SP, Greenway MJ, Orr NA, The influence of receptor fluid on in vitro percutaneous penetration. *Int J Pharm*, 53 (1989) 43-46

Jonsson DC, Angaard E, Biosynthesis and metabolism of prostaglandin E₂ in human skin. *Scand J Clin Lab Invest*, 29 (1972) 289-294

Juby PF, Goodwin WR, Hudyma TW, Partyka RA, Antiinflammatory activity of some indan-1-carboxylic acids and related compounds. *J Med Chem*, 15 (1972) 1297-1306

Kaidbey KH, Therapy of resistant psoriasis with topical corticosteroids and dimethyl-sulfoxide. *Dermatologica*, 152 (1976) 316-320

Kamali F, Gescher A, Slack JA, Medicinal azides. Part 3. The metabolism of the investigational antitumour agent meta-azidopyrimethamine in mouse tissue *in vitro*. *Xenobiotica*, 18 (1988) 1157-1164

Kapp JF, Koch H, Topert H, Kessler J, Gerhards E, Untersuchungen zur pharmakologie von 6 α -Fluor-11 β -hydroxy-16 α -methyl-3,20-dioxo-1,4-pregnadien-21-säure-butylester (Fluorcortin-butylester). *Arzneim Forsch*, 27 (1977) 2191-2204

Kappus H, Drug metabolism in the skin. In: Greaves MW, Shuster S (eds), *Handbook of Experimental Pharmacology*, 87/1. *Pharmacology of the Skin II*. Springer-Verlag, Berlin, (1989) pp 123-163

Katayama H, Kawada A, Exacerbation of psoriasis induced by indomethacin. *J Dermatol (Tokyo)*, 8 (1981) 323-327

Kato T, Rokugo M, Terui T, Tagami H, Successful treatment of psoriasis with topical application of active vitamin D₃ analogue. *Br J Dermatol*, 115 (1986) 431-433

Katz M, Poulsen BJ, Absorption of drugs through the skin. In: Brodie BB, Gillette J (eds), *Handbook of Experimental Pharmacology*, Vol 28/1. Springer Verlag, Berlin, (1971) pp 103-174

Keighley JH, Infra-red spectroscopy. In: Jones (ed) *Introduction to the spectroscopy of biological polymers*. Academic Press, New York, (1976) pp 17-80

King EJ, Prue JE, Precise measurements with the glass electrode of the ionization constants of benzoic, phenylacetic and β -phenylpropionic acids at 25°C. *J Chem Soc*, (1961) 275-279

Kirschner G, Scollar MP, Klivanov AM, Resolution of racemic mixtures via lipase catalysis in organic solvents. *J Am Chem Soc*, 107 (1985) 7072-7076

Kligman AM, The biology of the stratum corneum. In: Montagna W, Lobitz, Jr WC (eds) *The Epidermis*. Academic Press, New York, (1964), pp 387-433

Knox JH, Done JN, Fell AF, Gilbert MT, Pryde A, Wall RA, *High-Performance Liquid Chromatography*. Edinburgh University Press, Edinburgh, (1978)

Knutson K, Potts RO, Guzek DB, Golden GM, McKie JE, Lambert WJ, Higuchi WI, Macro- and molecular physical-chemical considerations in understanding drug transport in the stratum corneum. *J Control Rel*, 2 (1985) 67-87

Knutson K, Krill SL, Lambert WJ, Higuchi WI, Physicochemical aspects of transdermal permeation. *J Control Rel*, 6 (1987) 59-74

Kobza Black A, Greaves MW, Hensby CN, Plummer NA, Warin AP, The effects of indomethacin on arachidonic acid prostaglandins E₂ and F_{2 α} levels in human skin 24 h after u.v.B and u.v.C irradiation. *Br J Clin Pharmacol*, 6 (1978) 261-266

Koebner H, Fur aetiologie der psoriasis. *Vjschr Dermatol*, 8 (1876) 559-561

Kosower NS, Kosower EM, The glutathione status of cells. *Int Rev Cytol*, 54 (1978) 109-160

Kragballe K, Herlin T, Benoxaprofen improves psoriasis: a double-blind study. *Arch Dermatol*, 119 (1983) 548-552

- Kragballe K, Ternowitz S, Herlin T, Normalisation of monocyte chemotaxis precedes clinical resolution of psoriasis treated with benoxaprofen. *Acta Dermatol Venereol*, 65 (1985) 319-323
- Kragballe K, Pinnamaneni G, Desjarlais L, Duell EA, Voorhees JJ, Dermis-derived 15-hydroxy-eicosatetraenoic acid inhibits epidermal 12-lipoxygenase activity. *J Invest Dermatol*, 87 (1986a) 494-498
- Kragballe K, Duell EA, Voorhees JJ, Selective decrease of 15-hydroxyeicosatetraenoic acid (15-HETE) formation in uninvolved psoriatic dermis. *Arch Dermatol*, 122 (1986b) 877-880
- Kromann N, Green A, Epidemiological studies in the Upernavik district, Greenland. *Acta Med Scand*, 208 (1980) 401-406
- Krulig L, Farber EM, Grumet FC, Payne RO, Histocompatibility (HL-A) antigens in psoriasis. *Arch Dermatol*, 111 (1975) 857-860
- Larsson A, Orrenius S, Holmgren A, Mannervik B, In: *Functions of glutathione: Biochemical, Physiological, Toxicological and Clinical Aspects*. Raven Press, New York, (1983)
- Lassus A, Forstrom S, A dimethoxynaphthalene derivative (RSO43179 gel) compared with 0.025% fluocinolone acetonide gel in the treatment of psoriasis. *Br J Dermatol*, 113 (1985) 103-106
- Lee DC, Chapman D, Infrared spectroscopic studies of biomembranes and model membranes. *Bioscience Reports*, 6 (1986) 235-256
- Leinweber F, Possible physiological roles of carboxylic ester hydrolases. *Drug Metab Rev*, 18 (1987) 379-439
- Lever WF, Schaumburg-Lever G, Psoriasis. In: *Histopathology of the Skin*, 6th edn. J B Lippincott Company, Philadelphia, (1983) pp 139-146
- Li Wan Po A, Irwin WJ, High-performance liquid chromatography. Techniques and applications. *J Clin Hosp Pharm*, 5 (1980) 107-144

Lichtenstein J, Flowers F, Sherertz EF, Nonsteroidal anti-inflammatory drugs. Their use in dermatology. *Int J Dermatol*, 26 (1987) 80-87

Loftsson T, Effect of oleic acid on diffusion of drugs through hairless mouse skin. *Acta Pharm Nordica*, 1 (1989) 17-22

Loftsson T, Bodor N, Improved delivery through biological membranes IX: Kinetics and mechanism of hydrolysis of methylsulfinylmethyl 2-acetoxybenzoate and related aspirin prodrugs. *J Pharm Sci*, 70 (1981a) 750-755

Loftsson T, Bodor N, Improved delivery through biological membranes X: Percutaneous absorption and metabolism of methylsulfinylmethyl 2-acetoxybenzoate and related aspirin prodrugs. *J Pharm Sci*, 70 (1981b) 756-758

Lomholt G, Psoriasis: Prevalence, spontaneous course and genetics. A census study on the prevalence of skin diseases on the Faroe Islands, *GEC GAD*, Copenhagen, (1963)

Lorenzetti OJ, Propylene glycol gel vehicles. *Cos Dermatol*, 23 (1979) 747-750

Mak VHW, Potts RO, Guy RH, Oleic acid concentration and effect in human stratum corneum: non-invasive determination by attenuated total reflectance infrared spectroscopy in vivo. *J Control Rel*, 12 (1990a) 67-75

Mak VHW, Potts RO, Guy RH, Percutaneous penetration enhancement *in vivo* measured by attenuated total reflectance infrared spectroscopy. *Pharm Res*, 7 (1990b) 835-841

Mallet AI, Cunningham FM, Structural identification of platelet activating factor in psoriatic scale. *Biochem Biophys Res Commun*, 126 (1985) 192-198

Martin B, Watts O, Shroot B, Jamouille JC, A new diffusion cell - an automated method for measuring the pharmaceutical availability of topical dosage forms. *Int J Pharm*, 49 (1989) 63-68

- Marty J, Guy RH, Maibach HI, Percutaneous penetration as a method of delivery to muscle and other tissues. In: Bronaugh RL, Maibach HI (eds), *Percutaneous Absorption. Mechanisms-Methodology-Drug Delivery*. Marcel Dekker, New York, (1985) pp 469-487
- Masters DJ, McMillan RM, 5-Lipoxygenase from human leukocytes. *Br J Pharmacol*, 81 (1984) 70P
- Matoltsy AG, Downes AM, Sweeney TM, Studies of the epidermal water barrier part II: investigation of the chemical nature of the water barrier. *J Invest Dermatol*, 50 (1968) 19-26
- McKenzie AW, Stoughton RB, Methods of comparing percutaneous absorption of steroids. *Arch Dermatol*, 86 (1962) 608-610
- Meacock SCR, Kitchen EA, Dawson W, Effects of benoxaprofen and some other non-steroidal anti-inflammatory drugs on leukocyte migration. *Eur J Rheumatol*, 3 (1979) 23-28
- Meister A, Anderson ME, Glutathione. *Ann Rev Biochem*, 52 (1983) 711-760
- Metzler CM, Weiner DC, PCNONLIN, Statistical Consultants Inc, Lexington, Kentucky, USA, (1986)
- Meuller W, Hermann B, Cyclosporin A for psoriasis. *N Engl J Med*, 301 (1979) 555
- Meyerhoff JO, Exacerbation of psoriasis with meclofenamate. *N Engl J Med*, 309 (1983) 496
- Moffat AC, *Clarke's Isolation and Identification of drugs. In pharmaceuticals, body fluids and post-mortem material*. 2nd edn, The Pharmaceutical Press, London, (1986)
- Moldéus P, Quangan J, Importance of the glutathione cycle in drug metabolism. *Pharmac Ther*, 33 (1987) 37-40

- Montagna W, Parakkal PF, *The Structure and Function of the Skin*, 3rd edn. Academic Press, New York, (1974)
- Morimoto S, Yochikawa K, Kozuka T, Kitano Y, Imanaka S, Fukuo K, Koh E, Yumahara T, An open study of vitamin D₃ treatment in *Psoriasis vulgaris*. *Br J Dermatol*, 115 (1986) 421-429
- Mützel W, Pharmakokinetik und biotransformation von fluocortin-butyl ester beim menschen. *Arzneim Forsch*, 27 (1977) 2230-2233
- Møllgaard B, Hoelgaard A, Bundgaard H, Pro-drugs as drug delivery systems XXIII. Improved dermal delivery of 5-fluorouracil through human skin via N-acetyloxymethyl pro-drug derivatives. *Int J Pharm*, 12 (1982) 153-162
- Møllgaard B, Hoelgaard A, Vehicle effects on topical drug delivery. I. Influence of glycols and drug concentration on skin transport. *Acta Pharm Suec*, 20 (1983) 433-442
- Møllgaard B, Hoelgaard A, Vehicle effects on topical drug delivery. II. Concurrent skin transport of drugs and vehicle components. *Acta Pharm Suec*, 20 (1983b) 443-450
- Nacht S, Yeung D, Artificial membranes and skin permeability. In: Bronaugh RL, Maibach HI (eds), *Percutaneous Absorption. Mechanisms - Methodology - Drug Delivery*. Marcel Dekker, New York, (1985) pp 373-386
- Newton JA, Boodle KA, Dowd PM, Greaves MW, Topical NDGA (nordihydro-guaiaretic acid) in psoriasis. *Br J Dermatol*, 119 (1988) 404-406
- Nielsen NM, Bundgaard H, Prodrugs as drug delivery systems. 68. Chemical and plasma-catalyzed hydrolysis of various esters of benzoic acid: a reference system for designing prodrug esters of carboxylic acid agents. *Int J Pharm*, 39 (1987) 75-87
- Nielsen NM, Bundgaard H, Glycolamide esters as biolabile prodrugs of carboxylic acid agents: synthesis, stability, bioconversion, and physicochemical properties. *J Pharm Sci*, 77 (1988) 285-298

- Noonan PK, Wester RC, Cutaneous metabolism of xenobiotics. In: Bronaugh RL, Maibach HI (eds), *Percutaneous absorption. Mechanisms-Methodology-Drug Delivery*. Marcel Dekker, New York, (1985) pp 65-85
- Norholm-Pederson A, Infections and psoriasis, *Acta Dermatovenereol*, 32 (1952) 159-167
- Norrind R, Psoriasis following infections with haemolytic streptococci. *Acta Dermatovenereol*, 30 (1950) 64-72
- Ogiso T, Ito Y, Iwaki M, Atago H, Absorption of indomethacin and its calcium salt through rat skin: effect of penetration enhancers and relationship between *in vivo* and *in vitro* penetration. *J Pharmacobio Dyn*, 9 (1986) 517-525
- Oikarinen A, Viinikka L, Rytsala H, Kiistala U, Ylikorkala O, Prostacyclin, thromboxane and prostaglandin F_{2α} in suction blister fluid of human skin: effect of systemic aspirin and and local glucocorticoid treatment. *Life Sci*, 29 (1981) 391-396
- Ongpipattanakul B, Burnette RR, Potts RO, Francoeur ML, Evidence from infrared spectroscopy that oleic acid induces lipid phase separation within the stratum corneum. *Pharm Res* (in press)
- Ostrenga J, Steinmetz C, Poulsen B, Significance of vehicle composition I: relationship between topical vehicle composition, skin permeability, and clinical efficacy. *J Pharm Sci*, 60 (1971) 1175-1179
- Pannatier A, Jenner P, Testa B, Etter JC, The skin as a drug-metabolizing organ. *Drug Metab Rev*, 8 (1978) 319-343
- Panse VP, Zeiller P, Sensch KH, Zur perkutanen resorption von antiphlogistisch wirksamen substanzen. *Arzneim Forsch*, 24 (1974) 1298-1301
- Pedace J, Muller A, Winklemann RK, Biology of psoriasis: experimental study of Koebner phenomenon. *Acta Dermatovenereol*, 49 (1969) 390-400
- Penneys N, Ziboh V, Lord J, Simon P, Inhibitor(s) of prostaglandin synthesis in psoriatic plaque. *Nature*, 254 (1975) 351-352

Perrin DD, Dempsey B, *Buffers for pH and Metal Ion Control*. Chapman and Hall, London, (1974)

Pinkus H, Mehregan AH, Psoriasis. In: *A guide to dermatohistopathology*, 3rd edn. Appleton-Century-Crofts, New York, (1981) pp 101-104

Polano MK, Ponec M, Dependence of corticosteroid penetration on the vehicle. *Arch Dermatol*, 112 (1976) 675-680

Potts RO, Physical characterization of the stratum corneum: The relationship of mechanical and barrier properties to lipid and protein structure. In: Hadgraft J, Guy RH (eds), *Transdermal Drug Delivery: Developmental Issues and Research Initiatives*. Marcel Dekker, New York, (1989) pp. 23-57

Potts RO, Guzek DB, Harris RR, McKie JE, A noninvasive, in vivo technique to quantitatively measure water concentration of the stratum corneum using attenuated total-reflectance infrared spectroscopy. *Arch Dermatol Res*, 277 (1985) 489-495

Poulsen BJ, Diffusion of drugs from topical vehicles: an analysis of vehicle effects. *Adv Biol Skin*, 12 (1972) 495-509

Poulsen BJ, Young E, Coquilla V, Katz M, Effect of topical vehicle composition on the in vitro release of fluocinolone acetonide and its acetate ester. *J Pharm Sci*, 57 (1968) 928-933

Poulsen BJ, Chowhan ZT, Pritchard R, Katz M, The use of mixtures of topical corticosteroids as a mechanism for improving total drug bioavailability. A preliminary report. *Curr Probl Dermatol*, 7 (1978) 107-120

Prescott SM, The effect of eicosapentaenoic acid on leukotriene B production by human neutrophils. *J Biol Chem*, 259 (1984) 7615-7621

Pusey WMA, *The history of dermatology*. Charles C Thomas, Illinois, (1933)

Puttnam NA, Attenuated total reflectance studies of the skin. *J Soc Cosmet Chem*, 23 (1972) 209-226

- Puttnam NA, Baxter BH, Spectroscopic studies of skin in situ by attenuated total reflectance. *J Soc Cosmet Chem*, 18 (1967) 469-472.
- Rabinowitz JL, Feldman ES, Weinberger A, Schumacher HR, Comparative tissue absorption of oral ^{14}C aspirin and topical triethanolamine ^{14}C salicylate in human and canine knee joints. *J Clin Pharmacol*, 22 (1982) 42-48
- Ragaz A, Ackerman AB, Evolution, maturation and regression of lesions in psoriasis. *Am J Dermatopath*, 1 (1979) 199-214
- Reiss VW, Schmid K, Botta L, Die perkutane resorption von diclofenac. *Drug Res*, 36 (1986) 1092-1096
- Rigg PC, Barry BW, Shed snake skin and hairless mouse skin as model membranes for human skin during permeation studies. *J Invest Dermatol*, 94 (1990) 235-240
- Risum G, Psoriasis exacerbated by hypoparathyroidism with hypocalcaemia. *Br J Dermatol*, 89 (1973) 309-312
- Rougier A, Dupuis D, Lotte C, Roguet R, Schaefer H, In vivo correlation between stratum corneum reservoir function and percutaneous absorption. *J Invest Dermatol*, 81 (1983) 275-278
- Rougier A, Dupuis D, Lotte C, Roguet R, The measurement of the stratum corneum reservoir. A predictive method for in vivo percutaneous absorption studies: influence of application time. *J Invest Dermatol*, 84 (1985) 66-68
- Rougier A, Dupuis D, Lotte C, Roguet R, Wester RC, Maibach HI, Regional variation in percutaneous absorption in man: measurement by the stripping method. *Arch Dermatol Res*, 278 (1986) 465-469
- Rougier A, Lotte C, Maibach HI, In vivo percutaneous penetration of some organic compounds related to anatomic site in humans: predictive assessment by stripping method. *J Pharm Sci*, 76 (1987) 451-454
- Ruzicka T, Printz MP, Arachidonic acid metabolism in skin: a review. *Rev Physiol Biochem Pharmacol*, 100 (1984) 121-160

Ruzicka T, Simmet T, Peskar BA, Ring J, Skin levels of arachidonic acid-derived inflammatory mediators and histamine in atopic dermatitis and psoriasis. *J Invest Dermatol*, 86 (1986) 105-108

Salmon JA, Higgs GA, Tilling L, Moncada S, Vane JR, Mode of action of benoxaprofen. *Lancet*, 2 (1984) 848

Sanderson FD, *Absorption Models of Drug Delivery*. PhD Thesis, Aston University, (1986)

Schaefer H, Zesch A, Stüttgen G, Penetration, permeation and absorption of triamcinolone acetonide in normal and psoriatic skin. *Arch Dermatol Res*, 258 (1977) 241-249

Schaefer H, Stüttgen G, Zesch A, Schalla W, Gazith J, Quantitative determination of percutaneous absorption of radiolabeled drugs *in vitro* and *in vivo* by human skin. *Curr Prob Dermatol*, 7 (1978) 80-94

Schaefer H, Farber EM, Goldberg L, Schalla W, Limited application period for dithranol in psoriasis, *Br J Dermatol*, 102 (1980) 571-573

Schaefer H, Zesch A, Stüttgen G, *Skin Permeability*. Springer, Berlin, (1982)

Schalla W, Schaefer H, Localization of compounds in different skin layers and its use as an indicator of percutaneous absorption. In: Bronaugh RL, Maibach HI, (eds), *Percutaneous Absorption. Mechanisms - Methodology - Drug Delivery*. Marcel Dekker, New York, (1985) pp 281-303

Schalla W, Bauer E, Schaefer H, Beeinflussungsgrößen der penetration von steroidexterna. *Aktuel Dermatol*, 6 (1980) 3-11

Scheuplein RJ, Permeability of the skin: a review of major concepts. *Curr Prob Dermatol*, 7 (1978a) 172-186

Scheuplein RJ, Skin permeation. *J Physiol Pathophysiol*, 5 (1978b) 1693

Schroder JM, Christophers E, Identificaton of C5a des arg and an anionic neutrophil-activating peptide (ANAP) in psoriatic scales. *J Invest Dermatol*, 87 (1986) 53-58

Scott RC, Dugard PH, A potential model for studying absorption through abnormal stratum corneum. *J Pharm Pharmacol*, 33 S (1981) 2

Seville RH, The doctor-patient relationship. In: Mier PD, van de Kerkhof PCM (eds) *Textbook of Psoriasis*. Churchill Livingstone, Edinburgh, (1986) pp 277-284

Shahi V, Zatz JL, Effect of formulation factors on penetration of hydrocortisone through mouse skin. *J Pharm Sci*, 67 (1978) 789-792

Shen TY, *Drugs Exp Clin Res*, 2 (1977) 1

Shen TY, Nonsteroidal anti-inflammatory agents. In: *Burger's Medicinal Chemistry*, 4th edn, Part III. Wiley, New York, (1981) pp 1205-1271

Sherertz EF, Sloan KB, McTiernan RG, Effect of skin pretreatment with vehicle alone or drug in vehicle on flux of a subsequently applied drug: results of hairless mouse skin and diffusion cell studies. *J Invest Dermatol*, 89 (1987) 249-252

Shore PA, Brodie BB, Hogben CAM, The gastric secretion of drugs: a pH-partition hypothesis. *J Pharmacol Exp Ther*, 119 (1957) 361

Shrewsbury RP, Foster TS, Dittert LW, Quigley JW, Leavell UW, Percutaneous absorption of hydroxyurea through psoriatic lesions. *Curr Ther Res*, 28 (1980) 1002-1011

Siddiqui O, Physicochemical, physiological, and mathematical considerations in optimizing percutaneous absorption of drugs. *Crit Rev Ther Drug Carrier Systems*, 6 (1989) 1-38

Simpson CF, *Practical High Performance Liquid Chromatography*. Heyden, London, (1978)

Siver KG, Sloan KB, The effect of structure of Mannich base prodrugs of 6-mercaptapurine on their ability to deliver 6-mercaptapurine through hairless mouse skin. *Int J Pharm*, 48 (1988) 195-206

Skelly JP, Shah VP, Maibach HI, Guy RH, Wester RC, Flynn G, Yacobi A, FDA and AAPS report of the workshop on principles and practices of in vitro percutaneous penetration studies: relevance to bioavailability and bioequivalence. *Pharm Res*, 4 (1987) 265-267

Slack JA, Pashley SGH, Stevens MFG, Griffin RJ, Analysis and preclinical pharmacology of the new lipophilic DHFR inhibitor MZPES. *Proc Am Assoc Cancer Res*, 27 (1986) 403

Sloan KB, Bodor N, Hydroxymethyl and acyloxymethyl prodrugs of theophylline: enhanced delivery of polar drugs through skin. *Int J Pharm*, 12 (1982) 299-313

Sloan KB, Selk S, Haslam J, Caldwell L, Shaffer R, Acyloxyamines as prodrugs of anti-inflammatory carboxylic acids for improved delivery through skin. *J Pharm Sci*, 73 (1984a) 1734-1737

Sloan KB, Koch SAM, Siver KG, Mannich base derivatives of theophylline and 5-fluorouracil: synthesis, properties and topical delivery characteristics. *Int J Pharm*, 21 (1984b) 251-264

Sloan KB, Sheretz EF, McTiernan RG, The effect of structure of Mannich base prodrugs on their ability to deliver theophylline and 5-fluorouracil through hairless mouse skin. *Int J Pharm*, 44 (1988) 87-96

Smeyers YG, Cuéllar-Rodríguez S, Galvez-Ruano E, Arias-Pérez MS, Conformational analysis of some α -phenylpropionic acids with antiinflammatory activity. *J Pharm Sci*, 74 (1985) 47-49

Smith EL, Walworth ND, Holick MF, Effect of 1,25-dihydroxyvitamin D₃ on the morphologic and biochemical differentiation of cultured human epidermal keratinocytes grown in serum-free conditions. *J Invest Dermatol*, 86 (1986) 709-714

Smith EL, Pincus SH, Donovan L, Holick MF, A novel approach for the evaluation and treatment of psoriasis. *J Am Acad Dermatol*, 19 (1988) 516-528

Smith JB, Willis AL, Aspirin selectively inhibits prostaglandin production in human platelets. *Nature*, 231 (1971) 235-237

Squire B, Treatment of psoriasis by an ointment of chrysophanic acid. *Br J Dermatol*, 2 (1876) 819-820

Staros JV, Bayley H, Standring DN, Knowles JR, Reduction of aryl azides by thiols; implications for the use of photoaffinity reagents. *Biochem Biophys Res Commun*, 80 (1978) 568-572

Stevens MFG, Griffin RJ, Wong SK, The aromatic azido group in anti-cancer drug design: application in the development of novel lipophilic dihydrofolate reductase inhibitors. *Anti-Cancer Drug Design*, 2 (1987) 311-318

Stingl G, Wolff K, Origin and function of Langerhans cells and their role in disease. In: Goos M, Christophers E (eds) *Lymphoproliferative diseases of the skin*. Springer Verlag, Berlin, (1982), pp 34-40

Stoughton RB, Animal models for *in vitro* percutaneous absorption. In: Maibach HI (ed), *Animal Models in Dermatology*. Churchill Livingstone, New York, (1975) pp 121-132

Strakosch EA, Studies on ointments; local action of salicylic acid plus sulfur from various ointment bases. *Arch Dermatol Syph*, 48 (1943) 384-392

Stuart NSA, Crawford SM, Blackledge GRP, Newlands ES, Slack J, Hoffman R, Stevens MFG, A phase I study of meta-azidopyrimethamine ethanesulphonate (MZPES) - a new dihydrofolate reductase inhibitor. *Cancer Chemother Pharmacol*, 23 (1989) 308-310

Sugibayashi K, Hosoya KI, Morimoto Y, Higuchi WI, Effect of the absorption enhancer, Azone, on the transport of 5-fluorouracil across hairless rat skin. *J Pharm Pharmacol*, 37 (1985) 578-580

- Swerlick RA, Cunningham MW, Hall NK, Monoclonal antibodies cross-reactive with group A streptococci and normal and psoriatic human skin. *J Invest Dermatol*, 87 (1986) 367-371
- Täuber U, Metabolism of drugs on and in the skin. In: Brandau R, Lippold BH (eds), *Dermal and Transdermal Absorption*. Wissenschaftliche Verlagsgesellschaft, Stuttgart, (1982) pp 133-151
- Täuber U, Rost KL, Esterase activity of the skin including species variations. In: Shroot B, Schaefer H (eds), *Pharmacology of the Skin*, Vol 1. Karger, Basel, (1987) pp 170-183
- Täuber U, Toda T, Biotransformation von difluocortolonvalerianat in der haut von ratte, meerschweinchen und mensch. *Arzneim Forsch*, 26 (1976) 1484-1487
- Terano T, Salmon JA, Moncada S, Effect of orally administered eicosapentaenoic acid (EPA) on the formation of leukotriene B₄ and leukotriene B₅ by rat leukocytes. *Biochem Pharmacol*, 33 (1984) 3071-3076
- Ternowitz T, Monocyte and neutrophil chemotaxis in psoriasis. Relation to the clinical status and the type of psoriasis. *J Am Acad Dermatol*, 15 (1986) 1191-1199
- Tsuji K, Morozowich W, *GLC and HPLC Determination of Therapeutic Agents*, Parts 1-3. Marcel Dekker, New York (1978-79)
- Tsuzuki N, Wong O, Higuchi T, Effect of primary alcohols on percutaneous absorption. *Int J Pharm*, 46 (1988) 19-23
- Valdimarsson H, Baker BS, Jonsdottir I, Fry L, Psoriasis: a disease of abnormal keratinocyte proliferation induced by T lymphocytes. *Immunology Today*, 7 (1986) 256-259
- Van de Kerkhof PCM, Clinical features. In: Mier PD, van de Kerkhof PCM (eds) *Textbook of Psoriasis*. Churchill Livingstone, Edinburgh, (1986) pp 13-39

- Van Scott EJ, Ekel TM, Kinetics of hyperplasia in psoriasis. *Arch Dermatol*, 88 (1963) 373-381
- Vanderhook JY, Bryant RV, Bailey JM, Inhibition of leukotriene biosynthesis by the leukocyte product 15-hydroxy-5,8,11,13-eicosatetraenoic acid. *J Biol Chem*, 255 (1980) 10064-10066
- Vane JR, Inhibition of prostaglandin synthesis as a mechanism of action of the aspirin-like drugs. *Nature*, 231 (1971) 232-235
- Wada Y, Etoh Y, Ohira A, Kimata H, Koide T, Ishihama H, Mizushima Y, Percutaneous absorption and anti-inflammatory activity of indomethacin in ointment., *J Pharm Pharmacol*, 34 (1982) 467-468
- Wahba A, Cohen H, Bar Eli M, Callily R, Enhanced chemotactic and phagocytic activities of leukocytes in psoriasis vulgaris. *J Invest Dermatol*, 71 (1978) 186-188
- Wahlberg JE, "Disappearance measurements" a method for studying percutaneous absorption of isotope-labelled compounds emitting gamma-rays. *Acta Derm Venereol*, 45 (1965) 397-414
- Walker JR, Dawson W, Inhibition of rabbit PMN lipoxygenase activity by benoxaprofen. *J Pharm Pharmacol*, 31 (1979) 778
- Wallace TJ, Schriesheim A, Solvent effects in the base-catalysed oxidation of mercaptans with molecular oxygen. *J Org Chem*, 27 (1963a) 1514-1520
- Wallace TJ, Schriesheim A, Solvent effects in the oxidation of thiols IV. Base catalyzed oxidation of thiols and disulfides to sulfonic acids. *Tetrahedron Lett*, 17 (1963b) 1131-1136
- Walters KA, Penetration enhancers and their use in transdermal therapeutic systems. In: Guy RH, Hadgraft J (eds), *Transdermal Drug Delivery: Developmental Issues and Research Initiatives*. Marcel Dekker, New York, (1989) pp 197-246

Waranis RP, Sloan KB, Effects of vehicles and prodrug properties and their interactions on the delivery of 6-mercaptopurine through skin: bisacyloxymethyl-6-mercaptopurine prodrugs. *J Pharm Sci*, 76 (1987) 587-595

Waranis RP, Sloan KB, Effects of vehicles and prodrug properties and their interactions on the delivery of 6-mercaptopurine through skin: S⁶-acyloxy-methyl-6-mercaptopurine prodrugs. *J Pharm Sci*, 77 (1988) 210-215

Ward AJL, Tallon R, Penetration enhancer incorporation in bilayers. In: Osborne DW, Amann AH (eds), *Topical Drug Delivery Formulations*. Marcel Dekker, New York, (1990) pp 47-67

Watson W, Cann HM, Farber EM, Nall ML, The genetics of psoriasis. *Arch Dermatol*, 105 (1972) 197-207

Weigand DA, Gaylor JR, Removal of the stratum corneum in vivo: an improvement on the cellophane tape stripping technique. *J Invest Dermatol*, 60 (1973) 84-86

Weinstein GD, Frost P, Abnormal cell proliferation in psoriasis. *J Invest Dermatol*, 50 (1968) 254-259

Weinstein GD, McCullough JL, Cytokinetics in disease of epidermal hyperplasia. *Ann Rev Med*, 24 (1973) 345-352

Wester RC, Maibach HI, Cutaneous pharmacokinetics: 10 steps to percutaneous absorption. *Drug Metab Rev*, 14 (1983) 169-205

Wester RC, Maibach HI, Dermatopharmacokinetics: a dead membrane or a complex multifunctional viable process? In: Bridges JW, Chasseaud LF (eds), *Progress in Drug Metabolism*, Vol 9. Taylor and Francis Ltd, (1986) pp 95-109.

Wester RC, Noonan PK, Relevance of animal models for percutaneous absorption. *Int J Pharm*, 7 (1980) 99-110

Wester RC, Bucks DAW, Maibach HI, In vivo percutaneous absorption of hydrocortisone in psoriatic patients and normal volunteers. *J Am Acad Dermatol*, 8 (1983) 645-647

Whitehouse MW and Rainsford KD, Side-effects of anti-inflammatory drugs: are they essential or can they be circumvented? *Agents Actions*, Suppl. 3 (1977) 171-187

Wiechers JW, The barrier function of the skin in relation to percutaneous absorption of drugs. *Pharm Weekbl [Sci]*, 11 (1989) 185-198

Wiegrebbe W, Retzow A, Plumier E, Ersoy N, Garber A, Faro HP, Kunert R, Dermal absorption and metabolism of the antipsoriatic drug dithranol triacetate. *Arzneim-Forsch Drug Res*, 34 (1984) 48-51

Willan R, *On cutaneous diseases*, Vol 1. Kimber and Conrad, Philadelphia, (1809) pp 115

Winthrop GJ, Does meclofenamate help psoriasis and arthritis? *N Engl J Med*, 307 (1982) 1528

Woodford R, Barry BW, Penetration enhancers and the percutaneous absorption of drugs: an update. *J Toxicol Cut Ocular Toxicol*, 5 (1986) 167-177

Woollard PM, Stereochemical difference between 12-hydroxy-5,8,10,14-eicosatetraenoic acid in platelets and psoriatic lesions. *Biochem Biophys Res Commun*, 136 (1986) 169-176

Wotton PK, Møllgaard B, Hadgraft J, Hoelgaard A, Vehicle effect on topical drug delivery. III. Effect of azone on the cutaneous permeation of metronidazole and propylene glycol. *Int J Pharm*, 24 (1985) 19-26

Yano T, Nakagawa A, Tsuji M, Noda K, Skin permeability of various non-steroidal anti-inflammatory drugs in man. *Life Sci*, 39 (1986) 1043-1050

Yasuda T, Ishikawa E, Mori S, Psoriasis in the Japanese. In: Farber E, Cox A (eds) *Proceedings of the First International Symposium*. York Medical Books, New York, (1971) pp 25-34

Yu CD, Fox JL, Ho NFH, Higuchi WI, Physical model evaluation of topical prodrug delivery - simultaneous transport and bioconversion of vidarabine-5'-valerate. I & II. *J Pharm Sci*, 68 (1979) 1341-1357

Yu CD, Higuchi WI, Ho NFH, Fox JL, Flynn GL, Physical model evaluation of topical prodrug delivery - simultaneous transport and bioconversion of vidarabine-5'-valerate. III. Permeability differences of vidarabine and *n*-pentanol in components of hairless mouse skin. *J Pharm Sci*, 69 (1980a) 770-772

Yu CD, Fox JL, Ho NFH, Higuchi WI, Physical model evaluation of topical prodrug delivery - simultaneous transport and bioconversion of vidarabine-5'-valerate. IV. Distribution of esterase and deaminase enzymes in hairless mouse skin. *J Pharm Sci*, 69 (1980b) 772-775

Zachariae H, Epidemiology and genetics. In: Mier PD, van de Kerkhof PCM (eds) *Textbook of Psoriasis*. Churchill Livingstone, Edinburgh, (1986) pp 5-12

Zahler WL, Cleland WW, A specific and sensitive assay for disulfides. *J Biol Chem*, 243 (1968) 716

Zaks A, Klibanov AM, Enzymatic catalysis in nonaqueous solvents. *J Biol Chem*, 263 (1988) 3194-3201

Zesch A, Methods for evaluation of drug concentration in human skin. In: Brandau R, Lippold BH (eds), *Dermal and Transdermal Absorption*. Wissenschaftliche Verlagsgesellschaft, Stuttgart, (1982) pp 116-132

Zesch A, Hoffmann WD, Schaefer H, Distribution of a labelled pharmaceutical from four ointment bases in the human horny layer. *Pharmazie*, 29 (1974) 198-203

Zesch A, Schaefer H, Penetration of radioactive hydrocortisone in human skin from various ointment bases. II. In vivo experiments. *Arch Dermatol Forsch*, 252 (1975) 245-256

Ziboh VA, Casebolt TL, Marcelo CL, Voorhees JJ, Biosynthesis of lipoxygenase products by enzyme preparations from normal and psoriatic skin. *J Invest Dermatol*, 83 (1984) 426-430

Ziboh VA, Cohen KA, Ellis CN, Miller C, Hamilton TA, Kragballe K, Hydrick CR, Voorhees JJ, Effects of dietary supplementation of fish oil on neutrophil and epidermal fatty acids: Modulation of clinical course of psoriatic subjects. *Arch Dermatol*, 122 (1986) 1277-1282

APPENDICES

APPENDIX 1
LIST OF SUPPLIERS

<u>Chemical</u>	<u>Supplier</u>
Acetonitrile	FSA Laboratory Supplies
Azone	Nelson Research
<i>n</i> -Butyl- <i>p</i> -aminobenzoate	Sigma
Caffeine	BDH
Citric acid	Fisons
Deuterated water	Aldrich
Diethylamine	BDH
Dimethyl sulphoxide	BDH
Dithiothrietol	Sigma
Dodecylamine	Sigma
Ethyl salicylate	Aldrich
Glucose-6-phosphate	Sigma
Glucose-6-phosphate dehydrogenase	Sigma
HEPES	Sigma
Isopropyl myristate	Sigma
KH ₂ PO ₄	Fisons
MgCl ₂ .6H ₂ O	Sigma
Methanol	FSA Laboratory Supplies
Methyl paraben	Sigma
Methyl <i>p</i> -nitrobenzoate	Aldrich
NADP (sodium salt)	Sigma
N-decyl methyl sulphoxide	Boehringer-Mannheim
Na ₂ HPO ₄	Fisons
Na ₂ HPO ₄ . 2H ₂ O	Fisons
NaH ₂ PO ₄ . 2H ₂ O	Fisons
1-Octanesulphonic acid (sodium salt)	Sigma
Octan-1-ol	Fisons
Oleic acid	Hopkin & Williams
Orthophosphoric acid	Fisons

Potassium chloride	Fisons
<i>n</i> -Propyl salicylate	Graesser Salicylates Ltd
Propylene glycol	Fisons
Sodium chloride	Fisons
Theophylline	BDH
Tris (hydroxymethyl)aminomethane	Fisons
Tween 20	Sigma

APPENDIX 2
COMPOSITION OF BUFFERS

KH₂PO₄, NaOH buffer

Contains 50 ml 0.1 M KH₂PO₄ (13.60 g l⁻¹) and x ml 0.1 M NaOH, diluted to 100 ml.

pH at 25°C	x	KCl added (g/100 ml) to produce ionic strength of 0.5 M
5.80	3.6	3.327
6.20	8.1	3.289
6.50	13.9	3.219
6.80	22.4	3.147
7.20	34.7	2.987
7.80	44.5	2.759
8.00	46.1	2.714
8.50	47.6	2.647
9.00	48.2	2.599

Ionic strengths prior to addition of KCl were calculated by computer analysis and then adjusted to 0.5 M by the addition of appropriate amounts of KCl (see Perrin and Dempsey, 1974)

Phosphate buffer, pH 7.40

Na₂HPO₄ · 2H₂O 29.01g
 NaH₂PO₄ · 2H₂O 2.96g
 Distilled water to 1 litre

Phosphate buffered saline

NaCl 8.0g
 KCl 0.2g
 KH₂PO₄ 0.2g
 Na₂HPO₄ · 2H₂O 1.44g
 Distilled water to 1 litre

McIlvaine buffers

Contains x ml 0.1 M citric acid (21.01 g $C_6H_8O_7 \cdot H_2O$ l⁻¹) and (100 - x) ml 0.2 M disodium hydrogen phosphate (35.61 g $Na_2HPO_4 \cdot 2H_2O$ l⁻¹).

pH at 21 °C	x	KCl added (g/100 ml) to produce ionic strength of 0.5 M
3.4	72.4	2.83
3.6	68.7	2.72
3.8	65.2	2.61
4.0	61.9	2.46
4.2	59.0	2.31
4.4	56.3	2.20
4.6	53.8	2.09
4.8	51.4	1.94
5.0	49.0	1.86
5.2	47.0	1.71
5.4	44.8	1.64
5.6	42.6	1.49
5.8	40.2	1.42
6.0	37.5	1.34
6.2	34.6	1.19
6.4	31.1	1.12
6.6	27.1	1.04
6.8	22.8	0.969
7.0	17.8	0.746
7.2	13.0	0.522
7.4	9.4	0.298
7.6	6.5	0.075

From Perrin and Dempsey (1974).

For the preparation of a concentrated McIlvaine buffer, ten-fold amounts of all salts were used.

CONCENTRATED Tris(hydroxymethyl)aminomethane, HCl buffer

Contains 50 ml 1.0 M Tris (121.14 g l⁻¹) and x ml 1.0 M HCl, diluted to 100 ml.

pH	x
7.00	46.6
7.10	45.7
7.20	44.7
7.30	43.4
7.40	42.0
7.50	40.3
7.60	38.5
7.70	36.6
7.80	34.5
7.90	32.0
8.00	29.2
8.10	26.2
8.20	22.9
8.30	19.9
8.40	17.2
8.50	14.7
8.60	12.4
8.70	10.3
8.80	8.5
8.90	7.0
9.00	5.7

Adapted from Perrin and Dempsey (1974).

Where buffers were prepared in deuterated water, the pD value was obtained by the relationship:

$$\text{pD} = \text{meter reading} + 0.40$$

where the pH meter was calibrated using aqueous pH buffers.